Folate Receptor Mediated Targeting of Oral Cancer: Therapeutic and Mechanistic Investigations Against Tumour Cells and Tumour Associated Macrophages

THESIS

Submitted in partial fulfilment

of the requirements for the degree of

DOCTOR OF PHILOSOPHY

By

DWAIPAYAN BHATTACHARYA

ID. No.-2017PHXF0413H

Under the supervision of

Prof. Kumar Pranav Narayan

BITS Pilani
Pilani | Dubai | Goa | Hyderabad

BIRLA INSTITUTE OF TECHNOLOGY & SCIENCE, PILANI

2023

BIRLA INSTITUTE OF TECHNOLOGY AND SCIENCE,

PILANI, HYDERABAD CAMPUS

CERTIFICATE

This is to certify that the thesis entitled **"Folate Receptor Mediated Targeting of Oral Cancer: Therapeutic and Mechanistic Investigations Against Tumour Cells and Tumour Associated Macrophages"** submitted by **Dwaipayan Bhattacharya** ID No **2017PHXF0413H** for award of Ph.D. of the Institute embodies original work done by him under my supervision.

Kumar Pranav Narayan

Prof. KUMAR PRANAV NARAYAN
Supervisor
Professor
Department of Biological Sciences
Date:

Acknowledgement

In my research career so far, I have not just gained knowledge, but also valuable life lessons that hopefully I shall get to share some day with the world in my own way. I wish to gratefully thank and acknowledge the remarkable individuals who stayed with me throughout my journey and helped me believe in myself.

To begin with, I would like to thank my thesis supervisor, Prof. Kumar Pranav Narayan. He trusted me from the first day, no matter how challenging the task was. He taught me to be brave, hold my head high and give my best no matter how small the endeavour was. He trusted my instincts and allowed me to grow in the best possible way. Sir treated me like family and taught me to not just work methodically, but also to do so with kindness and concern for everyone around me. I shall forever be indebted to him for his guidance and insight which has helped me throughout my tenure at BITS Pilani Hyderabad Campus.

I wish to thank my DAC (Doctoral Advisory Committee) members, Dr. Piyush Khandelia and Prof. Onkar Kulkarni for their inspiring support and invaluable scientific suggestions from time to time. They always extended helpful hands towards me whenever I needed them.

I thank Prof. Sridev Mohapatra, DRC (doctoral research committee) convener, for his constant encouragement and support.

I express my sincere thanks to all the faculty members of Biological Sciences Department, BITS Pilani, Hyderabad campus for their kind help and encouragement in carrying out my research work.

I thank all the technical assistants of our Department and especially Poornima, Ramakrishna Sir and Imtiaz Sir for their kindness and prompt assistance whenever I needed them. My work would never run as smoothly without them.

It is my utmost pride and pleasure to acknowledge Dr. Rajkumar Banerjee, Principal Scientist, Indian Institute of Chemical Technology (IICT), Hyderabad for his constant encouragement and input. He has been eternally kind to me and I

am indebted to his help and blessings in sailing through my Doctoral journey. He always extended his helpful hands to me whenever I needed them.

Constant moral support extended to me by my friends and well-wishers is gratefully acknowledged. I thank my lab mates Kalyani, Chhavi, Ramchandra, Jayasheela and Abhiram for their constant support and patience with me. I would like to thank Bakhya, Dhansri, Shraddha, Swati, Jayasree, Suryansh and Pragati for their love which made my experience at BITS Pilani Hyderabad a memorable one. I also thank Rohit, Shiva, Aniket, Naresh, Harsha, Sumana, Gargi and Rolly for their love and support. I am really fortunate for sharing a wonderful friendship with them. Writing this thesis would be extremely difficult for me without their enormous support.

Financial assistance from BITS Pilani, Hyderabad is gratefully acknowledged. I am grateful to the Director, BITS Pilani Hyderabad for providing space and resources for carrying out my work. I thank the Centre for Human Diseases & Research (CHDR) for funding and resources. I also thank ICMR for awarding me with SRF which was a great financial aid for me throughout my tenure.

I appreciate the unending love and affection from my sister Darshana. Love you for your everlasting support extended towards me. Words are inadequate to express thanks and appreciation to my wife Srijani for all her love and support when I was irritable and depressed. Last but not the least, the undying love and sacrifice of my parents, Mr. Debashish Bhattacharya & Mrs. Damayanti Bhattacharya, can never be completely expressed with words alone. They have given up so much for me. I just hope this makes them proud. Their blessings have helped me in reaching this goal.

Dwaipayan Bhattacharya

Abstract:

Folate helps in DNA synthesis, methylation and repair besides a host of other physiological processes like RBC formation, neural tube formation during pregnancy and homocysteine breakdown. Apart from their natural ligand Folate, Folate receptors (FR) are known to bind reduced folic acid derivatives and facilitate their uptake and intracellular delivery**.** Before that, the cargo is converted from polyglutamate to monoglutamate for easy traversion across the lipid bilayer. In the context of receptor oriented targeted delivery, FR expressed on the cell surface can selectively transport folate-conjugated payloads. This was however discovered long after the advent of drugs like pemetrexed and methotrexate which target intracellular folate metabolism. Till date, the FR has emerged as a feasible target for targeted imaging and therapy given that a variety of cancers overexpress it. Biopsies of oral squamous cancer have also been found to express FR, more specifically the alpha isoform. However, TAMs (Tumour Associated Macrophages) in the surrounding stroma express FRβ and may thus be subjected to FR targeted nano delivery. Based on this principle, we fashioned carbon nanospheres (CSPs) from glucose and coupled them with our folate-based lipid FA8. These CSPs have active surfaces that are highly amenable to functionalization besides other physicochemical attributes conducive to the development of a targeted system with high payload capacity. Our drug is an Anthracycline which induces chemoresistance in most cancers including OSCC (Oral Squamous Cell Carcinoma). Apropos to this, receptor targeted delivery of drug has been shown to be more therapeutically favourable as opposed to convection or diffusion mediated chemotherapy. OSCC also hosts other challenges like possession of a mutated tp53 and an

immunologically cold TME (Tumour Microenvironment) that promotes aggressive tumour progression and MDR. In our case, FR targeted therapy induced apoptotic cell death selectively in malignant cells instead of necroptotic death that is characteristic of Doxorubicin. Following the assessment of drug uptake in vitro, in vivo investigation with an immunocompetent tumour model revealed selective drug localization in TAMs isolated from solid tumours. Mice administered with targeted CSPs indicated attenuated iNOS levels in tumour tissue besides observable downregulation of Vimentin as well as higher cleaved Caspase3 levels. All this combined with the downregulation of M2 TAM-specific marker expression indicated the possible convergence of multiple pathways resulting effectively in overall tumour size regression. Further studies on an ex-vivo platform of 3-dimensional OSCC spheroids established their potential as a suitable model for evaluating FR-targeted nanotherapeutics in the future.

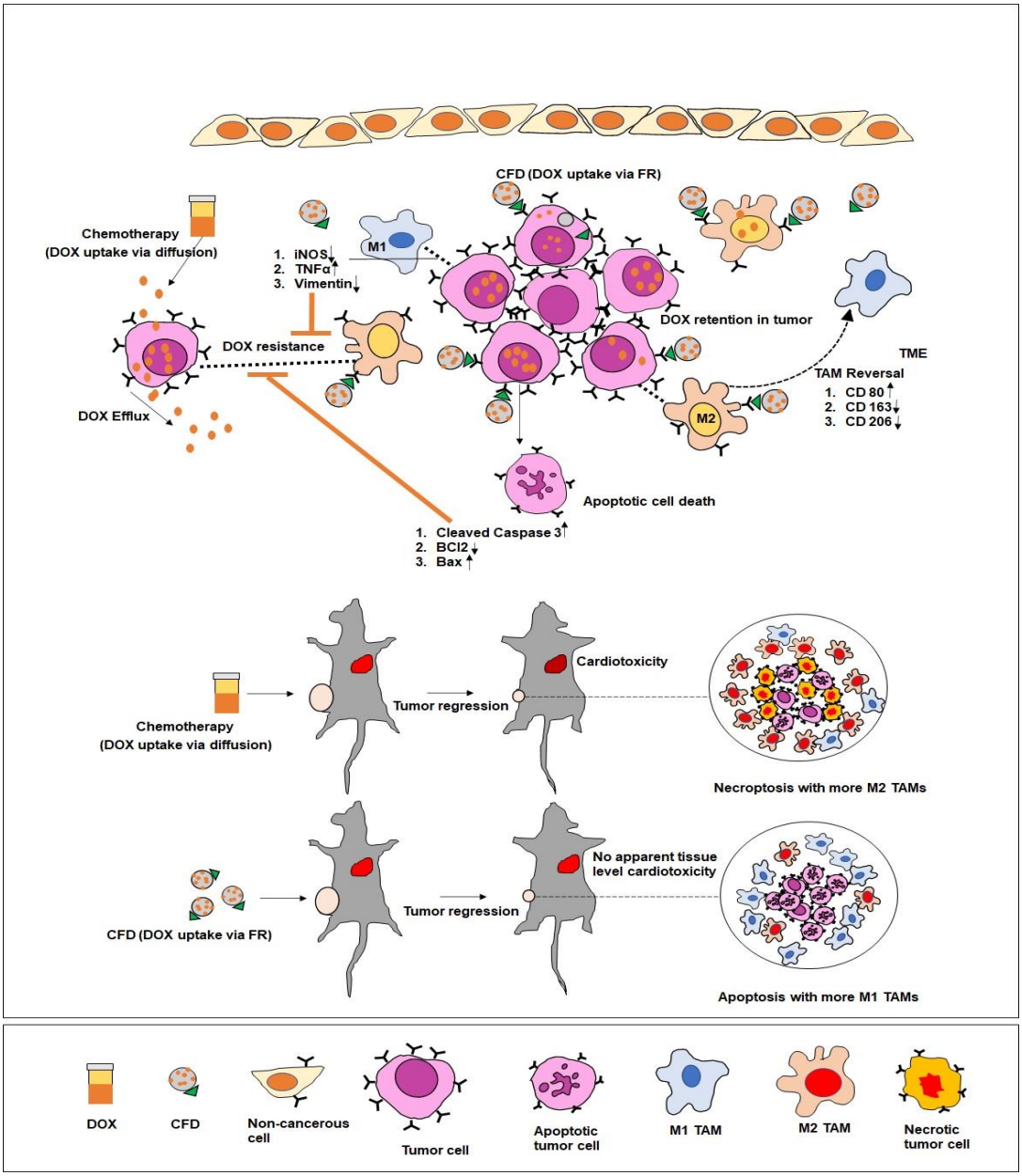

Scheme 1: A pictorial overview of the current work and its findings.

Table of Contents

List of Tables:

List of Figures:

List of Abbreviations:

- 5-FU- 5-Fluoro Uracil
- CAF- cancer Associated Fibroblasts
- CD- CSP-Doxorubicin
- CFD- CSP-FA8-Doxorubicin
- CSP- Carbon nanosphere
- DAPI- 4',6-diamidino-2-phenylindole
- DMEM- Dulbecco's Modified Eagle Medium
- DMSO- Dimethyl Sulfoxide
- DOX- Doxorubicin
- ECM- Extracellular Matrix
- EDTA- Ethylene Diamine Tetra acetic Acid
- EGF- Epidermal Growth Factor
- EGFR- Epidermal Growth Factor Receptor
- EMT- Epithelial to Mesenchymal transition
- FACS- Fluorescence Activated Cell sorter
- FITC- Fluorescein isothiocyanate
- FR- Folate Receptor
- GOF- Gain of Function
- GSH-Glutathione
- GTP- Guanosine triphosphate
- H&E- Haematoxylin & Eosin
- HCl- hydrochloric acid
- HDP- Host defence Peptide
- HNSCC- Head & Neck Squamous Cell Carcinoma
- HPV- Human Papillomavirus

- IDR- Innate Defence Regulator
- IMDM- Iscoves Modified Dulbecco Medium
- iNOS- Inducible Nitric Oxide Synthase
- JAK- Janus kinase
- MACS- Magnet Associated Cell Sorting
- MDR- Multi Drug Resistant
- MHC- Major Histocompatibility Complex
- miR- Micro RNA
- MOC- Mouse Oral Cancer
- MTT- 3-(4,5-dimethylthiazol-2-yl)-2,5-diphenyltetrazolium bromide
- Mutp53- Mutated p53
- NF-κB- Nuclear factor kappa-light-chain-enhancer of activated B cells
- NGS- Next Generation Sequencing
- NMR- Nuclear Magnetic Resonance
- NO- Nitric Oxide
- NOS- Nitric Oxide Synthase
- OLK- Oral Leukoplakia
- OSCC- Oral Squamous Cell Carcinoma
- PBS- Phosphate Buffer Saline
- PLGA- Poly (lactic-co-glycolic acid)
- PTX- Paclitaxel
- REDOX- Reduction-Oxidation
- RIPA- Radioimmunoprecipitation assay buffer
- ROS- reactive Oxygen Species
- RPMI- Roswell Park Memorial Institute
- SEM- scanning electron Microscope
- siRNA- RNA silencing
- SLN- Solid Lipid Nanoparticle
- TAM- Tumour associated Macrophage

- TGF- Transforming Growth Factor
- TME- Tumour Microenvironment
- TNF- Tumour Necrosis Factor
- tp53- Tumour suppressor p53
- VEGF- Vascular Endothelial Growth Factor
- WHO- World Health Organization

As per a projection by the World Health Organization (WHO), approximately 9.6 million deaths and 18.1 million new incidences of oral cancer were reported in 2018 alone. Globally, 1 in 5 men and 1 in 6 women are affected by cancer throughout their lifetime and when it comes to India, the number of cancer cases reported in 2018 alone is nearly 1.1 million, with the number of deceased patients reaching almost 784,821.

Rapidly dividing cells take up Folate to meet their increasing demands of DNA synthesis and proliferation. The Folate receptor (FR) is highly overexpressed in the epithelia of multiple cancers and plays an important role in regulating the expression of genes and transcription factors involved in cell proliferation, migration and invasion (**Cheung et al.,2016**). Anomalous situations like cancer (including OSCC) have been linked to a general deficiency of Folate, which can thus be countered by increasing the dietary intake of Folate as proven by certain reports (**Ulrich et al.,2007; Pelucchi et al.,2003**). Not surprisingly, studies on patients as well as epidemiological studies have proven higher risk of oral cancer in people who have low dietary intake of Folate and have chronic exposure to tobacco as well as alcohol.

The complex nature of cancer makes it difficult for a single strategy to effectively treat cancer. Both chemotherapy and radiation are potentially genotoxic and hence targeted delivery is being increasingly preferred. Another challenging aspect of cancer is the immunosuppressive nature of the TME. Of all the different stromal elements TAMs have always played a prominent role in tumour growth and aggressiveness (**Biswas et al.,2013; Joyce et al.,2009; Pollard et al.,2004**). Pro-tumoural M2 TAMs promote angiogenesis, metastasis and tumour spread right from the initial stages of the disease.

The Folate Receptor is a known prognostic as well as diagnostic marker for a number of different cancers. High levels of FR expression has been reported in squamous cell lesions of higher-grade cervical cancer, indicating the promise which FR-mediated anticancer therapy holds (**Pillai et al.,2003; Gupta et al.,2018**). Apart from targeted therapy, there have also been reports of the application of FR-mediated screening in the early detection and diagnosis of cancer. Predina et al.. explored ways to utilize the expression of FR on pulmonary squamous cell carcinomas for receptor-targeted intraoperative molecular imaging (**Predina et al.,2018**). Other reports hinting at the over-expression of FR in squamous cell carcinomas and its therapeutic potential also include studies on ovarian cancer patient samples (**Toffoli et al.,1997**). However, not much is clinically indicated regarding OSCC (oral squamous cell carcinoma). Hence, our study aims at finding out how effectively FR might serve as a means to target OSCC. The rationale behind this study is that cancer cells unlike normal cells require far greater quantities of nutrients like Folate, a molecule that is essential for DNA synthesis, among various other functions (**Wani et al.,2008**). The Folate Receptor often exhibits aberrant expression levels, with differential expression of its isoforms (α & β) in different organs/tissues of the body, which is principally a function of varying amounts of extracellular folate in or around different tissue types (**Akhter et al.,2011**). However, the expression of α & β FR isoforms has been found to be very low or negligible in normal tissues and cells as opposed to their overexpression on tumour tissues and cancer cells.

We fabricated glucose derived carbon nanospheres (CSPs) which are highly biocompatible and can access multiple organs in the body including the brain when conjugated to our Folate based cationic lipid FA8 **(Elechalawar & Bhattacharya et al.,2019)**. The drug conjugated to our delivery system is Doxorubicin (DOX) or Adriamycin, a popular

topoisomerase inhibitor and a widely reported anti-cancer drug. The primary objectives of the current study were as follows:

- Formulation and characterization of a delivery system using FA8 cationic lipid conjugated with carbon nanospheres (CSP) for targeting oral cancer cells expressing folate receptor.
- Testing the efficacy of the formulations for selective cancer cell killing and orthotopic tumour regression.
- Mechanistic investigation of the effect of formulation on tumour micro-environment (TME) including tumour-associated macrophages (TAM) and deciphering the role of TME and TAMs on oral cancer aggressiveness.

To summarize, a FR-targeted system which was first verified by us against advanced glioma was tested subsequently against an immunocompetent murine model of OSCC. We first assessed our targeted system for uptake and targeted cancer cytotoxicity in vitro using both human and mouse OSCC cell lines. Once commendable tumour regression was achieved thereafter in animal studies, we tested for and detected signs of possible M2 TAM attenuation. We also tested our formulation on 3D spheroids in a bid to establish its efficacy as a superior model for experimentation as compared to 2D culture systems. Few molecular markers reportedly linked to chemoresistance and overall tumour progression but not previously reported in the MOC2 in-vivo model were also investigated. Our findings from the current study are encouraging since we have tangible evidence of the potential that FR holds as a suitable mediator for targeted nano-therapy in OSCC.

Oral cancer is a multifaceted disease with more than one aspect that needs to be addressed. Since we intend to design and optimize a targeted delivery system that achieves localized drug delivery, we must first understand the nature of our target disease, its pathology and what makes it so challenging to cure. The current work specifically aims to approach the problem from two primary ends- cancer cells and their surrounding stromal elements. In this section we shall proceed to discuss the hallmarks of aggressive OSCC, the chemotherapeutic approaches conventionally used to address it, how Doxorubicin holds its own set of challenges and finally, how we may target the Folate receptor efficiently to address all these issues and achieve an overall improved therapeutic outcome.

2.1. Oral squamous Cell Carcinoma and its pathology

OSCC is still one of the most challenging malignancies as faced by our country as well as the rest of the world. This may be attributed to existing treatment loopholes like difficulty of diagnosis as well as lack of general awareness among regular users of tobacco and related products (**Soares et al.,2018**).

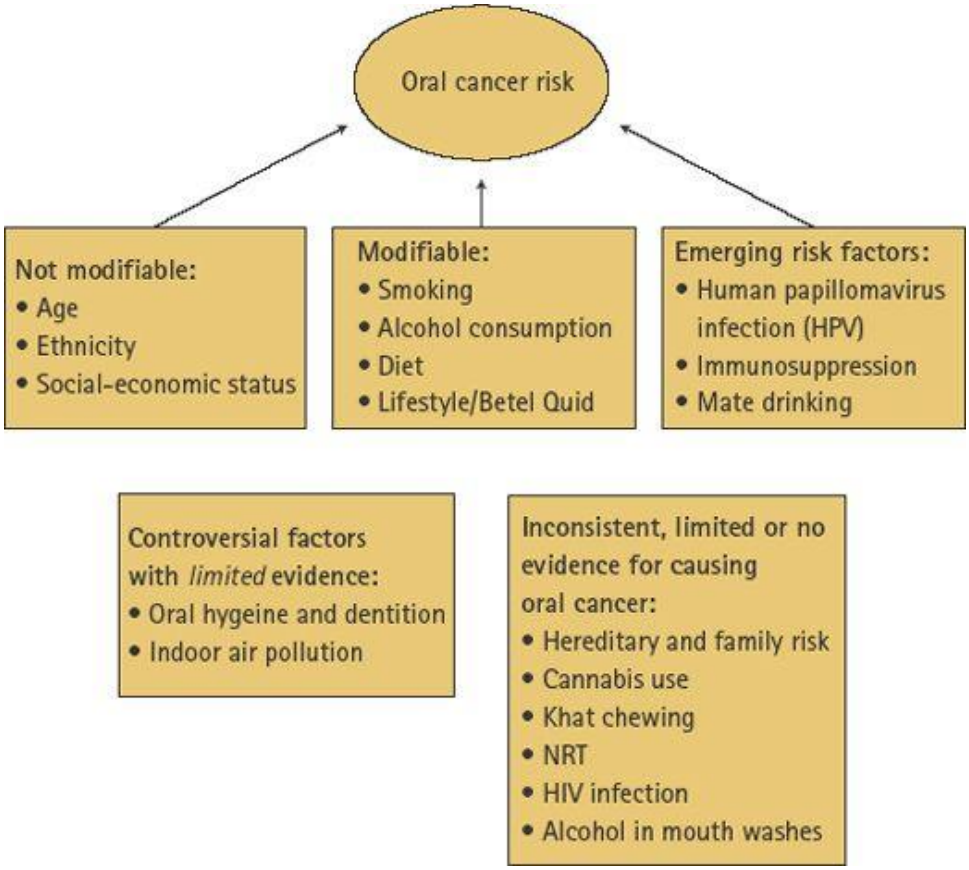

Fig 2.1. Common risk factors reported for oral cancer: Oral cancer may arise due to a variety of reasons which may be modifiable or non-modifiable. While emerging factors like immunosuppression and HPV infection are under intense investigation, factors such as use of cannabis or familial (hereditary) history are on the rise steadily. (**Warnakulasuriya et al. ,2010**)

One of the genes quite commonly found mutated in OSCC is TP53. The TP53 is popularly deemed as the guardian of the genome, owing to its indispensability in orchestrating apoptosis in a timely and context dependent manner (**George et al.,2011**). Besides, this gene has been shown to work in concert with several other tumour suppressors as well as downstream activators like PumA, MDM2, p21 etc. in deciding the fate of a cell which is passing through the divisional cycle (**Sherr et al.,2002**). Quite understandably, the functional absence of p53 protein might render a cell anomalous or abnormal, as in cancer. Scientific literature is rich in accounts documenting a range of different mutations in TP53 in various cancers as well as their repercussions (**Muller et al.,2013**). Mutations may broadly be classified as missense or nonsense. While the latter involves complete absence of p53 expression, the former usually entails the production of a non-functional protein (one that overexpresses but has no function) or one that confers multiple features advantageous to the survival and proliferation of the tumour (gain-of-function mutations). Gain of function mutations (GOFs) are well-reported in HNSCC as well as aggressive OSCC where they bestow distinct pro-tumoural features upon cancer cells, making them more evasive and chemoresistant (**Oren et al.,2010**).

Besides TP53 there are a host of other molecular players reported as being involved in OSCC drug resistance as well as aggressive proliferation. However, we shall discuss a bit about a few of them which we found to be linked to each other in concert, regulating cumulatively the malignant spread of OSCC in conjunction with the tumour stroma and its elements which we shall also discuss separately in a later portion of this brief literature review.

The role of nitric oxide and the enzyme responsible for its production, Nitric Oxide Synthase (NOS), in cancer biology is not yet clear. NO is a small gaseous molecule produced by three

different isoforms of NOS and is also involved in facilitation of immune and anti-pathogenic responses besides being vasoactive (**Vannini et al.,2015**). Over the years researchers have discovered that NO has a dual role in cancer. For the sake of discussion within the context of the current work, we note that NO has been proven to have anti-inflammatory effects on the TME, working as an immunosuppressant and a pro-oncogenic molecule (**Bader et al.,2020**). Reports also show that NO suppresses tumour suppressor genes while parallelly causing oncogene activation (**Grimm et al.,2013**). NO may act through either cGMP-dependent or cGMP- independent pathways, nitrosylating a host of important genes involved in pathways associated with cell death and tumour invasiveness (**Babykutty et al.,2012**). However, most of these actions are concentration dependent, including NO-induced effects on the tumour microenvironment. Of the three isoforms of NOS, iNOS is the one which produces the maximum amount of NO and that too in a calcium-independent manner (**Mattila et al.,2014**). This is the same NOS isoform that is intricately involved with tumour associated processes like metastasis, angiogenesis and malignant transformation. The popular notion regarding NO and its role in cancer is that during the stages of tumour growth, it is the tumour cells which use NO for tumourigenic progression whereas the stroma carries out the opposite function. NO is connected functionally to TP53 and NFkB, encouraging pro-tumourigenic functions like progression and metastasis in a variety of cancers (**Matsumoto et al.,2001**). Even though levels of iNOS and their effects may vary from one cancer type to another, it is maintained that high iNOS levels often leads to an unfavourable prognosis in case of oral squamous cell carcinomas (**Silva-Servato et al.,2019**). iNOS also has been recorded to have positive correlation with the accumulation of TP53 mutations.

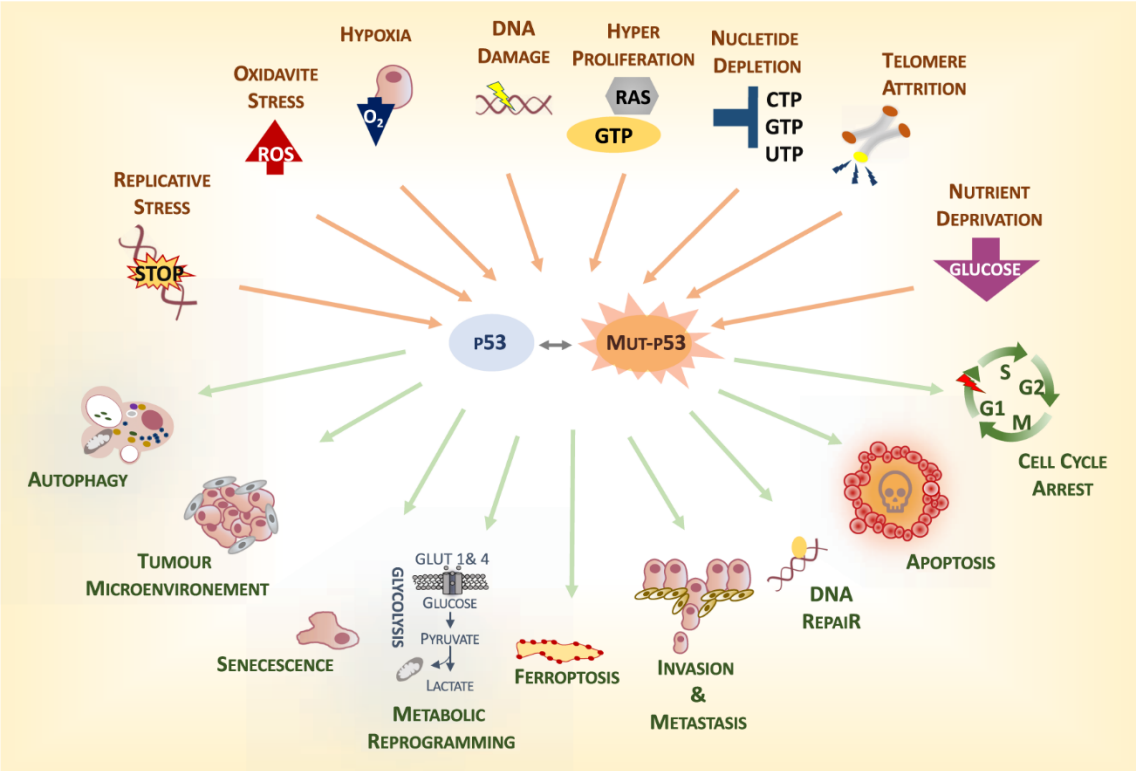

Fig 2.2. TP53 and its many roles: The above figure represents the complex interplay between functional and mutated p53 protein which often becomes the crux of most cancers and their aggressive expansion. The figure includes several factors which are kept under control by TP53 and may be destabilized by either the lack of functional p53 protein or an excess of its mutated counterpart, thus giving rise to diseased state. (**Amelio & Melino,2020**).

2.2. The role of TME resident pro-tumoural TAMs in OSCC etiology

Another aspect worth considering is the tumour microenvironment and its M2 tumour associated macrophages which aid in the maintenance of an anti-inflammatory or immunosuppressive state. OSCC has been reported to have an immunologically cold TME that is irresponsive to conventional immunotherapy (**Shi et al., 2022**). Oral squamous cancers typically possess highly pro-tumoural profiles in terms of cytokine and chemokine content (**Alves et al., 2021**). In addition to this, TAMs and dendritic cells in the OSCC TME often create conditions unsuitable for the infiltration of functional T-cytotoxic cells.

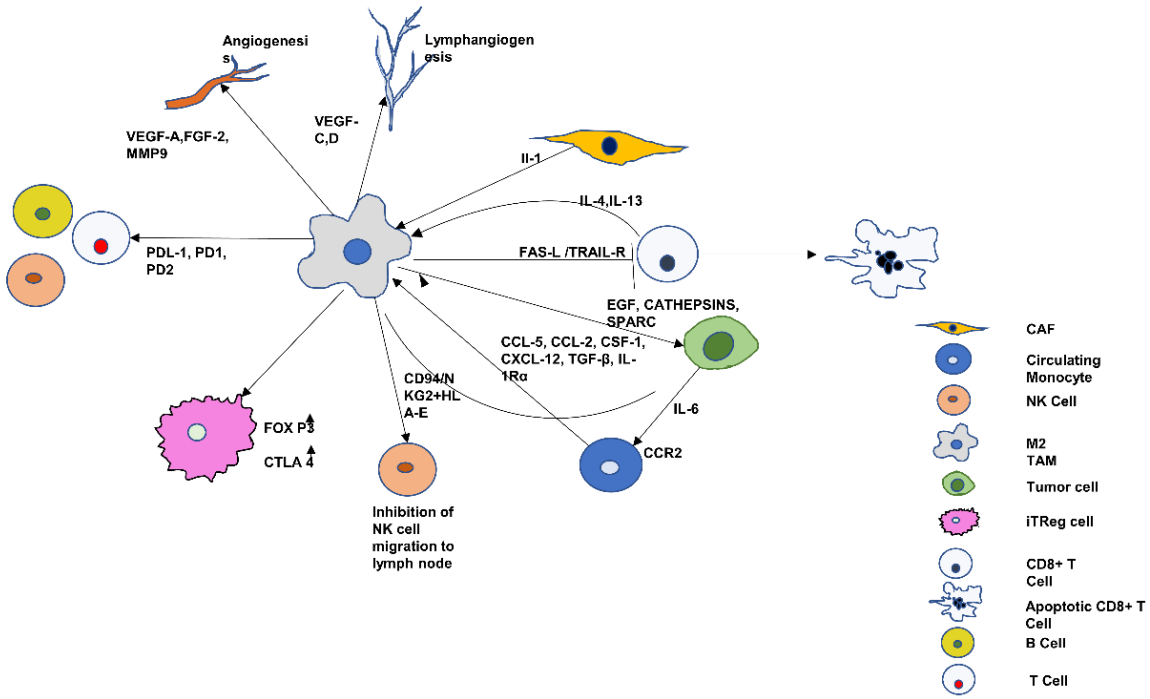

Fig 2.3. Interactions between M2 TAMs and other stromal elements in the TME: the above figure gives us an idea of the complex network of activities existing within the TME between TAMs and other stromal elements. These interactions help shape the immunological profile of a disease like cancer, essentially disabling pro-inflammatory markers while inducing a perpetual state of immunosuppression. (**Bhattacharya et al.,2021**).

Tumour associated macrophages or TAMs are well reported in multiple cancers and also in the context of oral squamous cell carcinoma. As discussed previously they may be pro-tumoural (M2) or anti-tumoural(M1) in nature, their activity defined by the set of cytokines they produce. (**Hagemann et al.,2008**). Some of the characteristic markers used to identify these cells are CD68 and CD163 where CD163 is specific to the M2 macrophages [19]. Other markers commonly reported for identification/characterization of pro-tumoural TAMs in the tumour microenvironment is CD206 (**Hu et al.,2017**). Similarly, an erstwhile characteristic marker reported for anti-tumoural M1 type TAMs is CD80 (**Moradi-Chaleshtori et al.,2021**). Both CD80 and CD206 are crucial markers with regards to anti-tumour immune responses mounted by the body. This is the reason both these markers have been experimented with extensively over the years leading investigators to conclude that they are valuable prognostic markers besides being promising targets for immunotherapeutic approaches. CD80 is a glycoprotein molecule that is present transiently on the surfaces of B cells, Dendritic cells as well as macrophages (**Yellin et al.,1994**). However, it has been reported to be present in low levels in pro-tumoural TAMs which are liable to evade anti-tumour immune responses launched by T cytotoxic cells. In fact, tumour cells with low or no CD80 expression have been shown to induce apoptosis in tumour infiltrating T cells, often rendering immunotherapeutic approaches redundant (**Mir, 2015**). Induction of higher CD80 levels either by transfection or other methods has thus started to prove itself a valid therapeutic approach in recent times (**Zhang et al.,2022**). In fact, it is proven that without the stable expression of CD80, it is difficult to carry out T-cell activation or even mount an anti-tumour immune response. Quite contrary to CD80, the CD206 marker has been found to be a prominent M2 marker, facilitating pro-tumoural conditions and the maintenance of a cold tumour microenvironment. Fan et al. reported

the prognostic significance of CD206 in liver cancer, experimentally showing that not only did high CD206 expression correlate with lower survival rates but it also indicated significantly higher chances of metastatic progression (**Fan et al., 2019**). Utilizing a short hairpin approach, they silenced CD206 in liver CSCs (cancer stem cells) which negatively impacted their invasiveness as well as migratory capabilities. Similar findings were reported by Haque et al. who studied the role of CD206 positive TAMs in OSCC progression using clinical samples. The authors reported that CD206 positive TAMs were the primary perpetrators of metastasis and invasiveness as compared to TAMs expressing other M2 markers like CD204 or CD163 (**Haque et al., 2019**). The authors went on to further point out that CD206 positive TAMs comprised of a particular TAM subset producing EGF in large quantities and also that conditioned media collected from such cultures reprogrammed other TAM subsets to become more proliferative and invasive in nature. Another notable therapeutic approach which investigators are studying these days is the use of HDPs (Host Defense Peptides), also termed IDRs (Innate Defense Regulators) for immunomodulatory purposes. One particular study used a certain IDR, which is essentially a synthetic peptide analog, to target CD206 positive TAMs and induce M2 to M1 reprogramming via the activation of the mannose receptor protein (CD206) (**Jaynes et al., 2020**). Needless to say, such indirect therapeutic approaches capable of modulating CD206 expression might open up new vistas for cancer immunotherapy in the near future.

M1 TAMs may subsequently undergo transformation to M2-type phages in the presence of factors like IL-6, CCL-2, PD-1/PD-L1 and CSF-1. CD47 and some other markers like PGE2, CC2R, and PD-1 are being investigated as possible targets for therapy, especially in approaches involving the prevention of M1-type to M2-type phage conversion (**Jiang et**

al.,2021). Wei et al. showed that in OSCC there is a continuous molecular crosstalk and exchange between tumour cells and TAMs where genesis of pro-tumourigenic M2-TAMs is often accompanied by a downregulation in E-Cadherin levels and a concomitant upregulation in the expression of Vimentin (**Wei et al.,2019**). Loss of E-Cadherin has earlier been reported to be characteristic of a more malignant phenotype, coupled with the upregulation of target genes whose transactivation often leads to metastasis (**Onder et al.,2008**). EMT is a cascade of sequential steps that bring about morphological and biochemical changes which gradually transform an epithelial cell to one with an increased mesenchymal phenotype. Zhou et al. reported low levels of E-Cadherin coupled with high Vimentin levels in metastatic OSCC, going on to stress that their levels are of prognostic value when dealing with advanced stage OSCC (**Zhou et al.,2015**). Concurrent findings were reported by Liu et al. where microarray studies revealed highest levels of upregulation in Vimentin expression in metastatic OSCC lines. They subsequently showed how siRNA mediated knock-down of Vimentin gave rise to a non-metastatic phenotype with reduced invasiveness (**Liu et al.,2016**).

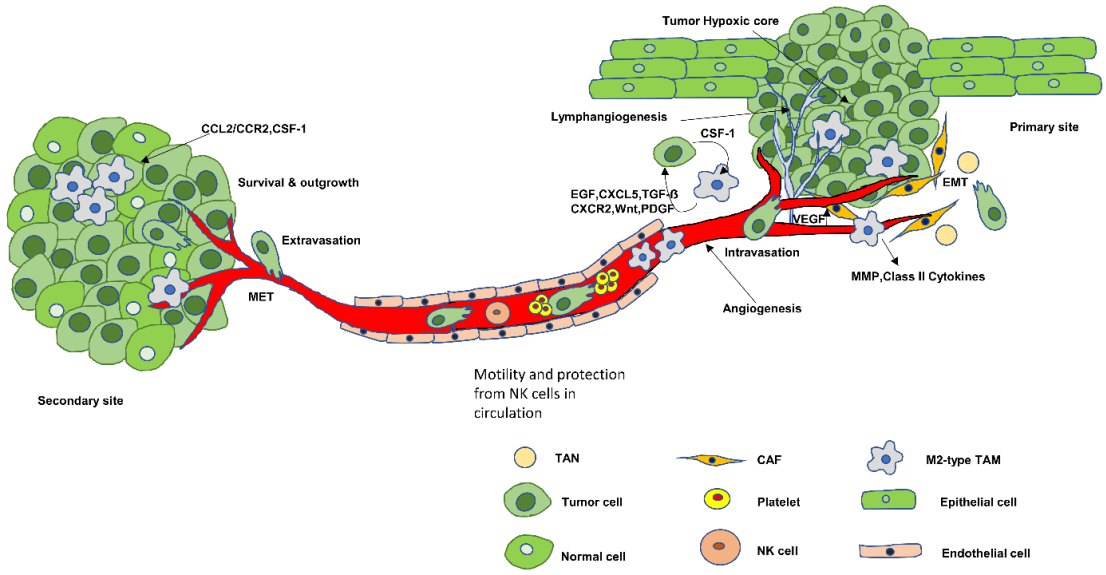

Fig 2.4. Tumour cells and TAMs coordinate to control EMT: The above figure is representative of a chain of events responsible for the orchestration of EMT and the subsequent development of a secondary site due to metastatic spread of tumor cells from the primary site and their subsequent colonization at distant locations. The role of TAMs in this process has been highlighted along-with other members of the TME like CAFs. (**Bhattacharya et al.,2021**).

TAMs express TGF-β, which influences tumour-associated epithelial cells to proliferate via many pathways including the STAT-3 pathway. A decrease in TGF-β followed by the STAT-3 level in the tumour lysate advocates the possibility that both TAMs and tumour cells are adversely affected by CFD. TGF-β is known to induce EMT, which leads to metastasis. A decrease in TGF-β evidently induces EMT reversal and reduces metastasis. It has been found through an immunohistochemical study that the extent of TAM polarization relates to tumour histopathology. For example, cases of lymphogenic metastasis exhibit a significantly higher population of resident TAMs expressing the markers CD63, CD168, MRC1, and CD11c, etc. coupled with more TAM polarization as well as infiltration (**Ramadan et al.,2020**). Lucio et al. performed a similar immunohistochemical study to quantify pro-tumoural TAMs in OSCC of the lower lip of 42 patients where they showed that while there was no apparent correlation between the number of M2 TAMs and M1 TAMs or the number of M2 TAMs and tumour size (**Lucio et al.,2016**). Petruzzi et al.,2017 reviewed the intricate role of cytokines like Il-4,6,8 and 10 and Axl, a receptor tyrosine kinase that controls M2 polarization as well as tumour progression in OSCC (**Petruzzi et al.,2017**). Their study revealed TGF-β to play a major part in mediating TAM polarization and tumour progression. The immunohistochemical study by Sun et al. reported the absence of CD68 positive macrophages in normal non-OSCC tissue besides a significantly higher VEGF expression in OSCC TAMs as compared to macrophages from healthy lymph nodes, a property that was attenuated upon inhibition of TGF- β, T- β RIII or Smad3 signalling (**Sun et al.,2018**). Lymph node metastasis has been shown to depend upon the relative density of CD163 positive TAMs, with higher amounts of VEGF, Il-10, and CCL22 being produced by RAW cells subjected to media from OSCC in vitro cultures (**Yamagata et al.,2017**). Haque et al.,2019 conducted an immunohistochemical study of patient-derived

OSCC samples to elucidate the relationship between densities of CD-163/204/68 positive TAM subsets and tumour progression in terms of cell proliferation, and they reported that the TAMs were probably using EGF to mediate these pro-tumoural effects (**Haque et al.,2019**). A positive correlation between M2 TAM density and nodal positivity as well as lymphatic and vascular invasion has been reported by multiple research groups (**Kumar et al.,2019; Mukherjee et al.,2019**). The number of CD4+ T cells and CD163+ TAMs in OSCC as well as OLK (oral leukoplakia) has been proven (**Stasikowska-Kanicka et al.,2018**). Kouketsu et al.,2019 studied the expression of Treg cell markers CD25 and FoxP3 as well as TAM markers CD163, CD204, etc. (markers for M2-TAMs) to show their association in controlling tumour invasiveness and nodal metastasis (**Kouketsu et al.,2019**). miRNAs too play a significant role in OSCC progression. Exosome enclosed miR-29a-3p was reported to mediate the M2 polarization of TAMs by upregulating p-STAT6 (**Cai et al.,2019**). The authors also reported miR-29a-3p mediated SOCS-1(cytokine transduction inhibitory factor-1) downregulation in aggressive OSCC. Interestingly, TAMs have also been shown to undergo M2 polarization when treated with areca nut extract, a common source of Nicotine (**Chang et al.,2019**). Reports indicate the possible role of CD169+ macrophages in the suppression of metastasis and tumour growth, without further details of the possible mechanism of action involved. However, Topf et al. did a study where they reported significantly lower density of CD169+ subcapsular macrophages in the subcapsular sinuses of metastatic OSCC samples (**Topf et al.,2019**). Among other popular pathways, the CCL12/CXCR4 axis maintains stemness via the recruitment and polarization of pro-tumoural TAMs. This ligand-receptor pair has been implicated in M2 polarization, chemotaxis of metastatic cells, enhanced proliferation of OSCC cells, and expression of stem cell markers like Oct-4, Sox-2, etc. (**Li et al.,2019**). Matsuoka et al. demonstrated in

their work that the overall survival rate of OSCC patients expressing a higher number of CD163 positive M2 TAMs was less when compared to patients expressing a lower number of such TAMs. For the same reason, the patients having a higher number of CD163 positive TAMs have been found to show increased resistance to 5-FU based chemotherapy (**Matsuoka et al.,2016**).

2.3. Involvement of TP53, NO and TNFα in TME modulation

The p53 protein and its mutant variants have a prominent role in the context of TAM maturation and cancer progression. Cancer cells possessing mutant p53 protein can reprogram TAMs to be tumour supportive. For example, one study showed that colon cancer cells with GOF muTP53 shed exosomes rich in miR-1246 and their subsequent uptake by neighbouring macrophages triggered a miR-1246-dependent TAM reprogramming process (**Cooks et al.,2018**). MuTP53-reprogammed TAMs favour anti-inflammatory immunosuppression with increased TGF-β activity. These findings, associated with poor survival in colon cancer patients, strongly support a microenvironmental role for GOF muTP53 in actively engaging the immune system and promoting cancer progression and metastasis (**Asl et al.,2023**). The NF-κB molecule too is important in shaping macrophage-initiated inflammatory responses. The exact role of TP53 in macrophage response to environmental challenges including chemotherapy is yet to be fully understood. Lowe et al. reported that NF-κB and TP53, which generally have opposing effects on cancer cells, co-regulate induction of pro-inflammatory genes in primary human monocytes and macrophages (**Lowe et al.,2014**). Using Nutlin-3 as a tool, they demonstrated that TP53 and NF-κB collectively induce IL-6 activity while transcriptome analysis showed global TP53/NF-κB mediated co-regulation of immune response genes

including several chemokines, effectively inducing human neutrophil migration. Additionally, it was found that TP53, activated by tumour cell paracrine factors, induces high basal levels of macrophage IL-6 in a TAM model system (Tumour-conditioned Macrophages [TCMs]). Compared to normal macrophages, TCMs exhibited higher p53 levels, enhanced p53 binding to the IL-6 promoter and reduced IL-6 levels upon p53 inhibition.

When it comes to the stromal effects of iNOS/NO in the tumour microenvironment, the activity is cancer stage dependent. In the early phases of tumour progression, stromal iNOS/NO usually has an anti-cancer role whereas with time and as the tumour progresses, there is more induction of pro-tumoural M2 TAMs and a concomitant reversal in the role of stromal iNOS/NO as well (**Vannini et al., 2015**). Interestingly, there are reports which deal specifically with the interaction between NO and Doxorubicin. In 1996, Sakai et al. showed how the anticancer drug epi-Doxorubicin attenuated levels of inducible NOS and NO levels both in vitro and in vivo (**Sakai et al.,1996**). The authors explained further how this finding might prove useful later specially considering the role of NO and iNOS in cancer. Later, Jung et al. showed that Doxorubicin treatment could reduce the expression levels of iNOS in colon cancer cells (**Jung et al., 2002**). Yet another report by Oktem et al. showed how Doxorubicin reduced iNOS expression levels in breast cancer cells, laying down the foundation for more work expecting to reduce iNOS levels as a result of DOX treatment (**Oktem et al., 2004**). NO produced by iNOS is also heavily regulated by the tumour stroma as earlier discussed. This phenomenon is primarily due to the reprogramming of M1 TAMs to M2 phenotype as observed by some authors (**Nath et al., 2020**). On many occasions this pro-tumoural influence of the stromal elements even goes as far as to induce chemoresistance to popular therapeutics (**Perrotta et al., 2018**). Quite interestingly, some

functions of iNOS have also been reported as being linked to the TP53 status in cases of oral squamous cell carcinoma, where levels of iNOS correlate inversely with the prognosis of the disease (**Yang et al., 2015**).

2.4. Other molecules in OSCC- future possibilities for therapy

Several significant targets have been discovered so far which can potentially be employed for developing novel therapeutics against OSCC. CXCL12 derived from Cancer-Associated Fibroblasts (CAF) was found to increase M2 macrophage infiltration in the tumour microenvironment following the promotion of Cancer Stem Cells (CSCs) expressing mostly Yamanaka factors. Thus, obstructing CXCR4 (CXCL12 receptor) can be beneficial wherein it prevents tumour progression and metastasis (**Zhou et al.,2019**). Dan et al., also published an article presenting their finding that the expression levels of Receptor for Activated C Kinase 1 (RACK1) on OSCC cells was associated with the extent of M2 macrophage infiltration, inhibition of THP1 migration, and M2 macrophage polarization, thus correlating negatively with OSCC prognosis and proving itself a potential therapeutic target (**Dan et al.,2020**). The other type of OSCC caused due to HPV infection is found to be resistant toward standard therapies with higher chances of recurrence within 3 years of treatment completion. Studies to explore novel and targeted treatment options against such cases is thus imperative.

2.5. Drug resistance and its challenges in conventional chemotherapy

Conventional chemotherapy is often a dead end in cancer therapy, paving the way for targeted delivery (**Bae et al.,2011**). There are several factors which may render a cancerous

growth drug resistant. One of these would be the acquisition of multiple mutations that subsequently aggregate and the tumour to evade conventional chemotherapy as well as immunotherapy (**Loeb et al.,1996**). Chemotherapeutic drugs make up one of the largest arsenals we currently possess against cancer. There are several drugs which have time and again been tested for therapeutic potential against OSCC. However, each of them has its own individual merits and demerits and it is up to the clinicians to choose any one based on factors like the extent of tumour spread or the genetic landscape of the individual being treated (**Brannon-Peppas et al.,2004**). Another way we could approach this situation would be to try and repurpose existing drug molecules (**Gonzales-Fierro,2021**). Numerous groups are working on developing combination therapies which are a coalition of distinctly different approaches and have proven successful on multiple occasions so far (**Webster,2016**).

Our study particularly concerns the well-known anthracycline Doxorubicin. The mechanism of action as well as the side effects and probable targets of this molecule have been extensively documented over the years (**Carvalho et al.,2009**). Several cancers including OSCC have developed resistance towards this molecule, making it crucial for us to understand some of the underlying reasons behind it (**Du et al.,2017**). Besides expelling the drug using microvesicles, exosomal vesicles and other similar microbodies, cancer cells utilize certain gene mutations to their advantage (**Bukowski et al.,2020**). Additionally, the increasing involvement of the tumour microenvironment and its constituent elements in rendering a cancerous entity untreatable demands our immediate attention (**Suh et al.,2014**). There are several publications which bear witness to the fact that these challenges don't exist as singular threats anymore but instead pose a collective burden that needs to be addressed by novel and multi-faceted therapeutic approaches.

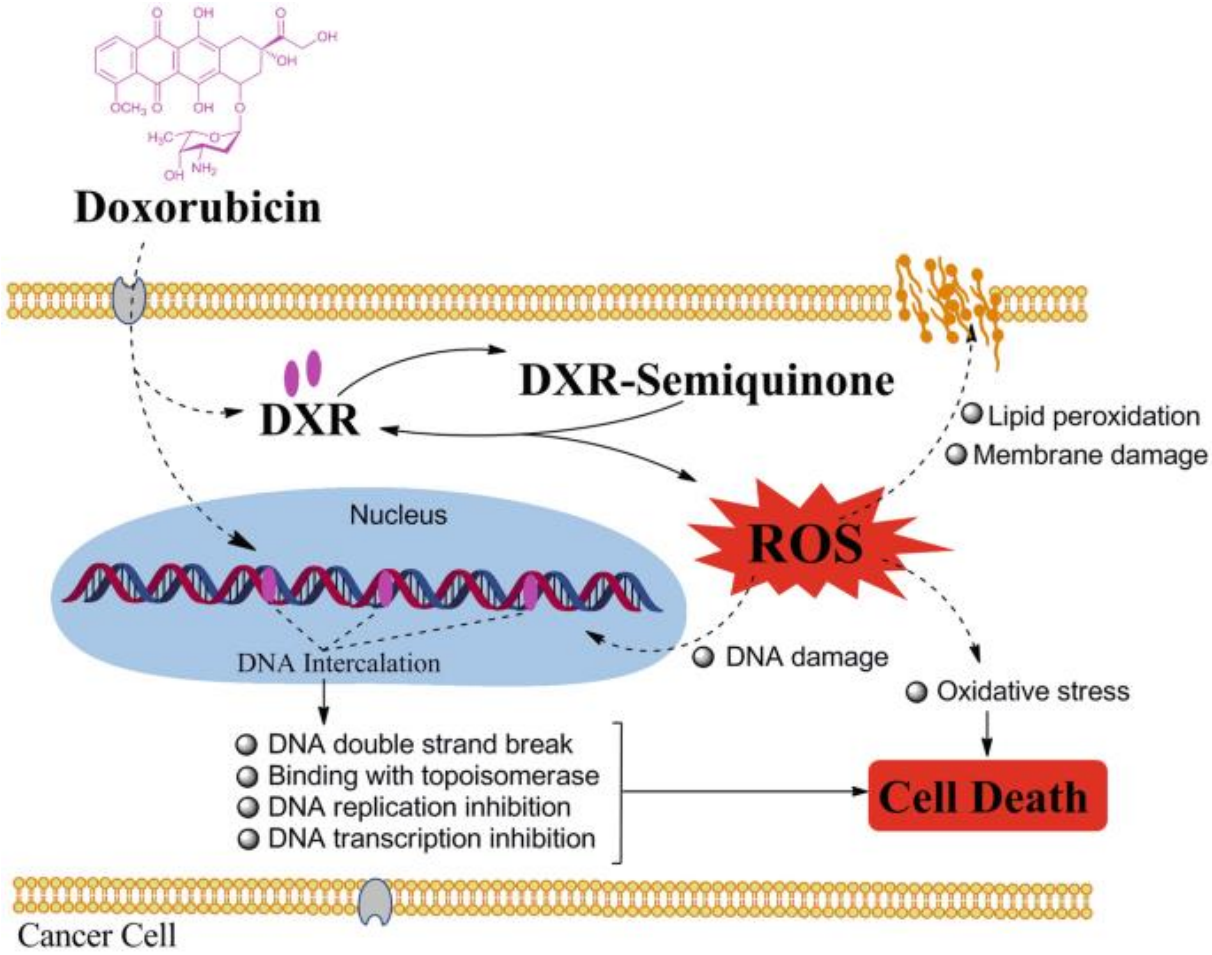

Fig 2.5. Mechanism of action of Doxorubicin: Doxorubicin or DOX attacks highly proliferative cells like cancer cells primarily by inducing DNA breaks besides inhibiting DNA replication as well as transcription. The above figure outlines the primary effects of DOX on target cells, highlighting its expected role in therapy. (**Shrestha et al.,2019**).

One of the biggest challenges that modern cancer therapeutics face today is that of drug resistance or chemoresistance (**Jo et al.,2018**). There are several factors that may contribute to any cancerous growth becoming drug resistant over the course of treatment. Cancer cells are set apart by their ability to adapt and survive in the face of any adverse condition. True to this fact, cancer cells have devised numerous ways to learn and evade the deleterious effects of chemotherapeutic drugs and small molecules, rendering treatment regimens essentially void after a period of time. There are various mechanisms that have been reported over the years as contributing to such a condition. Other factors that may contribute to chemoresistance include autophagy, activation of genes responsible for epithelial to mesenchymal transition, anti-apoptotic mechanisms, novel mechanisms for DNA repair and a plethora of RNA molecules like lncRNAs, miRNAs, circular RNAs etc (**Li et al.,2019; Wang et al.,2016; Wilson et al.,2009; Zhu et al.,2009; Ayers et al.,2017**). The tumour microenvironment (TME) plays a very important role in the regulation and maintenance of MDR (Multi Drug Resistance) (**Erin et al.,2020**). It has been proven that OSCC has a particularly cold tumour immune system where there is very little scope of T cell activation and which makes these tumours practically impervious to conventional immunotherapy. All these factors culminate in making oral cancer cells resistant to small molecules like Doxorubicin, Cisplatin etc. (**Perez-Sayans et al.,2010).** Mutations in genes like TP53, pRb etc also plays a major role in orchestrating drug resistance and aggressiveness in OSCC (**Karunakaran et al.,2020**). Cancer cells have developed the mechanism of excluding drugs or foreign small molecules from within themselves using microbodies like microvesicles, exosomes etc (**Lowry et al.,2015**). Newer ways of identifying and characterizing such exclusion bodies are being investigated so as to come up with novel cancer targeting strategies.

Doxorubicin or Adriamycin induces cell death as well as cell cycle arrest via a range of biochemical pathways (**Siu et al.,1999**). It primarily intercalates with cellular DNA and also orchestrates cell death aided by ROS generation (Ref). Besides apoptosis, Doxorubicin is also known to induce cell death by ferroptosis, necroptosis, necrosis etc. (**Tsang et al.,2003**). Doxorubicin inhibits Topoisomerase activity, preventing it from resealing DNA replication forks, which leads to the subsequent generation of Dox-DNA mono adducts which lead to cell death in conjunction with ROS (**Stornetta et al.,2017**). The transporter protein ABCB5 has been reported to be involved in Doxorubicin resistance in human melanoma (**Frank et al.,2005**). Small non coding molecules and RNAs have major contribution to doxorubicin resistance. The RNA molecule miR-221 was found to be present in high levels in oral squamous carcinoma cells, directly mediating chemoresistance by downregulating TIMP3 (**Du et al.,2017**). The overproduction of a particular class of lipids, the ceramides, has also been shown to render DOX resistance in patients after treatment, essentially affecting cell death by misregulating critical pathways like the MEK/ERK and Akt signalling pathways (**Liu et al.,2008**). However, the aspect of ceramides and their effects on DOX-induced chemoresistance has yet to be explored further in detail. Besides the involvement of tumour cells and their associated pathways, TAMs and pathways associated to the tumour microenvironment have also been shown to contribute to DOX resistance. In a study concerned with DOX mediated therapy of uterine Leiomyosarcoma, Zhang et al. demonstrated that the protein MELK induced M2 polarization in TAMS and the induction of Doxorubicin chemoresistance via the miR-34a/JAK2/STAT3 pathway (**Zhang et al.,2020**).

2.6. Molecular aspects of Doxorubicin chemoresistance

Mutations in the p53 protein and their effects are of active interest with regards to the current discussion. Tumours harbouring mutated TP53 are often reported to become resistant to standard chemotherapeutic drugs like Anthracyclines, EGFR-inhibitors, Estrogen inhibitors, anti-metabolites, Cisplatin etc., making the development of small molecules that may restore functional p53 activity essential. Studies dating as far back as to 1996 record the role of de novo mutations in TP53 in chemoresistance of breast cancer to Doxorubicin (**Aas et al.,1996**). The authors showed in this work how mutations in the zinc-binding domain of p53 may render the tumour chemoresistant. The discussion regarding mutated TP53 and its involvement in cancer and its disease pathology is crucial since the OSCC cell lines used for all experimentation as pertaining to the current thesis carry mutated TP53 (**Onken et al., 2014**). TP53 when functional assists in DOX induced cell death by responding to excessive DNA damage (**Hamilton et al.,2000**). However, as pointed out by Pitolli et al. in their review, mutations in the TP53 gene may have adverse effects on usual anti-cancer functions (**Pitolli et al.,2019**). The authors further discuss how gain of function mutations in TP53 may render the mutated protein dominant over its wild-type counterpart and lead to its stabilized overexpression in tumours harbouring GOF mutations of TP53 (**Blandino et al.,1999**). Indeed, there are reports describing how in murine models tumours often become dependent on such mutated (GOF) p53 for their growth as well as aggressive nature (**Olive et al.,2004**). Mutant p53 has far reaching effects on tumour growth as well as the regulation of TME elements like the MHCs, levels of Interleukins and various chemokines etc. It renders resistance to apoptosis, anoikis, as well as confers invasiveness to cancers. Mutant p53 interacts with NF-kB to regulate TNF α to create an inflammatory tumour microenvironment conducive to M2 polarization and reduced

sensitivity to immunotherapy (**Alvarado-Ortiz et al.,2021**). Mutant p53 has been reported to disrupt REDOX balance in cells, and confers stemness to cancer cells (**Eriksson et al., 2019**). These cancer stem cells are further difficult to target for therapy since the function of pro-apoptotic markers like Bax in TP53 mutated tumours is often disrupted (**Amanatullah et al.,2000**). Quite early in 1998, Rowley et al. showed the presence of mutated TP53 in oral cancer as well as oral dysplastic tissue by sequencing methods (**Rowley et al., 1998**). The authors showed that TP53 mutations in exons 5 and 6 were quite prevalent in both dysplasia as well as diagnosed cases of OSCC. This and several such reports since prove the prevalence of TP53 mutation in OSCC as in other malignancies. In recent times, Shi et al. have shown how mutated p53 protein may also drive the generation of a cold TME that is unresponsive to immunotherapy in OSCC (**Shi et al., 2022**). However, it is possible to restore some of the effects of functional p53 even in the absence of the concerned protein through otherwise unrelated pathways like those of ROS generation or other p53 independent pathways involving Bim (**Chae et al.,2008**). Hence theoretically, evasion of chemoresistance using a classic anthracycline like Doxorubicin might possibly involve the restoration of p53-like effects through such alternative pathways.

2.7. The Folate Receptor as a candidate for receptor-targeted chemotherapy in OSCC

Recently, our group has synthesized a new cationic folate-based lipid (FA8), which was later conjugated with glucose derived carbon spheres to give rise to targeted molecules for dual targeting of both TAMs and glioblastoma cells for effective tumour regression (**Elechalawar & Bhattacharya et al.,2019**). The FR is incidentally over-expressed on both TAMs and cancer cells. Interestingly, we could find higher expression of folate receptor in FaDu cells

using flow cytometry. Our hypothesis thus was that oral cancer cells as well as associated tumour macrophages can be targeted using a similar formulation for effective tumour regression. Reports of aberrant expression levels are quite common for the Folate receptor, especially in the context of cancer. The expression levels for α & β FR isoforms have been found to be lower in healthy tissues as compared to cancerous tissue (**Ross et al.,1994**). Folate receptor β expression is found to be high in tumour associated macrophages **(Tie et al.,2020).** However, between the two isoforms, Folate receptor α is better characterized and is found to have high affinity for Folic acid, its natural ligand. This receptor is present primarily in the plasma membrane and mediates Folate uptake and transport by means of endocytosis **(Sabharanjak et al.,2004)**. Quite understandably, the Folate Receptor may very well be explored in the context of targeted therapeutics that work on the principle of ligand-receptor interaction. Oral squamous cell carcinoma (OSCC) can be one of the many probable targets for this particular therapeutic approach owing to the overexpression of the Folate receptor α **(Mangeolle et al.,2019)**. There are several reports witnessing the fact that oral tumours or squamous cell carcinomas of the mouth possess multiple isoforms of the Folate receptor **(Pan et al.,2003)**. FR expression has also been found to be high in mouse orthotopic models of OSCC, allowing for efficient targeted therapy, as shown by Yang et al. (2017) who co-delivered Paclitaxel and Cisplatin to mice grafted with FaDu (HTB43) cells **(Yang et al.,2017).** Previously, we developed a Folate based cationic lipid (FA8) that could be easily conjugated to a variety of delivery systems and would permit easy release of payload within target cells **(Elechalawar et al.,2017)**.

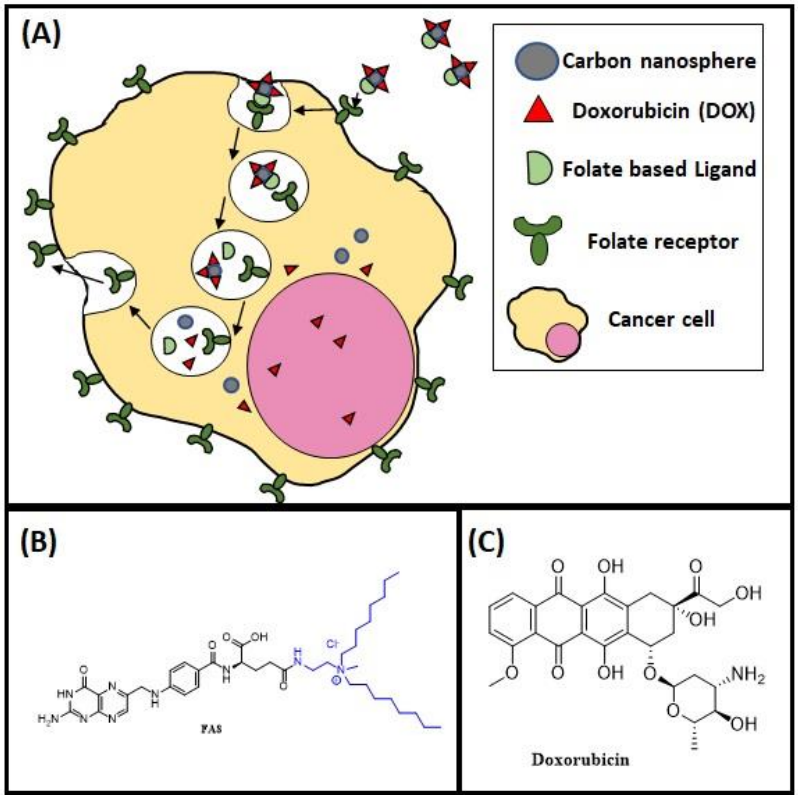

Fig 2.6. Folate based lipid FA8 and its role in DOX delivery by targeting the Folate receptor: (A) Scheme for FR mediated drug uptake (B) Chemical structure of FA8 (C) Chemical structure of Doxorubicin.

The FR has been used for developing successful receptor targeted therapeutics as well as imaging systems in recent times **(Alberti et al., 2017; Zwicke et al., 2012**). In 2011, van Dam *et al.*. scouted for ways to utilize the overexpressed status of FR overexpression in ovarian cancer for debulking and simplifying cytoreductive surgery **(Van Dam et al.., 2011)**. They used fluorescently tagged (FITC-labelled) Folate to target FRα-overexpressing cells in a case of epithelial ovarian cancer, significantly improving tumour staging and making surgical

tumour resection easier. The Folate receptor has also been targeted successfully for cancer immunotherapy. One study showed how the drug Farletuzumab (a FRα-specific mAb) induced autophagy mediated cancer cell and significantly suppressed growth in FRα overexpressing orthotopic tumours in a mouse model of ovarian cancer **(Wen et al., 2015)**. This study exemplified the dependence of ovarian epithelial cancer cells on folate metabolism. Building upon results from such studies people have also gone ahead to test antibody-drug conjugates to successfully combat cancer. In the wake of these findings, Ponte *et al.*. reported the successful use of an antibody-drug conjugate, IMGN853 (**Ponte et al.,2016**). On many occasions, the FR has been successfully used for dually targeting tumour cells as well as TAMs (**Elechalawar & Bhattacharya et al., 2019**). Earlier, the same ligand was used for liposome mediated delivery to treat melanoma in murine tumour models (**Elechalawar et al.., 2017**). One among many recent cases is where Raniolo et al. highlighted highly effective delivery of doxorubicin into FR overexpressing cancer cells (**Raniolo et al.., 2018**). Yu et al. developed a FR-targeted nanoparticle from the alcoholic extracts of Withania somnifera, a herb with medicinal value and elegantly demonstrated how FR can be a conduit for the delivery of natural compounds with anticancer properties (**Yu *et al..*, 2019**).

2.8. Targeted drug delivery and its importance today

Rigorous research is currently underway to develop better targeted therapeutics that will kill or inhibit specific proteins indispensable for the survival and proliferation of cancer cells (**A Baudino, 2015, Mukherjee et al., 2009,Manturthi et al., 2022 a&b**). According to Fojo and Parkinson, the risks posed by the myriad side effects and possibilities of systemic toxicity that accompany conventional chemotherapy still stand tall. This calls for the urgent advent of personalized medicine (**Fojo & Parkinson, 2010**). The relevance of this statement is enhanced further by numerous reports of chemotherapeutics not being beneficial and instead incurring deleterious side effects in patients. For example, there have been several cases of failed treatment involving patients who were irresponsive to Cetuximab on account of the presence of a mutated KRAS gene **(Karapetis et al., 2008)**. Likewise, gene mutations involving EGFR, MET, BRAF, etc have also had huge impact in terms of chemotherapy since the nature of their expression varies amongst patients, often rendering generalized chemotherapy schedules futile. In this regard, tools like the NGS (Next Generation Sequencing) are bound to be increasingly instrumental in exploring the area of predictive molecular pathology, paving the way for improved therapeutic advancements in the field of personalized medicine (**Dietel et al., 2015**). The occurrence of sub-clonal mutations is another challenge that we must address on account of its involvement in multi drug resistance. The current situation thus warrants intense focus on the genetic landscapes of cancer for the development of better diagnostic tools (**Schmitt, Loeb, & Salk, 2016**).

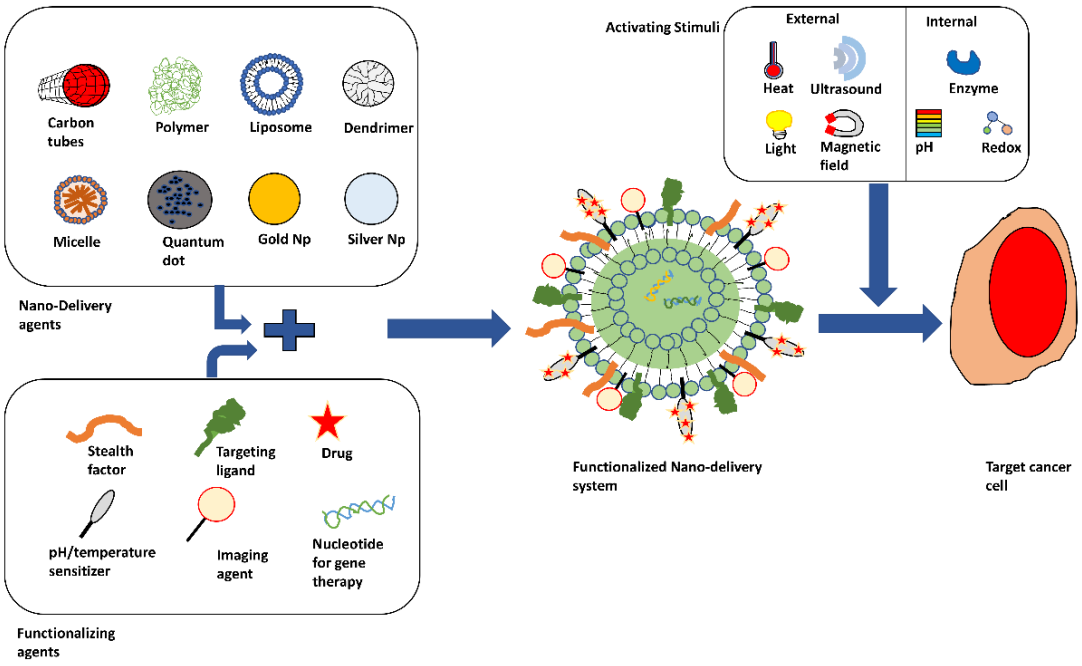

Fig 2.7. Types of targeted nano delivery systems: The above figure highlights the nano delivery systems popularly in use for therapy. It also shows the role of functionalization in developing cancer cell targeting delivery systems which shall garner maximal therapeutic effect with minimal systemic toxicity or damage. (**Mahadik et al.,2022**).

2.9. Targeted therapy against TAMs for TME modulation

Induced reversion of TAMs from M2 to M1 type is a popular anti-metastatic therapeutic approach that has been extensively reviewed by Dong et al. (**Li et al.,2023**). TAMs have been proven to be functionally linked with receptors that promote malignancy. Cytokines like TGF-β and IL-10 are frequently implicated in the polarization of anti-inflammatory M2 macrophages (**Zhang et al.,2016**). Using a monoclonal anti-MARCO antibody, La Fleur et al.. targeted the MARCO receptor present on TAMs residing in breast and colon cancers and elicited anticancer effects by reprogramming the TAM pool to a more pro-inflammatory state (**La Fleur et al.,2018**). In this context, our group has targeted TAMs on account of folate receptor over-expression (FR). The relationship between tumour cells and TAMs is bi-directional, where each element affects the other and carries forward towards the maintenance of a pro-tumoural state. Some of the many markers responsible for driving M2 TAM activation via STAT3 induction are IL-6 and IL-4. This is important to note since TGF-β and STAT3 are direct players in metastasis and immunosuppression orchestrated by M2 TAMs (**Nowak & Klink,2020**). Some select pro-tumoural cytokines like sICAM-1 and C5a and some anti-tumoural cytokines like IP-10 and IL-1ra were also found to be differentially regulated as a result of dual-targeting FR-mediated therapy in glioma. However, further investigation as to the exact nature of their involvement in tumour progression warrants further investigation. M2 TAMs have also been shown to directly induce higher levels of EMT via the upregulation of the EGFR/ERK1/2 pathway (**Gao et al.,2018**).

Stromal elements impart cancer cells all the essential characteristic features which make the disease undoubtedly one of the most elusive and challenging in the world. One such

feature is resistance to chemotherapy, to which TAMs have been proven to contribute to. Yin et al., 2019, studied the effects of hypoxia treated HNSCC (Head and neck squamous carcinoma) cells on TAM polarization and movement, where they found M2 type TAMs to induce resistance to Gefitinib in HNSCC cells with the help of paracrine signalling of the factor CCL15 (**Yin et al.,2019**). Efforts to affect tumour cells as well as TAMs by targeting the mTOR pathway using a four-way liposomal delivery system having Rapamycin (an mTOR inhibitor) and Regorafenib (an anti-angiogenic drug) has led to the repolarization of target TAMs expressing Mannose receptors and PD-L1 receptors, besides reducing angiogenesis and arresting tumour growth (**Chen et al.,2020**). In an effort to discover novel bioactive molecules capable of effectively reprogramming the tumour microenvironment, a Fungus-derived small molecule called Trichomicin was studied. Trichomicin was found to be effective in reducing levels of TNFα and Il-6, which subsequently lowered expression levels of PD-L1 on both tumour and stromal cells, leading to tumour regression in a murine model of colon cancer(subcutaneous) (**Zhao et al.,2020**). However, despite a slew of studies reporting the anti-cancer therapeutic efficacy of immunotherapeutic approaches, some reports indicate that a multimodal approach incorporating cancer cell-targeted therapy as well as immunotherapy at the same time may prove more potent. In line with such findings, a lipid-dendrimer-calcium-phosphate nanoparticle (TT-LDCP NP) was reported to successfully deliver anti-PD-L1 siRNA along-with Il-2 encoding plasmid DNA (**Huang et al.,2020**). Besides delivering anti-cancer genetic material the said delivery system also induced greater production of active T-cytotoxic cells thus effectively reprogramming the TME. Another novel approach worthy of mention is the induction of the systemic anticancer immune response by using non-viral oncolysis (**Kepp et al.,2020**). The current hour requires the establishment of newer approaches to physically/chemically

(non-viral approach) induce oncolysis in the tumour region and send off a systemic response against tumour antigens as well as factors mediating distant metastasis enabled by the release of danger-associated molecular patterns. Such non-viral oncolytic agents might encompass a range of materials such as cytotoxicants, ultrasonography, microwave, photothermal therapy, etc. among others. A lot of these therapeutic approaches though proven successful in a variety of cancer models have however not yet been implemented in the case of oral squamous cancer. We thus strongly believe that testing of these currently trending therapeutic approaches against OSCC would open up newer avenues to address what is becoming an increasingly challenging issue.

In their search for anti-TAM therapies using materials from natural sources, studies have gone as far as to use nanoparticles derived from Cuttlefish ink, which subsequently demonstrated commendable anti-cancer activity upon photothermal activation under NIR as well as TAM repolarization and tumour regression by downregulation of the MAPK pathway in an in-vivo model of lung metastasis (**Deng et al.,2019**). Similar studies using plant-derived materials include the use of Indocyanine green-conjugated C-phycocyanin as a targeted photothermal ablative against cancer (**Wan et al.,2020**). In another instance, Wang et al. report the use of Gold-Selenium nanoparticles coupled with Gold nanostars to initiate a two-headed attack comprising of chemotherapy and targeted photothermal therapy against tumour cells as well as TAMs (**Wang et al.,2020**). Yet another recent development in the context of targeted photothermal therapy is the reversal of tumour-induced immunosuppression, as well as TAM repolarization, achieved using a delivery system made of graphene oxide and Polyethylene glycol (**Deng et al.,2020**). This is one of the recent reports demonstrating how successfully TAMs can be targeted using PTT

(Photothermal therapy) as demonstrated by excellent tumour regression results from a mouse model of osteosarcoma.

2.10. Targeted immunotherapy- opportunities for the future

However, as discussed earlier, the use of multimodal approaches that incorporate nano therapy as well as targeted Immunotherapy will be our aim for the future. A recent report to exemplify such a therapeutic approach is the work done by Ramesh et al.,2020 who have used a dual kinase inhibitor loaded supramolecular nanoparticle which targeted both the CSF1-R and MAPK pathways at the same time to effect successful TAM repolarization (**Ramesh et al.,2020**). There are several such instances of TAM targeted immunotherapy which may be taken up as models for developing similar therapeutic systems for targeting OSCC in the future (**Table 2.1**). Nanotherapeutics targeting TAMs confer advantage with targeted delivery of drugs towards TAMs, increased circulation time along with the efficient reduction of tumour size (**Feng et al.,2019**). Even though Nanotherapeutics have shown exceptionally great results in the reduction of tumour progression, the aberrant tumour metastasis, immunosuppression, premature release of a drug, and poor biodegradability are some of the major challenges faced while developing novel Nano therapeutic strategies (**Dong et al.,2019**).

Table 2.1: Targeted Therapeutics that are reportedly TAM targeting: These functionalized small molecules have been shown to target TAMs and aid in achieving improved treatment response across cancer types. (**Bhattacharya et al.,2021**)

Sr. no	Drug/Bioactive component	Delivery system	Cancer type	Mechanism	Ref
1.	IL-2cP1	Nanoparticles	Melanoma	Repolarization of M2 TAMs to M1 phenotype	(**Wang et al.,2017**)
2.	Paclitaxel (PTX)	Nanoparticles with YI peptide	Colorectal cancer	Enhanced inhibition of tumour growth	(**Cao et al.,2018**)
3.	Hyaluronic acid (HA)	Mannan conjugated MnO_2 nanoparticles (Man-HA-MnO_2)	Breast tumour	Repolarization of M2 TAMs to M1 phenotype	(**Landstrom et al.,2017**)

Sr. no	Drug/Bioactive component	Delivery system	Cancer type	Mechanism	Ref
4.	Paclitaxel	Albumin modified Gold nanorods for photothermal-chemotherapy	Colon cancer	The temperature of the tumour microenvironment is 5-8^{0}C higher than normal cells. Paclitaxel inhibited M2 polarization.	(**Li et al.,2018**)
5.	Hydrazinocurcumin (HC)	Nanoparticles	Breast cancer	Inhibition of STAT3 and TAM repolarization to M1 phenotype.	(**Zhang et al.,2013**)
6.	Macrolide	Gold nanoparticles	Breast cancer	Reduction in the number of M2 TAMs.	(**Dreaden et al.,2012**)

Sr. no	Drug/Bioactive component	Delivery system	Cancer type	Mechanism	Ref
7.	RNA interference (RNAi) against VEGF	Peptide nanoparticles (NPs)	Lung cancer	Reduced angiogenic signals and enhanced tumour growth inhibition.	(**Conde et al.,2015**)
8.	Anti-CSF-1R siRNA	M2-like TAM dual-targeting nanoparticles (M2NPs)	Melanoma	Reduction in the density of M2 TAMs and an enhanced anti-tumour immune response.	(**Quian etal,2017**)
9.	Ginseng	Nanoparticles	Melanoma	Suppression of IL4, IL13, and increase in expression of TNFα, IL12, and IL6.	(**Cao et al.,2019**)

Sr. no	Drug/Bioactive component	Delivery system	Cancer type	Mechanism	Ref
				Sustained TAM repolarization.	
10.	A bioactive conjugate of the tumour-specific antigenic peptide (Hgp 100_{25-33}) with an immune stimulant (CpG) coated with a galactose inserted RBC membrane.	Baicalin loaded PLGA-NP	Melanoma	Reversal the M2 phenotype to the M1 phenotype.	**(Han et al.,2019)**
11.	O-carboxymethyl-chitosan (CMCS)	Sorafenib loaded cationic lipid nanoparticles	Hepatocellular carcinoma	Inhibition of IKKβ and repolarization of M2 type TAM. M-IMD-	**(Wang et al.,2019))**

Sr. no	Drug/Bioactive component	Delivery system	Cancer type	Mechanism	Ref
		(SF-CLN) and mannose modified IMD-0354 loaded cationic lipid-based nanoparticles (M-IMD-CLN)		CLN reduced the M2/M1 TAM ratio.	
12.	Hyaluronic acid (HA) ion-pairing	Liposomal nanoparticle between HA and Doxorubicin	Glioma	CD44 mediated targeting of tumour cells and CSCs, inhibition of	(**Yang et al.,2018**)

Sr. no	Drug/Bioactive component	Delivery system	Cancer type	Mechanism	Ref
		(DOX) forming DOX-HA-LPs		Vasculogenic mimicry channels (VMs).	
13.	Rabies virus glycoprotein (RVG)	PTX loaded NPs (RVG-PTX-NP)	Glioma	RVG enabled enhanced uptake in TAMs and their repolarization to M1 TAMs.	(**Zou et al.,2017**)
14.	miR155 (sPEG/GLC/155)	GLC nanoparticles coated with sPEG	Melanoma	MiR155 mediated targeting of the C/EBPβ pathway caused the repolarization of TAMs.	(**Liu et al.,2017**)

Sr. no	Drug/Bioactive component	Delivery system	Cancer type	Mechanism	Ref
15.	siRNA targeting NF-κβ proteins	Mannosylated copper nanoparticles	Ovarian tumour	Reduction in the number of tumour-promoting TAMs.	(**Ortega et al.,2016**)
16.	Doxorubicin (DOX)	Poly (lactic-co-glycolic) acid (PLGA) nanoparticles	Melanoma	PEGylated NPs deliver Doxorubicin to TAMs on account of Mannose overexpression on TAMs.	(**Niu et al.,2014**)
17.	PLX3397	Poly (lactic-co-glycolic acid) nanoparticles coated with M2	Melanoma	PLX3397 inhibits the CSF-1 pathway which is crucial for M2 TAM survival.	(**Pang et al.,2019**)

Sr. no	Drug/Bioactive component	Delivery system	Cancer type	Mechanism	Ref
		pep (peptide ligand binding specifically to M2 TAMs)			
18.	Epirubicin	Liposomes coated with sialic acid-cholesterol conjugate	Murine Sarcoma	Delivery of drug to TAMs on account of overexpression of Sialic acid.	(**Zhou et al.,2017**)
19.	Platinum and BLZ-945	$^{BLZ\text{-}945}$SCNs/Pt (Sensitive Cluster Nanoparticles)	Murine Breast cancer, Colon cancer, and Melanoma	BLZ-945 is an inhibitor of the CSF-1 receptor.	(**Wang et al.,2017**)

Sr. no	Drug/Bioactive component	Delivery system	Cancer type	Mechanism	Ref
20.	Sorafenib	Lipid coated poly-(lactic-co-glycolic acid) nanoparticles targeting CXCR4 modified with AMD3100 (CXCR4 antagonist)	Liver cancer	AMD3100 blocks CXCR4/SDF1signaling, leading to reduced TAM infiltration, delayed tumour progression.	(**Gao et al.,2015**)
21.	Paclitaxel (PTX) and Indocyanine green (ICG)	Hyaluronic acid (HA) layer-by-layer (LbL) nanoparticles	Breast tumour	Endocytosis mediated by HA-CD44 (CD44 is overexpressed on	(**Zhao et al.,2018**)

Sr. no	Drug/Bioactive component	Delivery system	Cancer type	Mechanism	Ref
				TAMs and tumour cells).	
22.	Trimethyl chitosan (PEG=MT) and poly-(allylamine hydrochloride)-citraconic anhydride	Conjugate nanoparticles of Pegylated mannose	Breast tumour	Upon receptor-mediated endocytosis of nanoparticles, the siRNA of VEGF and PIGF inhibit tumour progression and re-educate TAMs to M1 type.	(**Song et al.,2018**)

Cancer immunotherapy as already discussed in this review is currently one of the frontline treatment regimens under investigation. The said approach classically requires directly targeting TAMs to affect their polarization, programming as well as affecting other stromal elements which together with these TAMs mediate signalling pathways that regulate key functions like tumour proliferation, drug resistance metastasis, etc. Recent reports include the development of porous nanoparticles of Iron loaded with a PI3Kγ inhibitor to target TAMs via their Mannose receptors (**Fan et al.,2020**). This approach caused NFkB activation in TAMs thus causing their re-polarization to the M1 phenotype(anti-tumoural). In another study, TAM repolarization was achieved using a delivery system consisting of natural molecule Albiziabioside A conjugated with DCA(Dichloroacetate), a pyruvate dehydrogenase kinase inhibitor (**Narihira et al.,2018**). This delivery system inhibited glycolysis and restored oxidative phosphorylation, and also reduced levels of apoptosis and ferroptosis besides reducing the M2 TAM population. Natural products or molecules have also been attributed to the capability of TAM repolarization and TME associated immune modulation. There has been a report of a polysaccharide from Cordyceps militaris, CMPB90-1, that bound to TLR2 and caused repolarization of M2 TAMs to M1 TAMs, more specifically by downregulating the PD-L1- PD1 axis between TAMs and tumour cells(**Legge et al.,2019**).

In another independent investigation, Cabrita et al.,2020 revealed an interesting finding that revealed that the presence of CD20+ B cells along with T-cytotoxic cells in the tumour stroma led to the formation of a certain sort of lymphoid tertiary structure which enhances intratumoural immune responses such as those usually activated by checkpoint inhibitor therapy (**Li et al.,2020**). The presence of these B cells and their propensity to form the said lymphoid tertiary structures was also linked to a certain genetic signature. These findings

were corroborated when it was found that the presence of such B cells in the tumour made a big difference in terms of therapeutic response to ICB (Immune Checkpoint Blockade) owing to the differential expression of its associated genes among individuals, thus also highlighting the significance of these switched B cells and the consequences of their presence in tumours (**Wei et al.,2019**). Based on the same principle, Petitprez et al. reported their study of classifying a cohort of 608 cancer patients in terms of their gene expression profiles that would later help relate the formation of tertiary lymphoid structures and the resultant responsiveness of an individual to ICB therapy (**Bi et al.,2020**). Other ways of reprogramming TAMs include targeting CAMKII using a CAMKII inhibitor KN93 using a hybrid peptide hydrogel which resulted in reduced numbers of M2 TAMs as well as enhanced production of cytotoxic T cells (**Cabrita et al.,2020**).

We also come across newer ways of achieving dual-targeted therapy where no one single approach is exactly as another, underlining the fact that immunotherapy is currently one of the hot topics of cancer research with the applications and their ramifications yet to be understood in the scenario of oral cancer. Reported studies vary from the targeted delivery of CSF1R inhibitors using pH-responsive copolymer micelles to the liposomal delivery of chlorogenic acid in a targeted manner, all with the ultimate aim of TAM modulation/TAM mediated immunotherapy (**Helmink et al.,2020**; **Petitprez et al.,2020**). Among other receptors, the Folate Receptor has been an important target for targeted cancer treatment and associated investigations. This is primarily owing to the differential overexpression of the Folate Receptor on multiple cancers, which makes the Folate receptor an oft used marker for targeted therapy against TAMs and Tumour cells alike (**Dai et al.,2020**). Based on similar principles, Tie et al.,2020 have reported the use of a Folate-modified liposomal system carrying BIM-S plasmid to treat lung cancer cells as well as FRβ positive TAMs,

achieving tumour regression successfully in a mouse model of lung cancer (**Wang et al.,2020**).

A recent publication from our research group highlights the approach of dually targeting brain tumour (Glioma grade IV) cells and glioma resident tumour-associated macrophages using an anionic carbon nanosphere based delivery system that was primed with a Folate based cationic ligand for effective delivery of Doxorubicin to FR overexpressing TAMs and tumour cells (**Ye et al.,2020**). Not only did the said treatment alleviate tumour cell proliferation in vitro but also facilitated targeted TAM elimination and tumour regression along with improved overall survivability in a murine model of Glioblastoma. The use of targeted delivery systems for siRNA mediated therapy has been of no lesser importance either. The recent report by Shobaki et al. demonstrates the successful application of a lipid nanoparticle delivery system that targets TAMs directly by delivering siRNA against HIF-α and STAT-3 (**Shobaki et al.,2020**). Extended cancer-free survival compared with patients treated with conventional therapies and lower response rates are key advantages of manipulating TAMs with immunotherapy (**Canning et al.,2019**). However, inconsistent results from the treatment of/within different stages of the cancer are the major drawbacks observed (**Zhang et al.,2015**).

There are a variety of different targeted delivery systems that can be modified with/conjugated to any drug or bioactive molecule of choice and used thereafter to target aggressive incidences of oral squamous cancer. But at the same time, our findings make it clear that very few of these approaches are designed to target TAMs associated with the OSCC tumour microenvironment. While studies to date have revealed multiple approaches for selective drug or gene delivery to oral cancer cells, not many exist to substantiate our

claims of a greater therapeutic potential for TAM targeted approaches. Interestingly, we found that there are several cases where the drug/therapeutic targets for such functional small molecules are common to tumour cells and TAMs, and studies as to the assessment of their full therapeutic potential are necessary. In one recent study, Srivastava et al. developed a 5-FU conjugated PLGA nanoparticle-based delivery system that was functionalized with α-tocopherol to make the small molecule targeted. The said delivery drug-NP conjugate exhibited robust induction of apoptosis and cell death when treated to SCC15 oral cancer cells in vitro as shown by Flow cytometry (**Srivastava et al.,2019**). Interestingly, another study by Wei et al. showed how pro-tumoural M2 TAMs suppress the anti-cancer effects of 5-FU by secreting CCL22 which in its turn affects anti-5-FU chemoresistance via the PI3K/Akt and Caspase mediated apoptosis pathways (**Wei et al.,2019**). Based on the findings from these two reports, we may safely surmise that the therapeutic approach taken up by Srivastava et al. would have great potential against M2 TAMs in OSCC, an aspect worth investigating in the future. In another instance, Fan et al. developed a Glutathione sensitive and Folate receptor-targeted nanoparticle for the targeted delivery of Paclitaxel to highly metastatic HSC3 cells in vitro as well as to murine tumours in vivo (**Fan et al.,2020**). On the other hand, Sun et al. elegantly demonstrated the overexpression of Folate Receptor-β in pro-tumoural TAMs in OSCC, to the extent that it could be utilized for the development of robust Fluorescence-based imaging systems of great theranostic potential (**Sun et al.,2014**). This study again gives us enough evidence to believe that such FR-targeted delivery systems might work against tumour cells and M2 TAMs alike with comparable efficiency.

There are a few other reports that have a slightly different (but not any less exciting) approach and warrant studies as to their TAM-targeting potential in oral cancer (**Table 2.2**). Gupta et al. reported the design and use of a PLGA based nanoparticle system that would radiosensitize oral cancer cells by delivering Docetaxel, the same drug also known to effectively re-program pro-tumoural TAMs (**Gupta et al.,2018**). Wang et al., as well as Pan et al., used mesoporous Silica nanoparticles to deliver siRNA against MDR-1 demonstrating commendable results against oral cancer cells both in vitro as well as in vivo [**Wang et al.,2017; Pan et al.,2013**]. As reviewed by Bossennec et al., MDR-1 is a transmembrane transporter protein that is primarily concerned with the removal of tissue toxicity and with chemoresistance in the context of cancer specifically with regards to pro-tumoural TAMs (**Bossennec et al.,2018**). This is the reason we believe there should be further studies into assessing these MDR-1 targeted therapeutic molecules against M2 TAMs in OSCC. There are many other treatment options available that have been proven effective against oral cancer cells and which can be investigated for their potential effects on M2 TAMs wherever the targeting principle or therapeutic mechanism applies to both cancer cells and TAMs.

Table 2.2: Some Notable Nanotherapeutic approaches(targeted) reported so far against OSCC: The table lists a variety of different delivery systems conjugated with bio-active anti-cancer components derived from either synthetic or natural sources. These functionalized small molecules have different ways or mechanisms to target cancer and also exhibit potential as anti-TAM treatment options (**Bhattacharya et al.,2021**).

S. No.	Delivery system	Drug/Small molecule/Bioactive component		Target	Potential for anti-TAM therapy?	Reference
		Synthetic source	Natural source			
1	PECE hydrogel	HDACi SAHA & DDP(Cisplatin)		Deacetylation of hyperacetylated genes	Yes, Tran et al.., 2013	(**Li et al.,2012**)
2	Polymeric micellar nanoparticle	NC6004(CDDP/Cisplatin)		Improved intratumoural distribution with reduced nephrotoxicity	Yes, Chen and Chang, 2019	(**Endo et al., 2013**)
3	Chitosan nanoparticles		Ellagic acid	Anti-proliferative effect, DNA fragmentation	Yes NamKoong et al.., 2012	(**Arulmozhi et al.,2013**)
4	Thermosensitive Silica nanoparticles	Doxorubicin & Methotrexate		Matrix Metalloprotease 2	Yes Zheng et al.., 2017	(**Abbasi et al.,2014**)
5	Monomeric self-assembled nucleoside nanoparticle	5-Fluorouracil		Higher cancer cell toxicity, reduced proliferation, and	Yes Chen Wei et al.., 2019	(**Zhao et al.,2015**)

S. No.	Delivery system	Drug/Small molecule/Bioactive component		Target	Potential for anti-TAM therapy?	Reference
		Synthetic source	Natural source			
				greater accumulation in tumour		
6	Chitosan coated nanoparticles		Curcumin	Cancer cell-specific cytotoxicity	Yes Mukherjee et al.., 2016	(**Mazzarino et al.,2015**)
7	PLGA based hybrid nanoparticle	Quinacrine & Silver		Inhibition of BER (Base Excision Repair)	Yes Abdulghani et al.., 2016	(**Satapathy et al.,2018**)
8	Nanoemulsion with tocopherol moiety and Chitosan		Genistein	Antiproliferative activity	Yes Ning et al.., 2019	(**Gavin et al.,2015**)
9	Anti-Desmoglein antibody	TRAIL as ligand		Cancer cell-specific targeted apoptosis	Yes Gao et al.., 2019	(**Kouno et al.,2017**)
10	Anti-EGFR microbubbles	Bleomycin		EGFR	Yes Gao et al.., 2018	(**Hirabayashi et al.,2017**)
11	Mucoadhesive patch	Methotrexate		Mitochondrial membrane potential of cancer cell	Yes Lee et al.., 2019	(**Jin et al.,2018**)
12	Chitosan nanoparticles		Shrimp shell extract	VEGF, TNF-α	Yes Tamura et al.., 2020	(**Abd-el-fattah et al.,2018**)

S. No.	Delivery system	Drug/Small molecule/Bioactive component		Target	Potential for anti-TAM therapy?	Reference
		Synthetic source	Natural source			
13	Gold nanoparticles	Paclitaxel		Cancer cell proliferation	Yes Wanderley et al.., 2018	(**Asar et al.,2019**)

When debating over conventional/reported anti-OSCC therapeutics with possible utility as anti-TAM therapy in the future, we must not forget drugs or bioactive molecules which have been reported as having anti-cancer effects against oral squamous cell carcinoma even though not essentially in association or in conjugation with any targeted delivery system. The reason why these molecules deserve mention in this section is their prospective therapeutic functionality against tumour-associated macrophages in the OSCC TME. CSCs (Cancer stem cells) being well reported as being crucial drivers of tumour progression and metastasis were targeted by Hu et al. using Isoliquiritigenin which is a Flavonoid molecule isolated from the roots of licorice. The said treatment showed a high level of selectivity for OSCC-associated CSCs and reduced self-renewal besides affecting tumour growth and colony formation (**Hu et al.,2017**). The primary molecular targets of this naturally sourced bioactive compound were shown to be major players involved in pathways associated with stemness, metastasis, and chemoresistance, e.g: ALDH1, CD44, ABCG2, and GRP78. Wei and his colleagues have demonstrated how GP73(Golgi protein 73) regulates tumour growth and metastasis via the induction of GRP78 which mediates activation of ER (Endoplasmic Reticulum) stressors (**Wei et al.,2019**). Subsequently, ER stress activation and transmission results in the induction of pro-tumoural TAM phenotype increased TAM density and a poor prognosis. It is thus quite evident that Isoliquiritigenin may well be used in the future for TAM-targeted therapy. Epigenetic modulators are significant in the world of new age cancer therapy. Wang et al. reported the successful use of a Bromodomain and extra-terminal domain (BET) inhibitor, JQ1, to induce cell death in OSCC lines CAL27 and SCC25. Not only did JQ1 inhibit cell growth by downregulating FOXM1 and PD-L1 levels in a dose-dependent manner, but also exhibited tumour regression in vivo when used along with anti-Pd-L1 siRNA (**Wang et al.,2022**). We also find

a study revealing the direct correlation between PD-L1 expression on TAMs and its stimulatory effects on TAM proliferation, survival, and immune-suppressive conditions in the TME (**Hartley et al.,2018**). It could thus be well expected that an epigenetic regulator like JQ1 would potentially demonstrate robust anti-cancer effects if incorporated into a delivery system for targeted therapy of OSCC.

It's necessary to thoroughly understand the communication that occurs between stromal elements and tumour cells and the repercussions that of on Macrophage polarity and intra-tumoural immune response. Since TAMs and their polarization status are crucial factors that are involved in a complex interplay with interconnected biochemical pathways regulating tumour growth and spread, targeted approaches aimed either exclusively at TAMs or against TAMs and tumour cells both would compound the benefits of conventional OSCC therapy, ensuring improved overall survival as well as possible tumour growth remission. As evident from this review, current research on novel ways to target TAMs is mostly focused on cancers other than OSCC, where some significant progress has already been made. Recent findings suggest that approaches that involve targeting cancer associated pathways common to tumour cells and TAMs or multimodal approaches comprising of targeting common cancer associated kinases and pathways, TAM repolarization and tumour associated immune suppression might yield better therapeutic results in the future.

3.1. Chemical and Reagents:

Carbon nanospheres (CSP) were synthesized according to a previously published protocol (Elechalawar & Bhattacharya et al.,2019). Clinical grade injectable DOX was purchased as DOXOTERO, a product from ONCOLOGY MEDICINE, India. TAM isolation was done by Midi MACS separating kit containing Midi MACS separator (130-042-302), LS columns (130-042-401) and CD11b Micro beads (130-097-142) [Miltenyi Biotech Asia Pacific Pte Ltd, Singapore]. Folate Free RPMI -1640 media (Cat No: 27016021) was purchased from Thermo Fisher Scientific, USA. Antibiotics were purchased from Hi-media, India. DMEM (Cat No: 12800017), RPMI (Cat No: 31800022), IMDM (Cat No: 12200036) and F12 (Cat No: 21700075) were all purchased from Gibco (Invitrogen). All other reagents were purchased from local suppliers and used without further purification.

3.2. Antibodies and Apoptosis Kits:

Antibodies for Bax (Cat No: #2772), Bcl-2 (Cat No: #3498), E-Cadherin (Cat No: #3195), Vimentin (Cat No: #5741), Cleaved Caspase 3 (Cat No: 9664T), p53 (Cat No: #9282), iNOS (Cat No: #2982), β-Actin (Cat No: #4970) and TNFα (Cat No: #3707) were purchased from Cell Signalling Technology, Beverly, USA. Antibody for Folate Receptor whole (Cat No: sc-28997) was purchased from Santa Cruz Biotechnology, Texas, USA. Antibodies for Folate receptor α (Cat No: PA542004), CD68 (Cat No: 53-0681-82) and CD163 (Cat No: PA578961) were purchased from Thermo Fisher Scientific, USA. Antibodies for CD80 (Cat No: 104707), and CD206 (Cat No: 321103) were purchased from Biolegend, San Diego, USA. Annexin V-FITC based dead cell Apoptosis kit (Cat No: V13242) was purchased from Thermo Fisher Scientific, USA.

3.3. Maintenance of mammalian cell culture systems:

FaDu (human OSCC), CAL27 (human OSCC), HEK293 (non-cancerous line) were purchased from ATCC (Manassas, USA) and MOC2 (mouse aggressive OSCC) cells were purchased from Kerafast, Boston, USA. All the cells were mycoplasma free. Cells were cultured in prescribed culture medium as per culture instructions from selling agencies with 10% fetal bovine serum (Sigma Chemical, St Louis, MO), penicillin 50 mg/litre, streptomycin 50 mg/litre, kanamycin acid sulphate 100 mg/litre and 3.7gm/litre sodium bi-carbonate solution. Cultures of 85–90% confluency were used for all the experiments. The cells were trypsinized, counted, and plated as per standardized counts for different cell-based studies. The cells were allowed to adhere overnight before they were used for any experiment.

3.4. Procurement and procedures involving laboratory animals:

C57 Bl/6J mice were procured from Vyas Labs, Hyderabad, India and all studies carried out in accordance with IAEC regulations OF BITS Pilani Hyderabad Campus (Animal Facility Registration no.- 1912/PO/RE/S/16/CPCSEA). Mice were housed under standard conditions including ambient temperature and availability of feed and drinking water ad libitum. All surgical procedures were performed as per Institutional IAEC protocol under anaesthesia using Isoflurane. Any animal found to have compromised state of health was euthanized using CO_2 chamber as per humane standards.

3.5. Synthesis of CSPs:

CSPs were synthesized by the hydrothermal decomposition of Glucose in water kept in a Teflon-lined autoclave at 180^0C for 8h. The synthesis procedure was carried out in

collaboration with Dr. Rajkumar Banerjees Lab in CSIR-IICT, Hyderabad as per a previously published protocol **(Selvi et al.,2008; Elechalawar & Bhattacharya et al.,2019).** The steps taken are briefly as follows-

- 1.5g of D (+) was dissolved in 17 ml of deionized water to form a clear solution.
- It was placed in a 21 ml Teflon-lined sealed stainless-steel autoclave and maintained at 180^{o}C for 8h.
- After cooling the reaction vessel, the brown material formed was transferred to the centrifuge tube.
- The pure product was isolated by repeated centrifugation at 10000 rpm for 10 minutes using deionized water and ethanol.
- The purified product obtained was dried in an oven at 80^{0}C for 4h.
- The final product obtained was a brownish powder with a spheres range of 360-380 nm.

3.6. Synthesis of FA8 {(R)-N-(2-(4-(4-(((2-amino-4-oxo-3,4-dihydropteridin-6-yl) methyl) amino) benzamido)-4-carboxybutanamido) ethyl)-N-methyl-N-octyloctan-1-aminium chloride}:

The synthesis for Folate-based lipid FA8 was carried out in collaboration with Dr. Rajkumar Banerjees Lab in CSIR-IICT, Hyderabad as per a previously published protocol **(Elechalawar & Bhattacharya et al.,2019).** The steps taken are briefly as follows-

Step-1: Synthesis of tert-butyl (2-(dioctylamino)ethyl)carbamate (Compund-2):

- Monoboc-protected ethylenediamine (Compound-1, 1.8g) was added to Ethyl Acetate (20ml).
- To this mixture K_2CO_3 (6.4 g, 4eq) followed by 1-Bromo octane was added and stirred at 65 °C for 48 h.
- Reaction mass was filtered and the ethyl acetate was evaporated to get crude. Purification is done by column chromatographic separation using 60-120 mesh silica gel and 1% Methanol-Chloroform (v/v) as eluent.
- The separation yielded compound-2 as colourless liquid (3g, 70% yield).

1H NMR (300 MHz, $CDCl_3$):δ/ppm = 0.9 [m, 6H, CH3-(CH2)7-]; 1.1−1.6 [bs, 20H, -(CH2)10-; m, 9H, CO-O-C(CH3)3]; 1.5[m, 4H, -CH2-N-CH2-(CH2)4]; 2.3−2.5 [m,4, -CH2-N-(CH2)2-(CH2)2-]; 2.5[t, 2H, -NH-CH2-CH2-N-(CH2)2-];3.2 [m, 1H, -NH-CH2-CH2-N-(CH2)2-]; 3.6[t, 2H, -NH-CH2-CH2-N-(CH2)2-]; ESI-MS: m/z= 386 [M+1]+ for C23H48N2O2

Step-2 Synthesis of N-(2-((tert-butoxycarbonyl) amino) ethyl)-N-methyl-N-octyloctan-1-aminium iodide (Compound -3):

- Compound-2, 1.8g was added to Methyl Iodide (5ml) and stirred at room temperature for 12h.
- Methyl Iodide was evaporated to get crude.
- Purification is done by column chromatographic separation using 60-120 mesh silica gel and 2% Methanol-Chloroform (v/v) as eluent.
- The separation yielded compound-3 as white solid (2.5g, 80% yield).

1H NMR (300 MHz, CDCl3):δ/ppm = 0.9 [m, 6H, CH3-(CH2)7-]; 1.1-1.6 [bs, 20H, -(CH2)10-; m, 9H, CO-O-C(CH3)3]; 1.5[m, 4H, -CH2-N-CH2-(CH2)4]; 3.2-3.3 [s,3, -CH2-N(CH3)-(CH2)2-

(CH2)2-]; 3.4-3.6 [m, 4H, -CH2-N(CH3)-(CH2)2-(CH2)2-]; 3.6-3.8[m, 4H, -NH-CH2-CH2-N-(CH2)2-]; ESI-MS : m/z= 400 [M+1]+ for C24H51N2O2

Step-3 Synthesis of N-(2-aminoethyl)-N-methyl-N-octyloctan-1-aminium chloride (Compound -4)

- Compound-3, 2g was added and was dissolved in 2 mL dry $CHCl_3$, 1 mL of TFA was added and the mixture at 00C was allowed to stir for 3 h.
- TFA was removed with nitrogen flow and the residue was subjected to chloride ion exchange chromatography over amberlyst A-26 chloride ion exchange resin.
- The compound-4 obtained after chloride ion exchange was almost pure (1.2 g, 80% yield) and unstable and hence directly continued to next step.

Step-4: Synthesis of FA8

- Folic Acid, 1g was dissolved in DMSO (10ml), to this mixture HATU (1.03g, 1.2eq) was added.
- To this solution mixture of compound-4 (0.67g, 1 eq) and Triethylamine (0.459g, 2eq) in DMSO (5ml) was added.
- Reaction mass was stirred for overnight.
- 2N HCl 30 ml was added to reaction mass followed by filtration to get crude solid.
- Crude product was purified by using 60-120 mesh silica gel and 15% Methanol-Chloroform (v/v) as eluent.
- Yellow solid was then dissolved in acetone and filtered to get pure FA8 (0.6g, 36%. Yield).

1H NMR (400 MHz, CDCl3+ DMSO-d6): δ/ppm = 0.9 [m, 5.5H, CH3-(CH2)7-]; 1.1−1.4 [bs, 20H, -(CH2)10-;1.5[m, 4H, -CH2-N+(CH3)-(CH2)2-(CH2)2-]; 3−3.2 [s,3, -CH2-N+(CH3)-(CH2)2-(CH2)2-]; 3.4-3.6{ m, 8.1H, [-CH2-N+(CH3)-(CH2)2-(CH2)2-], [-NH-CH2-CH2-N-(CH2)2-]},4.4 -4.6[m, 3.1H, FA- 3C (-CH), FA- 8C(-Ph-NH-(CH2)-]: 6.6−6.7 [m, 2.8 H, FA-5C&7C]: 7.8 [m, 2.5H, FA- 4C & 6C]: 8.8−10 [s, 1.3H, FA- 9C]: ESI- MS : m/z= 723[M+1]+ for C38H60N9O5.

3.7. Synthesis and characterization of CSP conjugates:

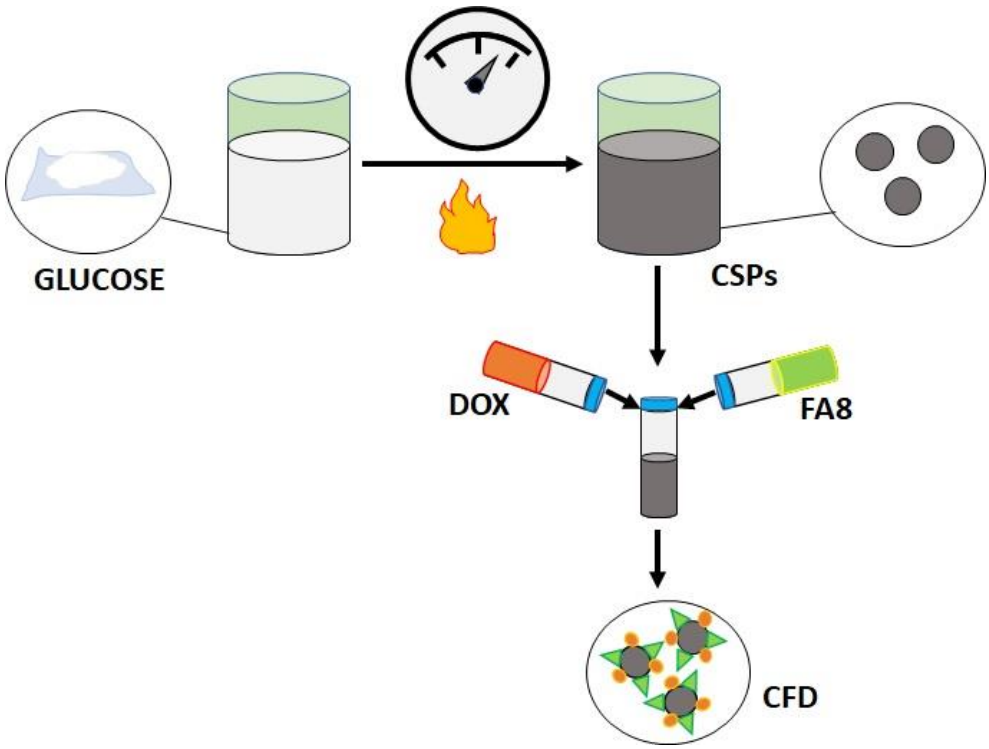

Fig.3.1. **Preparation of targeted delivery system CFD:** Above Schematic diagram represents the basic steps in the synthesis of CSPs from glucose under high temperature and pressure followed by their conjugation with DOX as well as Folate based lipid FA8.

- 5 mL of 1.5 mM solution of FA8 (M. wt. 757 g mol/l) was made using HPLC grade methanol. 10 mg of CSPs was added to the FA8 solution and kept stirring for 12 h at room temperature. CSPs were separated by centrifuging at 10,000 rpm for 10 min. The amount of FA8 adsorbed to CSPs was calculated from the amount present in the supernatant methanol solution of FA8 obtained by measuring the absorbance at 280 nm using a spectrometer at 27^{o}C. A prior calibration plot was obtained by measuring FA8 solutions at different concentrations for this purpose. About forty percent of FA8 was found adsorbed on 10 mg of CSPs. CSP-FA8-DOX (CFD) or CSP-DOX (CD) was prepared by adding 10 mg of CSP-FA8 or CSP to 5 mL of 2 mM methanol solution of DOX and it was stirred for 12 h at room temperature.
- The amount of DOX adsorbed to CSP conjugates (CSP-FA8 & CSP) was calculated by measuring the absorbance of DOX at 495 nm in the supernatant methanol solution. NMR (both 13C as well as proton) and Mass spectrometry were also done for FA8 to confirm its chemical identity (**Elechalawar & Bhattacharya et al.,2019**). Twenty percent DOX was loaded on the CSP surface as assessed by UV-Vis Spectrophotometry. The amount of DOX adsorbed to CSP conjugates (CSP-FA8 & CSP) was also calculated by measuring the HPLC area for DOX at 233 nm in the supernatant methanol solution. The amount of released DOX in supernatant as measured from the standard curve (DOX HPLC curve) was subtracted from total DOX added for reaction to obtain drug loading values in percentage. All samples (CFD,CD) were filtered using 0.45 µm syringe filter and then analyzed by HPLC(Shimadzu) with suitable dilution for estimation of drug content. A C-18 ZORBAX column(Agilent, USA) was used for separation using acidic (formic acid)buffer (pH 3) with (MeCN:MetOH) at 1:1 v/v as mobile phase in isocratic mode. Flow rate was maintained at 1ml/min

and PDA detector was used at 233 nm. The linearity response for DOX was calculated using a concentration range of 0-500 µg/ml.

- The drug release study was performed for targeted system CFD using the dialysis bag diffusion method for up to 36 hours. The drug release membrane bag (MWCO: 12-14 kDa, Himedia) was activated in PBS buffer pH 7.4 at 37°C for overnight. Thereafter, 3 ml of doxorubicin-loaded carbon sphere (CFD) was transferred into a dialysis bag and sealed with a plastic clip without leakage. This was followed by transfer into 250 mL BPS buffer which had been previously maintained at 37°C ± 0.5 °C temperature. The sample was kept thus on continuous stirring at 100 rpm. The sample was collected initially at 15 and 30 minutes followed by 1 hr, 2 hr, 4 hr, 6 hr, 8 hr, 12 hr, 24 hr and 36 hr time points respectively. 2 ml volume of release buffer was collected at each time point and an equal volume of fresh buffer was added or replaced for maintaining sink condition. All collected samples were eventually filtered using 0.45 µm syringe filter and then analyzed by HPLC(Shimadzu) with suitable dilution for estimation of drug content. A C-18 ZORBAX column(Agilent, USA) was used for separation using acidic (formic acid)buffer (pH 3) with (MeCN:MetOH) at 1:1 v/v as mobile phase in isocratic mode. Flow rate was maintained at 1ml/min and PDA detector was used at 233 nm. The linearity response for DOX was calculated using a concentration range of 0-500 µg/ml.
- The average particle size and the polydispersity of the particle-size distribution of the CSPs were determined by Zeta sizer. Empty CSPs or CSP with only DOX were used as controls. The homogenous distribution, surface morphology and diameter of the CSP conjugates were analysed by FE-SEM instrument (FEI TECHNAI 12).

3.8. Assessment of FR expression on OSCC cells & non-cancerous cells using western blot:

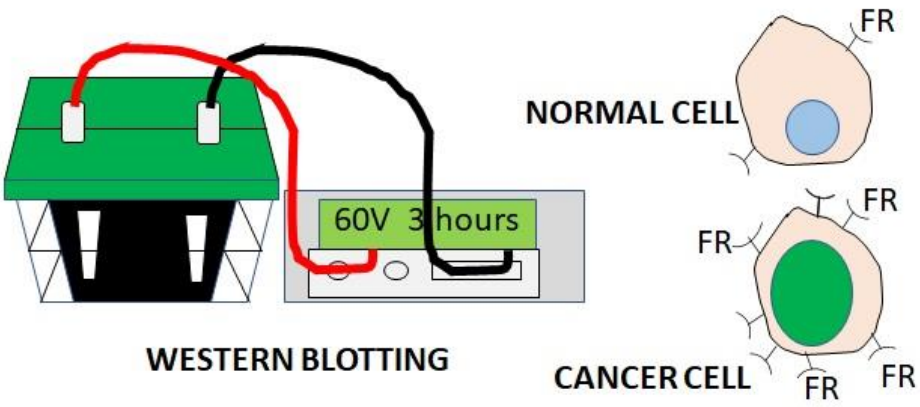

Fig.3.2. **Assessment of FR expression in OSCC & normal cells**: Schematic diagram representing the estimation of FR expression levels in both OSCC and non-cancerous cell lines using Western blot method. Higher expression of FR was evident in OSCC cells as compared to non-cancerous or normal cells.

- Cells were trypsinized from culture dishes and seeded in 6-well culture plates at a density of 3-5 x 10^5 cells/well.
- After 16-24 hours, cells were washed with 1X PBS and lysates were collected for protein studies using Laemmli buffer, pH 8. 60 µl of Laemmli buffer containing protease inhibitor cocktail was added to each well of a 6-well plate.
- Cells were incubated in Laemmli lysis buffer on ice for 10-15 minutes and sterile tips were used to collect the lysates from each well along-with cell debris into separate tubes.
- Lysates were centrifuged at 11000 rpm for 30 minutes at 4^0C and the supernatants were collected.

- Lysates thus obtained were assessed for protein concentration by the Bradford method, post which samples were prepared for loading with 2X loading dye and were boiled at 95^0C for 10 minutes in a dry bath before being loaded on a gel.
- For Folate pre-treatment studies, OSCC cells were seeded in a similar manner and treated with 100 µM of Folic acid for 30 minutes in Folate free culture media, post which, media was changed and any subsequent studies were continued under standard conditions, including collection of lysates at different time points as and when required.
- Amount of protein loaded for each protein sample was approximately 20µg (quantification done prior to loading as per Bradford method).
- SDS-PAGE gels were prepared with 12% resolving half. Proteins once run were transferred via the wet transfer method onto PVDF membranes which were subsequently blocked with 5% BSA (bovine serum albumin) for 1 hour.
- Post blocking, PVDF membrane was incubated with primary antibody at 4^0C overnight. The next day, membrane was washed with 1X PBST (0.1% Tween-20) and incubated with HRP-conjugated secondary antibody for 1-2 hours.
- Blots were then developed for chemiluminescence in Chemidoc imager.
- All target protein expression was normalized against respective internal control like β-Actin.

3.9. Drug uptake studies in 2D cell culture/in vitro samples:

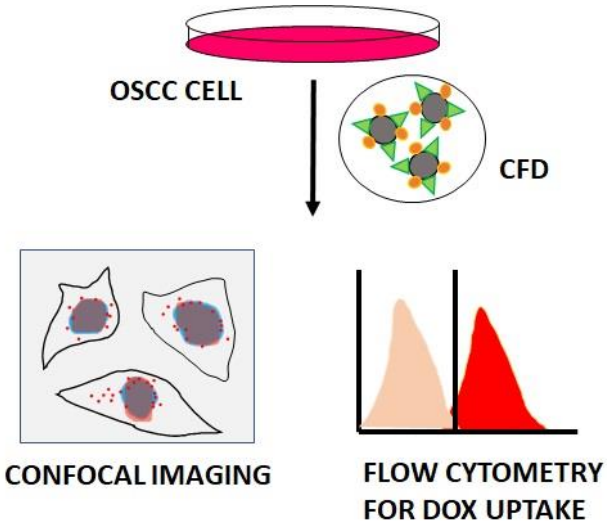

Fig.3.3. **DOX uptake in cells post targeted treatment:** Quantitation of DOX uptake was performed by Flow cytometry. Qualitative estimation as well as an assessment of intracellular compartmentalization of DOX in OSCC cells was performed by means of confocal microscopy.

3.9.1. Confocal imaging:

- Culture media was first aspirated out of the culture vessel and 1-2 washes given with 1X PBS (physiological buffer pH 7.2-7.4). Once wash was over, PBS was discarded and requisite amount of 0.25% Trypsin-EDTA was added (as suitable for the particular culture vessel).
- The culture vessel was then placed in the CO_2 incubator for 2-3 minutes till all cells could be found to have attained roundish morphology and floating, separated from their substratum.

- An equal volume of serum containing cell culture media (as much as the volume of Trypsin-EDTA used) was then added to the culture vessel to stop the action of Trypsin-EDTA. The cell suspension was then carefully collected in 15ml sterile centrifuge tubes and centrifugation was performed for 3-5 minutes at 1000 rpm (rotations per minute) to obtain cell pellet.
- The supernatant was shortly discarded and the pellet gently resuspended in requisite volume of culture media. Cell count was obtained from the suspension using a Neubauer's chamber.
- For qualitative confirmation of uptake, OSCC cell lines (FaDu, CAL27 and MOC2) were seeded in 6-well plates with square shaped coverslips (3-5 x 10^5 cells per well) inserted in them.
- After an incubation period of 12-16 hours cells were treated with CFD, CD and free drug (DOX) (6.4 µM drug equivalent).
- After 6 hours of treatment cells were washed with 1X PBS and fixed using 4% Paraformaldehyde for 15 minutes at room temperature. DAPI (0.5 mg/ml in 1X PBS) was added to each well and incubated for 15 minutes in dark for nuclear staining.
- Coverslips were then retrieved and mounted on glass coverslips with VECTASHIELD antifade mounting medium to produce permanent slides which were subsequently viewed under Confocal Microscope (Leica, Germany). Z-stacking was performed to assess degree or intensity of Doxorubicin localization signal in the nucleus.
- At least 5 different fields were visualized and captured for each sample or treatment group. Images were later analysed for fluorescence intensity using the Image J software.

- All fluorescence signal reads were normalized against their respective DAPI images wherever applicable.

3.9.2. Flow cytometry:

- OSCC cell lines FaDu, MOC2 & CAL27 alongside normal cell line HEK293 were selected for in vitro uptake studies.
- Cells were first checked for morphology as well as growth kinetics as reported previously by the selling agency (ATCC) and kept in a CO_2 incubator under standard conditions pertaining to CO_2, temperature and moisture conditions.
- Once cells were found to have reached 80-90% confluency, they were collected by mild trypsinization.
- Briefly, culture media was first aspirated out of the culture vessel and 1-2 washes given with 1X PBS (physiological buffer pH 7.2-7.4). Once wash was over, PBS was discarded and requisite amount of 0.25% Trypsin-EDTA was added (as suitable for the particular culture vessel).
- The culture vessel was then placed in the CO_2 incubator for 2-3 minutes till all cells could be found to have attained roundish morphology and floating, separated from their substratum.
- An equal volume of serum containing cell culture media (as much as the volume of Trypsin-EDTA used) was then added to the culture vessel to stop the action of Trypsin-EDTA. The cell suspension was then carefully collected in 15ml sterile centrifuge tubes and centrifugation was performed for 3-5 minutes at 1000 rpm (rotations per minute) to obtain cell pellet.

- The supernatant was shortly discarded and the pellet gently resuspended in requisite volume of culture media. Cell count was obtained from the suspension using a Neubauer's chamber.
- All cell lines were seeded in 12 well plates (1 x 10^5 cells per well) and allowed incubation under standard conditions overnight.
- Cells were then treated with targeted formulation CFD, non-targeted control CD and free drug (DOX) at a drug dose equivalent of 6.4 µM for 6 hours post which they were collected by mild trypsinization as described already and subsequently analyzed for drug uptake by Flow Cytometry.
- Flow cytometer (BD Aria III) was operated as per instructions provided in the respective instrument manual. 10,000 events were recorded for each sample analyzed and gating for all parameters was done with non-treated standards as blanks.
- Uptake of DOX was quantified in each sample as percentage of total population of cells with fluorescence beyond the gated threshold. Intensity of fluorescent signal or mean area under fluorescence was also obtained from respective sample histograms.

3.10. Studies for the assessment of targeted cancer cell death:

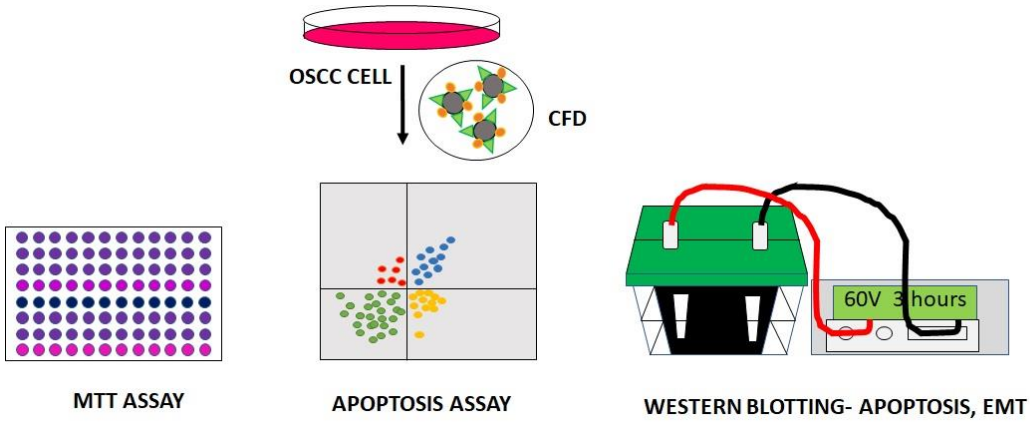

Fig.3.4. **Targeted cancer cell death and its underlying mechanisms**: Schematic diagram representing the different ways used to assess targeted OSCC cell death as induced by CFD. Figure involves three principal methods performed- MTT assay, Apoptosis assay (Live/Dead apoptosis kit) and western blot for markers pertaining to apoptotic and EMT pathways.

3.10.1. MTT assay:

- For cytotoxicity studies (MTT Assay), cells were trypsinized and seeded in 96-well culture plates at a density of 5-10,000 cells/well (depending on cell line) and incubated overnight
- Treatment was done with CFD (targeted formulation), CD (non-targeted formulation), free Doxorubicin, only CSP, CSP-F (CSP with FA8) and FA8(ligand). Treatment was administered at a concentration range of drug equivalent doses- 6.4μM, 3.2μM, 1.6 μM and 0.8μM.
- A media change was done at 6 hours post treatment and the culture plates kept back in incubation for the next 48 hours.

- After 48 hours, plates were added with MTT reagent (0.5 mg/ml) at 10ul for every 100ul of culture media.
- After addition of MTT reagent, culture plates were incubated for 3-4 hours and then retrieved. Culture media in the wells was carefully taken out and discarded.
- 100 µl of reagent grade DMSO was added to each well and the plate was placed on an orbital shaker for 10 minutes to ensure sufficient dissolution of Formazan crystals.
- Plates were subsequently kept covered in aluminum foil to avoid direct light exposure and processed for measurement of Absorbance values at 570 nm using an ELISA plate reader (Perkin Elmer).
- After subtracting O.D. for blank wells percent viability for each sample was calculated where untreated sample was considered as 100 % viable.

3.10.2. Apoptosis assay/Annexin V-FITC assay:

- For Flow cytometry-based study of Apoptosis, cells were trypsinized and seeded in 12-well plates (1-3 x 10^5 cells/well), for 16-24 hours.
- Treatment was then done with CSP formulations/groups as well as free drug (6.4 µm Doxorubicin).
- After 24 hours of treatment, cells were washed and collected by mild trypsinization and subsequently processed for Annexin V-FITC assay as per kit instructions (Apoptosis detection Kit, Invitrogen).
- Briefly, cells obtained by trypsinization were resuspended in 100ul 1X binding buffer (each sample) containing 5ul of Annexin V-FITC stain and 1 µl of PI (Propidium Iodide) working solution.

- Cells were kept thus in the dark at room temperature for 20 minutes and then 400 µl of binding buffer was added further to each sample tube.
- These tubes were then placed on ice and subsequently analyzed using BD FACS Aria III as per standard protocol.
- Respective percentages of early and late apoptotic cell populations were thus obtained from the Flow cytometry output where 10,000 events were counted for each sample analyzed.

3.10.3. Assessment of cell death by western blot:

- Cells were trypsinized from culture dishes and seeded in 6-well culture plates at a density of 3-5 x 10^5 cells/well.
- After an overnight incubation, cells were treated with different CSP formulations as well as free drug DOX and incubated for 6 hours. Media in the wells was then changed and the plate was incubated for the next 24 hours.
- After 24 hours, cells were washed with 1X PBS and lysates were collected for protein studies using Laemmli buffer, pH 8. 60 µl of Laemmli buffer containing protease inhibitor cocktail was added to each well of a 6-well plate.
- Cells were incubated in Laemmli lysis buffer on ice for 10-15 minutes and sterile tips were used to collect the lysates from each well along-with cell debris into separate tubes.
- Lysates were centrifuged at 11000 rpm for 30 minutes at 4^0C and the supernatants were collected.

- Lysates thus obtained were assessed for protein concentration by the Bradford method, post which samples were prepared for loading with 2X loading dye and were boiled at 95^0C for 10 minutes in a dry bath before being loaded on a gel.
- For Folate pre-treatment studies, OSCC cells were seeded in a similar manner and treated with 100 µM of Folic acid for 30 minutes in Folate free culture media, post which, media was changed and any subsequent studies were continued under standard conditions, including collection of lysates at different time points as and when required.
- Amount of protein loaded for each protein sample was approximately 20µg (quantification done prior to loading as per Bradford method).
- SDS-PAGE gels were prepared with 12% resolving half. Proteins once run were transferred via the wet transfer method onto PVDF membranes which were subsequently blocked with 5% BSA (bovine serum albumin) for 1 hour.
- Post blocking, PVDF membrane was incubated with different primary antibodies at 4^0C overnight. The next day, membranes were washed with 1X PBST (0.1% Tween-20) and incubated with HRP-conjugated secondary antibodies for 1-2 hours.
- Blots were then developed for chemiluminescence in a Chemidoc imager.
- All target protein expression was normalized against respective internal control like β-Actin.

3.11. In vivo studies to assess tumour and TAM attenuation:

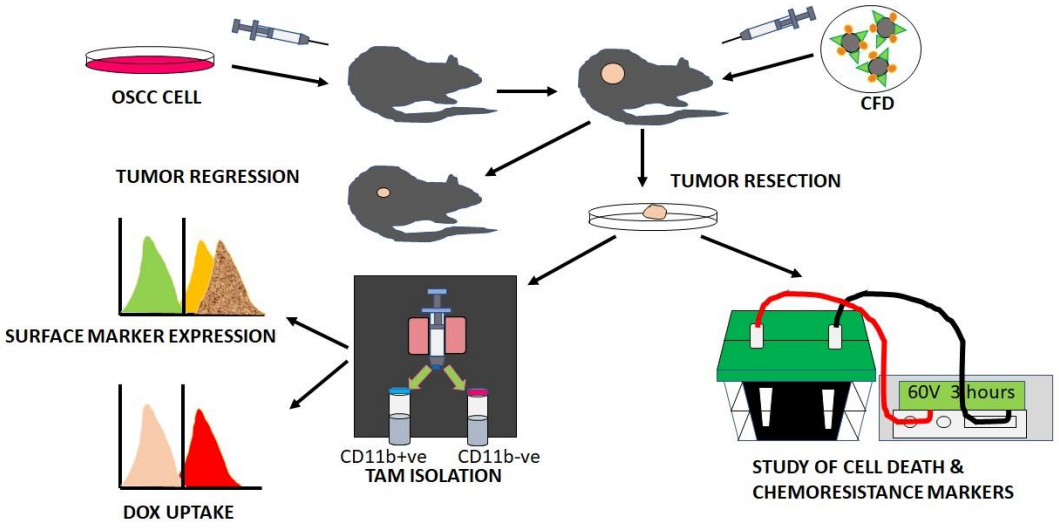

Fig.3.5. **Assessment of tumor and TAM targeted therapeutic outcome using animal model of aggressive OSCC**: Experimental outline for assessment of tumour and TAM attenuation. Experiments include TAM isolation and characterization, tumour regression study and western blotting for markers pertaining to chemoresistance, cell death and TAM attenuation.

3.11.1. Tumour regression study:

- $3x10^6$ cells of MOC-2(Mouse OSCC cell line) were injected subcutaneously into the right flank of female C57/BL6J mice (5-6 weeks).
- Tumour of approx. volume 50 mm^3(average) were observed on the 7th day post tumour cell inoculation.
- Mice were then randomly divided into groups and treated with CFD, CD, DOX, CSP & FA8 (5mg/kg Doxorubicin drug equivalent) intraperitoneally for 5 alternate dosings.

- Tumour size was measured every two days using vernier callipers and tumour volume calculated using the formula 1/2 x a x b^2 (where a= long axis, b=short axis of tumour).
- Mice were sacrificed on day 23 post tumour inoculation and tumours collected. Body weight measurement was also maintained every 3-4 days throughout the study starting a day before initiating treatment schedule.
- Tumour volumes of all animals in each group were recorded and tabulated till the end of the study marked by animal sacrifice. Post tumour and organ collection, all tumour dimensions and volumes tabulated and recorded till then were calculated to yield day-wise average tumour volume for each treatment group which were then compared for any statistically significant difference.
- Records for mice bodyweight were recorded in the same manner and tabulated at the end of the study.

3.11.2. Investigation of markers pertaining to cell death, chemoresistance and TAM attenuation:

- Tumour tissues were first isolated after animal sacrifice on day 20 post tumour inoculation and incubated in RIPA buffer supplemented with Protease Inhibitor cocktail on ice.
- Tissues were then lysed in RIPA by means of mechanical disaggregation at low temperatures using a bead beater (Bertin MiniLys from Bertin Corp., Rockville, USA).

- Disaggregated tissue suspensions in buffer were subsequently centrifuged at 12000rpm for 10 minutes (at 4 degrees) and the supernatant was collected and quantified for total protein concentration by the Bradford method.
- Amount of protein loaded for each protein sample was approximately 30 µg.
- SDS-PAGE gels were prepared with 12% resolving half. Proteins once run were transferred via the wet transfer method onto PVDF membranes which were subsequently blocked with 5% BSA (bovine serum albumin) for 1 hour.
- Post blocking, PVDF membrane was incubated with different primary antibodies at 4^0C overnight. The next day, membranes were washed with 1X PBST (0.1% Tween-20) and incubated with HRP-conjugated secondary antibodies for 1-2 hours.
- Blots were then developed for chemiluminescence in a Chemidoc imager.
- All target protein expression was normalized against respective internal control like β-Actin.

3.11.3. Study of in vivo drug uptake and TAM attenuation via flow cytometry:

- $3x10^6$ cells of MOC-2(Mouse OSCC cell line) were first counted and injected subcutaneously into the right flank of female C57/BL6J mice (5-6 weeks).
- Tumour of approx. volume 50 mm^3(average) were observed on the 7th day post tumour cell inoculation.
- Mice were then randomly divided into groups and treated with CFD, CD, DOX, CSP & FA8 (5mg/kg DOX) intraperitoneally.
- Tumours were collected from mice post sacrifice on Day 12 post tumour inoculation (after 3rd dosing) were kept on ice in 1X PBS and subsequently minced into tiny pieces using a short and sterile scalpel blade.

- These pieces were collected in a 50 ml centrifuge tube and subjected to treatment with Collagenase-I (1 mg/ml) at RT for 10 minutes.
- Enzymatic treatment was then neutralized using tissue culture media containing serum and the whole suspension was ground and washed into a fresh centrifuge tube over a 70 µm strainer.

3.11.3.a. Study of drug uptake in tumour/TAM:

- The uniform suspension thus obtained was processed by Flow cytometry for drug uptake studies.
- In case where TAM and non-TAM populations were to be separated and compared for drug uptake and expression levels for specific surface markers, whole tumour suspensions were further subjected to separation using CD11b coated magnetic beads by the MACS separator and columns (Miltenyi).
- Separated cell populations were further assessed for drug uptake or TAM marker expression studies as required using Flow cytometer (BD).
- For drug uptake, populations of CD11b-positive and negative cells were analyzed the same way as trypsinized cells obtained from 2D cultures.

3.11.3.b. Study of TAM-specific surface marker expression:

- For studies pertaining to expression levels of TAM or other cell specific surface markers, staining was performed with requisite fluorescence-tagged primary antibodies (commercially obtained) for Flow cytometry.
- Briefly, 1-2 x 10^5 cells were taken in each tube and stained with the specific tagged antibody for 20-30 minutes while being kept in the dark at 4^0C.

- After this, cells were pelleted by gentle centrifugation and washed with 1X PBS for the removal of unbound antibodies which could cause background signal.
- Stained cells were then suspended in 1X PBS and analyzed by Flow cytometry.
- DOX uptake as well as specific surface marker expression were quantified as percentage of total cell population analyzed.

3.11.4. Histopathological studies for the assessment of systemic toxicity after treatment:

- $3x10^6$ cells of MOC-2(Mouse OSCC cell line) were injected subcutaneously into the right flank of female C57/BL6J mice (5-6 weeks).

  Tumour of approx. volume 50 mm^3(average) were observed on the 7th day post tumour cell inoculation.
- Mice were then randomly divided into groups and treated with CFD, CD, DOX, CSP & FA8 (5mg/kg Doxorubicin drug equivalent) intraperitoneally for 5 alternate dosings.
- Tumour size was measured every two days using vernier callipers and tumour volume calculated using the formula $1/2 \times a \times b^2$ (where a= long axis, b=short axis of tumour).
- Mice were sacrificed on day 23 post tumour inoculation and tumours collected. Body weight measurement was also maintained every 3-4 days throughout the study starting a day before initiating treatment schedule.
- Organs (heart, liver, kidney and spleen) were collected were washed in 1X PBS and subsequently fixed by immersing in 4% PFA (paraformaldehyde).

- After overnight incubation in PFA at 4 degrees, specimens were washed once more with 1X PBS and stored at -80 degrees by immersing in 1X PBS containing 20% glycerol(volume/volume).
- Tissue samples were subsequently paraffin embedded and sectioned for H&E staining (Haematoxylin & Eosin). Stained samples were prepared for visualization under bright field microscope and analyzed subsequently for required parameters.

3.12. Ex-vivo studies on OSCC 3D spheroids:

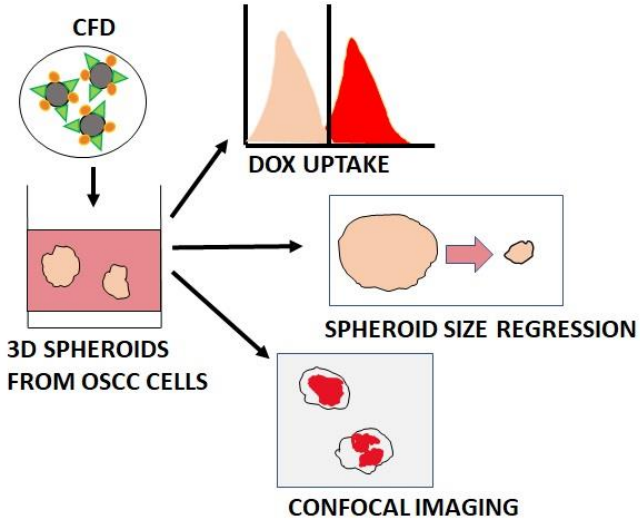

Fig.3.6. **Assessment of the effects of targeted DOX delivery on 3D spheroids of OSCC**: A schematic diagram representing ex-vivo studies on 3D spheroids of OSCC cells which encompass drug uptake, size regression as well as confocal imaging studies.

3.12.1. Studies to assess drug uptake in 3D spheroids:

3.12.1.a. Flow cytometry:

- For spheroid-based drug uptake studies, tumour spheroids were first cultured by seeding cells in 12 well culture plates ($1x10^5$cells per well) coated with low melting point agarose (0.6%).
- Briefly, cells were collected by mild trypsinization once they were 80-90% confluent and counted using the Neubauer's chamber. Low melting agarose was diluted in cell 1X culture media and kept warm at 55-60^0C so that it stayed fluid for plating. 200 µl of molten agarose was then added to each well in a laminar air flow hood under

sterile conditions and the culture dish placed in the incubator for 4-6 ours to allow the agarose to solidify.

- Cell suspension obtained by mild trypsinization and counted to a pre-determined number were then added to each agarose-coated well.
- Cells which could not attach on account of agarose coating either died or started giving rise to 3-D spheroids on Day 2-3 post seeding.
- Counting the day of seeding as day 0, spheroids were treated on day 3 with CFD, CD or DOX (6.4 µm DOX equivalent) for 24 hours and 48 hours.
- Spheroids were then harvested at these pre-designated time points and broken down into single cell suspensions by mild treatment with Trypsin-EDTA (0.5%) as well as light tapping.
- Cell suspension thus obtained was then freshly carried on ice and analyzed for drug uptake by Flow cytometry as in case of in vitro samples.

3.12.1.b. Confocal imaging:

- For spheroid-based drug uptake studies, tumour spheroids were first cultured by seeding cells in 12 well culture plates ($1x10^5$cells per well) coated with low melting point agarose (0.6%) as described earlier.
- Cells which could not attach on account of agarose coating either died or started giving rise to 3-D spheroids suspended in culture medium.
- Counting the day of seeding as day 0, spheroids were treated on day 3 with CFD, CD or DOX (6.4 µm DOX equivalent) for 6 hours.
- Spheroids were then fixed within their dishes with 2% paraformaldehyde and taken out carefully.

- Whole spheroids(fixed) were then mounted on glass slides and placed under coverslips with mounting media. Specimens were sealed to cut off air exposure.
- Slides were visualized under Confocal Microscope (Leica, Germany) under 20X magnification.

3.12.2. Study of effects of targeted therapy on 3D spheroid size:

- For spheroid-based drug uptake studies, tumour spheroids were first cultured by seeding cells in 12 well culture plates ($1x10^5$cells per well) pre-coated with low melting point agarose (0.6%).
- Cells which could not attach on account of agarose coating either died or started giving rise to 3-D spheroids suspended in culture medium.
- Counting the day of seeding as day 0, spheroids were treated on day 3 with CFD, CD or DOX (6.4 µm DOX equivalent) for 24 hours and 48 hours.
- Snapshots of these spheroids were subsequently obtained using a bright field microscope at 24 hour and 48-hour time points.
- 3-4 optical fields per well were imaged and captured. These images were later exported and spheroids were measured for long axis (a) and short axis (b) using Image-J software.
- Volumes for spheroids were calculated using the formula $0.5 \times a \times b^2$and compared between groups.
- Average spheroid size was attained for each treatment group and tabulated for comparison and analysis.

3.13. Statistical analysis:

Image J software was used to measure band intensities from Western blot images. Students t-test was performed to calculate statistical significance wherever necessary. All data were represented as Average ± SEM wherever applicable. All experiments were performed in triplicate and the average values obtained from triplicate experiments were evaluated for significance. A minimum of $p<0.05$ for any data was considered statistically significant.

Advanced nanomaterials are needed for improved drug delivery. To utilise the substantial therapeutic promise of nanomaterials, surface functionalization has to be performed. These include antibody conjugation, small molecule labelling, functionalization with biologically active targeting molecules etc. towards facilitating efficient and promising imaging and therapy. Hence, the general challenge in surface modification of nanocarriers lies in designing multifunctional small molecules or fabricating bioactive large molecules.

Among the HNSCC family of cancers, oral squamous cell carcinoma (OSCC), which is highly invasive and difficult to diagnose has been shown to inflict maximum mortality in patients (**Kademani, 2007**). The overall aggressiveness of OSCC is not only due to the tumour-associated malignant cells but also due to a special tumour-associated micro-environment (TME) created within the tumour mass. TME consists of malignant cancer cells, various heterogeneous cell components including cancer stem cells, tumour-associated vascular endothelial cells, lymphatic cells and also macrophages. Among them, the tumour-associated macrophages (TAMs), the most abundant immune cells in the tumour-mass, play a predominant role in tumour pro-proliferation, cell invasion, metastasis, angiogenesis, immunosuppression etc. OSCC-associated cancer stem cells promote tumour supportive TAM by secreting periostin that aids in TAM recruitment and polarization (**Siriwardena et al.,2006**). TAMs are differentiated monocytes that form in response to tumour-derived chemo-attractants such as M-CSF-1 (macrophage colony stimulating factor-1), various chemokines CCL2/3/4/5/9 and VEGF. Levels of these proteins in the tumour mass proportionately relate to overall TAM count in the tumour environment, although no correlation has been obtained between TAM count and patient prognosis. However, a majority of studies have showed that high TAM numbers are often linked with reduced patient survival. Many TME-associated factors and their corresponding receptors

expressed on TAMs work in tandem to maintain the overall aggressiveness. One such incidence is the involvement of expressed CSF-1 receptor (CSF-1R) that helps in survival of TAM. On depletion of CSF-1R, the intracranial GBM propagation was found to be halted (**Pyonteck et al.,2013**). However, the TAM population did not deplete, as expression of other survival factors gained importance. The invasiveness of OSCC mass is due to functional expression of many factors including TAM-expressed TGFβ, which in turn up-regulates STAT3 via IL-6 in cells of tumour mass (**Jensen et al.,2015**). Clearly, the direct target should be TAM for effective and long-term therapeutic benefit. Hence, TAM-targeting is increasingly gaining importance. Recently, TAM has been found to act as slow-release reservoir for nano formulation-delivered-drug to tumour mass (**Miller et al.,2015**).

More recently, carbon nanospheres are gaining attention due to their applications in various fields including drug delivery (**Nieto-Márquez et al.,2015**). Among them, glucose-derived CSPs are emerging as a new class of intracellular drug carriers in drug delivery. These apparently non-toxic CSPs are readily dispersible in water, can target cell nuclei and have the unique property of crossing the blood- brain barrier (BBB) in vivo (**Selvi et al.,2008**). Folate receptors (FR), the glycosyl phosphatidyl inositol (GPI)-anchored protein, are expressed on the surface of cell membrane and are often overtly expressed in many cancers as well as on TAM membrane surface (**Retnakumari et al.,2009**). As FR binds and internalises folate or folic acid into cells, folate targeted delivery systems especially for targeting FR-over expressing cancer cells are well known. FR-targeted drug/gene nano delivery systems are reported against OSCC tumours (**Fan et al.,2020**). However, the importance of targeting TAM for OSCC treatment is not adequately emphasized in a majority of those studies.

Here we describe the use of folate ligand-associated CSP for targeting FR-overexpressing tumour associated malignant cells and TAM. This ligand is cationic lipid modified folic acid and hence will strongly bind via electrostatic interactions to negatively charged CSP. With a high surface concentration of cationic folate, the targeted CSP showed enhanced tumour cell and TAM targeting simultaneously. Armed with a model anticancer drug Doxorubicin (DOX), the targeted nano-formulation exhibited significant tumour cell killing, tumour regression, and M2 TAM attenuation. Here, we found indication of DOX-mediated chemoresistance being by-passed along-with favourable findings in 3D-spheroid based ex-vivo studies. This dual strategy of targeting TAM and malignant cells exhibited overall improved outcome in an immunocompetent mouse model of aggressive oral cancer.

4.1. Preliminary characterization prior to synthesis of CSP conjugates:

Synthesis of FA8 was accomplished as per synthetic protocol described earlier (**Elechalawar et al.,2017**). CSP synthesis was accomplished as per the protocol described earlier (**Selvi et al.,2008**). C8 control molecule was prepared and characterized through 1HNMR and ESI mass (**Fig. 4.1**). CSP was then simultaneously associated with F8 and DOX or, only DOX. The sizes of CSP-FA8-DOX (CFD), CSP-DOX (CD) respectively were found in the range of 360 nm. Polydispersity index (PDI) of such CSP conjugates were less than 0.3, thereby clearly indicating the fairly homogenous size distribution of CSP conjugates. CFD was found to be stable in the presence of a varying range of serum concentrations (**Fig. 4.2-A**) IR spectra studies of CSP and their conjugated products indicated the association of ligands and/or drugs on CSP (**Fig. 4.2-B**).

A)

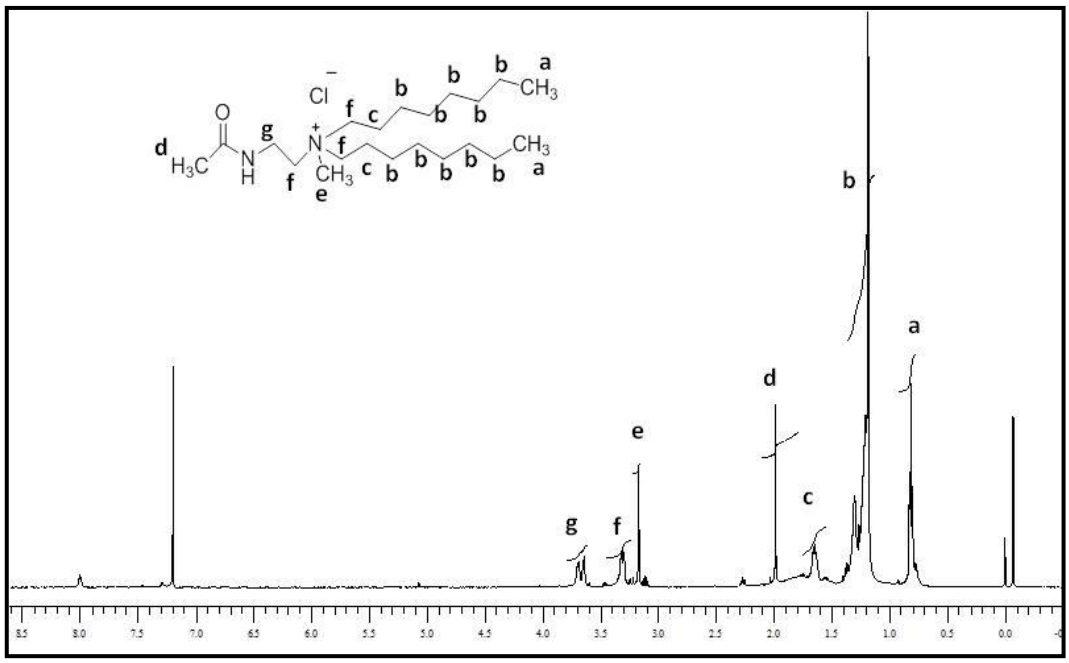

B)

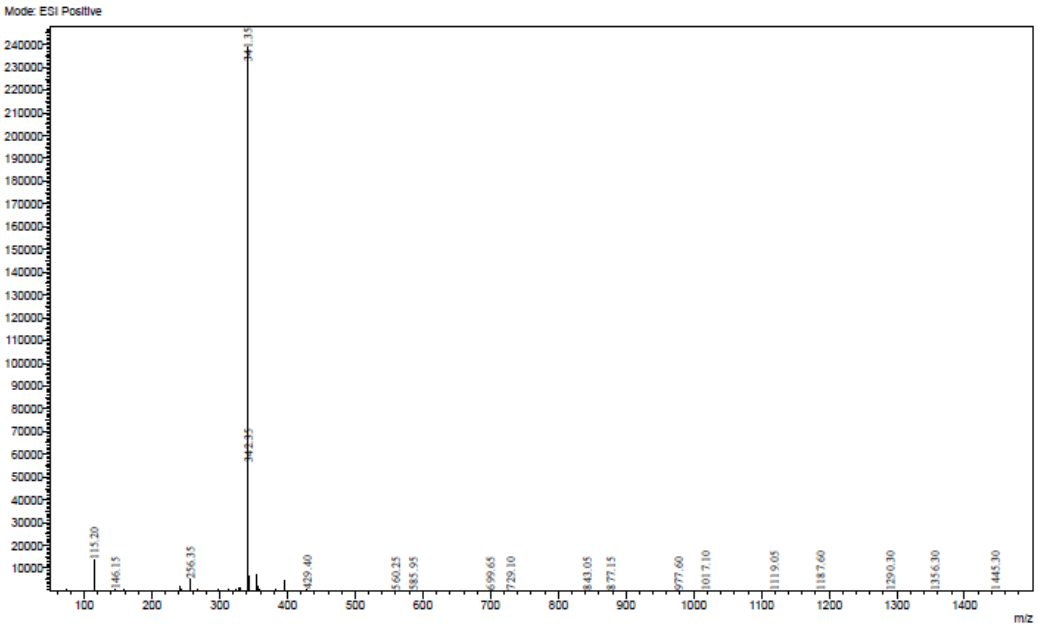

Fig.4.1. **ESI-Spectra and NMR**: Panel (A) 1H-NMR (300 MHz, CDCl3) Spectra of C8. Panel (B) ESI- Mass Spectra of C8. (**Elechalawar & Bhattacharya et al.,2019**)

A)

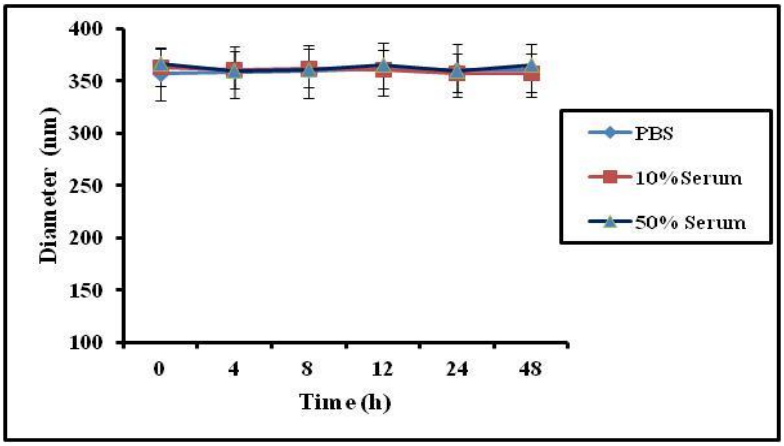

B)

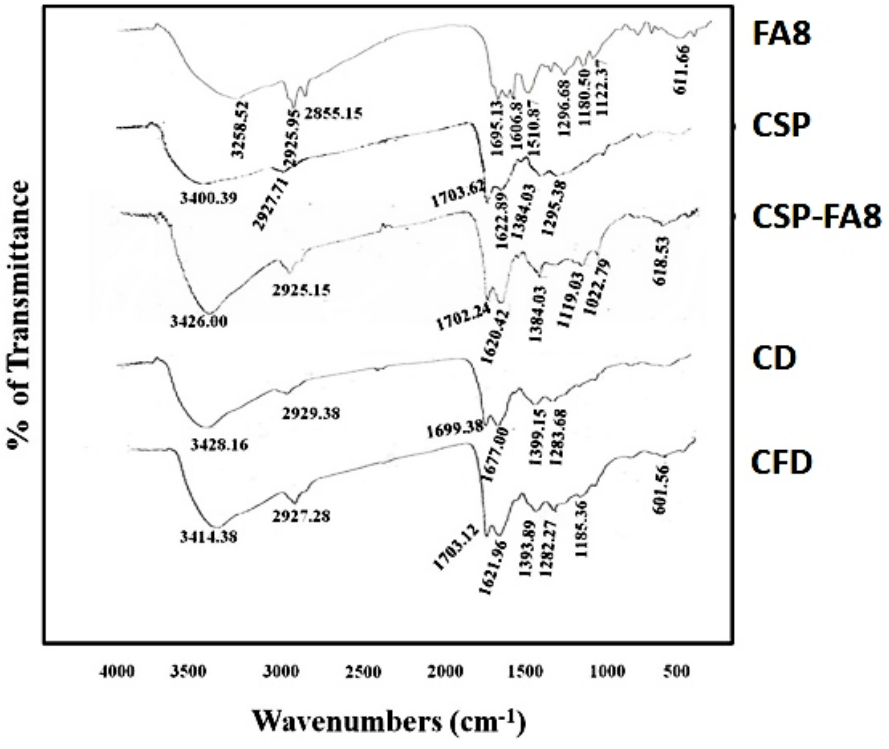

Fig.4.2. **Serum stability and FTIR- based characterization of CSP formulations: A)** Stability of CFD in different serum concentrations along with PBS. **B)** FTIR- Spectrum of different CSPs along with FA8. (**Elechalawar & Bhattacharya et al.,2019**)

The associated FA8 was ~32 percent (wt./wt.) or more with respect to CSP while DOX entrapments on CSP-F8 and CSP surfaces were in between 20-30 percent with respect to weight of CSPs. Drug absorption spectra were also generated for assessment of drug binding at later stages (**Fig. 4.3-A**). Besides FTIR-based estimation of CSP-ligand or CSP-drug conjugation, UV-Visible spectra for all CSP conjugates were also performed (**Fig. 4.3-B**).

4.2. Preparation and characterization of CSP conjugates:

Carbon nanospheres (CSPs) were synthesized according to a previously published protocol (**Elechalawar & Bhattacharya et al.,2019**). Synthesis of Folate based ligand FA8 was accomplished as per a synthetic protocol reported by us earlier (**Elechalawar et al.,2017**). These CSPs were then simultaneously conjugated with FA8 and DOX both, or only DOX .

The hydrodynamic diameter (size) and surface charge (zeta potential) of CSP-FA8-DOX (CFD), CSP-DOX (CD) and CSP were measured by electrophoretic mobility using a Zeta sizer (Malvern, UK). The sizes of CSP-FA8-DOX (CFD) and CSP-DOX (CD), respectively, are in the range of 340-360 nm (**Table 4.1**). The size of DOX and FA8-conjugated CSP [i.e., CFD] is stable up to 48 h in 50% serum in PBS. Additionally, SEM images show a homogeneously spherical structure for both conjugated systems CFD and CD (**Fig4.4-A**). Carbon-nanospheres have been recorded as having size up to 500 nm diameter, which is more than what was recorded in case of glucose derived CSPs in this case (Diez et al.,2021). An overall decrease in surface charge of CSP followed the conjugation with DOX.

About forty percent of FA8 was adsorbed on 10 mg of CSPs. CSP-FA8-DOX or CSP-DOX was prepared by adding 10 mg of CSP-FA8 or CSP to 5 mL of 2 mM methanol solution of DOX and it was stirred for 12 h at room temperature. The CSP conjugates were separated by

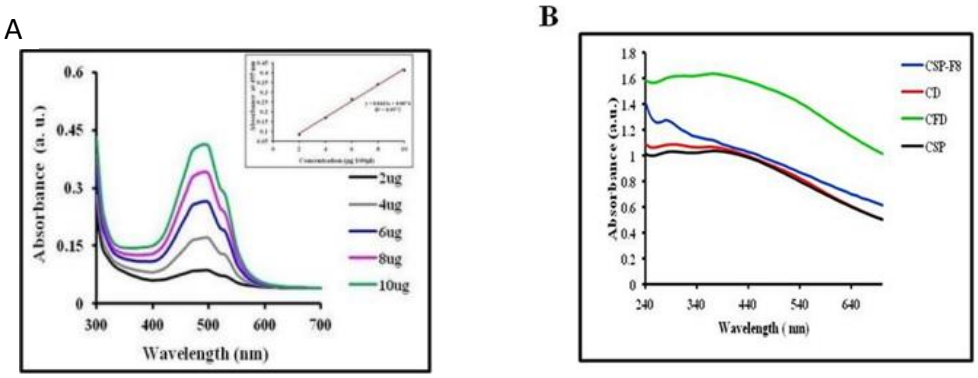

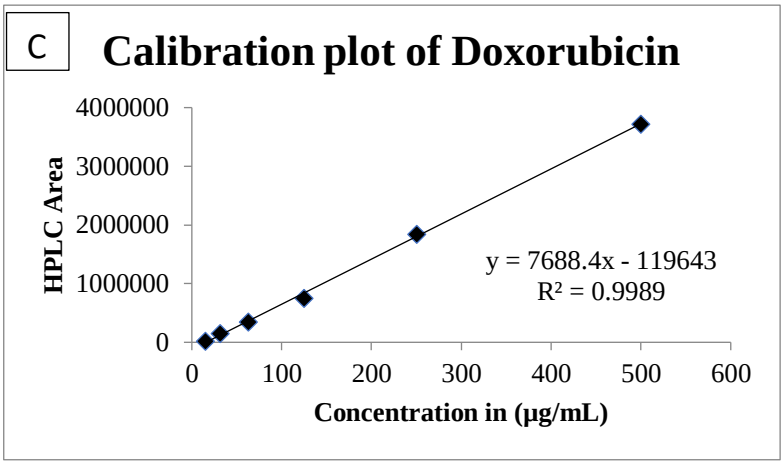

Formulations	Drug Loading
Formulation_CD	15.2 ± 0.66%
Formulation_CFD	24.3 ± 0.27%

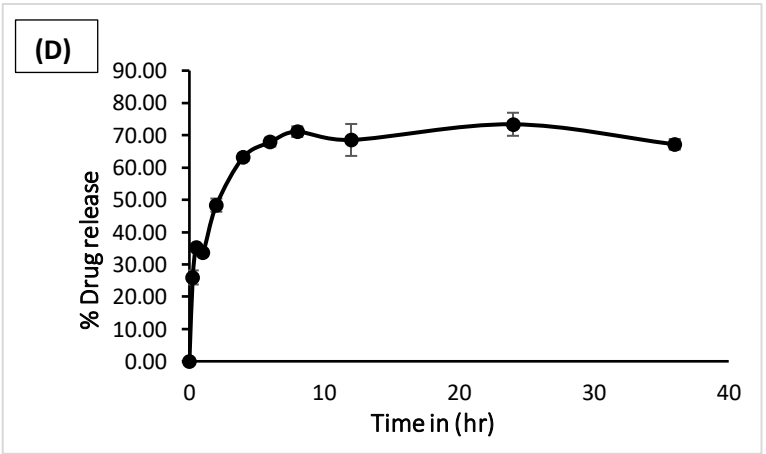

Fig.4.3. **DOX loading results and UV-VIS based characterization of CSP formulations**: A) Dose dependent absorption spectra of DOX. Absorption starts at 300-700nm.with abs max at 495nm. Corresponding standard curve for the confirmation of drug loading as an inset.

B) UV-VIS spectra of different CSP conjugates. (**Elechalawar & Bhattacharya et al.,2019**) C) Standard curve plotted to estimate DOX release with a range of drug concentrations. CFD was found to have a slightly higher drug loading at 24.3 ± 0.27% and CD at 15.2 ± 0.66% D) In vitro drug release profile of DOX from CSP formulation CFD in PBS (pH 7.4) at 37oC. Each point on the curve represents Average ± SEM values.

centrifugation. The amount of DOX adsorbed to CSP conjugates (CSP-FA8 & CSP) was calculated by measuring the absorbance of DOX at 495 nm in the supernatant methanol solution (**Fig. 4.5-B**). Approximately twenty percent DOX was found to have been loaded on the CSP surface (**Table 4.2**). However, HPLC based drug loading studies also revealed CFD to have a slightly higher drug loading at 24.3 ± 0.27% and CD at 15.2 ± 0.66%. As regards the release profile, the released amount of drug from DOX solution was quite negligible which is why it is not represented in the graph (**Fig 4.3-D**). A sharp spike of drug release was recorded for CFD at 30 minutes with 35.28 ± 0.79% release of DOX. From there onwards a gradual rise in drug release was recorded upto 24 hours at 73.39 ± 3.57% which indicated a sustained release pattern.

4.3. Expression of folate receptor in OSCC cells:

Our first requirement was to check for FR1 expression in all OSCC cell lines as well as in normal cell line to make sure that FR would be a valid candidate for cancer cell targeted therapeutic studies. All cell lines were treated with 100 µM Folate for 30 minutes after which media was changed. Lysates were collected for western blotting at different time

points post Folate (FA) treatment and subsequent media change (immediately, i.e. 0 hours, 3 hours and 5 hours). FR1 is present in two principal forms in a cell; a membrane bound p-glycoprotein as well as a free or circulating (solubilized) form once it binds with its ligand**.** In this folate treated condition, we assumed that any FR1 signal would primarily indicate levels pertaining to its freely circulating form. Western blots showed an increase in levels of FR1 (soluble form) immediately after 30 minutes of FA treatment, while being low or negligible in untreated samples. Receptors that are not exposed to ligand shall pre-dominantly remain as membrane-bound, thus accounting for low expression levels upon immunoblotting. Conversely, expression levels go up sometime after exposure to ligand (30-minutes lysates). However, expression levels were found to go down again gradually with time as the freely circulating receptors once again got recycled and were sent back to be re-instated as membrane bound receptor protein (**Fig.4.6**).

Flow cytometry revealed a similar pattern of expression. However, basal level of expression for FR1 in HEK293 normal cells was found to be much lower than what we found in OSCC cell lines FaDu, CAL27 and MOC2.

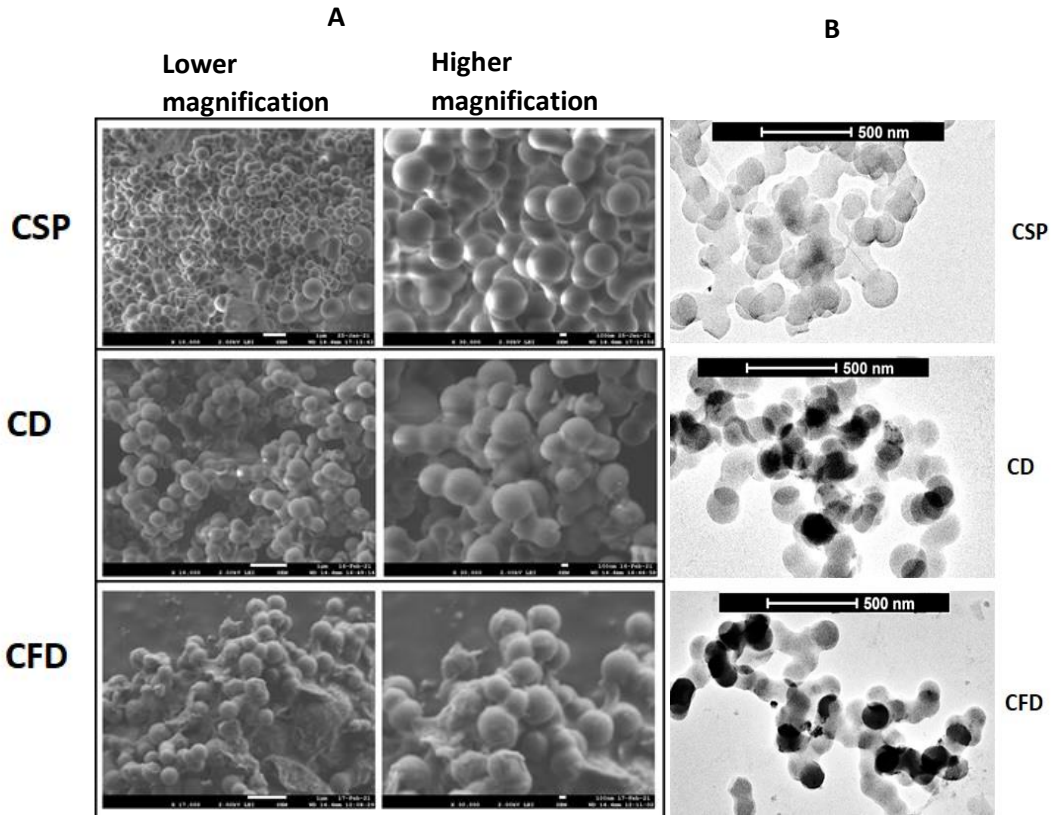

Fig.4.4. **SEM & TEM based characterization of CSP formulations**: (A) **Left panel**- SEM images at lower(left) and higher(right) magnifications (B) **Right panel-** TEM images for unconjugated & drug conjugated nanospheres.

Table 4.1. DLS based characterization of CSP formulations: Determination of size, zeta potential and PDI values for all CSP formulations as measured using Zeta-sizer

S. No.	Formulation	Hydrodynamic diameter (nm)	Zeta potential (mV)	PDI
1.	CSP	372.23 ± 35	-40.1 ± 0.3	0.23 ± 0.02
2.	CD	350.41 ± 38	-28.2 ± 0.3	0.18 ±0.06
3.	CFD	361.12 ± 42	-24.6 ± 0.4	0.27 ±0.08

4.4. Uptake of targeted carbon nanospheres in cancer cells is via the Folate Receptor

It was necessary for us to ascertain whether the uptake of ligand conjugated formulation CFD in cancer cells was indeed via the FR as intended. For this purpose, we pre-treated OSCC cells *in vitro* with 100 µM Folate for 30 minutes and then treated the cells as earlier with targeted, CFD and non-targeted, CD formulations. As control treatments, we also kept groups which underwent similar treatment but without any Folate pre-treatment. As seen in (**Fig. 4.7, Panel I),** there was significant difference in uptake (as quantitated by Flow Cytometry) between FA-pre-treated group and the group without any pre-treatment, especially with regards to CFD. This finding bears well with our hypothesis that CFD would be favoured for entry in cancer cells over CD specifically on account of its ligand-conjugated status and the overexpressed state of the FR in target OSCC cells.

A)

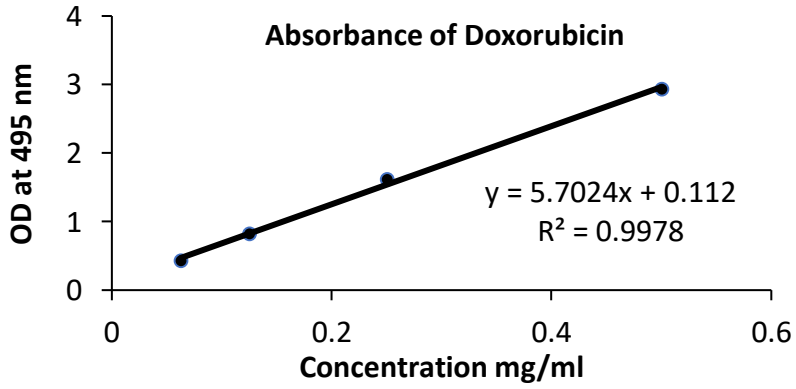

B)

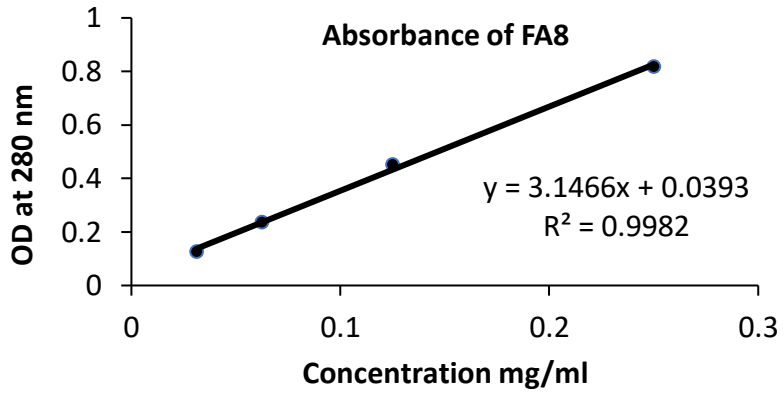

Fig.4.5. Preparation of DOX and FA8 standard curves based on absorbance at different wavelengths: Standard curves for calculation of concentration of (A) Doxorubicin and (B) FA8 at 495nm and 280nm respectively.

Table.4.2. Quantity of DOX and FA8 per unit amount of CSP formulation: Table representing DOX and FA8 concentrations in different CSP based formulations.

S. No.	Formulation	Quantity (mg)	Quantity of DOX (µg)	Quantity of FA8 (µg)
1.	CSP	1	-	-
2.	CD	1	113	-
3.	CFD	1	113	200

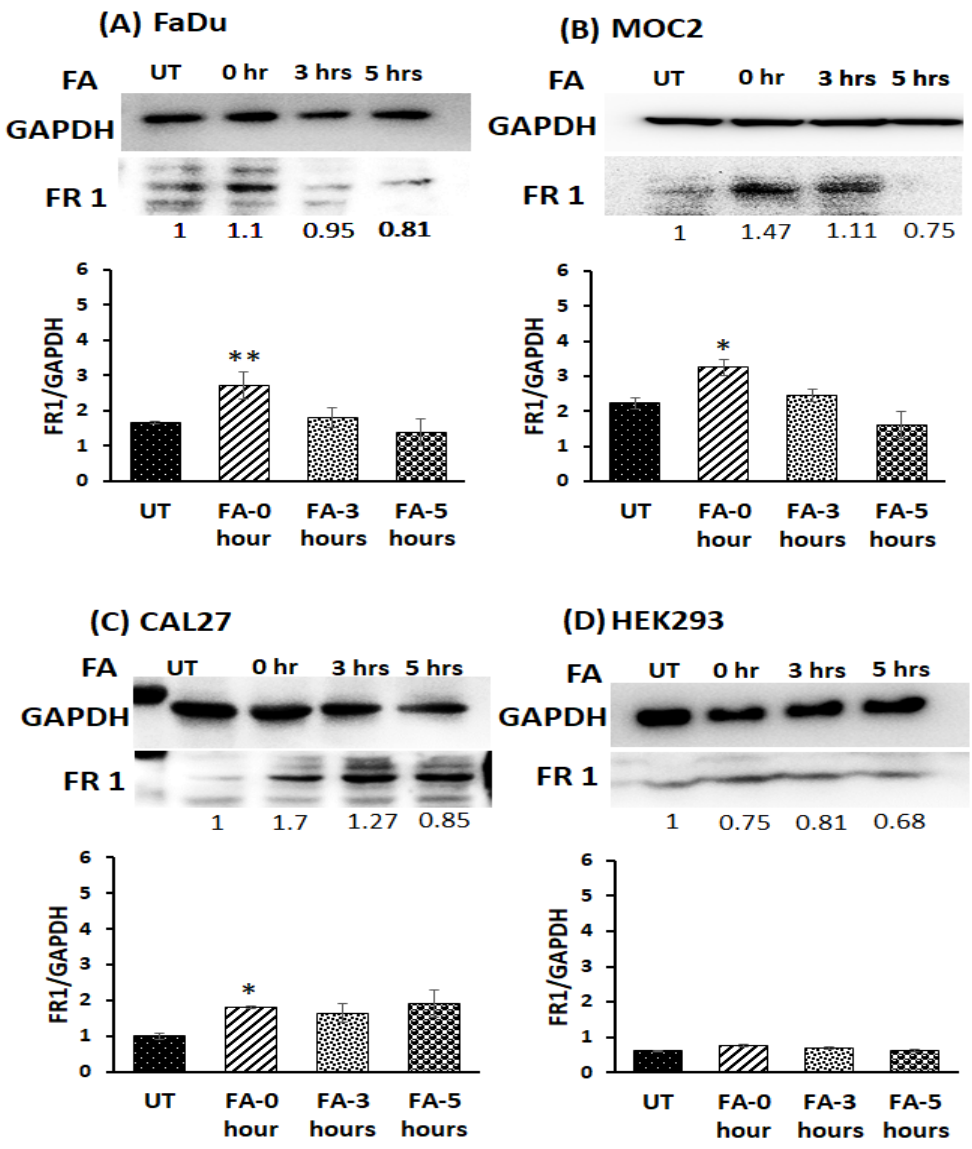

Fig.4.6. Experimental assessment of soluble Folate Receptor expression: Cells were treated in-vitro with Folate(FA) at a concentration of 100µM for 30 minutes and media was changed. Lysate was collected from samples at different time points after FA treatment- 0 hour (immediately after media change), 3 hours and 5 hours. Graphs represent densitometry data for different time points plotted as Average ± SEM values of FR1 normalized with corresponding GAPDH values. Blots developed by chemiluminescence were quantified using Image-J software. Statistical significance with respect to Untreated control (UT) represented by * where $p<0.05$-* and $p<0.01$-**.

As a further confirmation to our hypothesis, no significant difference in uptake was seen in uptake of non-targeted system CD whose levels as indicated by Flow cytometry results remained significantly lower than that of CFD. This observation was also corroborated by data representing mean area under fluorescence derived from the same set of experiments (**Fig. 4.7, Panel II**). Additionally, this observation was similar to earlier findings where pre-treatment of FR- overexpressing cancer cells with Folate was found to reduce CFD-mediated DOX uptake (**Elechalawar & Bhattacharya et al.,2019**).

In a further bid to compare and connect drug uptake (% cell uptake) with levels of soluble FR1 on a time course, a correlation was drawn between the two data sets obtained from experiments on the cell line MOC2 (**Fig. 4.8**). The first thing we noticed was that the levels of soluble FR was highest at 30 minutes of FA treatment, declining gradually as time went by. We found this observation to be in conjunction with published reports on how the membrane bound folate receptor shifts to its soluble form upon binding its ligand (Folate) and how it is subsequently recycled back to the membrane over time after it releases its ligand inside the cell (**Fernández et al.,2018**). Parallelly, it was also found using flow cytometry that CFD uptake was higher in OSCC cells (MOC2) at an earlier time point (3 hours earliest), declining gradually with time (5 hours). What was more interesting is that the difference between CFD and CD uptake levels was many folds higher at an initial stage of 3 hours post FA treatment than at a later time point (even though overall uptake for both CFD and CD had increased. All this indicated clearly that the difference of uptake between CFD and CD is quite possibly due to a time wise change in levels of circulating FR1 and a consequent change in the dynamics concerning the interaction between FR1 and folate-based ligand (FA8).

(I)

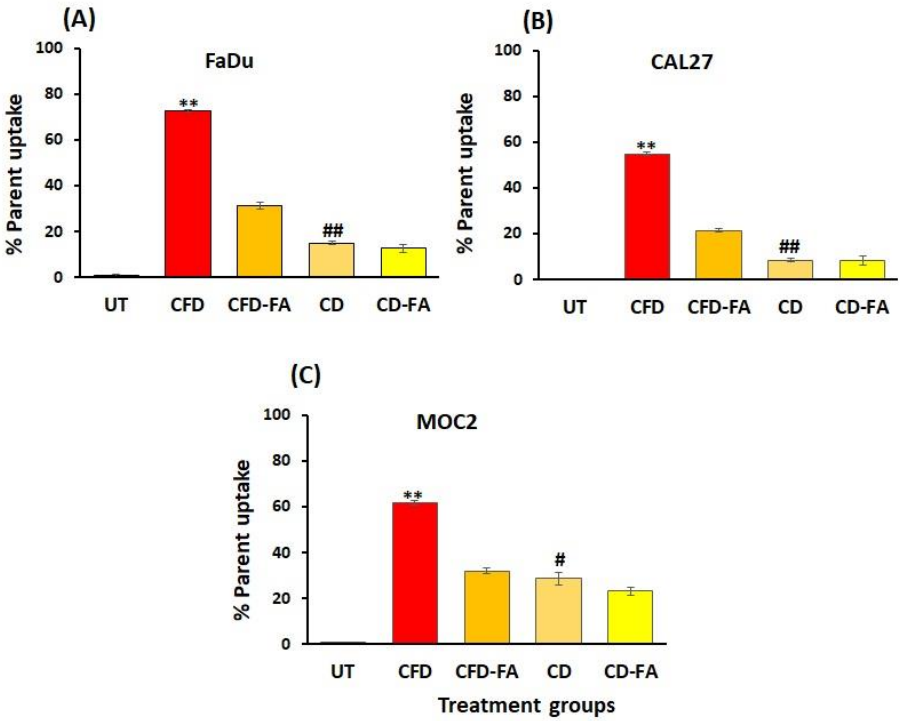
(A)
FaDu
% Parent uptake
100
80
60
40
20
0
**
##
UT
CFD
CFD-FA
CD
CD-FA
(B)
CAL27
% Parent uptake
**
##
UT
CFD
CFD-FA
CD
CD-FA
(C)
MOC2
% Parent uptake
**
#
UT
CFD
CFD-FA
CD
CD-FA
Treatment groups

(II)

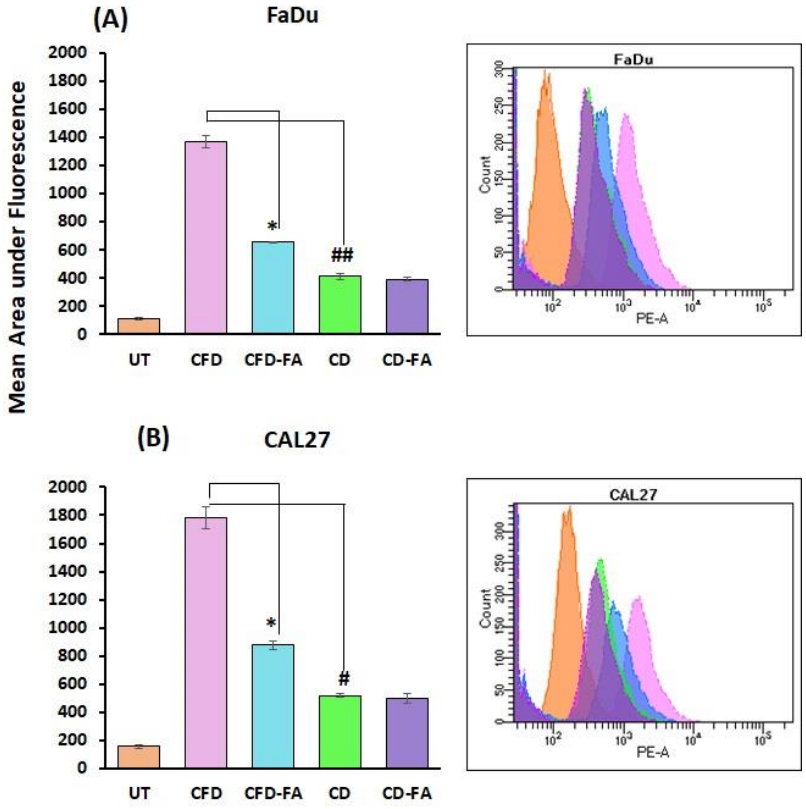
(A)
FaDu
Mean Area under Fluorescence
2000
1800
1600
1400
1200
1000
800
600
400
200
0
*
##
UT
CFD
CFD-FA
CD
CD-FA
FaDu
Count
PE-A
(B)
CAL27
*
#
UT
CFD
CFD-FA
CD
CD-FA
CAL27
Count
PE-A

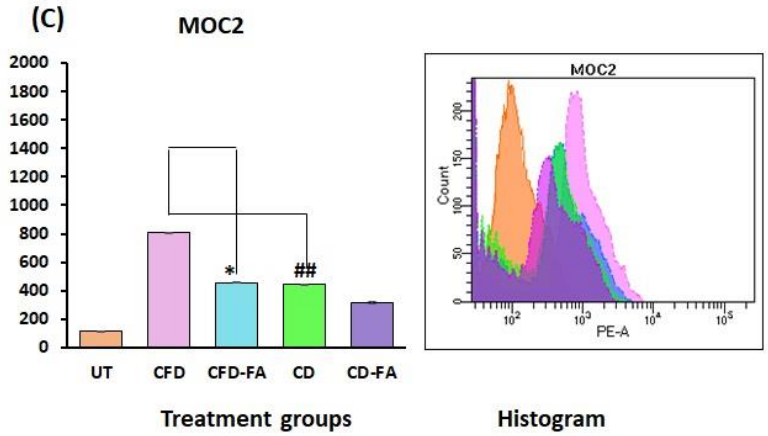

Fig.4.7. Flow cytometric quantification (comparative) of DOX uptake between Folate pre-treated and untreated OSCC cells: For pre-treatment Folate was treated at a concentration of 100 µM for 30 minutes. CSP formulations CFD & CD alongside free DOX were then treated to cells at a concentration of 6.4µM DOX. **Panel I:** Graphs represent Average ± SEM values of percent uptake of total population. **Panel II:** Graphs represent Average ± SEM values of mean area under DOX fluorescence. Statistical analysis was carried out w.r.t CFD-FA treated group as control using students t-test where *-p <0.05 & **-p<0.01. Similarly, # is used for significance w.r.t CFD as control.

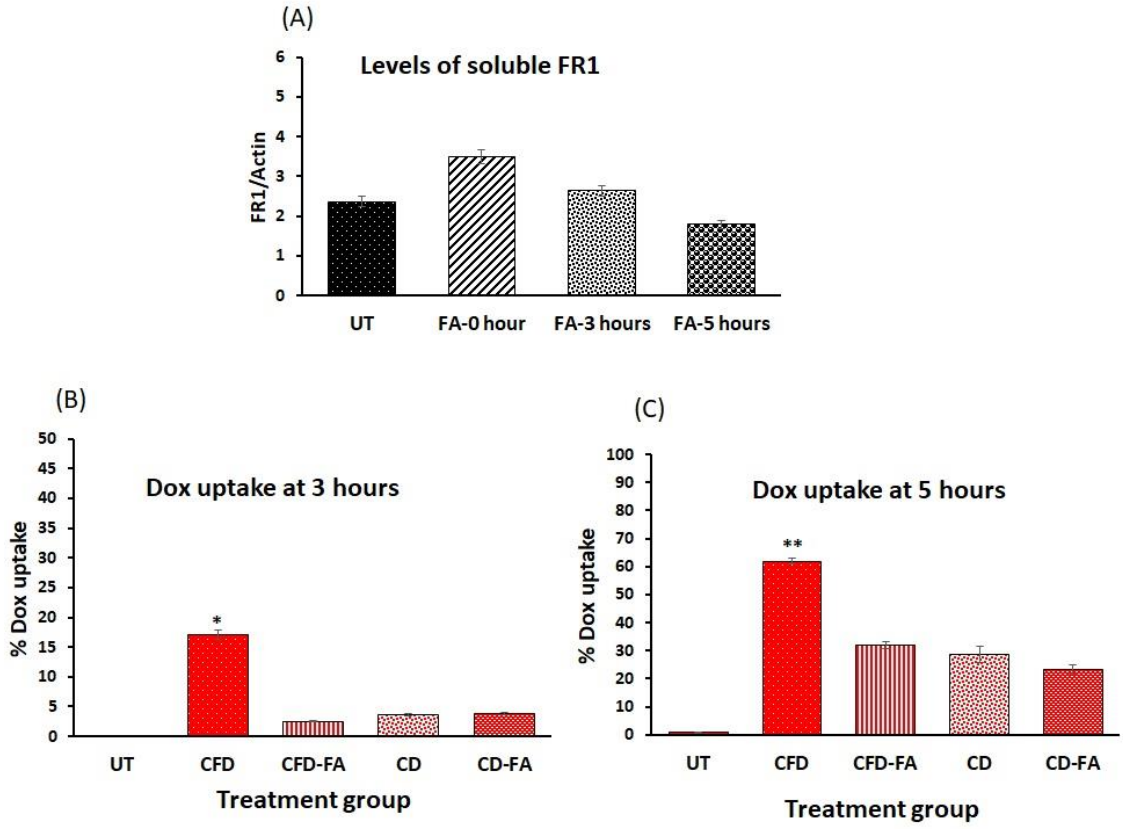

Fig.4.8. FR mediated DOX uptake through membrane bound FR1: MOC2 cells were pre-treated at a concentration of 100µM for 30 minutes and media was changed. Lysates were then collected post FA treatment at– 0.5 hours(FA-0), 3.5 hours(FA-3) and 5.5 hours(FA-5). Western blotting results obtained from lysates (A)were matched with flow cytometry data for DOX uptake in MOC2 at different time points (B & C). All graphs represent data as Average ± SEM values. Blot images were quantified using Image-J software. Statistical analysis was carried out wherever applicable using students t-test where *-$p < 0.05$, **-$p < 0.01$ with UT as control.

4.5. Targeted CSP (CFD) shows preferential drug uptake over CD and extended retention over pristine DOX in oral cancer cells:

However, as seen in (**Fig.4.9 & Fig. 4.10),** percent drug uptake as well as mean fluorescence area were higher in case of free DOX as compared to targeted formulation CFD. One of the primary reasons behind this observation would possibly be the fact that free drug enters cancer cells mostly by diffusion, unlike targeted delivery systems such as CFD, which is dependent on receptor-ligand interactions for net cellular uptake. Similar observations were retrieved from Confocal imaging studies on OSCC cells under similar experimental conditions **(Fig.4.11)**.

However, another set of uptake studies were conducted which were extended up to 24 hours instead of the usual 6 hours treatment for assessing uptake **(Fig.4.12).** Surprisingly, it was found that drug retention was more in case of CFD treated cells as compared to cells treated with free DOX after 24 hours. In fact, we found levels of non-targeted system CD to be at par with free DOX after 24 hours of treatment. Levels accounted for by CFD however remained highest across all OSCC cell lines tested.

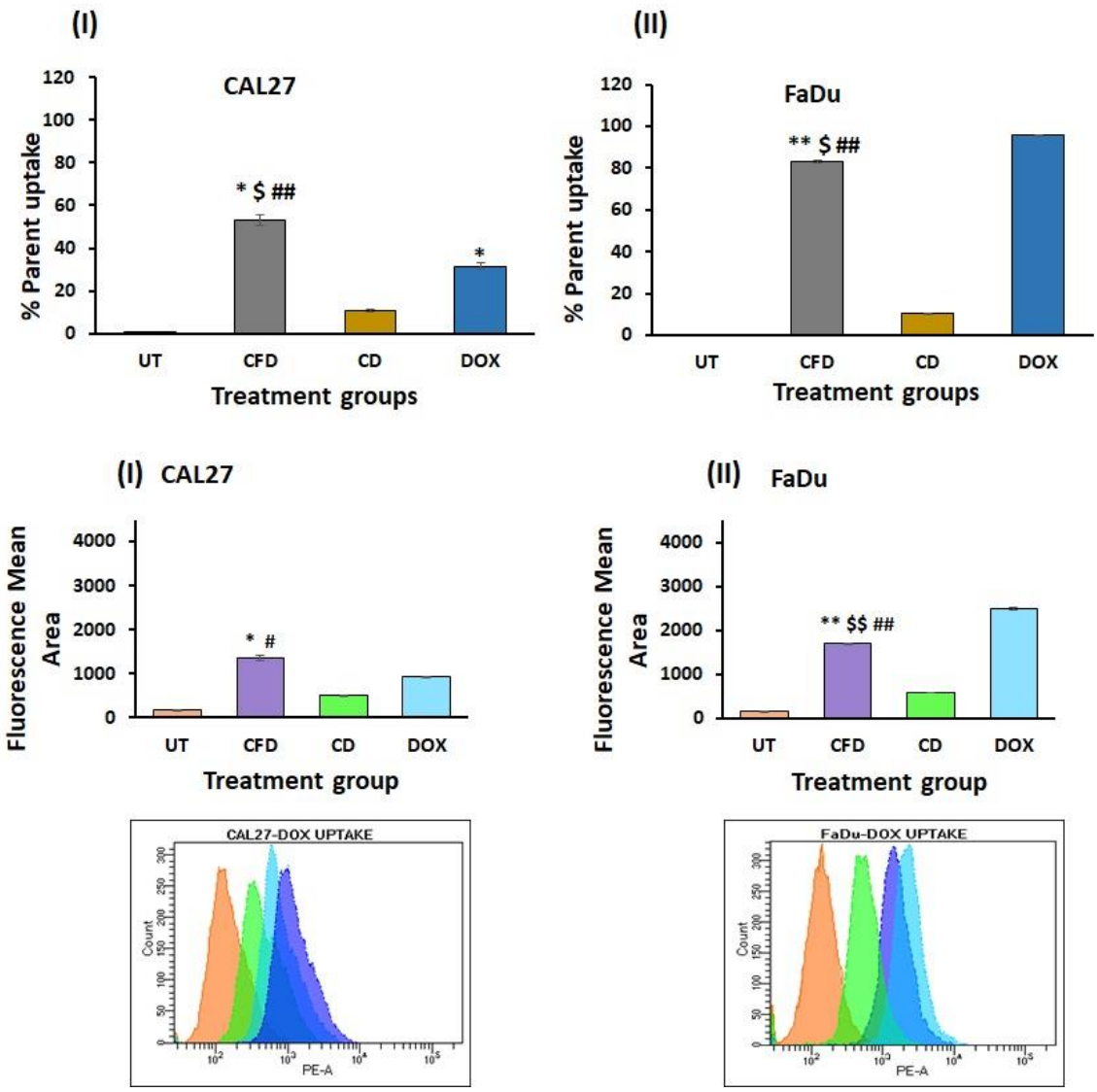

Fig.4.9. **Flow cytometric quantification (comparative) of DOX uptake in CAL27 and FaDu cells**: CSP formulations CFD & CD alongside free DOX were treated to OSCC cells (I)CAL27, (II)FaDu. After 6 hours of treatment cells were analysed. Upper panel of graphs represent data as Average ± SEM values of percentage of total. Lower panel of graphs represent data as Average ± SEM values representing mean area under Dox fluorescence along-with representative histograms. Statistical analysis was carried out using students t-test where *-p <0.05, **-p<0.01 with UT as control, $- p<0.05 with DOX as control and #- p<0.05, ##-p<0.01with CD as control.

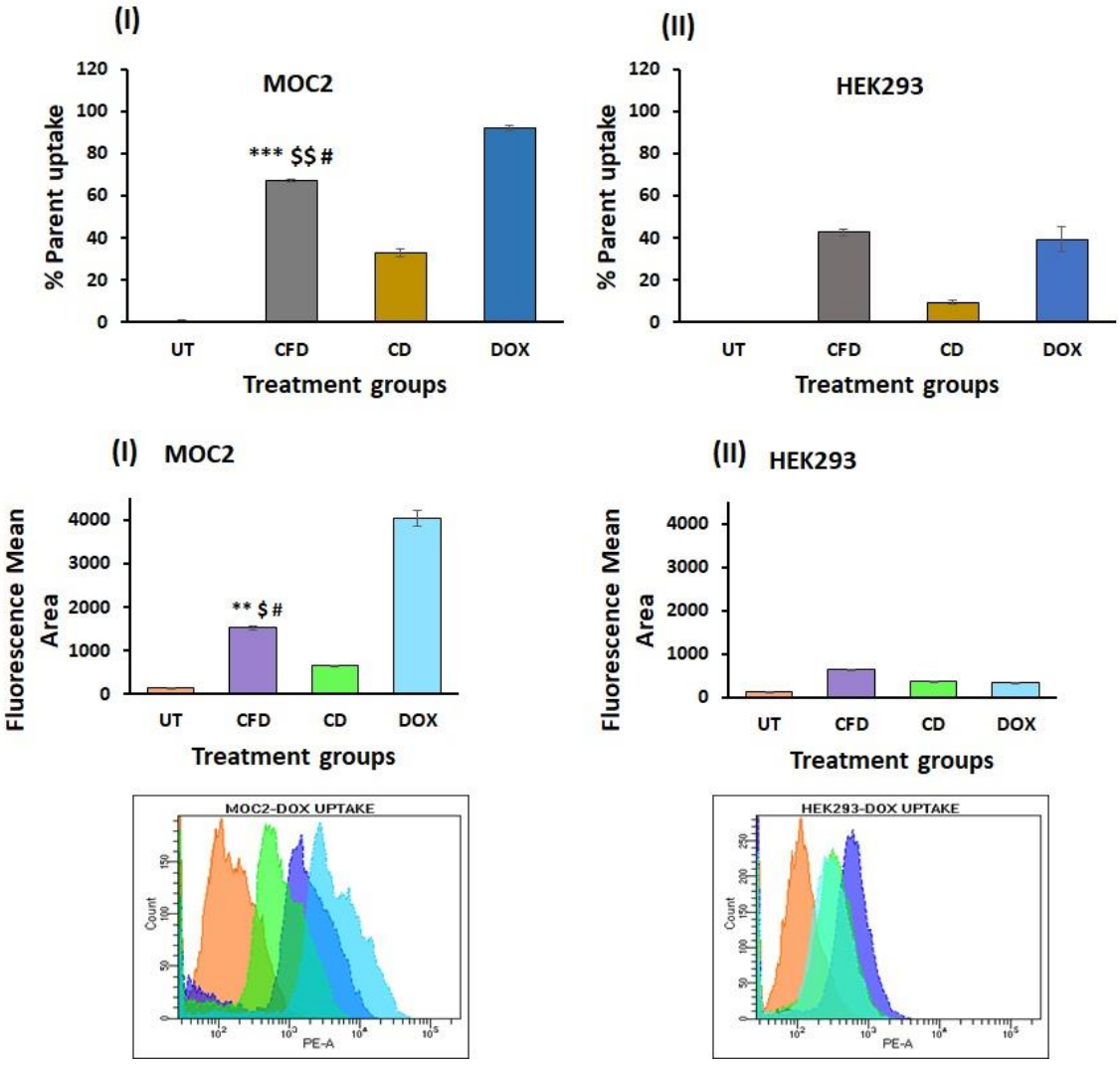

Fig.4.10. **Flow cytometric quantification (comparative) of DOX uptake in MOC2 and HEK293 cells**: CSP formulations CFD & CD alongside free DOX were treated to OSCC cells (I)MOC2, (II)HEK293. After 6 hours of treatment cells were analysed. Upper panel of graphs represent data as Average ± SEM values of percentage of total and lower for mean area under Dox fluorescence along-with representative histograms. Statistical analysis was carried out using students t-test where *-p <0.05, **-p<0.01 with UT as control, $- p<0.05 with DOX as control and #- p<0.05, ##-p<0.01with CD as control.

FaDu

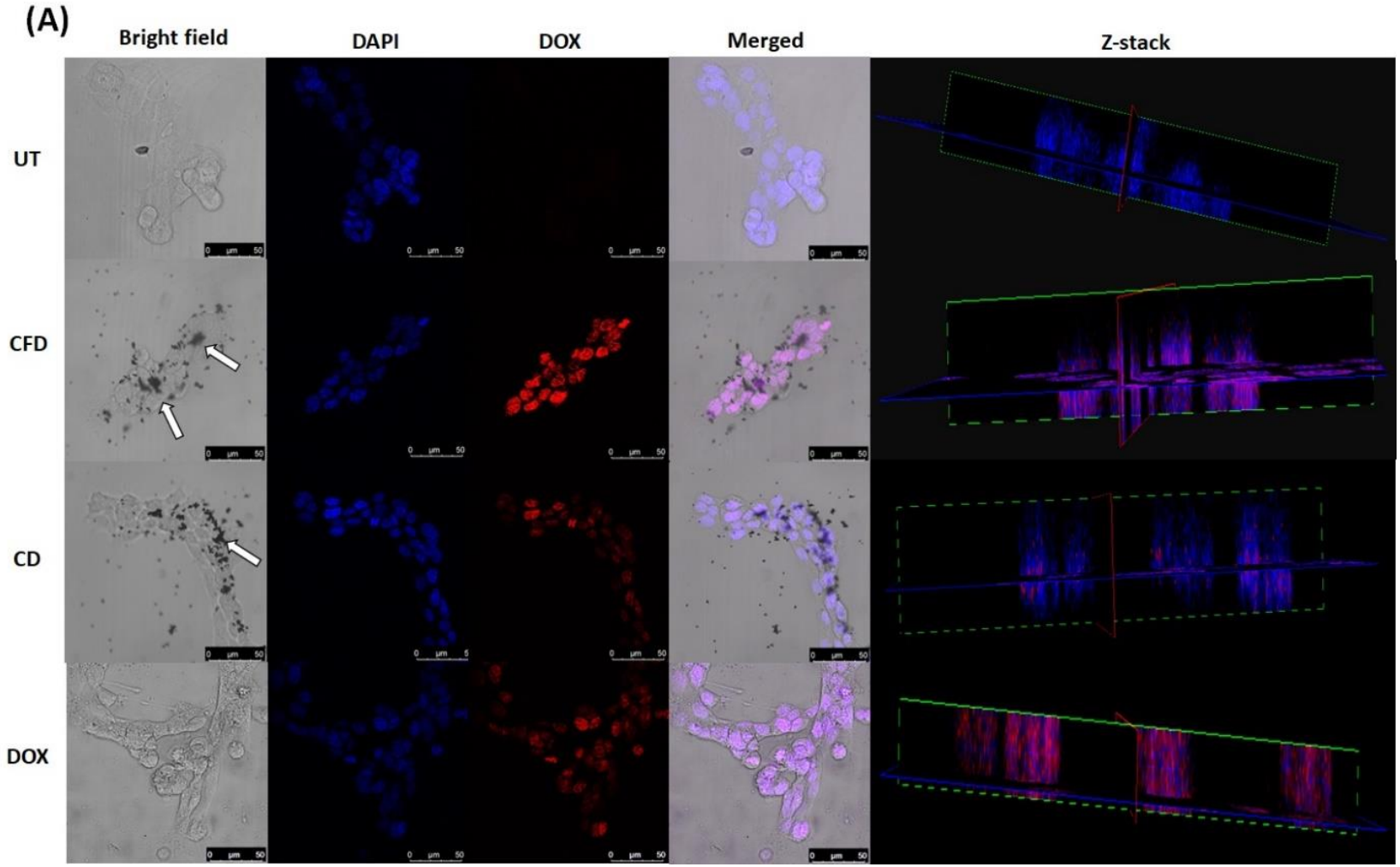

CAL27

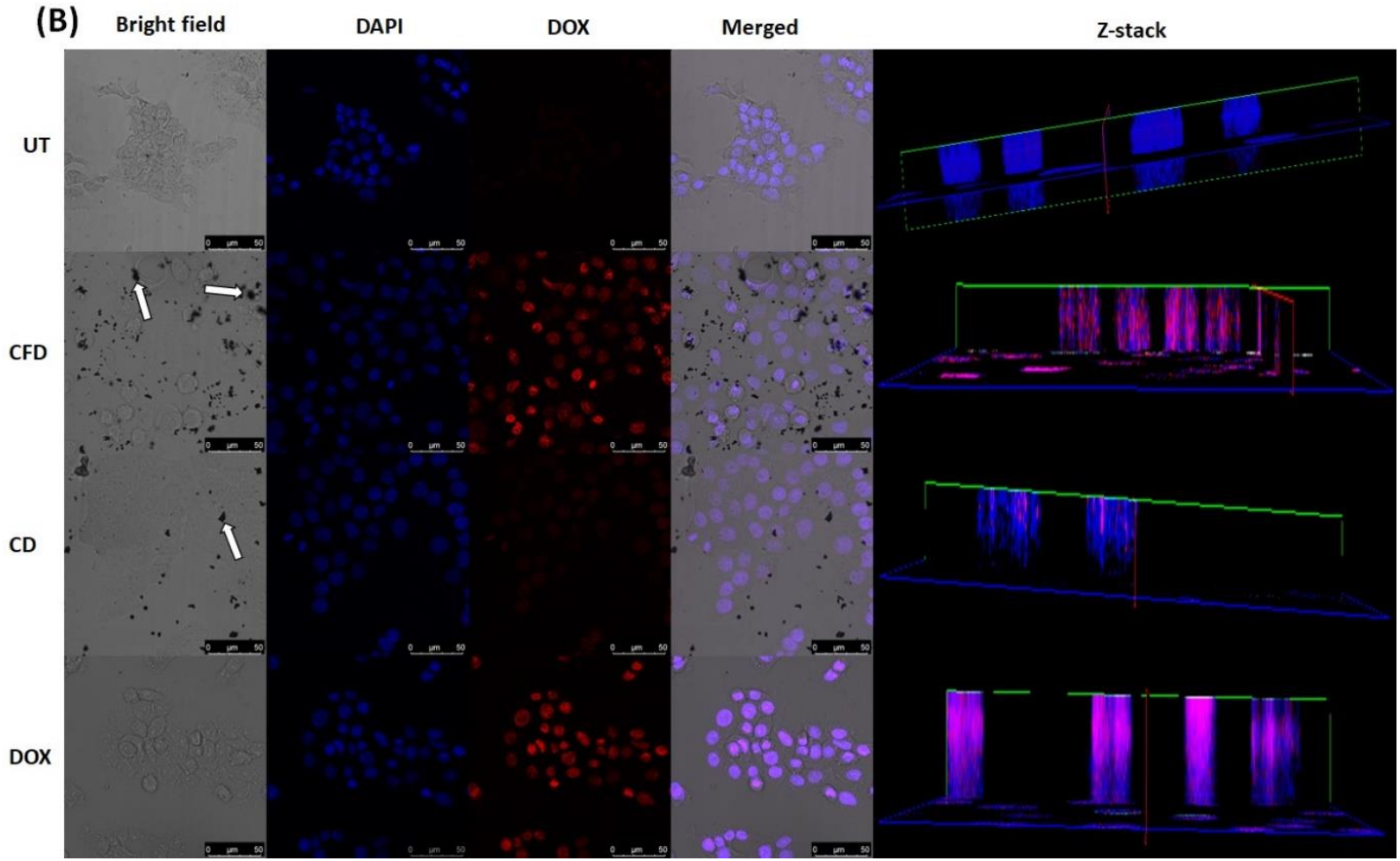

MOC2

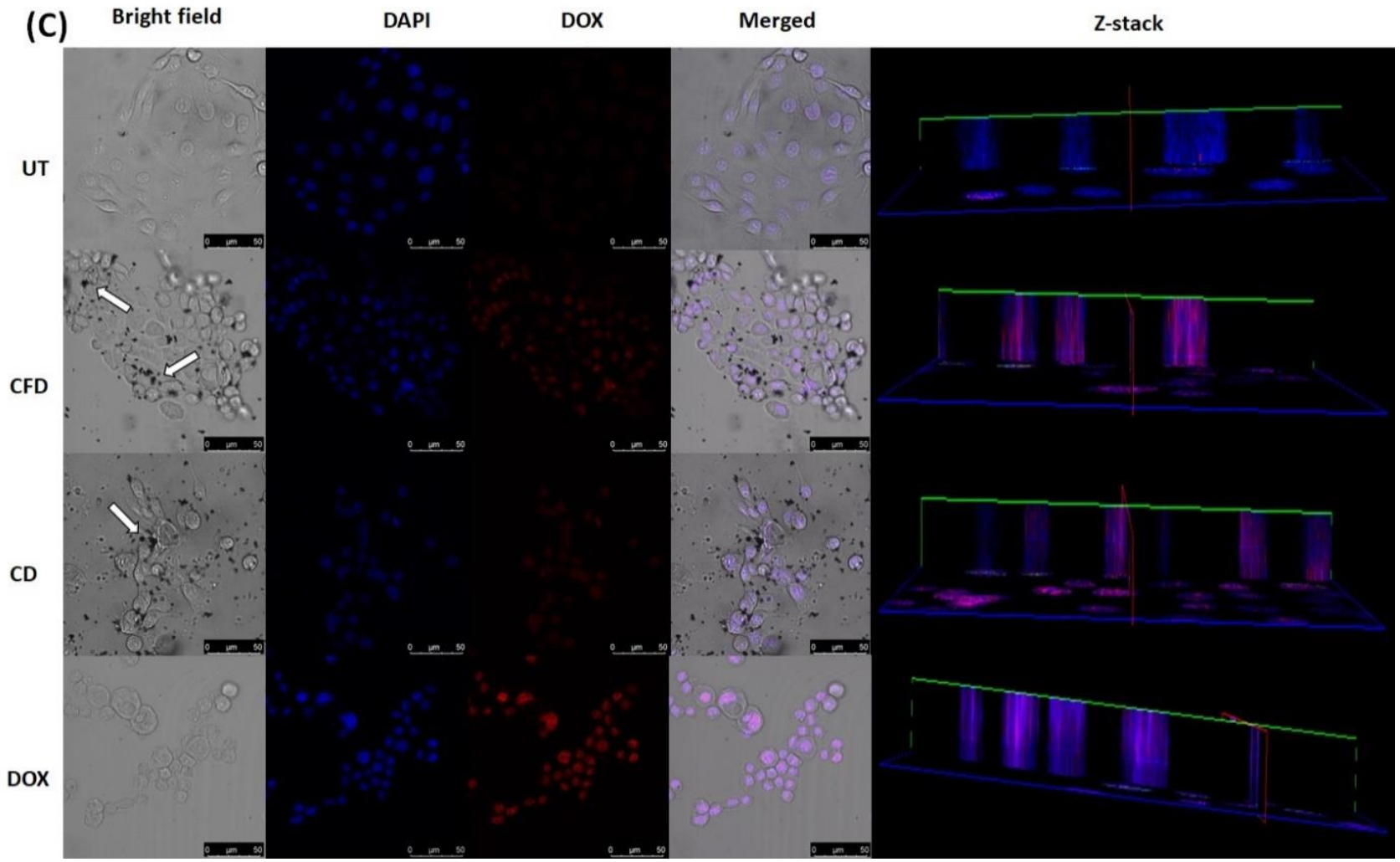

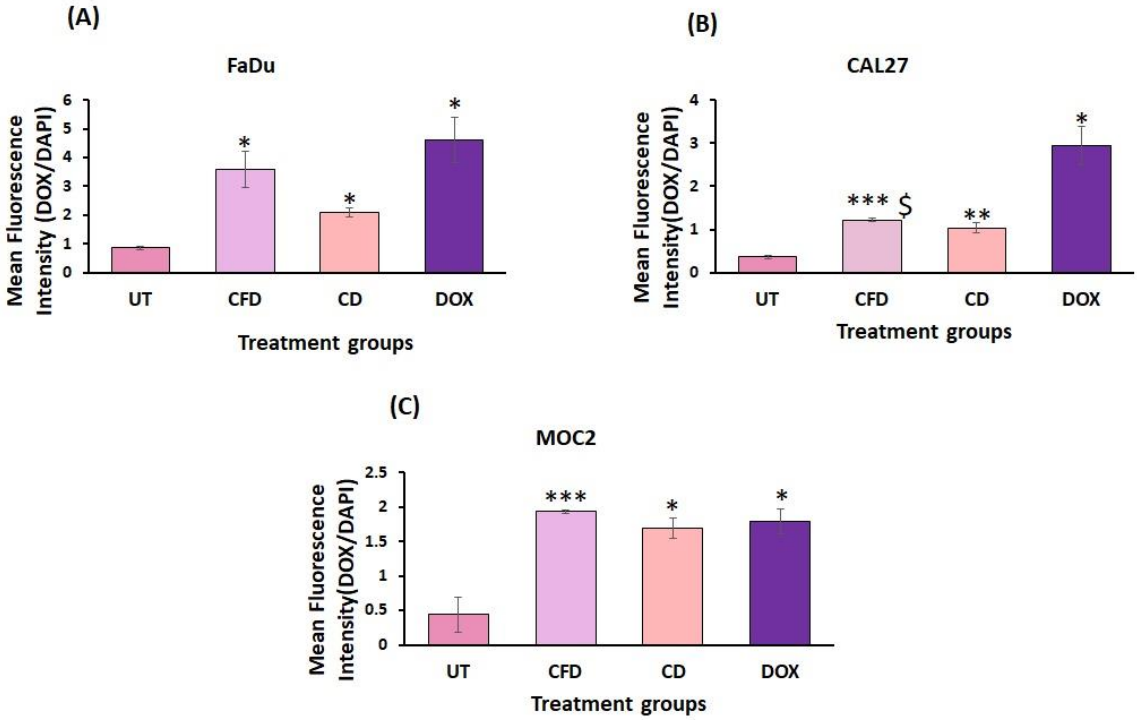

Fig.4.11. **Confocal studies to assess DOX uptake in cells**: OSCC cells were treated with different CSP combinations and free drug DOX for 6 hours. DOX fluorescence was qualitatively assessed in each treatment group. Arrows in bright field images indicate the position of CSPs inside cells. Panels A, B and C represent images for cell lines FaDu, CAL27 and MOC2 respectively. Panel D represents quantification data for drug fluorescence from stacked images as quantified by Image J software. Statistical analysis was carried out using students t-test where *-p <0.05, **-p<0.01 & ***-p<0.001 with UT as control, $- p<0.05 with DOX as control.

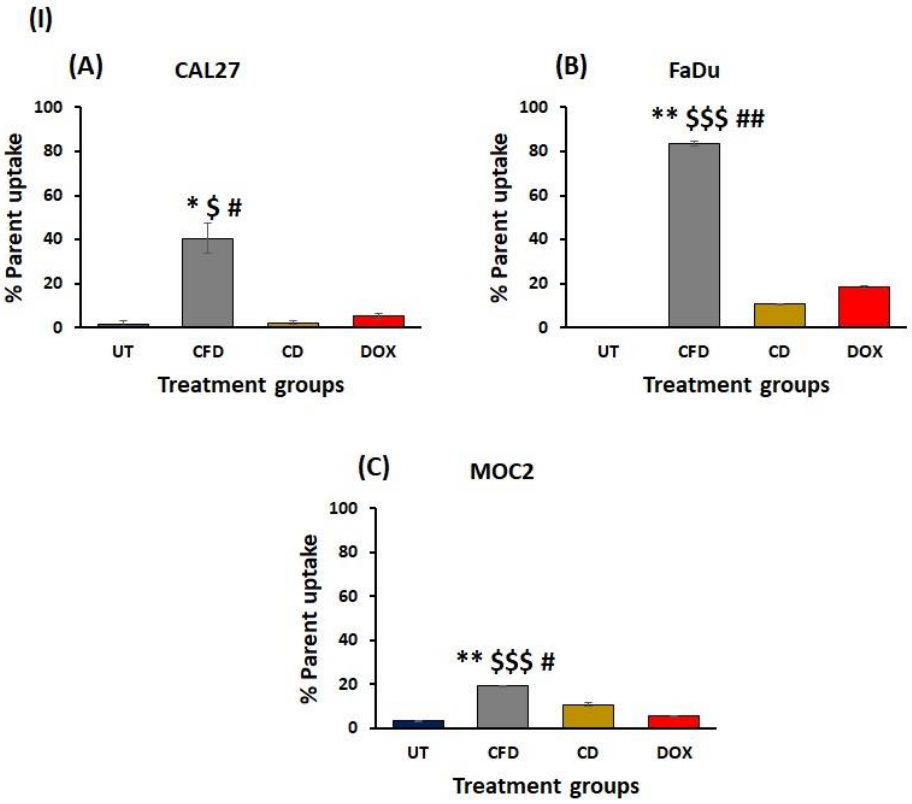
(I)
(A) CAL27
% Parent uptake
* $ #
UT
CFD
CD
DOX
Treatment groups
(B) FaDu
** $$$ ##
(C) MOC2
** $$$ #

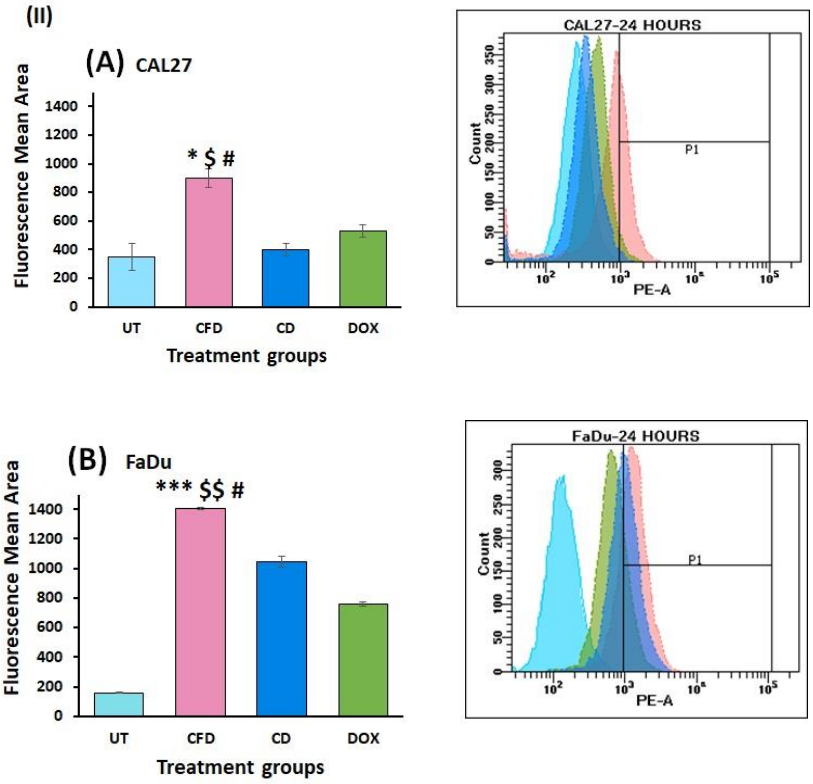
(II)
(A) CAL27
Fluorescence Mean Area
* $ #
Treatment groups
CAL27-24 HOURS
Count
P1
PE-A
(B) FaDu
*** $$ #
FaDu-24 HOURS

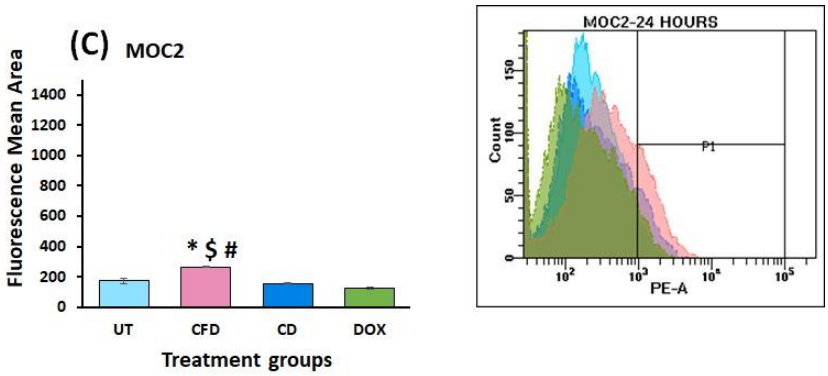

Fig.4.12. **Flow cytometric quantification of DOX uptake after 24 hours**: CSP formulations CFD & CD alongside free drug DOX were treated to OSCC cells(A) CAL27, (B)FaDu and (C)MOC2. After 6 hours of treatment media was changed and cells incubated for an additional 24 hours before being analysed. **Panel I:** Graphs represent data as Average ± SEM values of percentage of total. **Panel II:** Graphs represent data as Average ± SEM values representing mean area under DOX fluorescence along-with representative histograms. Statistical analysis was carried out using students t-test where *-p <0.05, **-p<0.01 with UT (Untreated) as control, $- p<0.05 with DOX as control & #- p<0.05 with CD as control.

To validate the above results from Flow cytometry studies, confocal imaging studies were conducted for MOC2 cells treated with CFD as well as pristine drug under similar experimental conditions (**Fig.4.13**). Images acquired after 24 hours showed that besides the drug's presence in the nucleus, there was substantial amount of drug (seen as red particles in figure 8) present in the cytoplasm as well as the peripheral regions in case of pristine drug treatment group (DOX only). On the other hand, most of the drug in case of CFD treated cells could be seen to be tightly accumulated within the nuclear margin of cells. Additionally, the drug fluorescence intensity was also found to be much higher within the nucleus in case of CFD treated cells as compared to only drug treatment group. This finding bears significance with respect to the fact that Doxorubicin is well-reported as targeting the nucleus and that exosomes or other eviction mechanisms are often known to prevent this in case of DOX-resistant cancer cells (**Chaikomon et al.,2018; Azmi et al.,2013**).

4.6. DOX loaded targeted CSPs induce cytotoxicity in a cancer cell selective manner

To test cytotoxicity, all cancer cells as well as normal cell line HEK293 were treated with CSPs and DOX for varied lengths of time and subsequently tested for cell death. Targeted formulation CFD exhibited significant cancer cell killing across all OSCC cell lines when compared to untreated control and non-targeted system CSP in MTT Assay (**Fig.4.14**). However, when tested under similar conditions on non-cancerous cell HEK293, no significant cancer cell death was evident. DOX (free drug) exhibited considerable cell death as expected but targeted system CFD exhibited yet higher levels of cytotoxicity even when compared to free drug in all OSCC cell lines tested. On the other hand, tests on non-cancerous cell line HEK293 showed CFD to have higher IC50 values with cell viability being maintained above 80% across all concentrations of CFD tested.

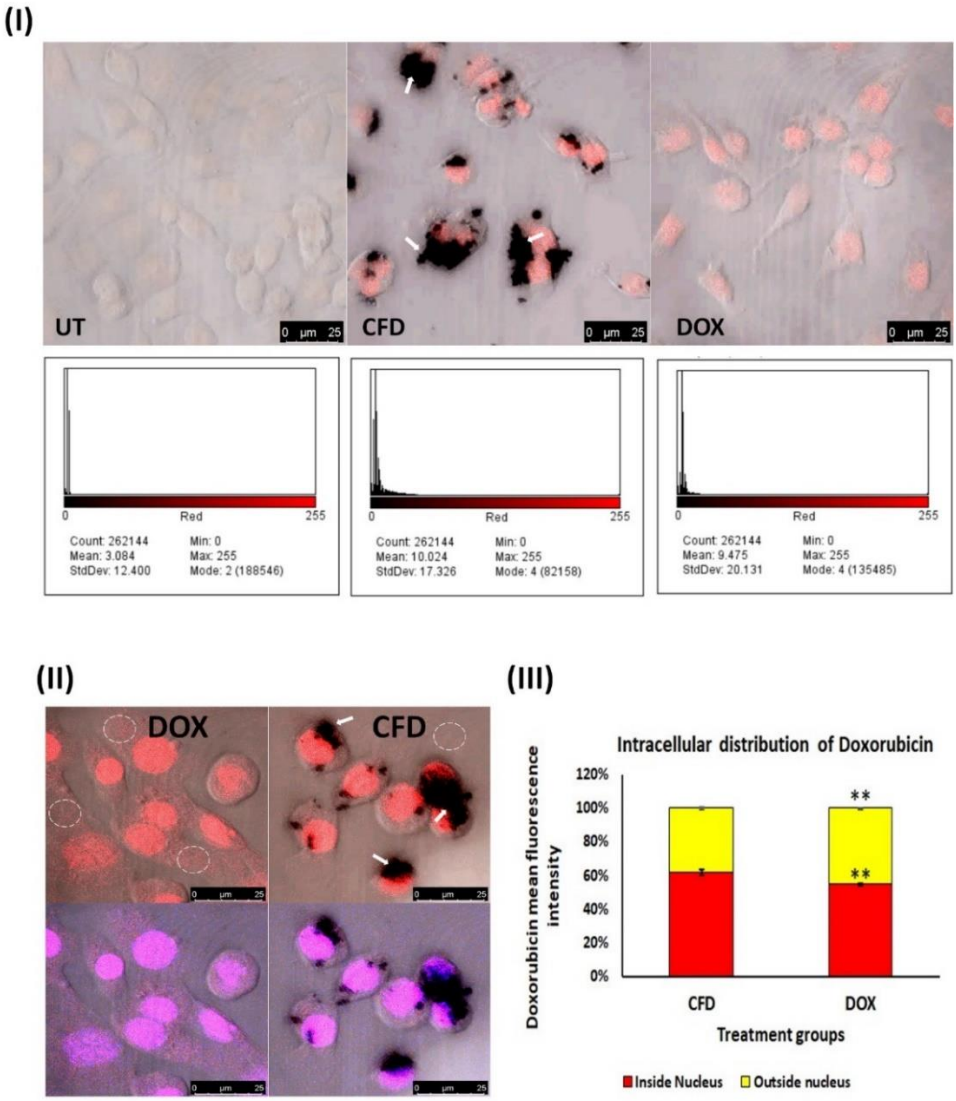

Fig.4.13. **Study of intracellular DOX localization**: MOC2 cells were treated with targeted CSP formulation CFD and free drug DOX for 6 hours, post which cells were washed and incubated for 24 hours. (I) Images representative of DOX fluorescence (relative). Arrows indicate clusters of CFD spheres in cells. (II) Images representative of CFD and DOX treatment. Arrows indicate CSP clusters. Rings indicate DOX located in cytoplasm and cell peripheral regions. (III) Graph of relative drug distribution for both treatment groups representative of images from Confocal microscopy (part II). Confocal images were quantified for mean fluorescence (DOX) using Image J software. Statistical analysis was carried out using students t-test where *-$p < 0.05$, **-$p < 0.01$ with CFD as control.

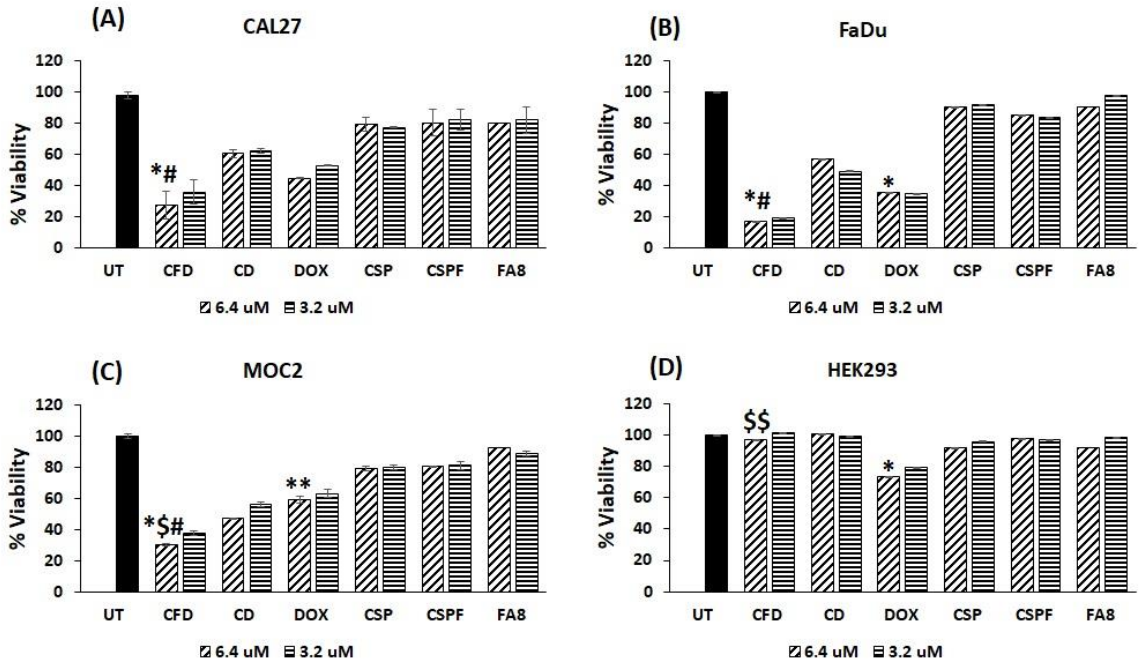

Fig.4.14. Cytotoxicity studies on OSCC and normal cell lines: OSCC cells FaDu, CAL27, MOC2 along-with normal cell line HEK293 were treated with CFD, CD, CSP, FA8 and DOX. After 48 hours of treatment, MTT assay was performed. Graphs represent data as Average ± SEM values of percent viability. Statistical analysis was carried out using students t-test where *-p <0.05, **-p<0.01 with UT as control and $- p<0.05 with DOX as control.

Subsequent results attained from Flow cytometry based Annexin V-FITC Assay corroborated with MTT assay results. Briefly, CFD induced significantly higher levels of apoptosis as compared to untreated control as well as non-targeted formulation CD and other treated groups (**Fig.4.15-a, b, c**). When it came to being compared with free drug DOX, levels of apoptosis elicited by CFD were found to be at par (higher in case of CAL27) even at 24 hours, demonstrating commendable cancer cell death. Additionally, CFD proved minimally toxic when tested upon normal cell HEK293 with the percentage of apoptotic cells produced being at par with that in the untreated control group **(Fig.4.15-d)**.

4.7. CFD induces apoptosis via the downregulation of Bcl-2:

DOX is well reported as inducing cell death via both apoptotic and necrotic pathways. However, it remained to be seen whether CFD induced cell death followed a similar mechanism as that of free DOX or if it was different. To test this, lysates were collected from in vitro cultures grown and treated under identical conditions as performed in the apoptosis FACS experiment and protein levels were assessed for both apoptotic and necrotic markers. CFD treated samples showed no or very low levels of the popular necroptotic protein RIP3 while its levels were higher in case of cells treated with free DOX (**Fig.4.18**). This indicated that CFD induced cell death was possibly not so much via the necroptotic pathway as via the apoptotic pathway (**de Almagro & Vucic, 2015**).

Markers pertaining to the apoptotic pathway of cell death were assessed for any signs of change in protein levels. Pro-apoptotic marker Bax and anti-apoptotic marker Bcl-2 were tested for this purpose and it was found that there was considerable downregulation in levels of Bcl-2 for cell samples treated in vitro with CFD as compared to untreated and CD treated groups. Interestingly, this observation held true for both FaDu and CAL27**(Fig.4.16)**.

However, for MOC2 a similar trend was found to be repeated only in case of Bcl-2. (**Fig.4.17**).

4.8. Tumour regression study:

In here, $3x10^6$ cells of MOC-2 (Mouse OSCC cell line) were injected subcutaneously into the right flank of female C57/BL6J mice (5-6 weeks) as per the protocol followed earlier by Onken et al. (**Onken et al.,2014**). Tumours of approx. volume 50 mm^3(average) were observed on the 7th day post tumour cell inoculation. Mice were then randomly divided into groups and treated with CFD, CD, DOX, CSP & FA8 (5mg/kg Dox drug equivalent) intraperitoneally for 5 alternate dosings. Tumour size was measured every 2 days with vernier callipers. Body weight for all treatment groups was also recorded throughout the study with a gap of 3 days in between. Mice were sacrificed on day 23 post tumour inoculation. Tumour size was found to be significantly lesser in case of CFD (compared to Untreated and other control groups) treatment group at the end of the treatment course **(Fig. 4.19b)**. Tumour sizes for CFD treated mice were also found to be smaller than mice treated with free drug, with apparent changes being statistically significant as found on the day of animal sacrifice and tumour collection **(Fig. 4.19c)**. Overall, targeted system CFD showed maximum tumour-regression among all treatment groups. With regards to body weight, CFD treated mice showed no statistically significant difference when compared to untreated mice at the end of the treatment course **(Fig. 4.19a)**. According to earlier studies, this was an indication of minimal overall toxicity on account of treatment (**Boyd, 1968**).

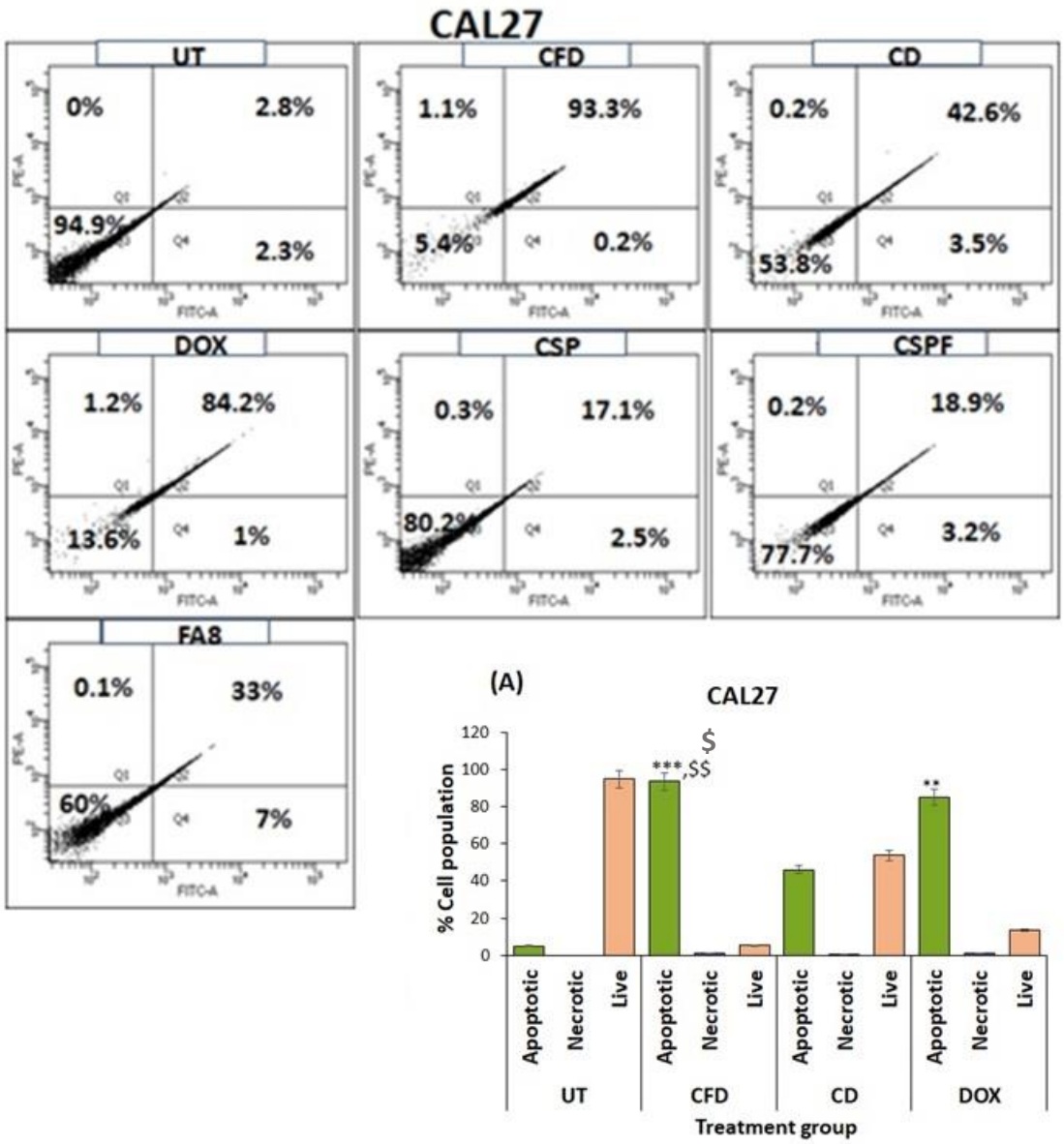

Fig.4.15a. Flow cytometric assessment of CAL27 cell death by Annexin-V Assay: Treatment was done with CFD (CSP-FA8-DOX), CD (CSP-DOX), CSP (only CSP), FA8 (Folate based Ligand)) and DOX for OSCC cells FaDu, CAL27, MOC2 along-with normal cell line HEK293. After 24 hours of treatment cells were collected by trypsinization and analysed by Flow Cytometry after staining with Annexin V-FITC and Propidium Iodide (PI) as per protocol. Graphs represent data as Average ± SEM values of percent apoptotic cells. Statistical analysis was carried out using students t-test where *-p <0.05, **-p<0.01, ***-p<0.001 with UT as control, $- p<0.05 with DOX as control and #- p<0.05 with CD as control.

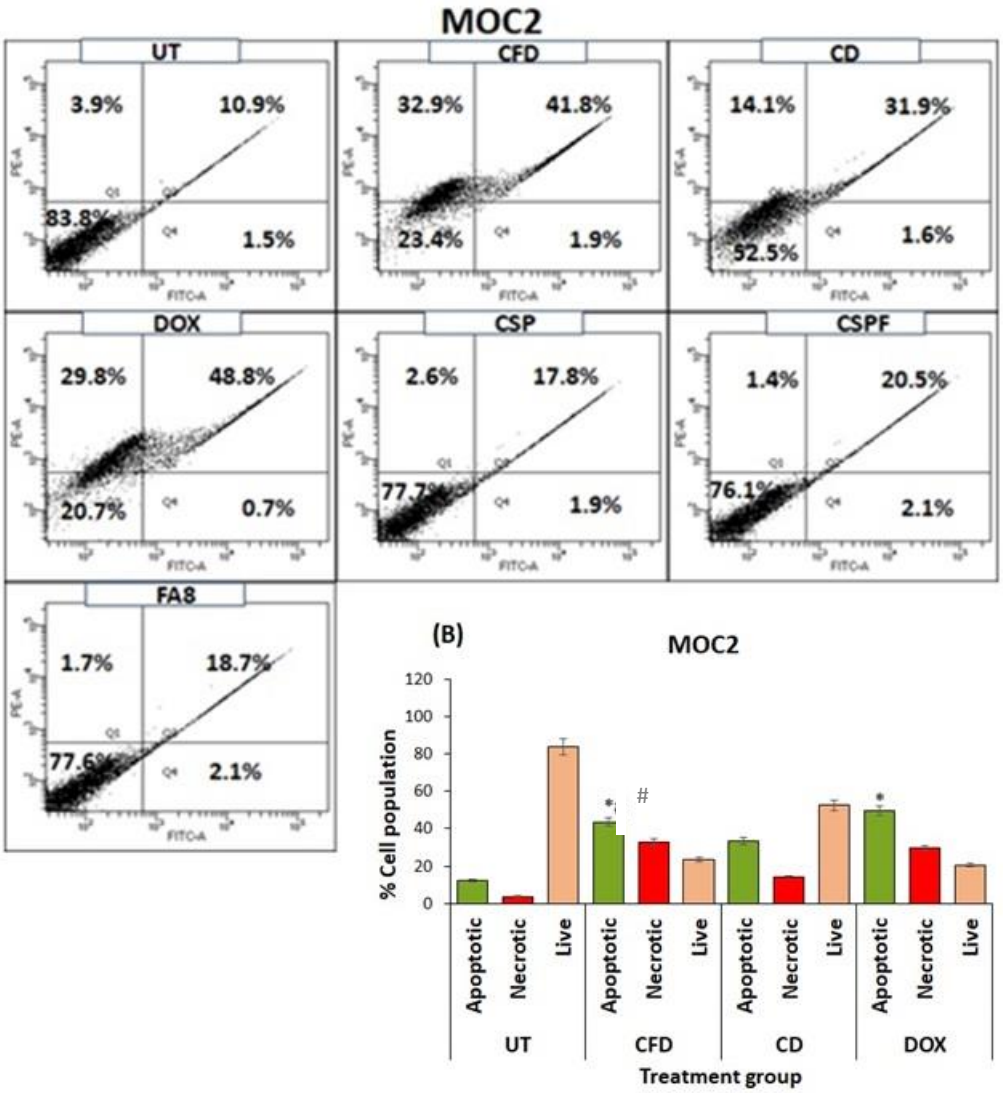

Fig.4.15b. Flow cytometric assessment of MOC2 cell death by Annexin-V Assay: Treatment was done with CFD (CSP-FA8-DOX), CD (CSP-DOX), CSP (only CSP), FA8 (Folate based Ligand)) and DOX for OSCC cells FaDu, CAL27, MOC2 along-with normal cell line HEK293. After 24 hours of treatment cells were collected by trypsinization and analysed by Flow Cytometry after staining with Annexin V-FITC and Propidium Iodide (PI) as per protocol. Graphs represent data as Average ± SEM values of percent apoptotic cells. Statistical analysis was carried out using students t-test where *-p <0.05, **-p<0.01, ***-p<0.001 with UT as control, $- p<0.05 with DOX as control and #- p<0.05 with CD as control.

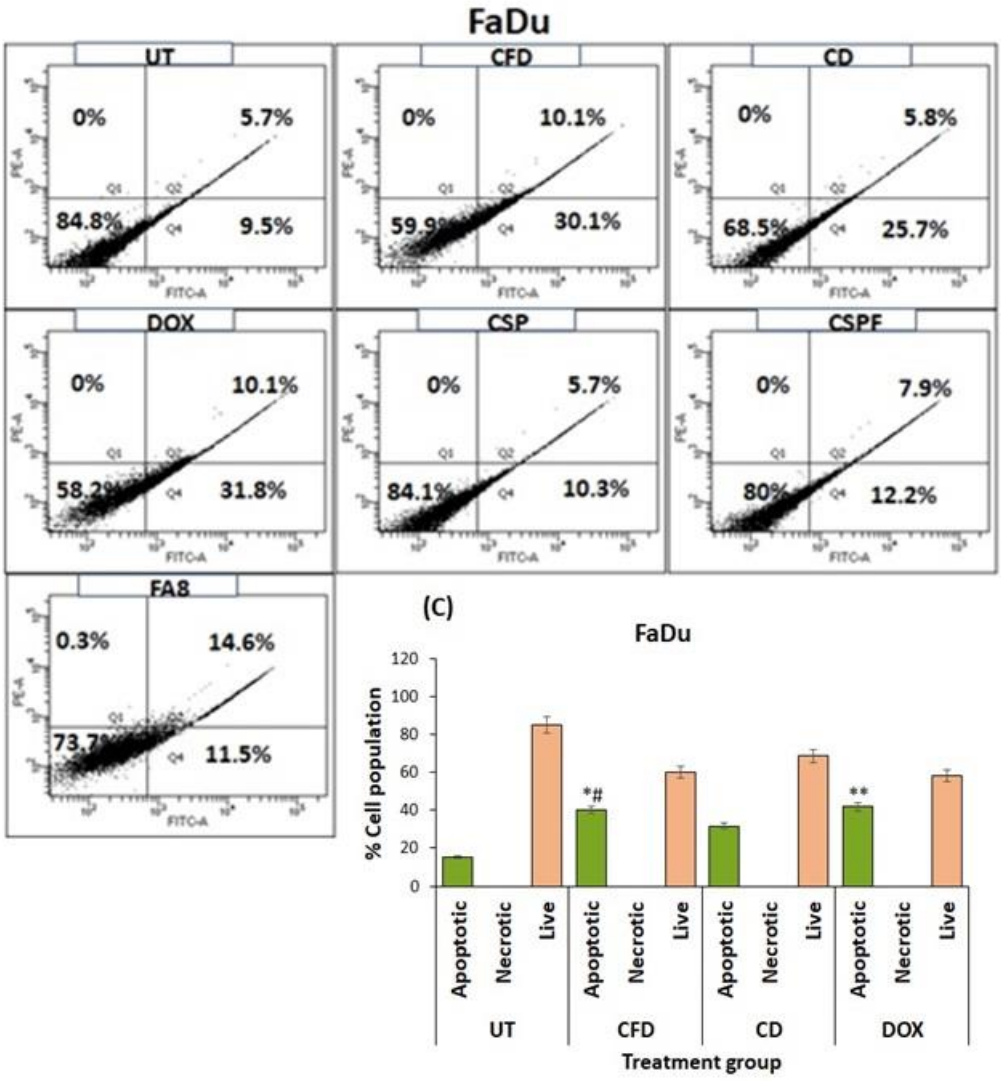

Fig.4.15c. Flow cytometric assessment of FaDu cell death by Annexin-V Assay: Treatment was done with CFD (CSP-FA8-DOX), CD (CSP-DOX), CSP (only CSP), FA8 (Folate based Ligand)) and DOX for OSCC cells FaDu, CAL27, MOC2 along-with normal cell line HEK293. After 24 hours of treatment cells were collected by trypsinization and analysed by Flow Cytometry after staining with Annexin V-FITC and Propidium Iodide (PI) as per protocol. Graphs represent data as Average ± SEM values of percent apoptotic cells. Statistical analysis was carried out using students t-test where *-p <0.05, **-p<0.01, ***-p<0.001 with UT as control, $- p<0.05 with DOX as control and #- p<0.05 with CD as control.

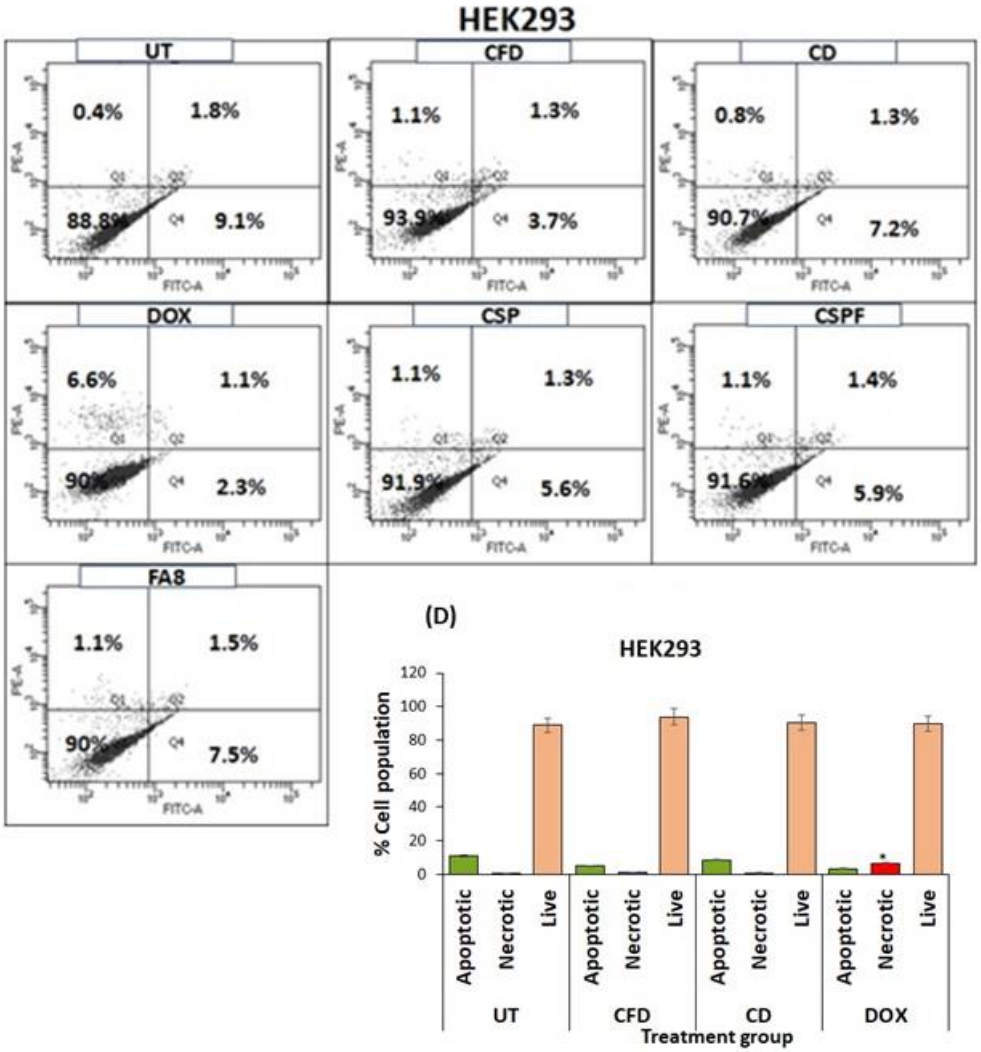

Fig.4.15d. Flow cytometric assessment of HEK293 cell death by Annexin-V Assay: Treatment was done with CFD (CSP-FA8-DOX), CD (CSP-DOX), CSP (only CSP), FA8 (Folate based Ligand)) and DOX for OSCC cells FaDu, CAL27, MOC2 along-with normal cell line HEK293. After 24 hours of treatment cells were collected by trypsinization and analysed by Flow Cytometry after staining with Annexin V-FITC and Propidium Iodide (PI) as per protocol. Graphs represent data as Average ± SEM values of percent apoptotic cells. Statistical analysis was carried out using students t-test where *-p <0.05, **-p<0.01, ***-p<0.001 with UT as control, $- p<0.05 with DOX as control and #- p<0.05 with CD as control.

Table.4.3. Comparison of apoptotic effect between CFD & CD: Table represents the percentage of apoptotic cells in each cell line induced by targeted formulation CFD and non-targeted formulation CD.

S.No.	Cell line	Percentage of apoptotic cells	
		CFD	CD
1.	FaDu	40.2	31.5
2	CAL27	93.5	46.1
3	MOC2	43.7	33.5
4	HEK293	5	8.5

Table.4.4. Variation of CFD induced apoptosis across OSCC cell lines: Table represents percentage of each cell subpopulation for individual OSCC cell lines post CFD treatment.

Cell subpopulation	OSCC cell lines		
	FaDu	CAL27	MOC2
Apoptotic	40.2	93.5	43.7
Necrotic	0	1.1	32.9
Live	59.9	5.4	23.4

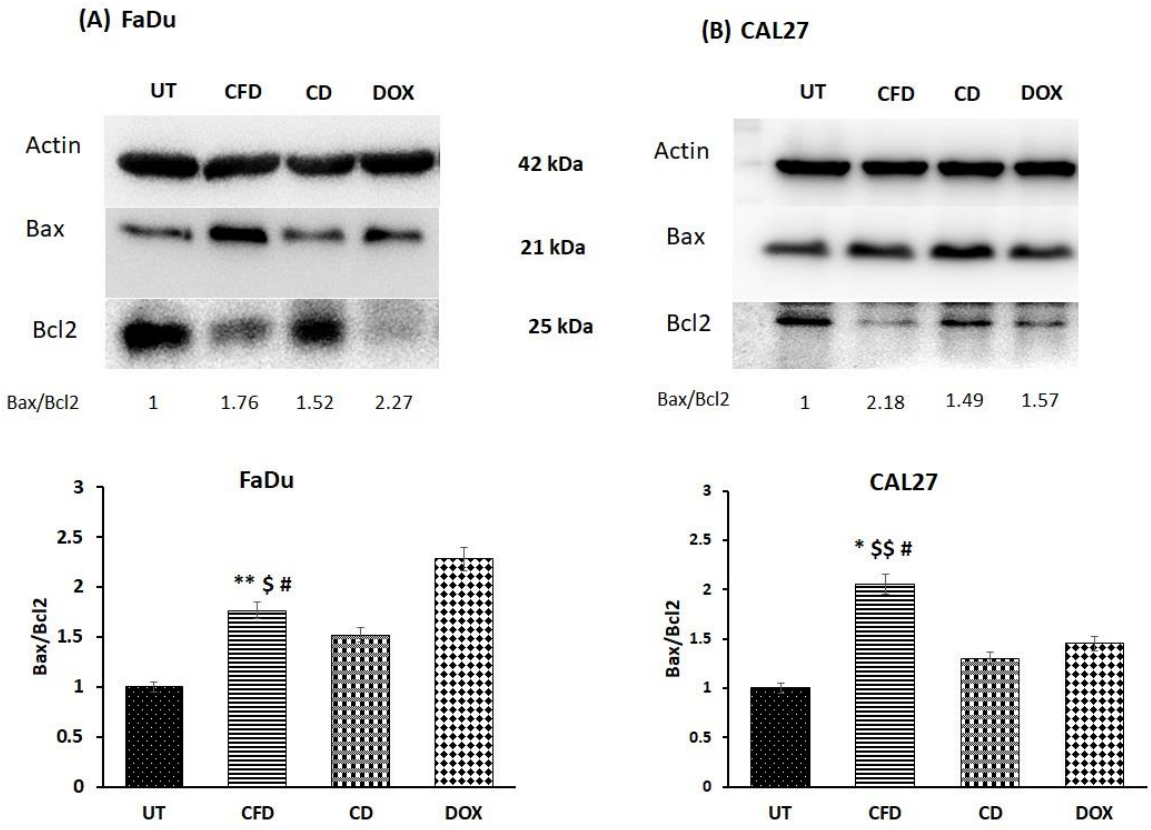

Fig.4.16. Western blotting for apoptotic pathway associated proteins Bax & Bcl-2: OSCC cells (A)FaDu and (B) CAL27 were treated in vitro with CSP formulations CFD(CSP-FA8-DOX) and CD(CSP-DOX) besides free drug DOX (6.4 µM). After 24 hours of incubation lysates were collected for Immunoblotting. Graphs represent levels of pro-apoptotic protein Bax normalized against levels of the anti-apoptotic protein Bcl-2 (individually normalized against house-keeping protein β-Actin). Data has been represented as Average ± SEM values. Blots were quantified using Image-J software. Statistical significance with respect to Untreated control represented by * where $p<0.05$-* and $p<0.01$-** , $- $p<0.05$ with DOX as control & #- $p<0.05$ with CD as control.

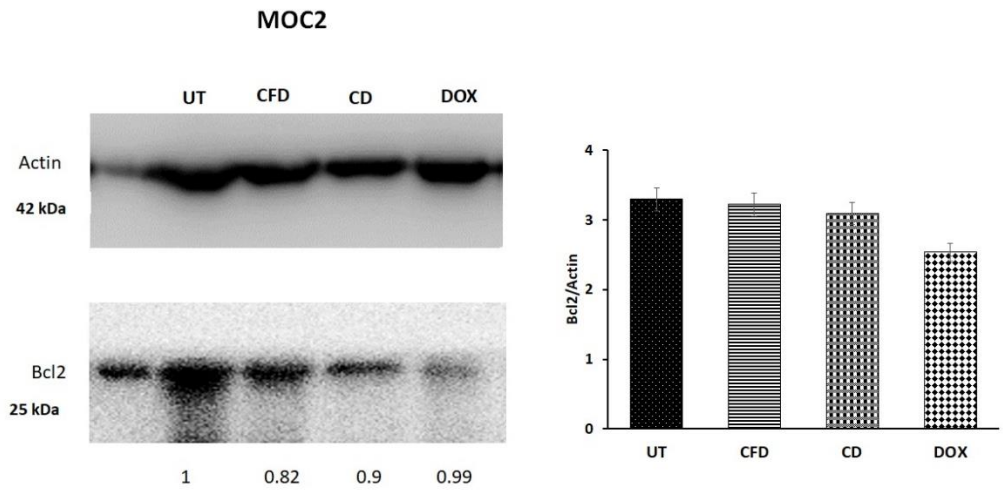

Fig.4.17: Western blotting for estimation of Bcl-2 expression in MOC2 cells: MOC2 cells were treated in vitro with CSP formulations or free DOX (equivalent to 6.4 µM DOX) and after 24 hours lysates were collected for Immunoblotting. Graphs represent levels of anti-apoptotic protein Bcl-2 (normalized against β-Actin). Data is represented as Average ± SEM values.

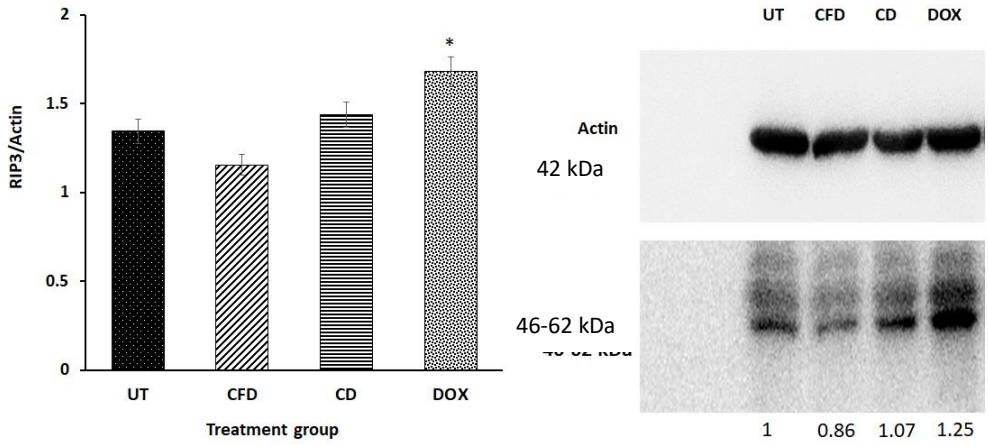

Fig 4.18: Western blotting for assessment of DOX induced necrosis: FaDu cells were treated in vitro with CSP formulations and free DOX (equivalent to 6.4 µM DOX) and after 24 hours lysates were collected for immunoblotting. Graphs represent levels of necroptotic marker RIP3 (normalized against β-Actin). Data is represented as Average ± SEM values.

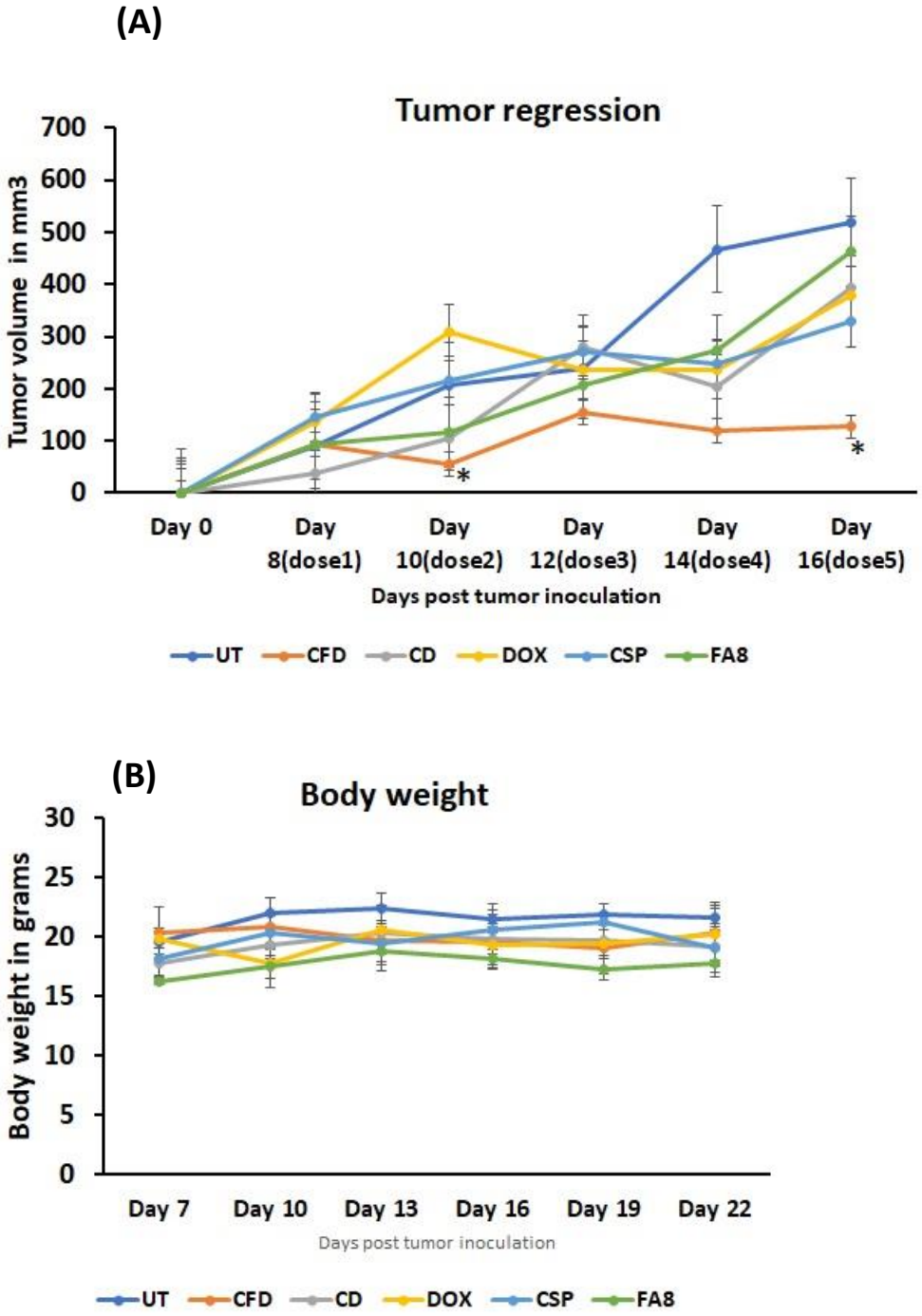

Fig.4.19a. CFD proves as maximally effective with no apparent toxicity: Plot (A) shows the change in tumour size (group size) as recorded over the course of treatment (Day 0 to Day 16. Plot (B) on the other hand shows change in body weight for the same treatment groups, with no toxicity evident in targeted delivery group. Statistical significance was evaluated using Students t-test where *-$p<0.05$ with Untreated group (UT) as control and $- $p<0.05$ with DOX as control.

(A)

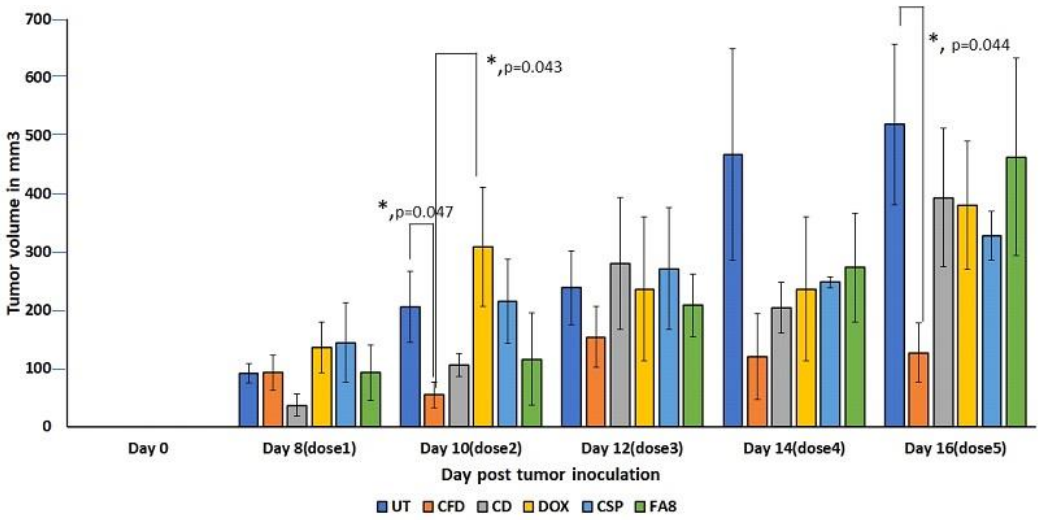

(B)

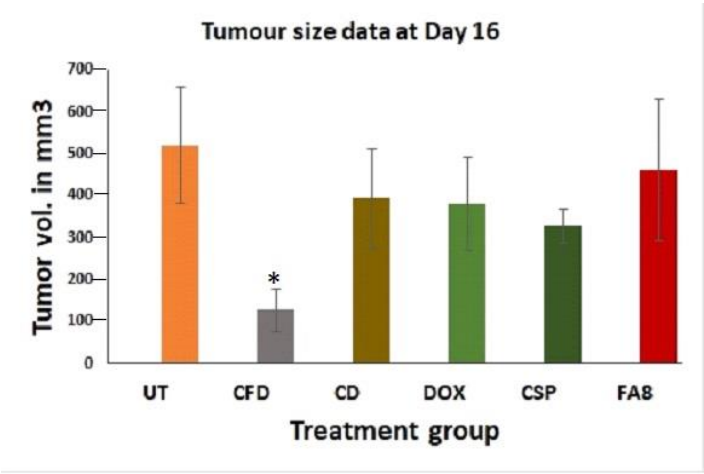

Fig.4.19b. CFD stalls tumour growth at an early stage of treatment: Graph (A) represents statistically significant change in CFD treated tumour size on day 16 (last day of dosing) as well as the inter-group tumour size difference on a dose-to-dose basis. Graph (B) shows the same data but only as representative of day 16. Statistical significance was evaluated using Students t-test where *-$p<0.05$.

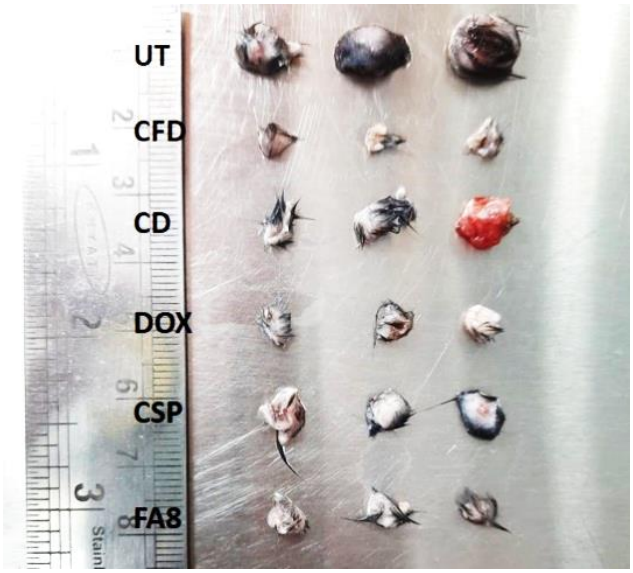

Fig.4.19c. CFD treatment has long standing therapeutic effect: MOC2 cells were inoculated (1 million per animal) subcutaneously in 4 weeks old female C57/BL6J mice. Treatment was started on day 8 (post tumour inoculation). Intraperitoneal injections (5 mg/kg Drug equivalent) for CFD (CSP-FA8-DOX), CD (CSP-DOX), CSP (only CSP), FA8 (Folate based Ligand) and DOX were administered intraperitoneally for 5 dosings on alternate days. Above Image represents tumour size difference as seen at the end of treatment course on day 23 post tumour inoculation. Statistical significance was evaluated using Students t-test where *- $p<0.05$ with Untreated group (UT) as control.

4.9. Western blotting experiments with MOC2 tumour lysates:

Subcutaneous tumours induced in mice were harvested after animal sacrifice and lysed for the purpose of carrying out western blotting experiments. Even though E-Cadherin levels showed no significant upregulation in treatment group CFD, a concomitant downregulation in levels of Vimentin was found in CFD treated samples, indicating a possibility of EMT reversal induction (**Fig.4.20**). This corroborates from earlier reports on Vimentin and its involvement in EMT (**Bonavida & Baritaki,2011**). Cleaved caspase-3 is a well-reported marker for apoptotic cell death (**Porter & Jänicke,1999**). Immunoblotting studies for this pro-apoptotic marker revealed higher expression levels in CFD treated samples as compared to the untreated control tumours.

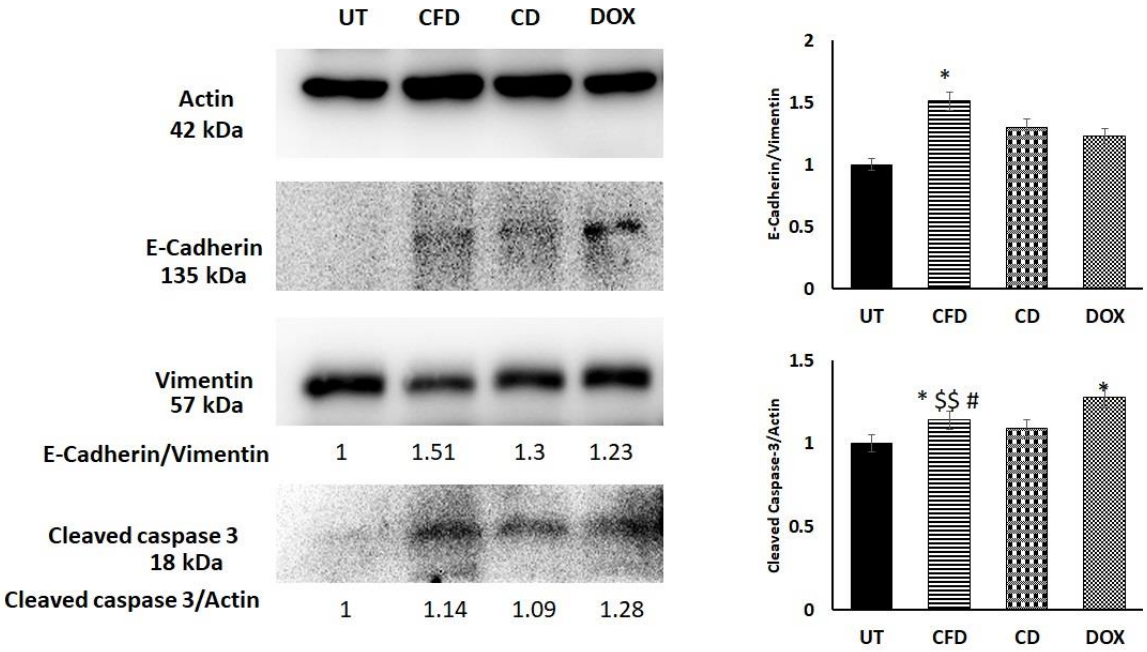

Fig.4.20. Western blotting for study of markers associated with EMT and apoptotic pathways in tumour lysates: MOC2 induced tumours inoculated subcutaneously in C57 mice were harvested treatment group-wise at the end of treatment schedule and lysed to obtain protein samples for Western blotting. Blots were immunoprobed for EMT associated markers E-Cadherin and Vimentin. Additional blotting was also performed for Cleaved caspase-3, a confirmatory marker associated with the apoptotic pathway. All blots were normalized against corresponding immunoblot of β-Actin. Graphs represent levels of particular proteins as Average ± SEM values. All blot images were quantified using Image-J software. Statistical significance with respect to Untreated control represented by * where $p<0.05$-*. Similarly, $ denotes $p<0.05$ with DOX as control & # denotes $p<0.05$ with CD as control.

4.10. Histopathology based toxicity studies:

$3x10^6$ cells of MOC-2(Mouse OSCC cell line) were injected subcutaneously into the right flank of female C57/BL6J mice (5-6 weeks). Tumours of approx. volume 50 mm^3(average) were observed on the 7th day post tumour cell inoculation. Mice were then randomly divided into groups and treated with CFD, CD, DOX, CSP & FA8 (5mg/kg DOX drug equivalent) intraperitoneally for 5 alternate dosings. Tumour size was measured every 2 days with vernier callipers. Mice were then sacrificed on day 23 post tumour inoculation and organs, namely the heart, liver, kidney and spleen were taken out and fixed with 4% paraformaldehyde. Post fixation organs were preserved in 1X PBS containing 20% glycerol till embedding them in paraffin blocks and obtaining sections using a Microtome. Upon observation, signs of myocardial vascular degeneration as well as some thickening in the middle layer of the coronary artery were found in the heart tissue samples of DOX treated mice **(Fig.4.21)**. Also, mild vacuolar/fatty degeneration of the coronary artery was observed in myocardium of heart for CD treated mice. In contrast, heart tissue from CFD treated mice was found to have normal morphology of the myocardium. Regarding the other organs observed, no apparent sign suggesting any loss of micro-architecture or perturbation in tissue structure could be observed across all the treatment groups. Notably, multifocal tumour emboli consisting of clusters of neoplastic cells could be observed in sections of liver from CD and DOX treated groups.

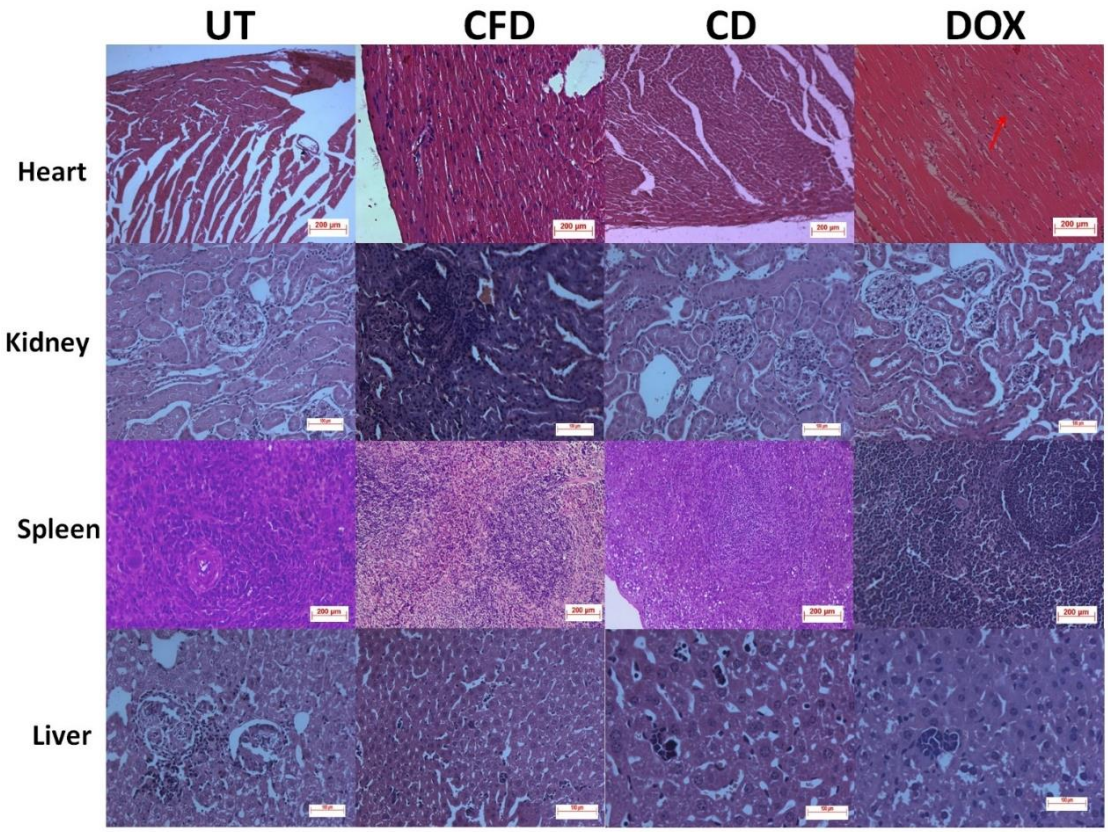

Fig.4.21. Organ histopathological studies for tissue toxicity: Above panel represents H&E (Haematoxylin and Eosin) stained images of different organ sections belonging to heart, kidney, liver and spleen. Images were taken under 100X and 200X magnification as required. Red arrow in the image representing Heart section of DOX treatment group shows myocardial vacuolar degeneration.

4.11. Assessment of DOX uptake in whole tumours and TAMs:

Subcutaneous tumours induced in mice were isolated fresh after sacrificing tumour bearing mice and were subsequently broken down by using Collagenase 1 to obtain a uniform suspension. Whole tumour cell suspensions were thus assessed via Flow Cytometry for the quantitation of drug (DOX) uptake. Drug uptake was found to be higher in case of CFD treated tumours as compared to DOX or CD treated groups (**Fig.4.22-A**). Subsequently the separation of CD11b positive (rich in TAMs) cell population from tumours was done and a comparative assessment of drug uptake was done between the CD11b-positive and negative cell populations. We found that DOX uptake was higher in the TAM-inclusive CD11b positive cell population, indicating significant uptake of the targeted system within the target stromal population (**Fig. 4.22-B**).

To assess and confirm the degree of FR expression on TAMs so isolated from murine tumours, a Flow cytometry-based receptor level quantitation was performed. Sufficient shift in fluorescence was detected after staining TAMs with FR-targeted antibody, which indicated substantial levels of FR expression on TAMs isolated from tumours. This also confirmed that the entry of drug was undoubtedly occurring via the Folate receptor **(Fig.4.22-C)**.

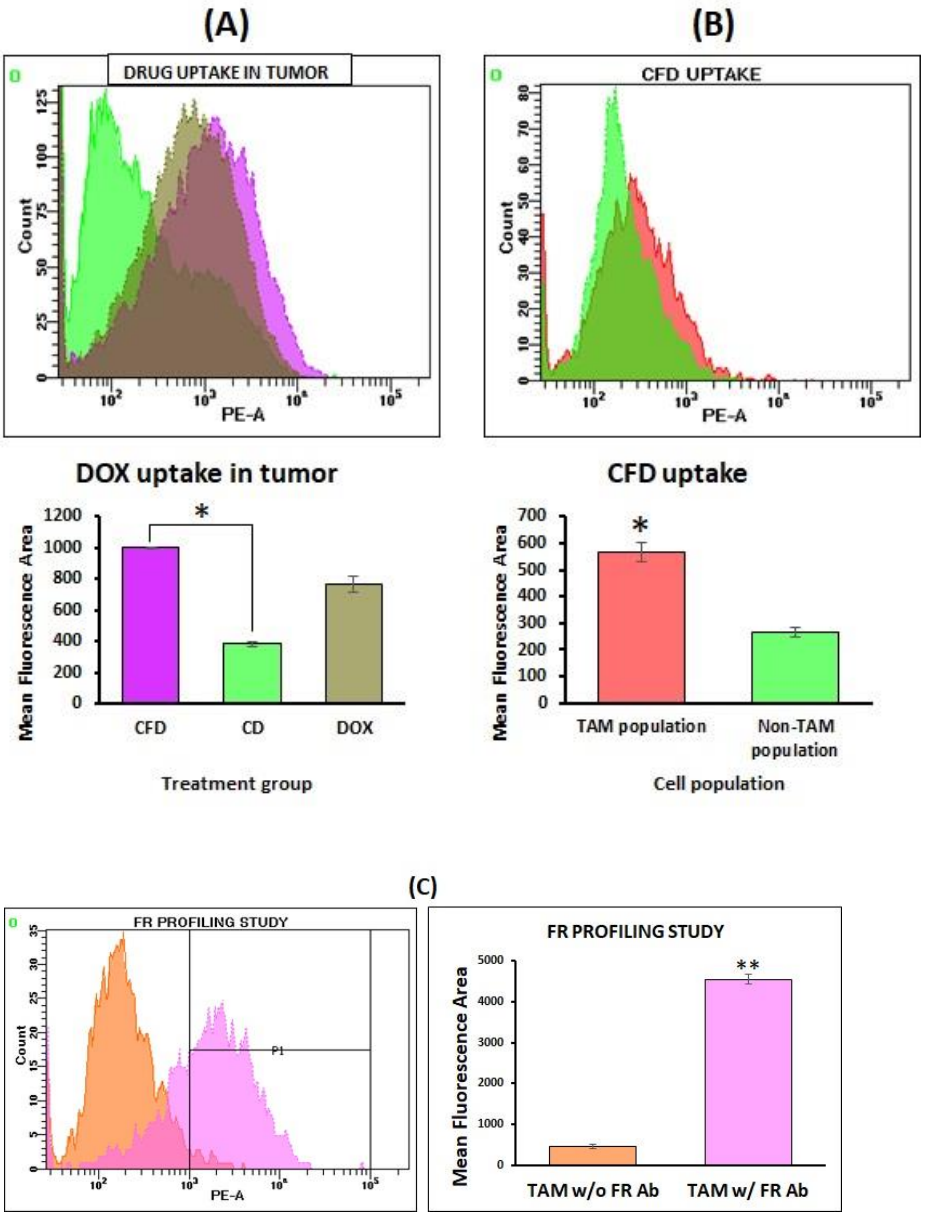

Fig.4.22. Flow Cytometry for drug quantitation in TAMs: MOC2 induced tumours from C57 mice were harvested treatment group-wise on the 10th day post tumour inoculation (after 2 treatment schedules or dosings) and broken down into single cell suspensions that could be processed for flow cytometry. Graphs represent mean area for fluorescence as Average ± SEM values. Statistical significance with respect to (A) CD and (B) Non-TAM population is represented by * which denotes that $p<0.05$. (C) Graph representing FR expression profile for TAMs isolated from murine tumour. ** represents statistical significance at $p<0.01$.

4.12. Assessment of TAM downregulation in the OSCC tumour microenvironment:

Subcutaneous tumours induced in mice were isolated fresh after sacrificing tumour bearing mice and were subsequently broken down by using Collagenase 1 to obtain a uniform suspension. Whole tumour cell suspensions were thus assessed via Flow Cytometry for the quantitation of TAM associated markers CD80, CD163, CD68 and CD206(**Fig 4.23**). For ease of assessment, calculations were performed for relative ratios of CD80(anti-tumoural) to CD206(pro-tumoural) and CD68 to CD163(both pro-tumoural). CD80/CD206 ratio in CFD treated group was found to be significantly higher than untreated group UT. At the same time, the CD68/CD163 ratios were higher for all treatment groups when compared to UT. Individually, CD80(M1 marker) expression was significantly higher in case of CFD group when compared to control group UT while for DOX treated group such was not the case (**Fig.4.24-A**). At the same time, CD163(M2 marker) expression was the lowest (statistically significant) only in case of CFD treated group and not for pristine DOX treatment (**Fig.4.24-B**). Since it has already been proven that it is possible to attenuate cancer aggressiveness by remodelling the TME, especially via the downregulation of CD206-positive markers, the findings from this particular experiment were encouraging (**Tu et al.,2020**).

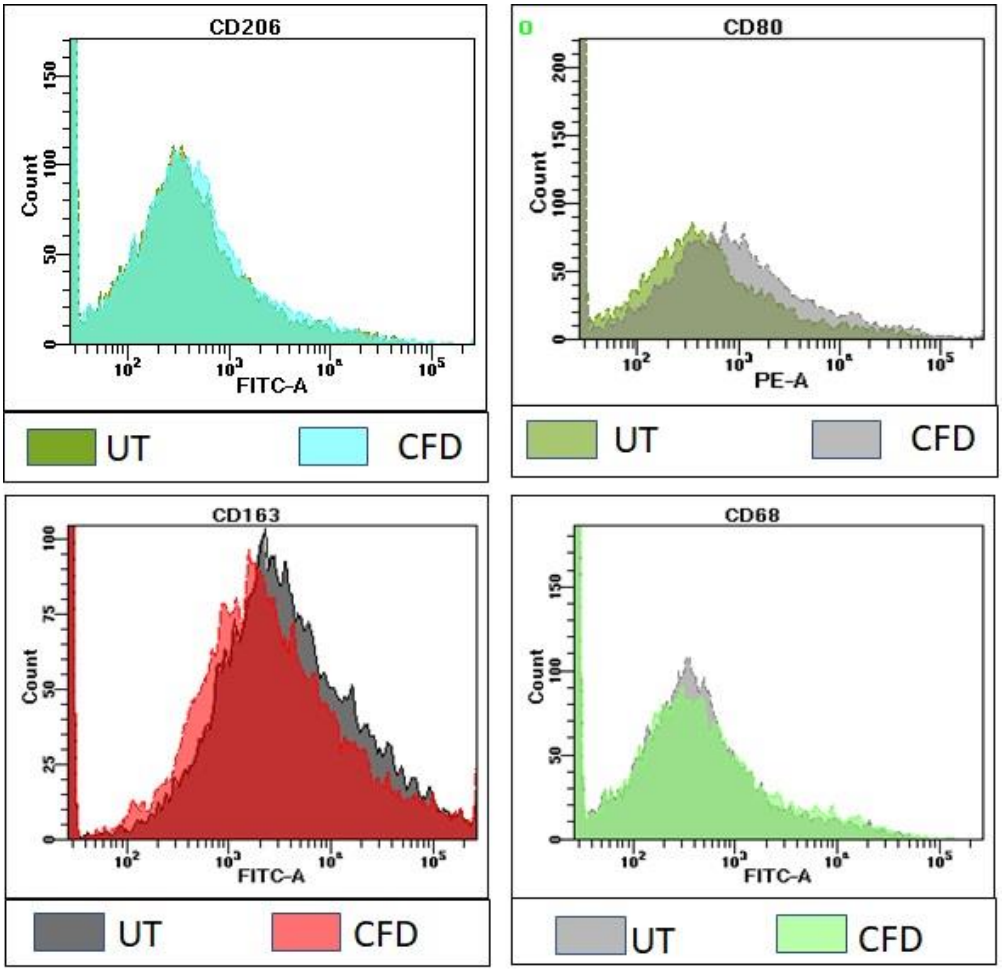

Fig.4.23. Flow Cytometry based quantitation of TAM specific markers: MOC2 induced tumours from C57 mice were harvested treatment group-wise on the 10th day post tumour inoculation (after 2 treatment schedules or dosing's) and broken down into single cell suspensions that could be processed for flow cytometry. Cd11b-positive TAM population was isolated from tumoural cell suspensions using CD11b-coated magnetic beads (Miltenyi Biotech) and assessed for expression levels of four TAM markers- CD80, CD206, CD68 and CD163(histograms).

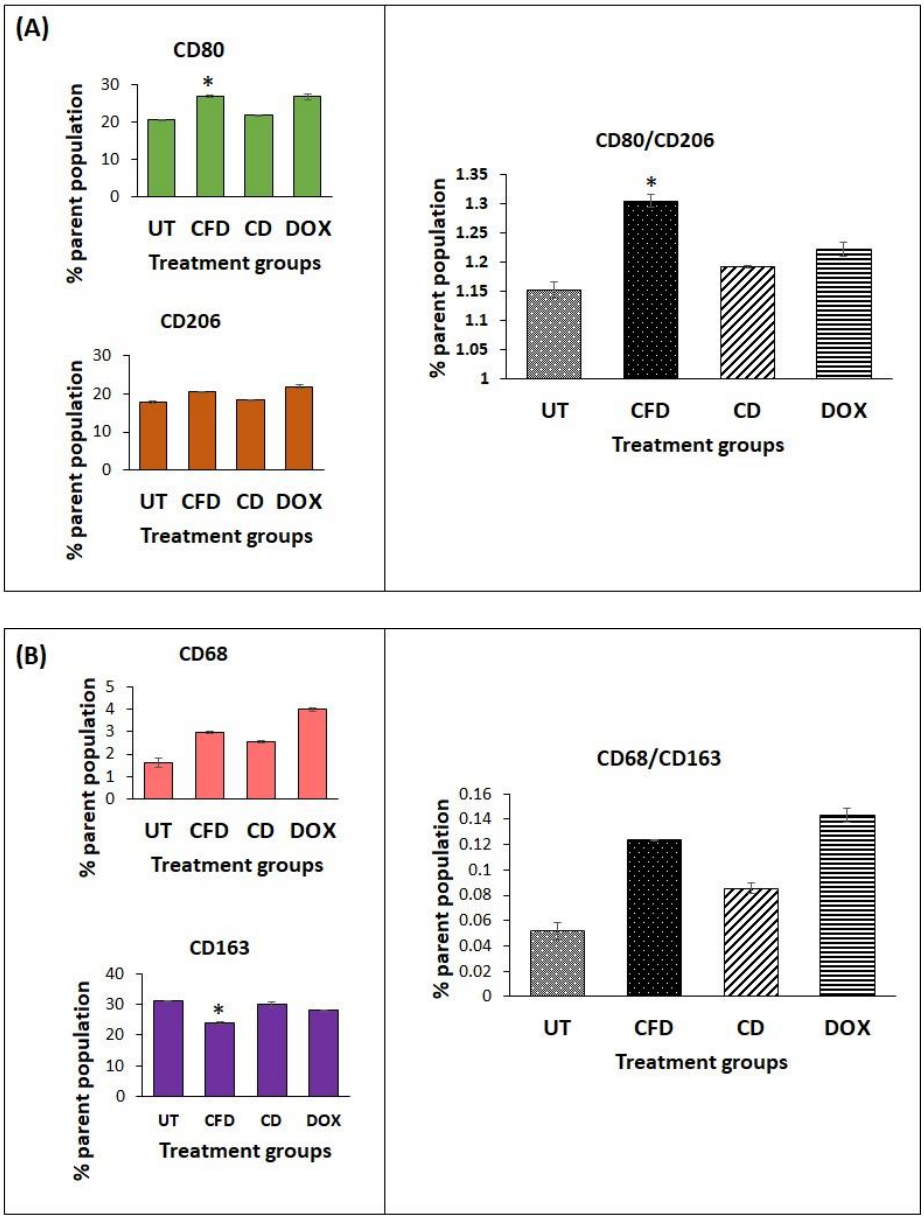

Fig.4.24. Flow Cytometry based quantitation of M2 TAM-associated markers: Tumours were harvested treatment group-wise at the end of treatment schedule and broken down into single cell suspensions that could be processed for flow cytometry. TAM positive population was assessed for (A) CD80 and CD206 (B) CD68 and CD163 using fluorescently tagged antibodies. Graphs represent mean area for fluorescence as Average ± SEM values. Statistical significance with respect to Untreated control represented by * where $p<0.05$ and $ where $p<0.05$ with DOX as control.

4.13. Protein level studies to confirm treatment effects on TME:

Subcutaneous tumours induced in mice were harvested after animal sacrifice and lysed for the purpose of carrying out western blotting experiments. In order to re-confirm the findings pertaining to Flow cytometry data for TAM markers, immunoblotting was performed for TAM markers CD80 and CD206. In this regard, CD80-positive macrophages are known to be an essential player to orient the TME towards an anti-cancer state (**Chang et al.,2007**). In concert with our flow cytometry data (**Fig.4.25**), CD80 levels were found to be highly upregulated in CFD treated mouse tumours when compared to other groups. Again, akin to Flow cytometry data, CD206 levels were found upregulated across all groups except CFD when compared to untreated samples. However, notably, upregulation in CD206 was negligible in CFD treated samples as compared to CD and DOX treated tumours.

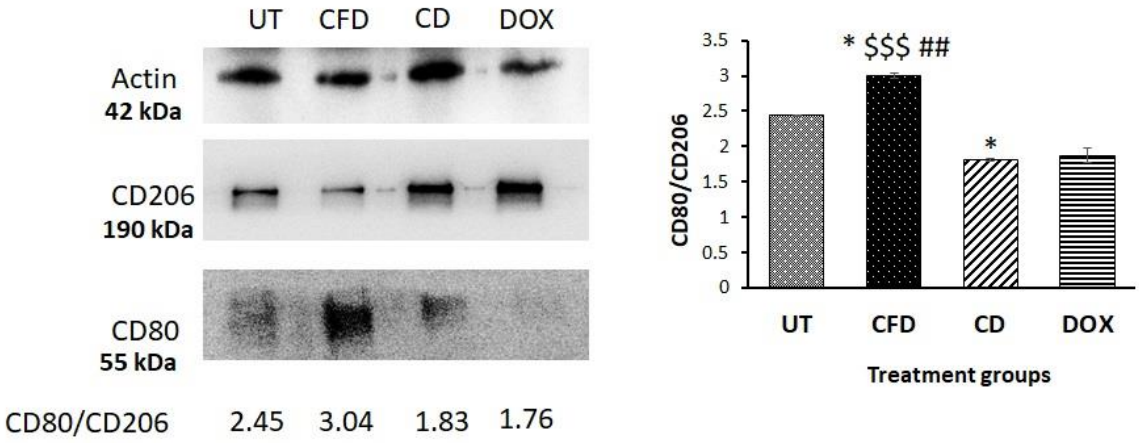

Fig.4.25. Western blotting for M1 marker CD80 and M2 marker CD206 in tumour lysates: MOC2 induced tumours inoculated subcutaneously in C57 mice were harvested on 20th day post tumour inoculation and lysed. Blots were immunoprobed for TAM markers CD80 and CD206. All blots were normalized against corresponding immunoblot of β-Actin. Graphs represent levels of particular proteins as Average ± SEM values. All blot images were quantified using Image-J software. Statistical significance with respect to Untreated control represented by * where $p<0.05$, $ where $p<0.05$ with DOX as control and # where $p<0.05$ with CD as control.

4.14. Western blotting to probe possible mechanism behind tumour cell and TAM attenuation:

Subcutaneous tumours induced in mice were harvested after animal sacrifice and lysed for the purpose of carrying out western blotting experiments. iNOS levels were found significantly downregulated in CFD treated tumours as compared to untreated control. Upregulation was noted in TNF α levels in CFD treated lysates but not as much as in case of CD and DOX treatment groups (**Fig.4.26**). Protein level for p53 in case of CFD treated group was found to be significantly downregulated with respect to untreated tumour group. This finding in particular was interesting in view of the fact that stable p53 expression (protein level) in cancers mutated for this gene is often indicative pro-cancerous conditions owing to possible gain of function (**Soussi & Lozano,2005**). Additionally, such GOF mutations may even work in concert with elevated iNOS expression to aid in cancer progression (**Yang et al.,2015**).

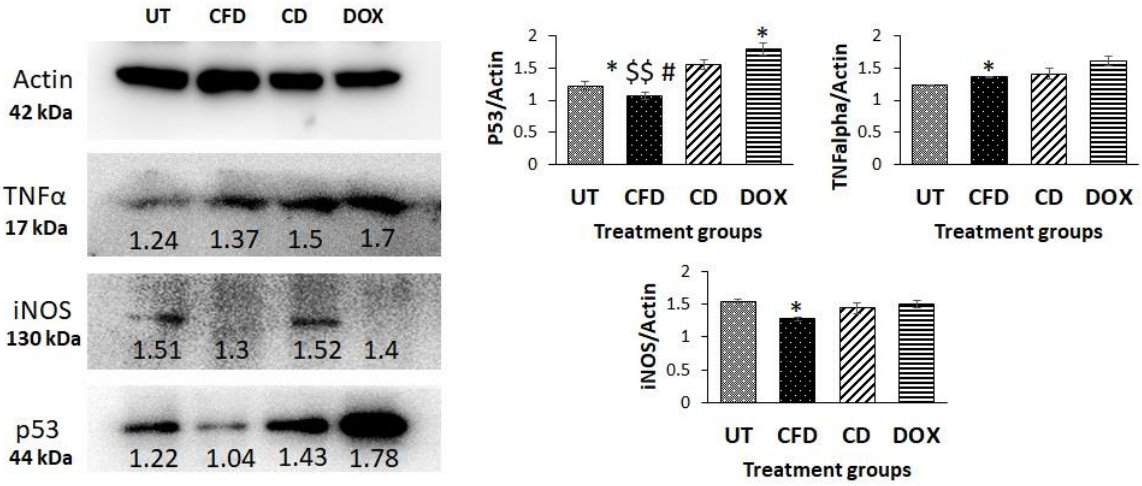

Fig.4.26. Western blotting for TNFα and iNOS in tumour lysates: MOC2 induced tumours inoculated subcutaneously in C57 mice were harvested treatment group-wise at the end of treatment schedule on 20th day post tumour inoculation and lysed to obtain protein samples for Western blotting. Blots were immunoprobed for EMT associated markers iNOS and TNFα as well as tumour suppressor protein p53. All blots were normalized against corresponding immunoblot of β-Actin. Graphs represent levels of particular proteins as Average ± SEM values. All blot images were quantified using Image-J software. Statistical significance with respect to untreated control (UT) is represented by * which denotes that $p<0.05$ and $ where $p<0.05$ with DOX as control.

4.15. Spheroid based ex-vivo studies for assessment of drug uptake:

Tumour spheroids were cultured for this particular experiment as it is a dependable ex-vivo platform and faithfully recapitulates in vivo tumour size regression experiments as well as drug uptake results without sacrificing experimental animals and also within a much shorter span of time (Ref). In this case, spheroids were assessed for drug uptake by Flow cytometric quantitation. For FaDu spheroids, uptake of CFD was found to be slightly less than that of DOX in 24 hours (**Fig.4.27**). However, drug uptake in CFD treated spheroids at 24 hours was still significantly higher than in case of those treated with non-targeted formulation CD. However, result of uptake studies at 48 hours showed comparable drug uptake between CFD and DOX treated spheroids with greater shift when compared to CD. However, this same experiment was also repeated in loose spheroids of aggressive mouse OSCC cell line MOC2 where CFD uptake was found to be much higher than CD but at the same time lower than that of free drug treated spheroids. Also, for both FaDu as well as MOC2, it was found that the uptake of drug reduced between 24 hours and 48 hours in case of DOX treated group while this depreciation was comparatively less for CFD treated spheroids.

FaDu spheroids were also cultured the same way and treated for uptake post which they were fixed and observed under the confocal microscope after 6 hours. Uptake of Dox was surprisingly found to be slightly higher in the CFD treated spheroids as compared to DOX treated spheroids. However, uptake in CD treated 3D spheroids was lower than CFD treated ones but almost at par with those treated with pristine drug. These results more or less corroborated with our flow cytometry results based on the same experimental outline (**Fig.4.28**).

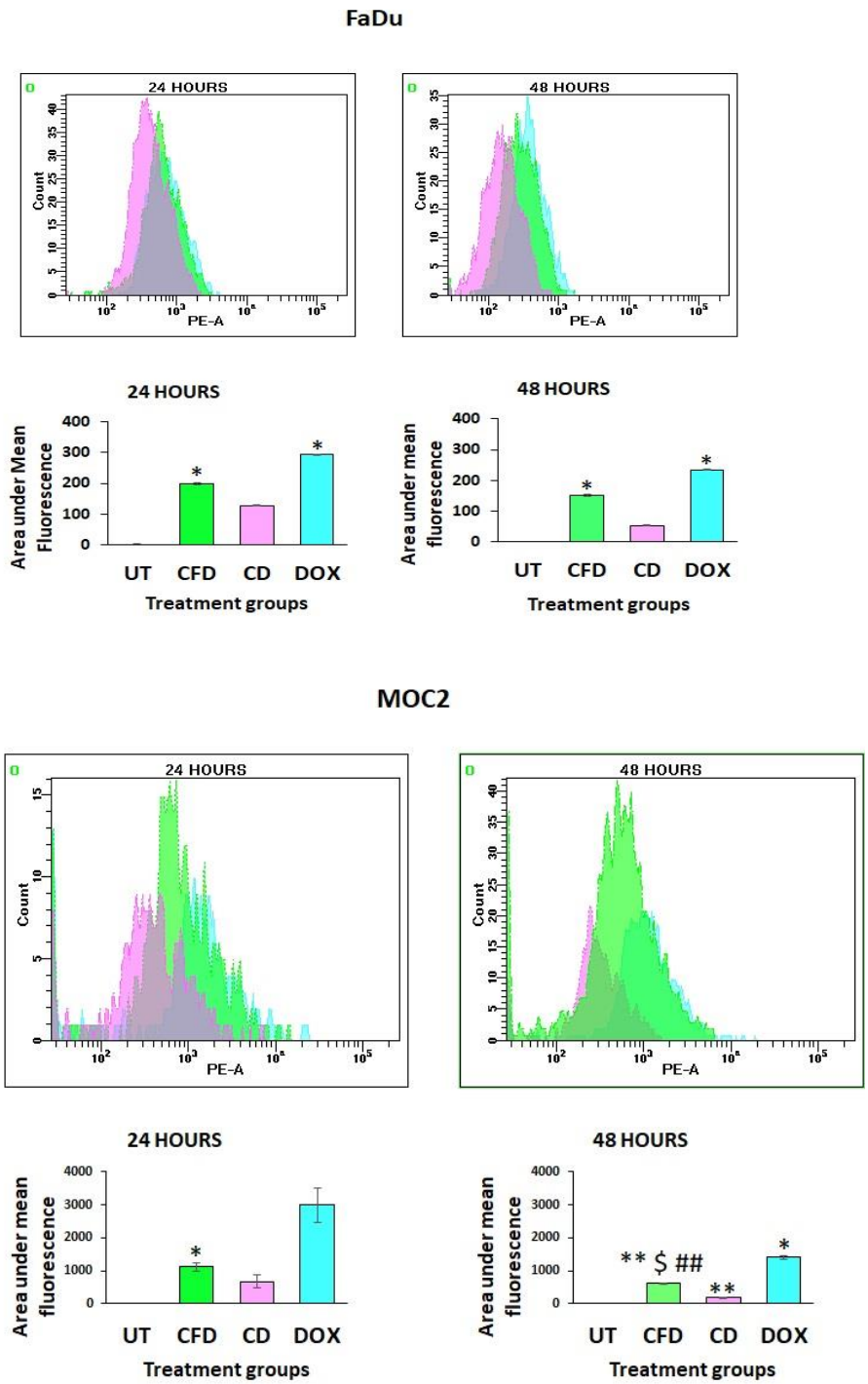

Fig.4.27. Flow Cytometry for quantitation of drug uptake in spheroids: MOC2 and FaDu spheroids were treated on day 3 post seeding and harvested at two time points, 24 hours and 48 hours post treatment. Graphs represent mean area under fluorescence as Average ± SEM values. * denotes p<0.05 w.r.t UT, $ denotes p<0.05 w.r.t DOX and # denotes p<0.05 w.r.t CD.

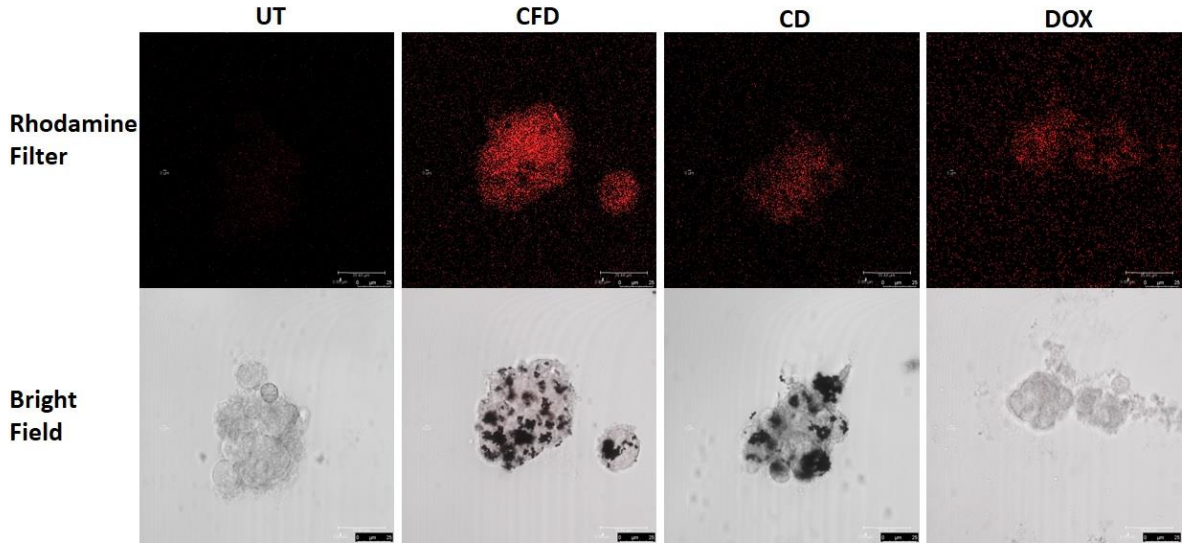

Fig.4.28. Confocal Imaging for qualitative assessment of drug uptake in FaDu spheroids: FaDu spheroids were treated on day 3 post seeding and harvested 6 hours post treatment. Spheroids were fixed with paraformaldehyde and mounted under coverslips on glass slides to produce permanent slides. Imaging was done under 20X magnification under two filters. Images represent various treated spheroid groups and their fluorescent images pertaining to DOX associated signal.

4.16. Study for assessment of treatment effects on ex-vivo cultured spheroid size:

Spheroids were treated in the same way as in case of spheroid based drug uptake studies and assessed via brightfield microscopy for changes in size or volume at 24 hours and 48 hours' time points. In case of FaDu, CFD treated spheroids were found to have significantly reduced size when compared to untreated group within 24 hours. While there wasn't much difference in size for CD treated group(non-targeted), DOX treated spheroids showed size depreciation as well, even though not statistically significant. At the 48 hours' time point we found statistically significant size depreciation for both CFD and DOX treated spheroids. In case of MOC2, the overall spheroid structure as well as size were found to be significantly altered after 24 hours of CFD treatment and this effect was still found to be persistent even at the 48 hours' time point. Once again, CD treated spheroids showed very little change in size which did not amount to being statistically significant (**Fig.4.29**).

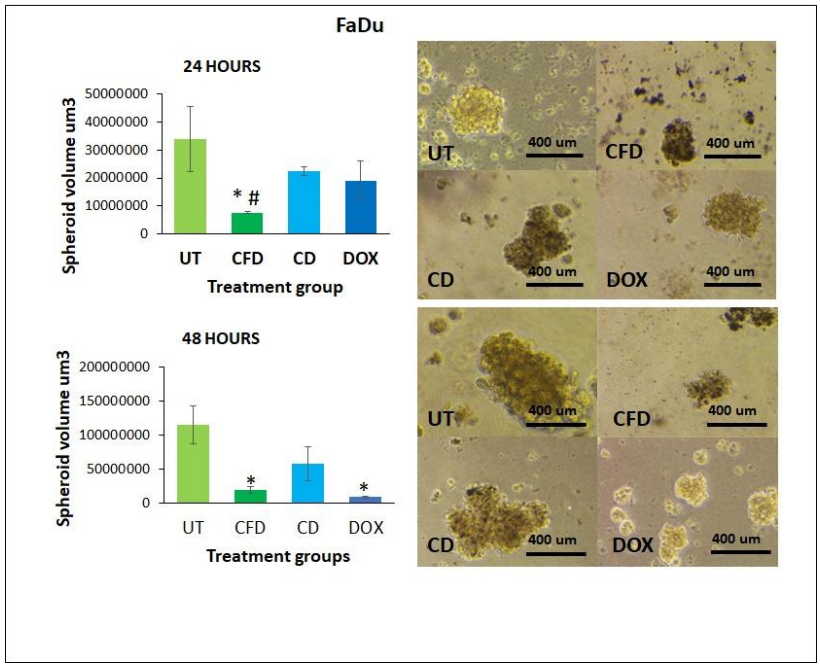

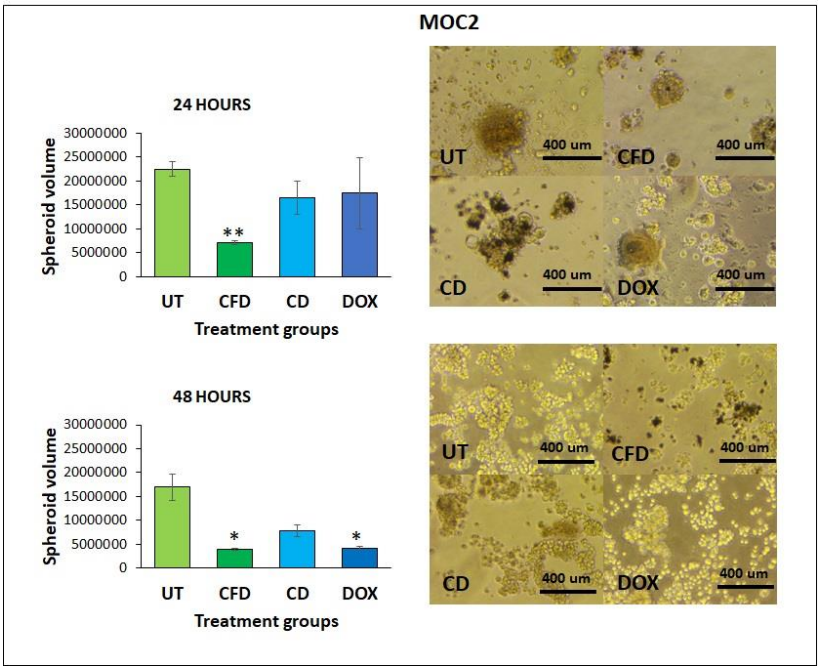

Fig.4.29. Bright field imaging for size regression analysis in 3D tumour spheroids: FaDu and MOC2 spheroids were treated on day 3 post seeding and imaged under 10X magnification 24 hours and 48 hours post treatment. Images were analysed using Image J software for spheroid size(volume) assessment. Graphs represent volume readings in μm^3 where statistical significance has been calculated with respect to untreated control UT where * represents $p<0.05$. # denotes $p<0.05$ where CD is control.

The usual course of treatment for OSCC in the clinical setting has mostly included surgical resection of the primary tumour to get rid of further progression and facilitation of disease-free survival (**Shah & Gil,2009**). But with time the nature of oral cancer, its genesis as well as repercussions in affected individuals have evolved, paving the path for multiple therapeutic approaches like radiotherapy, surgery, chemotherapy as well as combinations of these modalities.

Oral cancer is highly resistant to therapy and very difficult to diagnose, especially in its early stages (**Zhang & Li,2023**). One of the reasons behind this is the inherent ability of cancer cells to expel drugs or chemotherapeutic moieties using a variety of different mechanisms. The inability of drugs to be retained over extended time periods in cancer cells often poses a challenge to achieving long standing therapeutic outcome (**Liu, 2009**). Targeted chemotherapy making use of nanosized molecules or nano-sized delivery systems often tend to address the issue of drug retention by means of EPR or Enhanced Permeability and Retention, a phenomenon that allows passive circulation of nanosytems to the tumour site and its adjoining areas (**Shi et al.,2020**). This mostly happens either on account of the leaky vasculature possessed by these tumour sites or due to a lack of sufficient lymphatic draining which allows higher retention. MDR or Multi Drug Resistance arises due to multiple reasons. However, some of the primary ones are those that directly affect drug activity, namely the influx and efflux of drugs or small molecules at the tumour site. Most of the time these movements are under the control of membrane transporters like Pgp (**Loscher & Potschka,2005**). Ever since their discovery, these transporters have been deeply studied so as to develop them as druggable targets. As a result, there are currently

a host of drugs at our disposal which target these transporter proteins and thus effectively serve as efflux inhibitors (**Amin, 2013**). However, the other way this issue may be addressed is by means of site-targeted delivery as achieved by methods such as receptor targeted delivery. There have been multiple studies on drug retention and its targetability using inherently fluorescent molecules like Anthracyclines (**Krishan et al.,1987**). Most of these studies have tried to take advantage of the EPR effect by modulating the size, shape or other morphometric characteristics of the nano-sized delivery systems for effective delivery and subsequent retention (**Zhuo et al., 2018**). Some of these studies have reported the use of click reaction-based systems that are amenable to modification in size and structure when applied with an appropriate stimulus (**Han et al.,2017**). On the other hand, there are studies that elaborate on the advantages of nanodelivery systems that can circumvent or avoid efflux pumps such as those present in the cell membrane to achieve improved drug retention (**Ma & Mumper,2013**). In this context literature review brought up have come across multiple studies that have detailed the elegant workings of such therapeutic molecules that manage to be retained on account of their surface functionalizations and other chemical or physical modifications (**Osman et al.,2022**). It is common knowledge that drugs like Doxorubicin enter cells by means of diffusion. This means their entry is smooth but at the same time, they are subject to being evicted by membrane-based efflux pumps like Pgp (**Kim et al.,2020**). On the other hand, the same molecule when modified or conjugated to a targeted system is taken up by cells by means of the endocytic pathway, marking a major way in which they are subsequently sorted once within the cell (**Ma & Mumper,2013**). Endocytosis also provides these delivery systems immunity from efflux pumps and transporter proteins (**Goren et al.,2000**). One particular work involved the use of a modified nanodelivery system that reduced or scavenged the

tumour site of GSH(Glutathione), thus effectively chemosensitizing the cancer cells while serving the purpose of photoacoustic imaging (**Yang et al.,2020**). In the context of the current work, we did manage enhanced DOX retention (**Fig. 4.12**). This was possibly because of Folate Receptor mediated endocytosis which surely must have gained advantage over efflux transporters that otherwise render these cancer cells resistant. However, a deeper understanding of the exact mechanism or the particular efflux effectors that may have been involved has not yet been entirely delineated and would provide for more detailed investigation in the future. There was enough evidence showing higher retention of DOX for longer periods of time when delivered via the FR, affecting tumour cells and TAMs alike. This finding also matches with the observation of previous authors who have outlined a clear correlation between longer retention and evasion of drug efflux.

5.1. Targeting FR in oral squamous cell carcinoma

The aim of the current work was to develop a delivery system that would faithfully carry drug payload specifically into cancer cells. The receptor chosen to target is the FR which was initially discovered as a ubiquitous target for the delivery of agents that were otherwise difficult to deliver to the interior of cells (**Lu et al.,2002**). The idea of conjugating such molecules or other payloads to a naturally sourced Vitamin molecule was like striking gold in its initial stages, especially when it achieved successful delivery even to plant cells (**Low et al.,2008**). However, further studies soon revealed that the FR was overexpressed on cancer cells as well as cells in a variety of diseased conditions (**Hilgenbrink & Low,2005**). This made FR a popular choice for targeted delivery to cancer cells as well as tumour associated macrophages (TAMs) (**Nagai et al.,2009**). The Folate based cationic lipid reported previously was shown to have higher affinity for the FR as compared to the

natural ligand Folate (**Elechalawar et al.,2017**). Targeted drug delivery was achieved using glucose-based carbon nanospheres in melanoma and grade-4 glioma besides TAMs, which express FR. A variety of nano formulations are used for the diagnosis and therapy of oral cancer. These include liposomes, polymeric nanospheres/nanocapsules, nanocrystals, dendrimers, gold and magnetic nanoparticles etc. For treatment of oral cancer, mesoporous silica nanoparticle with DOX, co-encapsulated with other drug, or chitosan nanoparticle loaded with levulinic acid derivative targeted through FR have been tested on animal models of OSCC (**Wang et al.,2018**; **Lim et al.,2018**). Together with the heterogeneity of cancer types in oral cavity and the difficulty in attaining high local concentration of drug in the diseased sites, it is paramount to look for delivery systems that offer the advantage of dual targetability. In glucose based nanospheres (CSPs) the negatively charged surface carries multiple carboxylic anions formed from glucose moieties which render it selectively accessible to cancer cells having relatively higher expression of sialic acid moiety. Adsorbed folate cationic lipid on CSP provides this extra selectivity to target and deliver higher concentration of drug cargo to cancer cells. This ensured minimal accumulation of drug in non-cancerous areas, thus reducing potential collateral damages, as is evidenced by higher accumulation of CFD compared to pristine DOX at a given time point within OSCC cells (**Fig. 4.13**).

FR targeted delivery was proven in this work by receptor attenuation studies (**Fig. 4.7**). However, higher concentration of folate (100 µm was required, indicating a strong affinity possessed by our Folate based ligand FA8 for the Folate receptor. We are aware of the phenomenon of FR circulation between the cell surface/membrane and the cytoplasm (**Hilgenbrink et al.,2005**). FR is initially present as a membrane bound glycoprotein which upon binding to a suitable ligand dislodges from the membrane and enters the cell via an

endocytic pathway. Upon entry into the cell, it releases its cargo and the free receptor is re-circulated to the cell surface where it proceeds to bind a greater number of ligand molecules. For western blotting studies the buffer used for in vitro lysate collection was Laemmli. Laemmli buffer is not well suited for the extraction of membrane bound glycoproteins, suggesting that whatever protein levels of FR were detected most likely corresponded to the freely circulating FR isoform (**Gurnett et al.,1996**). Subsequent blotting studies revealed a spike in the levels of FR immediately within 30 minutes of Folate treatment. These levels were then gradually seen to wane off within a few hours, indicating that it had possibly been recycled back to the cell surface. This was a probable indication that targeted delivery system CFD would be endocytosed rapidly once it faced the surface FRs on cancer cells leading to robust uptake followed by recycling in less than 6 hours. Levels of FR expression as a function of folate exposure conducted on a time scale study, revealed interesting facts. Regulation of soluble FR1 levels post-folate treatment in FaDU and MOC2 were different than CAL27 but exhibited much higher levels than that in non-cancer cell, HEK293 (**Fig. 4.6**). This indicated FR-targeted entry of CFD in OSCC cells.

5.2. Further benefits of FR targeted therapy

When it comes to targeted therapy, its crucial to understand how such systems would enter cells and how effective payload delivery would be. There is a comprehensive review article providing detailed insight on the use of endocytic mechanisms for targeted delivery (**Bareford & Swaan,2007**). Based on their findings from literature, the authors argue that targeted delivery which follows uptake and internalization along the endo-lysosomal pathway hold great promise for disease specific therapies that can deliver cargo in a directed manner to specific compartments or sites of the cell. Receptors such as the Folate

receptor are present on the membrane and upon binding a high affinity ligand are endocytosed in vesicles that carry the delivery system inside till it is broken down by endo-lysosomal formations for effective release of cargo (**Sabharanjak & Mayor,2004**). This way, the therapeutics are saved from eviction by efflux pumps or transporters as well. Such approaches hold great potential for illnesses that suffer from drug resistance, including cancer.

In this case, uptake of the targeted system is via the caveolin mediated endocytic pathway (as is reported for Folate based entry) where the caveosome, a type of late endosome, releases its cargo and the free receptor is recycled back to the surface (**Suen & Chau,2014**). Results from receptor internalization studies corroborated with these findings and supported the model of FR mediated targeted drug uptake (**Fig. 4.6; Fig. 4.8**) Further, Zhang et al. have highlighted the importance of molecular interactions between targeted nano-delivery systems and membrane components for achieving better cellular uptake (**Zhang et al.,2021**). In the particular context of the folate receptor, the authors explain how FR, a glycoprotein, interacts with a suitable ligand or therapeutic entity and allows for its internalization and subsequent rapid disintegration for efficient release of therapeutic payload. However, the question that remained was whether targeted nanotherapeutics could evade or resist MDR.

An elaborate review on this topic has been published by (**Xue et al.,2020**). The authors have stressed upon advantages such as narrow size distribution, evasion of efflux pumps and longer circulation as well as higher accumulation in target site for targeted nanoparticles which provide them therapeutic advantage over standard approaches. Since designated Pgp inhibitors and similar molecules have certain known disadvantages, use of

alternative methods like siRNAs, antisense oligos or photodynamic therapy seems to be a better choice. In this regard, Kim et al. reported a targeted therapy module where they have elegantly incorporated the use of a microbubble-nanoparticle combinatorial platform. This system was shown to successfully deliver drug payload on the basis of micellar delivery whereupon photodynamic therapy induced release of Ce6 which incapacitated ABCG2 efflux pumps, allowing the efficient release and accumulation of Doxorubicin payload by nanoparticles at the target site (**Kim et al.,2020**). In another case, Yuan et al. authored a review on nanotherapeutic approaches to reversing MDR in resistant breast cancer (**Yuan et al.,2017**). Xu et al. reported the successful use of SLNs (solid lipid nanoparticles) for delivering Paclitaxel efficiently to drug resistant breast cancer cells (**Xu et al.,2018**). The authors elegantly demonstrated that SLN mediated drug uptake was much higher in resistant cells due to probable evasion of efflux pumps and they also verified endocytic uptake mechanisms by using specific inhibitors for Clathrin and Caveolin mediated endocytosis (**Suen et al.,2014**). However, at the end they have also concluded that whether the endocytic pathway followed by SLNs in case of resistant and sensitive cells is the same or different is not entirely clear and requires further investigation. In spite of relatively discouraging reviews so far, Efflux inhibitors are also being used by some investigators in conjunction with standard chemotherapeutics on a targeted delivery platform (**Dong et al.,2019**). In this study, Confocal scanning microscopy imaging of treated cells revealed that within cells treated with pristine DOX, drug shifted from the nuclear region to the cytoplasm and cell peripheral areas. Contrastingly, cells treated with CFD showed higher retention of drug within the nucleus (**Fig. 4.13**). This indicated the systems potential to resist the usual drug removal/eviction mechanisms make effective chemotherapy a challenge for multiple drugs, including DOX.

Distant metastasis in OSCC is quite common, even though it has been noted to happen in cases of late or advanced tumour growth. Metastasis in OSCC may lead to secondary tumours as well as primary tumours at distant sites. A patient cohort study conducted in 2016 showed the different sites in the body where metastasis from HNSCC may occur. Other than the lungs, distant metastasis was found to attack the heart, a variety of bones in the body, and the brain as well. However, apart from the knowledge of the spreading pattern of metastatic oral cancer, it is crucial to have an understanding of the underlying molecular biology as well. A review article on this matter explains how EMT is important for local recurrence as well as lymph node mediated distant metastasis (**Toll et al.,2013**). EMT is basically of 3 types-type 1, type 2 and type 3 where type 3 corresponds to the kind that contributes to cancer growth and progression. Among the primary molecular targets of EMT in oral cancer are E-cadherin, Vimentin, SNAIL, ZEB and TWIST (**Joseph et al.,2018**). Hence for the current study, E-cadherin and Vimentin levels were assessed in in-vivo samples or tumour lysates (**Fig. 4.20**). Additionally, a detailed review article by Ling et al. was found which documents how the tumour microenvironment also has a direct role in EMT occurrence (**Ling et al.,2021**). The TME as is known comprises of an array of stromal elements. Ling et al. have stressed on the role of such major members of the OSCC TME-the CAFs (Cancer Associated Fibroblasts) and TAMs (Tumour associated Macrophages). M2 pro-tumoural TAMs as well as M1 TAMs and their possible involvement in the entire process of EMT and tumour growth have been discussed later in this report.

5.3. Overcoming drug resistance for induction of cancer cell apoptosis

Doxorubicin is popularly known to induce apoptosis by overriding anti-apoptotic signals in cancer cells (**Fiandalo & Kyprianou,2012**). Cancer cells often exhibit chemoresistance as a

result of dysregulation in the balance between pro-and anti-apoptotic markers. It is quite common to find tumours that have upregulated expression of anti-apoptotic proteins such as Bcl-2, coupled with (not always) a concomitant downregulation of pro-apoptotic proteins like Bax (**Cho et al.,2006**). Oftentimes, such perturbations in the apoptotic balance are due to mutations in proteins that are part of either the intrinsic or extrinsic apoptotic pathways. This makes targeted therapies aimed at such dysregulated proteins a lucrative therapeutic option, especially in case of chemoresistant cancers that also harbour mutated tp53 (**Radha & Raghavan 2017**). The targeted system discussed here carries a cytotoxic molecule and hence it was logical that one should expect some activation of the apoptotic pathway (**Christidi & Brunham,2021**). However, this would require downregulation of Bcl-2, which would otherwise promote further genetic dysregulation and unchecked cellular proliferation to give rise to highly invasive cancer. This would be also be relevant especially considering the fact that the cell lines used in this study are all reportedly mutated for tp53 and also exhibit characteristic signs of DOX chemoresistance. When it comes specifically to oral squamous cell carcinoma, Bcl-2 overexpression has been recorded in multiple reports using 2D cultures or animal models of OSCC (**Duan et al.,2017**). However, there is a lot of disparity when it comes to comparing these observations with findings regarding clinical samples, where a large portion consistently shows high expression levels of Bax and Bcl-2 expression levels vary to a huge degree, making matters largely inconclusive (**Jordan et al.,1996**). Interestingly, the work reported by Pratt et al. discusses the regulation of Bcl-2 expression by mutated tp53 in Estrogen Receptor positive breast cancer cells, pointing out that stable expression of the mutated p53 caused moderately higher levels of Bcl-2 production while adenovirus mediated overexpression of wild type tp53 caused downregulation of Bcl-2 expression (**Pratt et al.,2007**). Yet another study by Emi et al.

discusses the therapeutic outcome of targeting Bcl-2 in breast cancer cells (**Emi et al.,2005**). The authors elegantly demonstrated how downregulation of Bcl-2 with antisense constructs increased their chemosensitivity to a host of different drugs (**Yamanaka et al.,2005**). In one study on the effects of tea tree oil (TTO), Ramadan et al. studied two types of cells, malignant melanoma and squamous cell carcinoma of the liver (**Ramadan et al.,2019**). The authors treated these cells with TTO and found a resultant increase in expression levels of tp53 and Bax accompanied by an attenuation of Bcl-2 protein levels. Teni et al. did an expression analysis for Bcl-2 and Bax in clinical samples of chewing tobacco induced OSCC using patient samples for diseased tumour tissue as well as lesions. They found irregularities in Bcl-2 expression but a majority of the samples had mutations in one or more of this particular set of genes-Bax, Bcl-2 and tp53, clearly outlining their importance in the context of the disease and its implications (**Teni et al.,2002**). Arumugam et al. have briefly reviewed the expression status of Bcl-2 in oral squamous cell carcinoma in patient samples and the prospects of the same as a prognostic marker (**Arumugam et al.,2017**). The authors have also stressed on how Bcl-2 contributes to negative prognosis and the importance of Bcl-2 inhibitors as a treatment option in the future. However, Bax or its possible role in cancer development and propagation must not be overlooked. Alam et al. found that Bax was mostly deregulated in a cohort of 127 OSCC patient samples via the tp53/Akt pathway and that its progressive downregulation is often responsible for the chemoresistant and invasive nature of this particular malignancy (**Alam et al.,2019**). A healthy and balanced ratio between Bax and Bcl-2 proteins is thus important for effective therapeutic outcome to be obtained (**Singh et al.,2019**).

OSCC is usually resistant to Doxorubicin, on account of upregulation of miR-221 as pointed out in their research article by Du et al. (**Du et al.,2017**). This was experimentally proven

by the use of anti-miR-221 oligonucleotides which downregulated miR-221 and effectively upregulated TIMP3 levels, leading to increased chemosensitivity in treated OSCC cells. As discussed earlier, OSCC often possesses mutated tp53. This again might lead to further chemoresistance towards DOX and its cytotoxic effects (**Chan & Lung,2004**). However, targeted delivery of Doxorubicin may overcome this hurdle by means of a variety of strategies, both direct and indirect (**Wang et al.,2011**). Such approaches might include re-activation of suppressed tp53 or depletion of a stable gain-of-function mutant protein. Additionally, targeted transfection with functional tp53 may be performed to achieve cancer cell death (**Sharma et al., 2016, Sridharan et al., 2020, Mukherjee et al.,2009**). However, it must be remembered that targeted delivery has ability to achieve successful therapeutic outcome for drugs like Doxorubicin which otherwise induces chemoresistance as a pristine molecule. El-Hamid et al. reported a liposome coated nano-doxorubicin formulation (Doxil) which they found to induce apoptosis in a much greater proportion of cells than when compared to pristine Doxorubicin (**Abd El-Hamid et al.,2019**). At the same time, they also showed that the percentage of necrotic cells was much higher in case of Doxorubicin treatment than the Doxil treated group. This particular report corroborates with findings from this study where CFD (targeted system) induced comparable or sometimes slightly higher levels of apoptosis than free DOX, while showing little upregulation in TNFα or RIP3 when compared to drug alone (**Fig. 4.15; Fig. 4.18; Fig. 4.26**). This would likely be more efficacious. Additionally, there would probably be very little possibility of CFD having necroptotic effects like cardiotoxicity as free DOX in vivo. Somewhat akin to this approach, Lu et al. reported the use of a dual function nanoparticle that was decorated with Folic acid for receptor mediated delivery of Doxorubicin (**Lu et al.,2018**). The authors reported better targeted uptake as well as longer retention and

circulation in vivo among other encouraging findings, providing evidence as to the much more streamlined and efficient system of DOX delivery than when the drug alone is administered to drug resistant cancer cells. With increased drug efflux, drug resistance becomes more evident. Induction of resistance against drugs like DOX is a known fact. Initially, cytotoxic effects of free DOX are higher than CFD in OSCC cells (**Fig. 4.15**). This finding, when considered in light of the 24-hour uptake study, gave a clear indication that anti-cancer effects of CFD were comparatively more long-lasting owing to better retention post-uptake. At an earlier time, point (6h), uptake of pristine DOX was highest compared to other groups (**Fig. 4.10**). However, at the 24-hour time point, CFD showed the highest uptake compared to other treatment groups in all OSCC cells (**Fig. 4.12**). Efflux pumps are present in all kinds of cells irrespective of whether they are mammalian, fungal or bacterial (**Van Bambeke et al.,2000**). Efflux pumps have a variety of functions which serve crucial physiological purposes. For example, efflux pumps in cells of the gastrointestinal tract help in getting rid of toxins, and those in the kidney aid in excretion of drugs (**Ughachukwu & Unekwe,2012**). However, the function of these efflux pumps changes its nature in the context of cancer cells, where they tend to overexpress and eliminate drugs or other therapeutic small molecules, effectively diminishing treatment outcome (**Modok et al.,2006**). The presence of such pumps and transporters is one of the major reasons behind multiple drug resistance (MDR), a challenging feature most resistant cancers exhibit. However, when it comes to avoiding or countering this problem, efflux pump inhibitors are still considered out of bounds. Some of the reasons behind this is the toxicity such inhibitors have been found to cause as they promote retention of chemotherapeutics to extents much higher than required, bringing about more damage than recovery (**Wu et al.,2019**). Efflux pump inhibitors have also been reported to affect pumps in cells of

unaffected areas, negatively impacting enzymatic activity of P450 (**Kuzin et al.,2018**). It is thus logical that other ways to evade the activity of efflux pumps or their effects in case of cancer therapy be searched for. This calls for detailed knowledge of the various effectors related to the working of these efflux pumps so as to possibly target them in conjunction with targeted delivery of chemotherapeutics. In this regard there have been few breakthroughs in recent times. Chen et al. have shown how the overexpressed status of efflux pumps and related transporters is reached in a progressive manner as cancer cells are induced to become drug tolerant over a series of passages (**Chen et al.,2016**). The authors treated breast cancer cells with Tamoxifen over a long stretch of time and several passages to give rise to potentially resistant cells. As expected, they found these tolerant or resistant cells to have overexpression of a number of transporters like Pgp, BRCP, MRP2 etc., showing how the two factors are directly correlated. Not long ago, Kurimchak et al. have shown how the well-known efflux pump MDR1 promotes intrinsic and acquired resistance to PROTACs (Proteolysis targeting chimeras), an upcoming and profoundly promising class of drugs (**Kurimchak et al.,2022**). Needless to say, efflux mediated MDR and its implications are of serious concern to those concerned with targeting cancer effectively.

5.4. Possibilities of EMT reversal

As already discussed, E-Cadherin is a major protein which is severely dysregulated in OSCC and affects tumour invasiveness as well as progression. An immunohistochemical study on patient samples revealed how loss of expression for E-Cadherin in cells at the invasive front is a negative prognostic marker (**Mehendiratta et al.,2014**). However, the authors also mentioned that they did not find any direct correlation between lowered E-cadherin

expression and lymph node status or tumour size. In another study on patient samples, Verdin et al. recently showed that mRNA levels of E-Cadherin are significantly higher in cells at the invasive fronts of tumours than cells at the centre (**Verdin et al.,2019**). The authors again confirmed that this low expression of E-cadherin was responsible for local recurrence as well as lower survivability. Vimentin however, is a mesenchymal marker whose expression pattern is quite the opposite to that of E-Cadherin, both in terms of expression levels as well as prognosis. Liu et al. reported a detailed analysis of Vimentin expression and its prognostic value using cell lines as well as patient samples (**Liu et al.,2016**). The authors showed that TGFβ-mediated upregulation of Vimentin expression was reversed when siRNA against Vimentin was used. Also, patient samples provided enough evidence to show that high Vimentin expression was a negative prognostic factor and indicated high potential of lymph node metastasis. Similar observations have been recorded and reiterated elegantly in the recent review article published by Mogre et al. (**Mogre et al.,2022**).

For the mouse aggressive cell line (MOC2) used in the current study, no reports recording relative levels of E-Cadherin or Vimentin could be found. However, protein levels from western blotting showed very low levels of basal E-Cadherin expression and high basal levels of Vimentin expression. Based on this and how CFD or DOX treated lysates have responded, it may very well be seen that CFD exhibits clear indication of EMT reversing capabilities (**Fig. 4.20**). This result has relevance even in drug resistant cancers like OSCC since it has been established that EMT reversal may be one way of overcoming MDR in cancers (**Erin et al.,2020**).

However, the particular approach for targeting EMT reversal in OSCC has not yet been explored to its full potential in spite of having some encouraging evidence from existing publications. According to a review by Wise-Draper et al., the most practical ways of addressing metastatic oral cancer would include identifying them as PDL1-expressing or not, ablative approaches wherever appropriate, and targeted anti-angiogenic therapy (**Wise-Draper et al.,2022**). For especially resistant cancers, targeting cancer stem cells for resistance reversal is also a practical approach (**Nunes et al.,2018**). This might prove to be particularly effective since cancer stem cells have self-renewal properties and often promote metastasis. Discovery of novel biomarkers to be used as potential therapeutic targets is also of utmost importance. For example, Sun et al. demonstrated how downregulation of cyclin dependent kinase 5(CDK5) activity by targeting the STAT3/miR-21 axis in HNSCC cell lines reduces Vimentin expression while increasing levels of E-Cadherin expression (**Sun et al.,2015**). In one miRNA based therapeutic study on 65rd3ed3d cell lines, overexpression of miR-485-5p was found to result in increase in E-Cadherin levels and a concomitant decrease in Vimentin levels, leading to EMT reversal and hence an overall downregulation in invasiveness (**Lin et al.,2017**). Some molecules like bovine lactoferrin and Metformin are now being newly discovered as prospective of reversing EMT in OSCC (**Chea et al.,2018; Qu et al.,2014**).

5.5. M2 TAM attenuation aids in overall tumour regression

With a dosage of drug so chosen for in vivo tumour regression studies, superior therapeutic outcome was witnessed for CFD-mediated therapy compared to pristine DOX treatment. With possibly higher retention of DOX through simultaneous dual targeting, first evidently through FR and also hypothetically through CSP's interaction with tumour-associated OSCC

cell surface, CFD-mediated tumour regression was far more prominent when compared to the other treated groups (**Fig. 4.19c**). In future, further dosage customization is necessary to achieve improved therapeutic outcome. A deeper understanding of the possible reasons behind the observed intracellular drug-retention as well as tumour size regression influenced by the targeted system CFD is required. To sum up, there was evidence of better delivery as well as retention of DOX as mediated by the FR targeted nano-formulation. Besides tumour regression, it was of interest to check whether the targeted delivery system made any difference in terms of alleviating the usual cardiotoxic effects of Doxorubicin (**Podyacheva et al.,20121**). There have been reports that have documented their findings from investigations into the probable mechanisms behind DOX induced cardiomyopathy. One such study showed how the upregulation of death receptors by Doxorubicin induces TRAIL-mediated apoptosis in cardiomyocytes (**Zhao & Zhang,2017**). A recent review on this topic lists multiple ways in which Doxorubicin may induce cardiotoxicity, including mitochondrial damage, inhibition of the Tyrosine kinase pathway, autoimmune inhibition, lipid peroxidation and ROS generation among others (**Rawat et al.,2021**). There have been numerous studies that have tried to simulate DOX associated toxicity in animal models like rabbits, rats, mice etc. Features simulated primarily include histological and ultrastructural perturbations in the myocardium (**Huang et al.,2021**). In this study, the results from histopathology-based toxicity studies concur with published findings, also indicating that the chances of incurring similar debilitating effects when using the targeted delivery system CFD are negligible to none (**Fig. 4.21**).

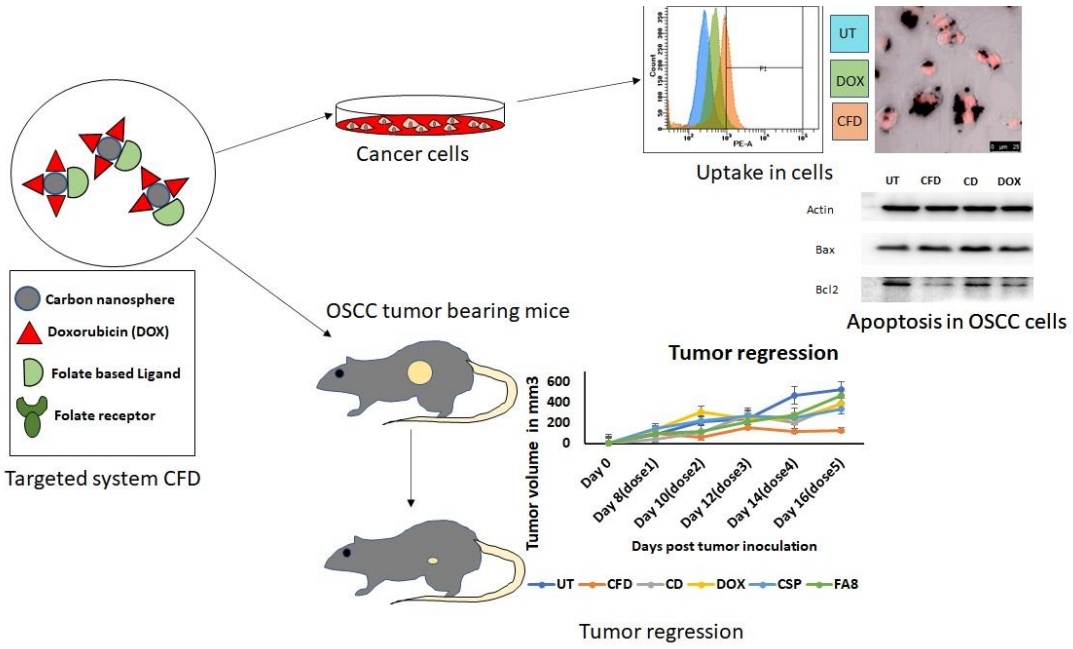

Fig.5.1. Schematic figure representing CFD mediated uptake, targeted apoptosis and tumour regression in MOC2 mouse model.

The establishment of a syngeneic OSCC model using MOC2 was necessary in the context of the current work since a large portion of it deals with the stromal elements residing in the TME and hence necessitates the use of an immunocompetent animal model (**Mendes et al.,2020**). However, the tumour regression data observed this time exhibited the same trend as the last report and this was evidence that the targeted delivery system was not only well capable at affecting sizeable regression in tumour size in an aggressive cancer model but was also more effective when compared to pristine drug alone (**Fig. 4.19a**). This finding further suggested that CFD might possibly be affecting the pro-tumoural stromal elements in the TME so as to cause an overall remission in tumoural growth. There have been enough studies in recent times which have showcased the higher anti-cancer efficacy for molecules or targeted systems which target not just the tumour cells but also pro-

tumoural macrophages in the TME, underlining repeatedly the vital role that the TME and its resident macrophages play in tumour progression as well as chemoresistance (**Ge & Ding,2020**). Earlier reports with the same targeted delivery system showcased efficient drug uptake in the TAM population residing in immunocompetent mice models of glioma (**Elechalawar & Bhattacharya et al.,2019**). It was thus imperative to verify whether achieve similar outcome could be achieved in a syngeneic model of aggressive OSCC. Upon assessment drug uptake was found to be slightly higher in TAMs than in the rest of the tumour cell populations (**Fig. 4.22-B**). On top of that drug uptake was assessed in whole tumours and uptake of CFD was found to be comparable to or even slightly higher than that of DOX (**Fig. 4.22-A**). The next objective was to assess any changes in TAM polarization that might have happened as a result of targeted therapy. The CD80 is a glycoprotein molecule that is present transiently on the surfaces of B cells, dendritic cells as well as macrophages (**Santin et al.,1999**). Interestingly, it has been reported by multiple authors that levels of CD80 expression are particularly low in cancer cells, making them highly evasive towards anti-tumour immune responses launched by T-cytotoxic cells (**Tirapu et al.,2006**). Indeed, tumour cells with low or no CD80 expression have been shown to induce apoptosis in tumour infiltrating T cells, often rendering allied immunotherapeutic approaches redundant (**Mir, 2015**). Conversely, induction of higher CD80 expression levels either by transfection or other methods has proven itself a valid therapeutic approach in recent times (**Zhang et al.,2016**). In fact, it is proven now that the activation of T-cells and the mounting of an appropriate anti-tumour immune response is quite challenging in the absence of stable CD80 expression. Contrary to this, the CD206 marker has been found to be a prominent M2 marker, facilitating pro-tumoural conditions and the maintenance of a cold tumour microenvironment. Fan et al. reported the prognostic significance of CD206 in

liver cancer, experimentally showing that not only did high CD206 expression correlate with lower survival rates but also increased chances of metastatic progression significantly (**Fan et al.,2019**). Utilizing a short hairpin approach, they silenced CD206 in liver CSCs (cancer stem cells) and showed that it impacted their invasiveness and migratory capabilities. Similar findings were reported by Haque et al. who studied the role of CD206 positive TAMs in OSCC progression using clinical samples. The authors reported that CD206 positive TAMs were the primary perpetrators of metastasis and invasiveness as compared to TAMs expressing other M2 markers like CD204 or CD163 (**Haque et al., 2019**). The authors went on to further point out that CD206 positive TAMs comprised of a particular TAM subset producing EGF in large quantities and also that conditioned media collected from such cultures reprogrammed other TAM subsets to become more proliferative and invasive in nature. Another notable therapeutic approach which investigators are studying these days is the use of HDPs (Host Defense Peptides), also termed IDRs (Innate Defense Regulators) for immunomodulatory purposes. Needless to say, such indirect therapeutic approaches hold immense promise for immunotherapy. This makes the findings for the current work encouraging since they are indicative of M2 to M1 reprogramming. Flow cytometry data in this regard was clearly suggestive of a significant increase in CD80 expression levels with no noticeable depreciation in CD206 levels. However, findings on TAM repolarization as a CD80/CD206 ratio were more encouraging when compared to either untreated or DOX treated samples (**Fig. 4.24**). At the same time, western blotting results from tumours collected at a relatively later time point were more evident of an improved CD80/CD206 ratio in case of treatment with the targeted system CFD (**Fig. 4.25**). Apart from this it was also found that targeted delivery system CFD had the highest drug uptake in TAMs among all the treatment groups, signifying that it had adeptly targeted

TAMs on the basis of FA8-conjugation and managed to unload its drug payload therein for maximal therapeutic outcome (**Fig. 4.22**). As a last leg of the experiment, it was also found that drug uptake on account of CFD was much higher in the TAM-positive stromal subpopulation of cells as compared to the CD11b-negative non-TAM stromal subpopulation. All this data indicated that targeting TAMs was possibly being achieved with success by the targeted CSPs, bringing about a holistic chemo-immunotherapeutic effect on aggressive tumours of oral squamous cell carcinoma. Even though such a report is probably yet to be published in terms of oral cancer, there are examples of earlier instances where the targeted delivery of Doxorubicin by functionalized nano-delivery systems has managed to target pro-tumoural TAMs for elimination or reversal besides exerting conventional chemotherapeutic effect. Niu et al. synthesised Doxorubicin loaded PLGA nanoparticles which were primed with Mannose for targeting TAMs and they successfully managed to show that these nanoparticles were capable of inducing tumour regression to a much higher extent as opposed to free DOX mediated chemotherapy alone (**Niu et al.,2013**). A few years later Yang et al. published their report where Doxorubicin alone had been used as a conjugate for ZnO nanoparticles and these NPs could achieve targeted reversal of pro-tumoural TAMs towards a more favourable M1 phenotype (**Yang et al.,2019**). It is thus clear that Doxorubicin when used in a specialized and targeted manner may perform wonders in terms of targeting multiple classes of pro-tumoural cells in a tumour for improved treatment.

Cancer cells harbouring mutated tp53(mutp53) have been reported to reprogram macrophages to a tumour supportive and anti-inflammatory state (**Nakamura & Smyth,2020**). This information is vital in the present context especially owing to the fact

that the platform cell line used here (MOC2) possesses mutated tp53, even though exact nature of the same is not entirely clear so far (**Onken et al.,2014**). Mutp53-reprogammed TAMs reportedly favour anti-inflammatory immunosuppression with increased activity of TGF-β. These findings, associated with poor survival in colon cancer patients, strongly support a microenvironmental GOF (gain of function) role for mutp53 in actively engaging the immune system and facilitating cancer progression and metastasis (**Stein et al.,2019**). While NF-κB is prominent in macrophage-initiated inflammatory responses, little is known about the role of tp53 in modulating macrophage responses to challenges like chemotherapy. It was hence decided to investigate any changes in p53 expression that might be detectable upon treatment. Strangely, repeated western blotting experiments showed a clear downregulation in the levels of stable p53 protein expression in CFD treated tumour samples (**Fig. 4.26**). There have been several reports which have documented the presence of stabilized mutant p53 in multiple cancers including OSCC which are in many cases gain of function changes that encourage tumour growth and therapeutic resistance (**Dolma & Muller,2022; Chan et al.,2004)**. The findings from the present study regarding p53 protein levels or the change therein post treatment is thus indicative at best since there is yet insufficient knowledge as to the exact nature of the p53 mutation which MOC2 particularly has. Also, the exact mechanism behind these low p53 levels in case of the CFD treated group is not yet clear even though we might possibly assume it to be an indirect effect from Bcl-2 downregulation as shown earlier (**Fig. 4.17**). Further delineation of the same and its subsequent effects on the pathophysiology of MOC2 induced tumours in future might help throwing light on this interesting aspect.

5.6. Possible mechanism behind FR mediated anti-tumour effects

Another gene which reportedly assists in DOX mediated cell death is TNFα. TNFα is a glycoprotein which is selectively cytotoxic against malignant cells as reported for a range of different cancers (**Waters et al.,2013**). One way that this molecule might be used now is as a response modifier, especially in case of tumours which are irresectable or have become resistant to chemotherapeutic drugs like DOX (**Cao et al.,2006**). Some of the earlier works show that TNFα is especially useful in inducing death against cancer cells lacking functional p53 protein (**Rokhlin et al.,2000**). In one particular study, Cao et al. demonstrated the use of TNFα along with DOX in successfully targeting DOX resistant breast cancer cells for death, primarily evading chemoresistance (**Cao et al.,2006**). Assessment of TNFα protein levels revealed an increase in expression for both targeted and non-targeted treatment groups while the maximum expression was seen in DOX treated group (**Fig. 4.26**). From this it may be surmised that the increase in TNFα levels was probably DOX mediated and not necessarily a direct effect of FR mediated drug delivery. This finding as to the effect of drug alone is in consort with the findings of Kaczmarek et al. who showed the upregulation of TNF in lavage fluid from mice injected intraperitonially with Doxorubicin (**Kaczmarek et al.,2013**).

The role of nitric oxide and the enzyme responsible for its production, Nitric Oxide Synthase (NOS), in cancer biology is not yet entirely clear. In the context of the current work, it must be noted that NO has been proven to have anti-inflammatory effects on the TME, working as an immunosuppressant and a pro-oncogenic molecule (**Penarando & Rodriguez-Ariza,2019**). There have also been reports that NO suppresses tumour suppressor genes while parallelly inducing oncogene activation by nitrosylating a host of important genes

involved in cell death and tumour invasiveness (**Baritaki et al.,2010**). Of the three isoforms of NOS, iNOS is the one which produces the maximum amount of NO which is intricately involved with tumour associated processes like metastasis, angiogenesis and malignant transformation (**Panaro et al.,2003**). Action of NO has been connected functionally with p53 and NFkB expression, encouraging pro-tumourigenic functions like progression and metastasis in a variety of cancers (**Muntane & De-la-Mata,2010**). Even though levels of iNOS and their effects may vary from one cancer type to another, it is maintained that high iNOS levels often lead to an unfavourable prognosis in case of squamous cell carcinomas (**Brennan et al.,2008**). Overall, it may be safe to say that targeted drug delivery has possible role in the downregulation of iNOS levels with possible suppression in protein levels of functional p53 in tumours essentially mutated for tp53 (**Fig. 4.26**).

5.7. An ex-vivo model of OSCC for the assessment of targeted chemotherapy

Spheroids are currently a popular experimental platform for development and screening of targeted nanotherapeutics. There are multiple reasons as to why 3D spheroids are preferred over 2D in vitro cultures (**Pinto et al.,2020**). Firstly, they have added features like cell-cell and cell-ECM interactions, spatial distribution akin to tumours, as well as a heterogenous nature that can be modulated and designed to mimic a tumour with a surrounding TME and its constituent stromal elements. 2D cell cultures can't be depended upon to faithfully provide us an idea of the true potential of any therapeutic moiety, not only because it has no interactive TME but also because of its homogeneous nature in terms of cell type. A 3D tumour spheroid on the other hand has in built gradients for pH and O_2 levels, characteristics that usually define actual tumours (**Nunes et al.,2018**). In terms of metastatic potential, it has been seen that tumour spheroids are better models

for studies pertaining to EMT since the cells in the outermost layer of a spheroid behave like cells present in the invasive front of tumours. Besides this, the very formation of a spheroid demands changes in a number of proteins that constitute core elements controlling cell-cell interactions. For example, induction of E-cadherin expression is required for the formation of 3-dimensional spheroid structures, even if its detrimental to tumour growth in vivo (**Powan et al.,2017**). On top of that, spheroids have also been found to have upregulated levels of proteins such as ZEB, TWIST and Vimentin, all of which promote EMT. In this very regard, spheroids are better models than 2D cultures for studies on invasion and cell migration as has been demonstrated by many studies using spheroids on Matrigel coated Boyden chambers (**Guyon et al.,2020**). This likely brings us to question their status in terms of drug resistance. Surely enough, a thorough literature search showed us enough evidence to establish the fact that spheroids consist of cells that are more resistant to chemotherapy than 2D cultures (**Hamilton & Rath,2019**). As a result, spheroids are also perfect for testing candidate therapeutics whose aim is to either directly or indirectly affect MDR. In the context of the current work, spheroids were tried as a model to assess drug uptake and any possible effects of targeted chemotherapy in OSCC. There have been several studies in the past that are witness to spheroids proving themselves as remarkable platforms for large scale screening of anti-cancer nanotherapeutics. Depending on features like size, charge and surface functionalization, a number of different nano-therapeutics have been evaluated and validated on different kinds of spheroid models that cater to a variety of scientific interests. Overall, spheroids in most studies could demonstrate penetrability and drug delivery by multiple nano-delivery systems, effectively serving to reduce the number of candidate drugs that reach in vivo testing and thus minimizing unnecessary wastage of time as well as resources. According

to a review article, the physical characteristics of nano-delivery systems play a very important role in deciding their bioactivity and other features responsible for biosafety as well as therapeutic efficiency (**Hasirci et al.,2006**). The authors conclude that nanodelivery systems of a particular size (less than 100 nm) and charge(negative) are usually favoured more for entry into 3D spheroids for targeted drug delivery. In this case, the glucose derived CSPs used are close to 300 nm diameter and negatively charged, which would mean that they are expected to have moderate penetrability in spheroids (**Fig. 4.28; Fig. 4.29**). The authors have also mentioned that biosafe and biodegradable materials serve better which bears well for glucose derived biocompatible nanospheres. Lastly, there have been numerous reports where the use of a targeting ligand has proven advantageous for targeted delivery to all parts of a tumour spheroid (**Huang & Gao,2018**). This sits well with the results from the current investigation which are from a delivery system targeted specifically against the Folate Receptor (**Fig. 4.27**). As already discussed, the Oxygen gradient characteristic of solid tumours is featured by 3D spheroids as well. This leads to the formation of a hypoxic core with upregulation of factors like HIF-1α, Pgp and VEGF, all of which contribute to heightened drug resistance. Factors like the presence of an acidic microenvironment (low pH) and the presence of cancer stem cells also facilitate spheroids to exhibit drug resistance quite like any in vivo tumour (**Milane et al.,2011**). The particular model of 3D spheroid used for the current work doesn't provide the scope for studying tumour-stroma interactions or even tumour-ECM interactions. However, these issues can be taken care of by means of 3D bioprinting or novel fabrication methods that could be used for making organ-on-chip systems that would serve as effective platforms for anticancer studies (**Ma et al.,2021**).

Overall, this study delineates the success of targeting the Folate receptor for effective attenuation of oral squamous cell carcinoma as well as its associated stromal elements.

5.8. The need to gain a better understanding of the implications of FR-targeting in cancer

So far in this thesis, we have observed that there are many advantages (in terms of possible therapeutic outcome) to targeting the Folate Receptor for site specific or cancer cell directed delivery of drugs or other therapeutic cargo. Receptor oriented targeting may help overcome certain shortcomings often seen in case of conventional chemotherapy-induction of chemoresistance, eviction via efflux mechanisms, systemic toxicity that harms surrounding normal tissues and cells etc.. We started off with the simple objective of testing the potential of the Folate receptor as a possible therapeutic target in the treatment of aggressive oral cancer. Hence our primary goal would be to develop a delivery system that would prove as being FR-targeted and would thus achieve cancer cell targeted delivery of DOX with negligible drug delivery to surrounding normal cells in the vicinity. As expected, in a large number of the experiments, CFD performed significantly better than CD, whether it was with regards to uptake, cancer cell toxicity or changes in levels of M2 TAM specific marker expression. This wasn't surprising given that we had already established the FR-targeting capabilities of CFD in the initial part of the study. However, in the course of observing and analyzing our findings we discovered that our targeted system CFD showed possibilities of a better treatment outcome as compared to pristine molecule DOX in some cases. Such differences (statistically significant) were noted in case of results of drug retention (in vitro & in vivo), expression of certain molecular markers (associated with cell death, chemoresistance, TAM reversal etc.) as well as tumour size regression (specific time points). These findings inspite of being interesting do not allow us to claim that our targeted system is better in any way than DOX as an anti-cancer agent. However, they do give us the hope that with further in-depth studies on systems such as CFD in future, we might gain a better understanding of the merits of FR-targeted chemotherapy in OSCC with the possibility of achieving improved and sustained disease-free survival for patients.

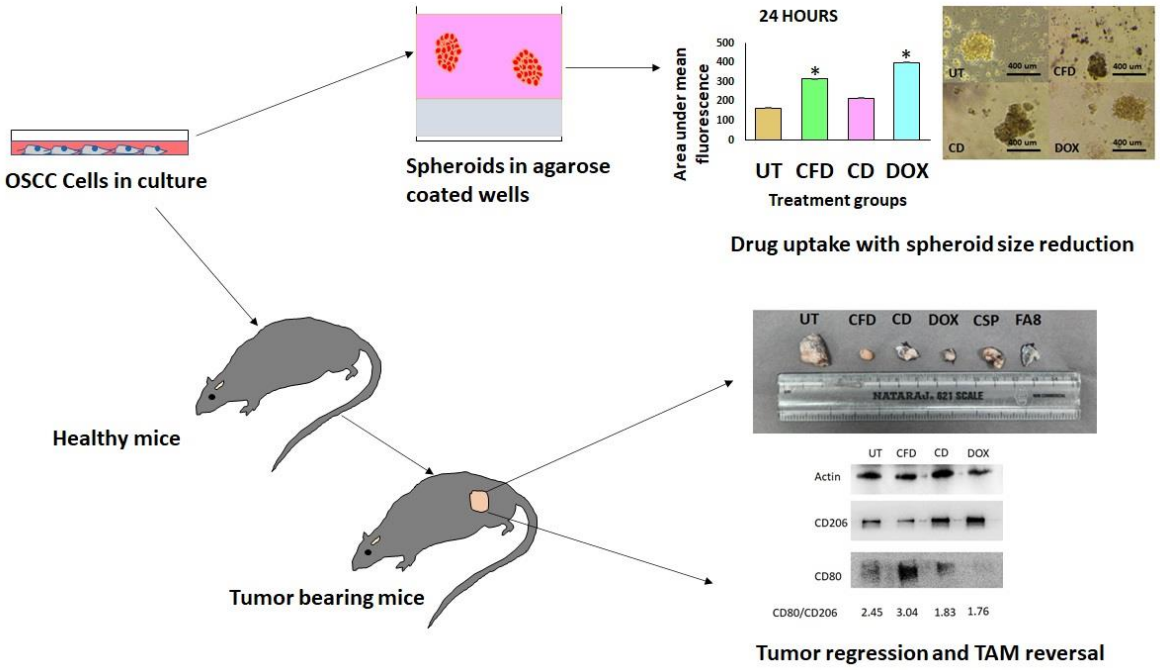

Fig.5.2. Schematic figure representing CFD mediated uptake in 3D tumour spheroids, spheroid size reduction and TAM attenuation.

Oral cancer is the 6th most prevalent cancer type in the world and is plagued by severe challenges like difficulty in diagnosis and treatment. Oral squamous cell carcinoma becomes malignant and aggressive very fast, considering the fact that it is riddled with lymph nodes. OSCC is also infamous for its immunologically cold TME which is irresponsive to conventional immunotherapeutic approaches. The particular in vivo model used in the current work is an aggressive mouse model of OSCC in immunocompetent C57 mice. Besides being mutated for p53, most OSCC cell lines and their derivative tumours possess anomalies in crucial genes involved with pathways responsible for cell proliferation, metastasis and multi-drug resistance. Targeted nano-delivery systems are making headway in present times owing to huge leaps in technological advancements. In this work glucose derived biocompatible carbon nanospheres (CSPs) conjugated to a cationic folate-based ligand were used. Attempting targeted drug delivery via the Folate receptor enabled targeting both tumour cells and tumour associated macrophages for improved and site directed drug delivery. The drug used is Doxorubicin, an Anthracycline less popular these days on account of misgivings like systemic toxicity, widespread induction of chemoresistance and ineffectiveness against highly metastatic cancers like OSCC. Possibilities at overcoming most of these therapeutic challenges were evident since efficient uptake was achieved in tumour regions as well as M2 pro-tumoural TAMs. Following their endocytosis, drug accumulation happened in a sustained manner for durations longer than what was noted in case of the pristine drug. Apoptotic death could be witnessed in treated cancer cells with some indication of EMT reversal. Further investigation on possible TME-related effects indicated M2 TAM attenuation as well as increase in relative percentage of pro-tumoural M1 TAMs. M2 Tams exhibited high uptake of ligand-conjugated targeted system CFD and overall tumour regression was evident from

in vivo studies. Further studies involving 3D spheroid models exhibited regression in size as well as efficient uptake of drug-conjugated CSPs showing that spheroid models of OSCC may serve well as efficient platforms for screening novel anti-cancer therapies, especially in malignancies resistant against conventional chemotherapeutics like Doxorubicin. Carbon nanospheres are biocompatible delivery systems that offer a lot of scope for surface functionalization and efficient drug loading. Their size, charge as well as receptor-targeted nature present opportunities for the development of efficient dual-targeting delivery systems with potential for clinical translation in the near future.

Specific conclusions of the thesis are-

- Oral squamous cell carcinoma cells were found to have relatively high expression for Folate Receptor and may well be targeted for therapy via the FR.
- Targeted delivery of ligand conjugated delivery system CFD took place via the Folate receptor as shown by receptor inhibition studies.
- Retention of DOX was found to be comparatively more in CFD treated cells than those treated only with DOX.
- Entry of CFD occurred selectively in cancer cells while non-cancerous cells showed no significant cytotoxicity upon treatment with CFD.
- CFD induced apoptotic cell death in OSCC cells principally via the downregulation of Bcl-2 and the overall upregulation of Bax/Bcl-2 ratio. CFD treatment exhibited no upregulation of RIP3 like what was seen in case of DOX treatment.
- CFD exhibited highest levels of tumour regression in vivo with minimal toxicity in an immunocompetent murine model of OSCC developed using MOC2 cells.

Histopathological studies revealed no signs of apparent cardiotoxicity at tissue level in case of CFD treated group as compared to DOX treated animals.

- CFD showed highest drug accumulation in mice tumours post treatment as compared to all other groups including DOX. Particularly, uptake of CFD was found to be slightly higher in TAM-specific tumour cell population than the rest of the tumour cells. TAMs isolated from tumour showed relatively high expression of FR.
- When compared to untreated mouse tumours, CFD treated tumours were found to have higher number of CD80-positive M1 TAMs and lower proportion of CD163-positive M2 TAMs.
- CD80/CD206 ratio was found to be the highest in lysates from CFD treated tumours.
- Targeted system CFD showed decent uptake in 3D tumour spheroids generated from OSCC cell lines, which was at par to that of DOX. This was validated using confocal imaging (6 hours) as well as flow cytometry(24 hours and 48 hours).
- CFD treated tumours also showed upregulated levels of TNFα (though not as much as in case of DOX treated tumours) and downregulated protein levels of iNOS. These along with a depreciation in p53 levels (as observed) upon treatment with CFD might possibly contribute to the mechanistic basis behind CFD mediated tumour cell death as well as M2-TAM attenuation in a p53-mutated and immunologically cold model of oral squamous cell carcinoma.
- Further investigation as to the probable mechanisms behind the uptake and utilization of DOX-conjugated targeted nano-delivery systems shall provide a better understanding of possible ways to overcome challenges like chemoresistance and pro-tumoural stromal effects more effectively in future.

Specific Contributions:

The Folate receptor is a viable target for the efficient delivery of nano delivery systems and functionalized nanoparticles carrying therapeutic payloads. Folate based cationic ligand FA8 demonstrated high FR-binding capacity when conjugated to glucose derived biocompatible carbon nanospheres. Our carbon nanospheres also demonstrated appreciable drug binding capacity and drug delivered thus via the Folate receptor was found to be retained at target site within cancer cells for much longer than pristine drug molecule. Targeted delivery system was found to affect cancer cells with high specificity, eliciting apoptotic cell death along-with indicative EMT reversal. Targeted system CFD also performed well in terms of permeabilization and therapy (size reduction) both for murine tumours as well as 3D tumour spheroids. Data indicative of M2 TAM suppression was obtained in terms of TAM-specific marker expression, and this was found to correlate with the expression profile of iNOS. Overall, the murine model of aggressive OSCC was found to be a promising in-vivo model for studying FR-mediated treatment options against p53-mutated OSCC. This work shall hopefully encourage further exploration of the potential of FR-mediated targeted therapy for countering drug resistance.

Future scope of work:

- Even though drug was found to be retained for longer when sent via CFD, the exact mechanism behind this observation was not investigated in the current work. More specifically, future studies pertaining to efflux pumps like Pgp and their function pertaining to receptor mediated drug delivery may be conducted.
- Any effects of FR mediated targeted drug delivery on ROS generation as well as status of mitochondria post stress may be studied in detail.
- In the present study a subcutaneous tumour model of MOC2 was used. However, the establishment and standardisation of an orthotopic model of OSCC using the same cell line would surely provide an improved platform for OSCC related in vivo studies.
- It was gathered from earlier reports that p53 in MOC2 cell line is mutated. However, further studies to ascertain the exact functional nature of this mutation is required in order for this model to serve better for understanding OSCC biology in depth.
- The effects of targeted treatment upon the TME may further be elucidated by looking at other important stromal elements like T cells and MDSCs which would give us more insight on immunotherapeutic potential.
- Preclinical and clinical studies for CSP based FR-targeted systems may be carried out.
- CFD may be tested for diagnostic as well as therapeutic potential against an array of FR-related diseases.

References:

- A Baudino, T., 2015. Targeted cancer therapy: the next generation of cancer treatment. *Current drug discovery technologies*, *12*(1), pp.3-20.
- Aas, T., Børresen, A.L., Geisler, S., Smith-Sørensen, B., Johnsen, H., Varhaug, J.E., Akslen, L.A. and Lønning, P.E., 1996. Specific P53 mutations are associated with de novo resistance to doxorubicin in breast cancer patients. *Nature medicine*, *2*(7), pp.811-814.
- Abbasi, M.M., Jahanban-Esfahlan, R., Monfaredan, A., Seidi, K., Hamishehkar, H. and Khiavi, M.M., 2015. Oral and IV dosages of doxorubicin-methotrexate loaded-nanoparticles inhibit progression of oral cancer by down-regulation of matrix Methaloproteinase 2 expression in vivo. *Asian Pacific Journal of Cancer Prevention*, *15*(24), pp.10705-10711.
- Abd El-Hamid, E.S., Gamal-Eldeen, A.M. and Eldeen, A.M.S., 2019. Liposome-coated nano doxorubicin induces apoptosis on oral squamous cell carcinoma CAL-27 cells. *Archives of oral biology*, *103*, pp.47-54.
- Abd-el-fattah DS, Mohammed WS, Ellithy MM. Effect of shrimp shell extract nanoparticles o oral squamous cell carcinoma cell line: in vitro study 2018;5:45-9.
- Alam, M., Kashyap, T., Mishra, P., Panda, A.K., Nagini, S. and Mishra, R., 2019. Role and regulation of proapoptotic Bax in oral squamous cell carcinoma and drug resistance. *Head & neck*, *41*(1), pp.185-197.
- Alberti, D., Protti, N., Franck, M., Stefania, R., Bortolussi, S., Altieri, S., Deagostino, A., Aime, S. and Geninatti Crich, S., 2017. Theranostic nanoparticles loaded with

References:

imaging probes and rubrocurcumin for combined cancer therapy by folate receptor targeting. *ChemMedChem*, *12*(7), pp.502-509.

- Alvarado-Ortiz, E., de la Cruz-López, K.G., Becerril-Rico, J., Sarabia-Sánchez, M.A., Ortiz-Sánchez, E. and García-Carrancá, A., 2021. Mutant p53 gain-of-function: role in cancer development, progression, and therapeutic approaches. *Frontiers in cell and developmental biology*, *8*, p.607670.
- Alves, A., Diel, L., Ramos, G., Pinto, A., Bernardi, L., Yates 3rd, J. and Lamers, M., 2021. Tumor microenvironment and Oral Squamous Cell Carcinoma: A crosstalk between the inflammatory state and tumor cell migration. *Oral Oncology*, *112*, p.105038.
- Amanatullah, D.F., Reutens, A.T., Zafonte, B.T., Fu, M., Mani, S. and Pestell, R.G., 2000. Cell-cycle dysregulation and the molecular mechanisms of prostate cancer. *Frontiers in Bioscience-Landmark*, *5*(3), pp.372-390.
- Amelio, I. and Melino, G., 2020. Context is everything: extrinsic signalling and gain-of-function p53 mutants. Cell Death Discovery, 6(1), p.16.
- Amin, M.L., 2013. P-glycoprotein inhibition for optimal drug delivery. *Drug target insights*, *7*, pp.DTI-S12519.
- Arulmozhi, V., Pandian, K. and Mirunalini, S., 2013. Ellagic acid encapsulated chitosan nanoparticles for drug delivery system in human oral cancer cell line (KB). *Colloids and Surfaces B: Biointerfaces*, *110*, pp.313-320.
- Arumugam, J., Jeddy, N., Ramamurthy, A. and Thangavelu, R., 2017. The expression of Bcl-2 in oral squamous cell carcinoma—A review. *Journal of Orofacial Sciences*, *9*(2), p.71.

References:

- Asar, S.L., El-Sheikh, S.M., El-Didi, F.H., Essawy, M.M., Ramadan, H.S. and Afifi, M.M., 2019. Therapeutic effect of Paclitaxel loaded on gold nanoparticles in treatment of induced oral squamous cell carcinoma. *Alexandria Dental Journal*, *44*(1), pp.17-23.
- Asl, E.R., Rostamzadeh, D., Duijf, P.H., Mafi, S., Mansoori, B., Barati, S., Cho, W.C. and Mansoori, B., 2023. Mutant P53 in the formation and progression of the tumor microenvironment: Friend or foe. *Life Sciences*, p.121361.
- Ayers, D. and Vandesompele, J., 2017. Influence of microRNAs and long non-coding RNAs in cancer chemoresistance. *Genes*, *8*(3), p.95.
- Azmi, A.S., Bao, B. and Sarkar, F.H., 2013. Exosomes in cancer development, metastasis, and drug resistance: a comprehensive review. Cancer and Metastasis Reviews, 32, pp.623-642.
- Babykutty, S., Suboj, P., Srinivas, P., Nair, A.S., Chandramohan, K. and Gopala, S., 2012. Insidious role of nitric oxide in migration/invasion of colon cancer cells by upregulating MMP-2/9 via activation of cGMP-PKG-ERK signaling pathways. *Clinical & experimental metastasis*, *29*, pp.471-492.
- Bader, J.E., Voss, K. and Rathmell, J.C., 2020. Targeting metabolism to improve the tumor microenvironment for cancer immunotherapy. *Molecular cell*, *78*(6), pp.1019-1033.
- Bae, Y.H. and Park, K., 2011. Targeted drug delivery to tumors: myths, reality and possibility. *Journal of controlled release*, *153*(3), p.198.
- Bareford, L.M. and Swaan, P.W., 2007. Endocytic mechanisms for targeted drug delivery. *Advanced drug delivery reviews*, *59*(8), pp.748-758.

References:

- Baritaki, S., Huerta-Yepez, S., Sahakyan, A., Karagiannides, I., Bakirtzi, K., Jazirehi, A. and Bonavida, B., 2010. Mechanisms of nitric oxide-mediated inhibition of EMT in cancer: inhibition of the metastasis-inducer Snail and induction of the metastasis-suppressor RKIP. *Cell cycle*, *9*(24), pp.4931-4940.
- Bhattacharya, D., Sakhare, K., Narayan, K.P. and Banerjee, R., 2021. The prospects of nanotherapeutic approaches for targeting tumor-associated macrophages in oral cancer. Nanomedicine: Nanotechnology, Biology and Medicine, 34, p.102371.
- Bi, S., Huang, W., Chen, S., Huang, C., Li, C., Guo, Z., Yang, J., Zhu, J., Song, L. and Yu, R., 2020. Cordyceps militaris polysaccharide converts immunosuppressive macrophages into M1-like phenotype and activates T lymphocytes by inhibiting the PD-L1/PD-1 axis between TAMs and T lymphocytes. *International Journal of Biological Macromolecules*, *150*, pp.261-280.
- Biswas, S.K., Allavena, P. and Mantovani, A., 2013, September. Tumor-associated macrophages: functional diversity, clinical significance, and open questions. In *Seminars in immunopathology* (Vol. 35, pp. 585-600). Springer Berlin Heidelberg.
- Blandino, G., Levine, A.J. and Oren, M., 1999. Mutant p53 gain of function: differential effects of different p53 mutants on resistance of cultured cells to chemotherapy. *Oncogene*, *18*(2), pp.477-485.
- Bonavida, B. and Baritaki, S., 2011. Dual role of NO donors in the reversal of tumor cell resistance and EMT: Downregulation of the NF-κB/Snail/YY1/RKIP circuitry. Nitric oxide, 24(1), pp.1-7.
- Bossennec, M., Roio, A.D., Caux, C. and Ménétrier-Caux, C., 2018. MDR1 in immunity: friend or foe? OncoImmunology 7, e1499388.

References:

- Boyd, E.M., 1968. Predictive drug toxicity. Assessment of drug safety before human use. Canadian Medical Association Journal, 98(6), p.278.
- Brannon-Peppas, L. and Blanchette, J.O., 2004. Nanoparticle and targeted systems for cancer therapy. *Advanced drug delivery reviews*, *56*(11), pp.1649-1659.
- Brennan, P.A., Dennis, S., Poller, D., Quintero, M., Puxeddu, R. and Thomas, G.J., 2008. Inducible nitric oxide synthase: correlation with extracapsular spread and enhancement of tumor cell invasion in head and neck squamous cell carcinoma. *Head & Neck: Journal for the Sciences and Specialties of the Head and Neck*, *30*(2), pp.208-214.
- Bukowski, K., Kciuk, M. and Kontek, R., 2020. Mechanisms of multidrug resistance in cancer chemotherapy. *International journal of molecular sciences*, *21*(9), p.3233.
- Cabrita, R., Lauss, M., Sanna, A., Donia, M., Skaarup Larsen, M., Mitra, S., Johansson, I., Phung, B., Harbst, K., Vallon-Christersson, J. and van Schoiack, A., 2020. Tertiary lymphoid structures improve immunotherapy and survival in melanoma. *Nature*, *577*(7791), pp.561-565.
- Cai, J., Gao, N., Qiao, B., Lin, N. and He, W., OSCC-derived exosomes promote M2-subtype macrophage polarization mediated by exosome-enclosed miR-29a-3p 2.
- Canning, M., Guo, G., Yu, M., Myint, C., Groves, M.W., Byrd, J.K. and Cui, Y., 2019. Heterogeneity of the head and neck squamous cell carcinoma immune landscape and its impact on immunotherapy. *Frontiers in cell and developmental biology*, *7*, p.52.
- Cao, D., Liang, L., Xu, Y., Sun, J., Lei, M., Wang, M., Wei, Y. and Sun, Z., 2018. Tumor associated macrophages and angiogenesis dual-recognizable nanoparticles for

References:

enhanced cancer chemotherapy. *Nanomedicine: Nanotechnology, Biology and Medicine*, *14*(3), pp.651-659.

- Cao, M., Yan, H., Han, X., Weng, L., Wei, Q., Sun, X., Lu, W., Wei, Q., Ye, J., Cai, X. and Hu, C., 2019. Ginseng-derived nanoparticles alter macrophage polarization to inhibit melanoma growth. *Journal for immunotherapy of cancer*, *7*, pp.1-18.
- Cao, W., Ma, S.L., Tang, J., Shi, J. and Lu, Y., 2006. A combined treatment TNF-α/doxorubicin alleviates the resistance of MCF-7/Adr cells to cytotoxic treatment. *Biochimica et Biophysica Acta (BBA)-Molecular Cell Research*, *1763*(2), pp.182-187.
- Carvalho, C., Santos, R.X., Cardoso, S., Correia, S., Oliveira, P.J., Santos, M.S. and Moreira, P.I., 2009. Doxorubicin: the good, the bad and the ugly effect. *Current medicinal chemistry*, *16*(25), pp.3267-3285.
- Chae, H.D., Kim, B.M., Yun, U.J. and Shin, D.Y., 2008. Deregulation of Cdk2 causes Bim-mediated apoptosis in p53-deficient tumors following actin damage. *Oncogene*, *27*(29), pp.4115-4121.
- Chaikomon, K., Chattong, S., Chaiya, T., Tiwawech, D., Sritana-Anant, Y., Sereemaspun, A. and Manotham, K., 2018. Doxorubicin-conjugated dexamethasone induced MCF-7 apoptosis without entering the nucleus and able to overcome MDR-1-induced resistance. Drug design, development and therapy, pp.2361-2369.
- Chan, K.T. and Lung, M.L., 2004. Mutant p53 expression enhances drug resistance in a hepatocellular carcinoma cell line. *Cancer chemotherapy and pharmacology*, *53*, pp.519-526.

References:

- Chang, L.Y., Hsiao, M.P.J., Lu, M.C.Y., Lin, Y.C., Hung, S.L. and Lai, Y.L., 2019. ARECA NUT EXTRACT ENHANCED M2-LIKE MACROPHAGE POLARIZATION AND fiBROBLAST ACTIVATION. *Oral Surgery, Oral Medicine, Oral Pathology and Oral Radiology*, *128*(1), p.e49.
- Chang, Y.J., Huang, J.R., Tsai, Y.C., Hung, J.T., Wu, D., Fujio, M., Wong, C.H. and Yu, A.L., 2007. Potent immune-modulating and anticancer effects of NKT cell stimulatory glycolipids. Proceedings of the National Academy of Sciences, 104(25), pp.10299-10304.
- Chen, C., Lu, L., Yan, S., Yi, H., Yao, H., Wu, D., He, G., Tao, X. and Deng, X., 2018. Autophagy and doxorubicin resistance in cancer. *Anti-cancer drugs*, *29*(1), pp.1-9.
- Chen, Z., Shi, T., Zhang, L., Zhu, P., Deng, M., Huang, C., Hu, T., Jiang, L. and Li, J., 2016. Mammalian drug efflux transporters of the ATP binding cassette (ABC) family in multidrug resistance: A review of the past decade. *Cancer letters*, *370*(1), pp.153-164.
- Cheung, A., Bax, H.J., Josephs, D.H., Ilieva, K.M., Pellizzari, G. and Opzoomer, J., Targeting folate receptor alpha for cancer treatment. Oncotarget. 2016; 7: 52553–74.
- Cho, H.J., Kim, J.K., Kim, K.D., Yoon, H.K., Cho, M.Y., Park, Y.P., Jeon, J.H., Lee, E.S., Byun, S.S., Lim, H.M. and Song, E.Y., 2006. Upregulation of Bcl-2 is associated with cisplatin-resistance via inhibition of Bax translocation in human bladder cancer cells. *Cancer letters*, *237*(1), pp.56-66.
- Christidi, E. and Brunham, L.R., 2021. Regulated cell death pathways in doxorubicin-induced cardiotoxicity. *Cell death & disease*, *12*(4), p.339.

References:

- Conde, J., Bao, C., Tan, Y., Cui, D., Edelman, E.R., Azevedo, H.S., Byrne, H.J., Artzi, N. and Tian, F., 2015. Dual targeted immunotherapy via in vivo delivery of biohybrid RNAi-peptide nanoparticles to tumor-associated macrophages and cancer cells. *Advanced functional materials*, *25*(27), pp.4183-4194.
- Cooks, T., Pateras, I.S., Jenkins, L.M., Patel, K.M., Robles, A.I., Morris, J., Forshew, T., Appella, E., Gorgoulis, V.G. and Harris, C.C., 2018. Mutant p53 cancers reprogram macrophages to tumor supporting macrophages via exosomal miR-1246. *Nature communications*, *9*(1), p.771.
- Dai, X., Meng, J., Deng, S., Zhang, L., Wan, C., Lu, L., Huang, J., Hu, Y., Zhang, Z., Li, Y. and Lovell, J.F., 2020. Targeting CAMKII to reprogram tumor-associated macrophages and inhibit tumor cells for cancer immunotherapy with an injectable hybrid peptide hydrogel. *Theranostics*, *10*(7), p.3049.
- Dan, H., Liu, S., Liu, J., Liu, D., Yin, F., Wei, Z., Wang, J., Zhou, Y., Jiang, L., Ji, N. and Zeng, X., 2020. RACK1 promotes cancer progression by increasing the M2/M1 macrophage ratio via the NF-κB pathway in oral squamous cell carcinoma. *Molecular oncology*, *14*(4), pp.795-807.
- de Almagro, M.C. and Vucic, D., 2015, March. Necroptosis: Pathway diversity and characteristics. In Seminars in cell & developmental biology (Vol. 39, pp. 56-62). Academic Press.
- Deng, R.H., Zou, M.Z., Zheng, D., Peng, S.Y., Liu, W., Bai, X.F., Chen, H.S., Sun, Y., Zhou, P.H. and Zhang, X.Z., 2019. Nanoparticles from cuttlefish ink inhibit tumor growth by

References:

- Deng, X., Liang, H., Yang, W. and Shao, Z., 2020. Polarization and function of tumor-associated macrophages mediate graphene oxide-induced photothermal cancer therapy. *Journal of Photochemistry and Photobiology B: Biology*, *208*, p.111913.
- Dietel, M., Jöhrens, K., Laffert, M.V., Hummel, M., Bläker, H., Pfitzner, B.M., Lehmann, A., Denkert, C., Darb-Esfahani, S., Lenze, D. and Heppner, F.L., 2015. A 2015 update on predictive molecular pathology and its role in targeted cancer therapy: a review focussing on clinical relevance. *Cancer gene therapy*, *22*(9), pp.417-430.
- Dolma, L. and Muller, P.A., 2022. GOF Mutant p53 in Cancers: A Therapeutic Challenge. *Cancers*, *14*(20), p.5091.
- Dong, H., Pang, L., Cong, H., Shen, Y. and Yu, B., 2019. Application and design of esterase-responsive nanoparticles for cancer therapy. *Drug delivery*, *26*(1), pp.416-432.
- Dong, Y., Liao, H., Yu, J., Fu, H., Zhao, D., Gong, K., Wang, Q. and Duan, Y., 2019. Incorporation of drug efflux inhibitor and chemotherapeutic agent into an inorganic/organic platform for the effective treatment of multidrug resistant breast cancer. *Journal of Nanobiotechnology*, *17*, pp.1-15.
- Dreaden, E.C., Mwakwari, S.C., Austin, L.A., Kieffer, M.J., Oyelere, A.K. and El-Sayed, M.A., 2012. Small molecule–gold nanorod conjugates selectively target and induce macrophage cytotoxicity towards breast cancer cells. *Small*, *8*(18), pp.2819-2822.
- Du, L., Ma, S., Wen, X., Chai, J. and Zhou, D., 2017. Oral squamous cell carcinoma cells are resistant to doxorubicin through upregulation of miR-221. *Molecular Medicine Reports*, *16*(3), pp.2659-2667.

References:

- Duan, Y., He, Q., Yue, K., Si, H., Wang, J., Zhou, X. and Wang, X., 2017. Hypoxia induced Bcl-2/Twist1 complex promotes tumor cell invasion in oral squamous cell carcinoma. *Oncotarget*, *8*(5), p.7729.
- Elechalawar, C.K., Bhattacharya, D., Ahmed, M.T., Gora, H., Sridharan, K., Chaturbedy, P., Sinha, S.H., Jaggarapu, M.M.C.S., Narayan, K.P., Chakravarty, S. and Eswaramoorthy, M., 2019. Dual targeting of folate receptor-expressing glioma tumor-associated macrophages and epithelial cells in the brain using a carbon nanosphere–cationic folate nanoconjugate. *Nanoscale Advances*, *1*(9), pp.3555-3567.
- Elechalawar, C.K., Sridharan, K., Pal, A., Ahmed, M.T., Yousuf, M., Adhikari, S.S. and Banerjee, R., 2017. Cationic folate-mediated liposomal delivery of bis-arylidene oxindole induces efficient melanoma tumor regression. *Biomaterials science*, *5*(9), pp.1898-1909.
- Emi, M., Kim, R., Tanabe, K., Uchida, Y. and Toge, T., 2005. Targeted therapy against Bcl-2-related proteins in breast cancer cells. *Breast cancer research*, *7*, pp.1-13.
- Endo, K., Ueno, T., Kondo, S., Wakisaka, N., Murono, S., Ito, M., Kataoka, K., Kato, Y. and Yoshizaki, T., 2013. Tumor-targeted chemotherapy with the nanopolymer-based drug NC-6004 for oral squamous cell carcinoma. *Cancer science*, *104*(3), pp.369-374.
- Eriksson, S.E., Ceder, S., Bykov, V.J. and Wiman, K.G., 2019. p53 as a hub in cellular redox regulation and therapeutic target in cancer. *Journal of molecular cell biology*, *11*(4), pp.330-341.

References:

- Erin, N., Grahovac, J., Brozovic, A. and Efferth, T., 2020. Tumor microenvironment and epithelial mesenchymal transition as targets to overcome tumor multidrug resistance. *Drug Resistance Updates*, *53*, p.100715.
- Fan, H.Y., Zhu, Z.L., Zhang, W.L., Yin, Y.J., Tang, Y.L., Liang, X.H. and Zhang, L., 2020. Light stimulus responsive nanomedicine in the treatment of oral squamous cell carcinoma. *European journal of medicinal chemistry*, *199*, p.112394.
- Fan, L., Wang, J., Xia, C., Zhang, Q., Pu, Y., Chen, L., Chen, J. and Wang, Y., 2020. Glutathione-sensitive and folate-targeted nanoparticles loaded with paclitaxel to enhance oral squamous cell carcinoma therapy. *Journal of materials chemistry B*, *8*(15), pp.3113-3122.
- Fan, W., Yang, X., Huang, F., Tong, X. and Zhu, L., 2019. Identification of CD206 as a potential biomarker of cancer stem-like cells and therapeutic agent in liver cancer. *Oncology letters*, *18*(3), pp.3218-3226.
- Feng, J., Byrne, N.M., Al Jamal, W. and Coulter, J.A., 2019. Exploiting current understanding of hypoxia mediated tumour progression for nanotherapeutic development. *Cancers*, *11*(12), p.1989.
- Fernández, M., Javaid, F. and Chudasama, V., 2018. Advances in targeting the folate receptor in the treatment/imaging of cancers. Chemical science, 9(4), pp.790-810.
- Fiandalo, M.V. and Kyprianou, N., 2012. Caspase control: protagonists of cancer cell apoptosis. *Experimental oncology*, *34*(3), p.165.
- Fojo, T. and Parkinson, D.R., 2010. Biologically targeted cancer therapy and marginal benefits: are we making too much of too little or are we achieving too little by giving too much?. *Clinical Cancer Research*, *16*(24), pp.5972-5980.

References:

- Frank, N.Y., Margaryan, A., Huang, Y., Schatton, T., Waaga-Gasser, A.M., Gasser, M., Sayegh, M.H., Sadee, W. and Frank, M.H., 2005. ABCB5-mediated doxorubicin transport and chemoresistance in human malignant melanoma. *Cancer research*, *65*(10), pp.4320-4333.
- Gao, D.Y., Lin, T.T., Sung, Y.C., Liu, Y.C., Chiang, W.H., Chang, C.C., Liu, J.Y. and Chen, Y., 2015. CXCR4-targeted lipid-coated PLGA nanoparticles deliver sorafenib and overcome acquired drug resistance in liver cancer. *Biomaterials*, *67*, pp.194-203.
- Gao, L., Zhang, W., Zhong, W.Q., Liu, Z.J., Li, H.M., Yu, Z.L. and Zhao, Y.F., 2018. Tumor associated macrophages induce epithelial to mesenchymal transition via the EGFR/ERK1/2 pathway in head and neck squamous cell carcinoma. *Oncology reports*, *40*(5), pp.2558-2572.
- Ge, Z. and Ding, S., 2020. The crosstalk between tumor-associated macrophages (TAMs) and tumor cells and the corresponding targeted therapy. *Frontiers in oncology*, *10*, p.590941.
- George, P., 2011. p53 how crucial is its role in cancer. *Int J Curr Pharm Res*, *3*(2), pp.19-25.
- Gonzalez-Fierro, A. and Dueñas-González, A., 2021, January. Drug repurposing for cancer therapy, easier said than done. In *Seminars in cancer biology* (Vol. 68, pp. 123-131). Academic Press.
- Goren, D., Horowitz, A.T., Tzemach, D., Tarshish, M., Zalipsky, S. and Gabizon, A., 2000. Nuclear delivery of doxorubicin via folate-targeted liposomes with bypass of multidrug-resistance efflux pump. *Clinical Cancer Research*, *6*(5), pp.1949-1957.
- Grimm, E.A., Sikora, A.G. and Ekmekcioglu, S., 2013. Molecular Pathways: Inflammation-Associated Nitric-Oxide Production as a Cancer-Supporting Redox

References:

Mechanism and a Potential Therapeutic TargetInflammation-Associated Nitric-Oxide Supporting Melanoma. *Clinical Cancer Research*, *19*(20), pp.5557-5563.

- Gupta, P., Singh, M., Kumar, R., Belz, J., Shanker, R., Dwivedi, P.D., Sridhar, S. and Singh, S.P., 2018. Synthesis and in vitro studies of PLGA-DTX nanoconjugate as potential drug delivery vehicle for oral cancer. *International Journal of Nanomedicine*, *13*(sup1), pp.67-69.
- Gurnett, A.M., Ward, J., Raper, J. and Turner, M.J., 1986. Purification and characterisation of membrane-form variant surface glycoproteins of Trypanosoma brucei. *Molecular and biochemical parasitology*, *20*(1), pp.1-13.
- Guyon, J., Andrique, L., Pujol, N., Røsland, G.V., Recher, G., Bikfalvi, A. and Daubon, T., 2020. A 3D spheroid model for glioblastoma. *JoVE (Journal of Visualized Experiments)*, (158), p.e60998.
- Hagemann, T., Lawrence, T., McNeish, I., Charles, K.A., Kulbe, H., Thompson, R.G., Robinson, S.C. and Balkwill, F.R., 2008. "Re-educating" tumor-associated macrophages by targeting NF-κB. *The Journal of experimental medicine*, *205*(6), pp.1261-1268.
- Hamilton, A., Larsimont, D., Paridaens, R., Drijkoningen, M., Van de Vijver, M., Bruning, P., Hanby, A., Houston, S., Treilleux, I., Guastalla, J.P. and Van Vreckem, A., 2000. A study of the value of p53, HER2, and Bcl-2 in the prediction of response to doxorubicin and paclitaxel as single agents in metastatic breast cancer: a companion study to EORTC 10923. *Clinical breast cancer*, *1*(3), pp.233-240.
- Hamilton, G. and Rath, B., 2019. Applicability of tumor spheroids for in vitro chemosensitivity assays. *Expert Opinion on Drug Metabolism & Toxicology*, *15*(1), pp.15-23.

References:

- Han, M., Huang-Fu, M.Y., Guo, W.W., Guo, N.N., Chen, J., Liu, H.N., Xie, Z.Q., Lin, M.T., Wei, Q.C. and Gao, J.Q., 2017. MMP-2-sensitive HA end-conjugated poly (amidoamine) dendrimers via click reaction to enhance drug penetration into solid tumor. *ACS applied materials & interfaces*, *9*(49), pp.42459-42470.
- Han, S., Wang, W., Wang, S., Wang, S., Ju, R., Pan, Z., Yang, T., Zhang, G., Wang, H. and Wang, L., 2019. Multifunctional biomimetic nanoparticles loading baicalin for polarizing tumor-associated macrophages. *Nanoscale*, *11*(42), pp.20206-20220.
- Haque, A.R., Moriyama, M., Kubota, K., Ishiguro, N., Sakamoto, M., Chinju, A., Mochizuki, K., Sakamoto, T., Kaneko, N., Munemura, R. and Maehara, T., 2019. CD206+ tumor-associated macrophages promote proliferation and invasion in oral squamous cell carcinoma via EGF production. *Scientific reports*, *9*(1), p.14611.
- Hartley, G.P., Chow, L., Ammons, D.T., Wheat, W.H. and Dow, S.W., 2018. Programmed Cell Death Ligand 1 (PD-L1) Signaling Regulates Macrophage Proliferation and ActivationPD-L1 Regulates Macrophage Proliferation and Activation. *Cancer immunology research*, *6*(10), pp.1260-1273.
- Hasirci, V.A.S.I.F., Vrana, E., Zorlutuna, P., Ndreu, A., Yilgor, P., Basmanav, F.B. and Aydin, E.R.K.İ.N., 2006. Nanobiomaterials: a review of the existing science and technology, and new approaches. *Journal of Biomaterials Science, Polymer Edition*, *17*(11), pp.1241-1268.
- Helmink, B.A., Reddy, S.M., Gao, J., Zhang, S., Basar, R., Thakur, R., Yizhak, K., Sade-Feldman, M., Blando, J., Han, G. and Gopalakrishnan, V., 2020. B cells and tertiary lymphoid structures promote immunotherapy response. *Nature*, *577*(7791), pp.549-555.

References:

- Hilgenbrink, A.R. and Low, P.S., 2005. Folate receptor-mediated drug targeting: from therapeutics to diagnostics. *Journal of pharmaceutical sciences*, *94*(10), pp.2135-2146.
- Hirabayashi, F., Iwanaga, K., Okinaga, T., Takahashi, O., Ariyoshi, W., Suzuki, R., Sugii, M., Maruyama, K., Tominaga, K. and Nishihara, T., 2017. Epidermal growth factor receptor-targeted sonoporation with microbubbles enhances therapeutic efficacy in a squamous cell carcinoma model. *PLoS One*, *12*(9), p.e0185293.
- Hu, F.W., Yu, C.C., Hsieh, P.L., Liao, Y.W., Lu, M.Y. and Chu, P.M., 2017. Targeting oral cancer stemness and chemoresistance by isoliquiritigenin-mediated GRP78 regulation. *Oncotarget*, *8*(55), p.93912.
- Hu, J.M., Liu, K., Liu, J.H., Jiang, X.L., Wang, X.L., Chen, Y.Z., Li, S.G., Zou, H., Pang, L.J., Liu, C.X. and Cui, X.B., 2017. CD163 as a marker of M2 macrophage, contribute to predict aggressiveness and prognosis of Kazakh esophageal squamous cell carcinoma. *Oncotarget*, *8*(13), p.21526.
- Huang, B.W. and Gao, J.Q., 2018. Application of 3D cultured multicellular spheroid tumor models in tumor-targeted drug delivery system research. *Journal of controlled release*, *270*, pp.246-259.
- Huang, C., Qiu, S., Fan, X., Jiao, G., Zhou, X., Sun, M., Weng, N., Gao, S., Tao, X., Zhang, F. and Chen, W., 2021. Evaluation of the effect of Shengxian Decoction on doxorubicin-induced chronic heart failure model rats and a multicomponent comparative pharmacokinetic study after oral administration in normal and model rats. *Biomedicine & Pharmacotherapy*, *144*, p.112354.
- Huang, K.W., Hsu, F.F., Qiu, J.T., Chern, G.J., Lee, Y.A., Chang, C.C., Huang, Y.T., Sung, Y.C., Chiang, C.C., Huang, R.L. and Lin, C.C., 2020. Highly efficient and tumor-

References:

selective nanoparticles for dual-targeted immunogene therapy against cancer. *Science advances*, *6*(3), p.eaax5032.

- Jaynes, J.M., Sable, R., Ronzetti, M., Bautista, W., Knotts, Z., Abisoye-Ogunniyan, A., Li, D., Calvo, R., Dashnyam, M., Singh, A. and Guerin, T., 2020. Mannose receptor (CD206) activation in tumor-associated macrophages enhances adaptive and innate antitumor immune responses. *Science translational medicine*, *12*(530), p.eaax6337.
- Jensen, D.H., Dabelsteen, E., Specht, L., Fiehn, A.M.K., Therkildsen, M.H., Jønson, L., Vikesaa, J., Nielsen, F.C. and Von Buchwald, C., 2015. Molecular profiling of tumour budding implicates TGFβ-mediated epithelial–mesenchymal transition as a therapeutic target in oral squamous cell carcinoma. The Journal of pathology, 236(4), pp.505-516.
- Jiang, Z., Sun, H., Yu, J., Tian, W. and Song, Y., 2021. Targeting CD47 for cancer immunotherapy. *Journal of Hematology & Oncology*, *14*(1), pp.1-18.
- Jin, B.Z., Dong, X.Q., Xu, X. and Zhang, F.H., 2018. Development and in vitro evaluation of mucoadhesive patches of methotrexate for targeted delivery in oral cancer. *Oncology letters*, *15*(2), pp.2541-2549.
- Jo, Y., Choi, N., Kim, K., Koo, H.J., Choi, J. and Kim, H.N., 2018. Chemoresistance of cancer cells: requirements of tumor microenvironment-mimicking in vitro models in anti-cancer drug development. *Theranostics*, *8*(19), p.5259.
- Jordan, R.C.K., Catzavelos, G.C., Barrett, A.W. and Speight, P.M., 1996. Differential expression of bcl-2 and bax in squamous cell carcinomas of the oral cavity. *European Journal of Cancer Part B: Oral Oncology*, *3.*

References:

- Joseph, J.P., Harishankar, M.K., Pillai, A.A. and Devi, A., 2018. Hypoxia induced EMT: A review on the mechanism of tumor progression and metastasis in OSCC. *Oral oncology*, *80*, pp.23-32.
- Joyce, J.A. and Pollard, J.W., 2009. Microenvironmental regulation of metastasis. *Nature reviews cancer*, *9*(4), pp.239-252.
- Jung, I.D., Lee, J.S., Yun, S.Y., Park, C.G., Han, J.W., Lee, H.W. and Lee, H.Y., 2002. Doxorubicin inhibits the production of nitric oxide by colorectal cancer cells. *Archives of pharmacal research*, *25*, pp.691-696.
- Kaczmarek, A., Krysko, O., Heyndrickx, L., Løve Aaes, T., Delvaeye, T., Bachert, C., Leybaert, L., Vandenabeele, P. and Krysko, D.V., 2013. TNF/TNF-R1 pathway is involved in doxorubicin-induced acute sterile inflammation. *Cell Death & Disease*, *4*(12), pp.e961-e961.
- Kademani, D., 2007, July. Oral cancer. In Mayo Clinic Proceedings (Vol. 82, No. 7, pp. 878-887). Elsevier.
- Karapetis, C.S., Khambata-Ford, S., Jonker, D.J., O'Callaghan, C.J., Tu, D., Tebbutt, N.C., Simes, R.J., Chalchal, H., Shapiro, J.D., Robitaille, S. and Price, T.J., 2008. K-ras mutations and benefit from cetuximab in advanced colorectal cancer. *New England Journal of Medicine*, *359*(17), pp.1757-1765.
- Karunakaran, K. and Muniyan, R., 2020. Genetic alterations and clinical dimensions of oral cancer: a review. *Molecular biology reports*, *47*, pp.9135-9148.
- Kepp, O., Marabelle, A., Zitvogel, L. and Kroemer, G., 2020. Oncolysis without viruses—Inducing systemic anticancer immune responses with local therapies. *Nature Reviews Clinical Oncology*, *17*(1), pp.49-64.

References:

- Kim, D., Park, S., Yoo, H., Park, S., Kim, J., Yum, K., Kim, K. and Kim, H., 2020. Overcoming anticancer resistance by photodynamic therapy-related efflux pump deactivation and ultrasound-mediated improved drug delivery efficiency. *Nano Convergence*, *7*(1), pp.1-12.
- Kouketsu, A., Sato, I., Oikawa, M., Shimizu, Y., Saito, H., Tashiro, K., Yamashita, Y., Takahashi, T. and Kumamoto, H., 2019. Regulatory T cells and M2-polarized tumour-associated macrophages are associated with the oncogenesis and progression of oral squamous cell carcinoma. *International Journal of Oral and Maxillofacial Surgery*, *48*(10), pp.1279-1288.
- Kouno, M., Minabe, M., Tachikawa, T. and Stanley, J.R., 2017. Oral cancer treatment by targeted drug delivery system with an anti-desmoglein monoclonal antibody. *Journal of Dermatological Science*, *86*(2), p.e27.
- Krishan, A., Sridhar, K.S., Davila, E., Vogel, C. and Sternheim, W., 1987. Patterns of anthracycline retention modulation in human tumor cells. *Cytometry: The Journal of the International Society for Analytical Cytology*, *8*(3), pp.306-314.
- Kumar, A.T., Knops, A., Swendseid, B., Martinez-Outschoom, U., Harshyne, L., Philp, N., Rodeck, U., Luginbuhl, A., Cognetti, D., Johnson, J. and Curry, J., 2019. Prognostic significance of tumor-associated macrophage content in head and neck squamous cell carcinoma: a meta-analysis. *Frontiers in oncology*, *9*, p.656.
- Kurimchak, A.M., Herrera-Montávez, C., Montserrat-Sangrà, S., Araiza-Olivera, D., Hu, J., Neumann-Domer, R., Kuruvilla, M., Bellacosa, A., Testa, J.R., Jin, J. and Duncan, J.S., 2022. The drug efflux pump MDR1 promotes intrinsic and acquired resistance to PROTACs in cancer cells. *Science Signaling*, *15*(749), p.eabn2707.

References:

- Kuzin, M., Schoretsanitis, G., Haen, E., Stegmann, B., Hiemke, C., Gründer, G. and Paulzen, M., 2018. Effects of the proton pump inhibitors omeprazole and pantoprazole on the cytochrome P450-mediated metabolism of venlafaxine. *Clinical pharmacokinetics*, *57*, pp.729-737.
- La Fleur, L., Boura, V.F., Alexeyenko, A., Berglund, A., Pontén, V., Mattsson, J.S., Djureinovic, D., Persson, J., Brunnström, H., Isaksson, J. and Brandén, E., 2018. Expression of scavenger receptor MARCO defines a targetable tumor-associated macrophage subset in non-small cell lung cancer. *International Journal of Cancer*, *143*(7), pp.1741-1752.
- Landstrom, A.P., Dobrev, D. and Wehrens, X.H., 2017. Calcium signaling and cardiac arrhythmias. *Circulation research*, *120*(12), pp.1969-1993.
- Legge, C.J., Colley, H.E., Lawson, M.A. and Rawlings, A.E., 2019. Targeted magnetic nanoparticle hyperthermia for the treatment of oral cancer. *Journal of Oral Pathology & Medicine*, *48*(9), pp.803-809.
- Li, D., Zhang, M., Xu, F., Chen, Y., Chen, B., Chang, Y., Zhong, H., Jin, H. and Huang, Y., 2018. Biomimetic albumin-modified gold nanorods for photothermo-chemotherapy and macrophage polarization modulation. *Acta Pharmaceutica Sinica B*, *8*(1), pp.74-84.
- Li, J., Gong, C., Feng, X., Zhou, X., Xu, X., Xie, L., Wang, R., Zhang, D., Wang, H., Deng, P. and Zhou, M., 2012. Biodegradable thermosensitive hydrogel for SAHA and DDP delivery: therapeutic effects on oral squamous cell carcinoma xenografts. *PLoS One*, *7*(4), p.e33860.
- Li, K., Lu, L., Xue, C., Liu, J., He, Y., Zhou, J., Xia, Z., Dai, L., Luo, Z., Mao, Y. and Cai, K., 2020. Polarization of tumor-associated macrophage phenotype via porous

References:

hollow iron nanoparticles for tumor immunotherapy in vivo. *Nanoscale*, *12*(1), pp.130-144.

- Li, L., Zhen, M., Wang, H., Sun, Z., Cao, X., Li, J., Liu, S., Zhao, Z., Zhou, C., Wang, C. and Bai, C., 2023. Tumor microenvironment-modulated multiple nanotherapeutic system for potent cancer immunotherapy and metastasis inhibition. *Nano Today*, *48*, p.101702.
- Li, X., Bu, W., Meng, L., Liu, X., Wang, S., Jiang, L., Ren, M., Fan, Y. and Sun, H., 2019. CXCL12/CXCR4 pathway orchestrates CSC-like properties by CAF recruited tumor associated macrophage in OSCC. *Experimental Cell Research*, *378*(2), pp.131-138.
- Li, X., Zhou, Y., Li, Y., Yang, L., Ma, Y., Peng, X., Yang, S., Liu, J. and Li, H., 2019. Autophagy: A novel mechanism of chemoresistance in cancers. *Biomedicine & Pharmacotherapy*, *119*, p.109415.
- Lim, E.K., Chung, B.H. and Chung, S.J., 2018. Recent advances in pH-sensitive polymeric nanoparticles for smart drug delivery in cancer therapy. *Current drug targets*, *19*(4), pp.300-317.
- Lin, X.J., He, C.L., Sun, T., Duan, X.J., Sun, Y. and Xiong, S.J., 2017. hsa-miR-485-5p reverses epithelial to mesenchymal transition and promotes cisplatin-induced cell death by targeting PAK1 in oral tongue squamous cell carcinoma. *International Journal of Molecular Medicine*, *40*(1), pp.83-89.
- Ling, Z., Cheng, B. and Tao, X., 2021. Epithelial-to-mesenchymal transition in oral squamous cell carcinoma: Challenges and opportunities. *International journal of cancer*, *148*(7), pp.1548-1561.

References:

- Liu, F.S., 2009. Mechanisms of chemotherapeutic drug resistance in cancer therapy—a quick review. *Taiwanese Journal of Obstetrics and Gynecology*, *48*(3), pp.239-244.
- Liu, L., Yi, H., He, H., Pan, H., Cai, L. and Ma, Y., 2017. Tumor associated macrophage-targeted microRNA delivery with dual-responsive polypeptide nanovectors for anti-cancer therapy. *Biomaterials*, *134*, pp.166-179.
- Liu, S., Liu, L., Ye, W., Ye, D., Wang, T., Guo, W., Liao, Y., Xu, D., Song, H., Zhang, L. and Zhu, H., 2016. High vimentin expression associated with lymph node metastasis and predicated a poor prognosis in oral squamous cell carcinoma. *Scientific reports*, *6*(1), p.38834.
- Liu, Y.Y., Yu, J.Y., Yin, D., Patwardhan, G.A., Gupta, V., Hirabayashi, Y., Holleran, W.M., Giuliano, A.E., Jazwinski, S.M., Gouaze-Andersson, V. and Consoli, D.P., 2008. A role for ceramide in driving cancer cell resistance to doxorubicin. *The FASEB Journal*, *22*(7), pp.2541-2551.
- Loeb, L.A. and Christians, F.C., 1996. Multiple mutations in human cancers. *Mutation Research/Fundamental and Molecular Mechanisms of Mutagenesis*, *350*(1), pp.279-286.
- López-Verdín, S., de la Luz Martínez-Fierro, M., Garza-Veloz, I., Zamora-Perez, A., Grajeda-Cruz, J., González-González, R., Molina-Frechero, N., Arocena, M. and Bologna-Molina, R., 2019. E-Cadherin gene expression in oral cancer: clinical and prospective data. *Medicina oral, patologia oral y cirugia bucal*, *24*(4), p.e444.
- López-Verdín, S., de la Luz Martínez-Fierro, M., Garza-Veloz, I., Zamora-Perez, A., Grajeda-Cruz, J., González-González, R., Molina-Frechero, N., Arocena, M. and

References:

Bologna-Molina, R., 2019. E-Cadherin gene expression in oral cancer: clinical and prospective data. Medicina oral, patologia oral y cirugia bucal, 24(4), p.e444.

- Löscher, W. and Potschka, H., 2005. Drug resistance in brain diseases and the role of drug efflux transporters. *Nature Reviews Neuroscience*, *6*(8), pp.591-602.
- Low, P.S., Henne, W.A. and Doorneweerd, D.D., 2008. Discovery and development of folic-acid-based receptor targeting for imaging and therapy of cancer and inflammatory diseases. *Accounts of chemical research*, *41*(1), pp.120-129.
- Lowe, J.M., Menendez, D., Bushel, P.R., Shatz, M., Kirk, E.L., Troester, M.A., Garantziotis, S., Fessler, M.B. and Resnick, M.A., 2014. p53 and NF-κB coregulate proinflammatory gene responses in human macrophages. *Cancer research*, *74*(8), pp.2182-2192.
- Lowry, M.C., Gallagher, W.M. and O'Driscoll, L., 2015. The role of exosomes in breast cancer. *Clinical chemistry*, *61*(12), pp.1457-1465.
- Lu, Y. and Low, P.S., 2002. Folate-mediated delivery of macromolecular anticancer therapeutic agents. *Advanced drug delivery reviews*, *54*(5), pp.675-693.
- Lu, Y.J., Lin, P.Y., Huang, P.H., Kuo, C.Y., Shalumon, K.T., Chen, M.Y. and Chen, J.P., 2018. Magnetic graphene oxide for dual targeted delivery of doxorubicin and photothermal therapy. *Nanomaterials*, *8*(4), p.193.
- Lúcio, P.S.C., Ribeiro, D.C., Aguiar, M.C.F.D., Alves, P.M., Nonaka, C.F.W. and Godoy, G.P., 2016. Tumor-associated macrophages (TAMs): clinical-pathological parameters in squamous cell carcinomas of the lower lip. *Brazilian oral research*, *30*.
- Ma, C., Peng, Y., Li, H. and Chen, W., 2021. Organ-on-a-chip: a new paradigm for drug development. *Trends in pharmacological sciences*, *42*(2), pp.119-133.

References:

- Ma, P. and Mumper, R.J., 2013. Anthracycline nano-delivery systems to overcome multiple drug resistance: A comprehensive review. *Nano today*, *8*(3), pp.313-331.
- Mahadik, N., Bhattacharya, D., Padmanabhan, A., Sakhare, K., Narayan, K.P. and Banerjee, R., 2022. Targeting steroid hormone receptors for anti-cancer therapy—A review on small molecules and nanotherapeutic approaches. Wiley Interdisciplinary Reviews: Nanomedicine and Nanobiotechnology, 14(2), p.e1755.
- Mangeolle, T., Yakavets, I., Lequeux, N., Pons, T., Bezdetnaya, L. and Marchal, F., 2019. The targeting ability of fluorescent quantum dots to the folate receptor rich tumors. *Photodiagnosis and Photodynamic Therapy*, *26*, pp.150-156.
- Manturthi, S., Bhattacharya, D., Sakhare, K.R., Narayan, K.P. and Patri, S.V., 2022. Nicotinic acid-based cationic vectors for efficient gene delivery to glioblastoma cells. New Journal of Chemistry, 46(43), pp.20886-20899.
- Manturthi, S., Bhattacharya, D., Sakhare, K.R., Narayan, K.P. and Patri, S.V., 2022. Cimetidine-Based Cationic Amphiphiles for In Vitro Gene Delivery Targetable to Colon Cancer. ACS omega, 7(35), pp.31388-31402.
- Matsumoto, H., Hayashi, S., Hatashita, M., Ohnishi, K., Shioura, H., Ohtsubo, T., Kitai, R., Ohnishi, T. and Kano, E., 2001. Induction of radioresistance by a nitric oxide-mediated bystander effect. *Radiation research*, *155*(3), pp.387-396.(a)
- Matsuoka, Y., Nakayama, H., Yoshida, R., Hirosue, A., Nagata, M., Tanaka, T., Kawahara, K., Sakata, J., Arita, H., Nakashima, H. and Shinriki, S., 2016. IL-6 controls resistance to radiation by suppressing oxidative stress via the Nrf2-antioxidant pathway in oral squamous cell carcinoma. *British journal of cancer*, *115*(10), pp.1234-1244.

References:

- Mattila, J.T. and Thomas, A.C., 2014. Nitric oxide synthase: non-canonical expression patterns. *Frontiers in immunology*, *5*, p.478.
- Mazzarino, L., Loch-Neckel, G., Bubniak, L.D.S., Mazzucco, S., Santos-Silva, M.C., Borsali, R. and Lemos-Senna, E., 2015. Curcumin-loaded chitosan-coated nanoparticles as a new approach for the local treatment of oral cavity cancer. *Journal of nanoscience and nanotechnology*, *15*(1), pp.781-791.
- Mehendiratta, M., Solomon, M.C., Boaz, K., Guddattu, V. and Mohindra, A., 2014. Clinico-pathological correlation of E-cadherin expression at the invasive tumor front of Indian oral squamous cell carcinomas: An immunohistochemical study. *Journal of oral and maxillofacial pathology: JOMFP*, *18*(2), p.217.
- Mendes, N., Dias Carvalho, P., Martins, F., Mendonça, S., Malheiro, A.R., Ribeiro, A., Carvalho, J. and Velho, S., 2020. Animal models to study cancer and its microenvironment. *Tumor Microenvironment: The Main Driver of Metabolic Adaptation*, pp.389-401.
- Milane, L., Duan, Z. and Amiji, M., 2011. Role of hypoxia and glycolysis in the development of multi-drug resistance in human tumor cells and the establishment of an orthotopic multi-drug resistant tumor model in nude mice using hypoxic pre-conditioning. *Cancer cell international*, *11*, pp.1-16.
- Miller, M.A., Zheng, Y.R., Gadde, S., Pfirschke, C., Zope, H., Engblom, C., Kohler, R.H., Iwamoto, Y., Yang, K.S., Askevold, B. and Kolishetti, N., 2015. Tumour-associated macrophages act as a slow-release reservoir of nano-therapeutic Pt (IV) pro-drug. Nature communications, 6(1), p.8692.
- Mir, M.A., 2015. *Developing costimulatory molecules for immunotherapy of diseases*. Academic Press.

References:

- Modok, S., Mellor, H.R. and Callaghan, R., 2006. Modulation of multidrug resistance efflux pump activity to overcome chemoresistance in cancer. *Current opinion in pharmacology*, *6*(4), pp.350-354.
- Mogre, S., Makani, V., Pradhan, S., Devre, P., More, S., Vaidya, M. and Dmello, C., 2022. Biomarker Potential of Vimentin in Oral Cancers. *Life*, *12*(2), p.150.
- Moradi-Chaleshtori, M., Bandehpour, M., Soudi, S., Mohammadi-Yeganeh, S. and Hashemi, S.M., 2021. In vitro and in vivo evaluation of anti-tumoral effect of M1 phenotype induction in macrophages by miR-130 and miR-33 containing exosomes. *Cancer Immunology, Immunotherapy*, *70*, pp.1323-1339.
- Mukherjee, A., Narayan, K.P., Pal, K., Kumar, J.M., Rangaraj, N., Kalivendi, S.V. and Banerjee, R., 2009. Selective cancer targeting via aberrant behavior of cancer cell-associated glucocorticoid receptor. Molecular Therapy, 17(4), pp.623-631.
- Mukherjee, A., Spadigam, A., Dhupar, A., Carvalho, K. and Syed, S., 2019. Tumor associated macrophages: tagging aggressiveness in oral squamous cell carcinoma. *Oral Surgery, Oral Medicine, Oral Pathology and Oral Radiology*, *128*(1), p.e83.
- Muller, P.A. and Vousden, K.H., 2013. p53 mutations in cancer. *Nature cell biology*, *15*(1), pp.2-8.
- Muntané, J. and De la Mata, M., 2010. Nitric oxide and cancer. *World journal of hepatology*, *2*(9), p.337.
- Nagai, T., Tanaka, M., Tsuneyoshi, Y., Xu, B., Michie, S.A., Hasui, K., Hirano, H., Arita, K. and Matsuyama, T., 2009. Targeting tumor-associated macrophages in an experimental glioma model with a recombinant immunotoxin to folate receptor β. *Cancer immunology, immunotherapy*, *58*, pp.1577-1586.

References:

- Nakamura, K. and Smyth, M.J., 2020. Myeloid immunosuppression and immune checkpoints in the tumor microenvironment. *Cellular & molecular immunology*, *17*(1), pp.1-12.
- Narihira, K., Watanabe, A., Sheng, H., Endo, H., Feril, L.B., Irie, Y., Ogawa, K., Moosavi-Nejad, S., Kondo, S., Kikuta, T. and Tachibana, K., 2018. Enhanced cell killing and apoptosis of oral squamous cell carcinoma cells with ultrasound in combination with cetuximab coated albumin microbubbles. *Journal of Drug Targeting*, *26*(3), pp.278-288.
- Nath, N. and Kashfi, K., 2020. Tumor associated macrophages and 'NO'. *Biochemical pharmacology*, *176*, p.113899.
- Nieto-Márquez, A., Romero, R., Romero, A. and Valverde, J.L., 2011. Carbon nanospheres: synthesis, physicochemical properties and applications. Journal of Materials chemistry, 21(6), pp.1664-1672.
- Niu, C., Wang, Z., Lu, G., Krupka, T.M., Sun, Y., You, Y., Song, W., Ran, H., Li, P. and Zheng, Y., 2013. Doxorubicin loaded superparamagnetic PLGA-iron oxide multifunctional microbubbles for dual-mode US/MR imaging and therapy of metastasis in lymph nodes. *Biomaterials*, *34*(9), pp.2307-2317.
- Niu, M., Naguib, Y.W., Aldayel, A.M., Shi, Y.C., Hursting, S.D., Hersh, M.A. and Cui, Z., 2014. Biodistribution and in vivo activities of tumor-associated macrophage-targeting nanoparticles incorporated with doxorubicin. *Molecular Pharmaceutics*, *11*(12), pp.4425-4436.
- Nowak, M. and Klink, M., 2020. The role of tumor-associated macrophages in the progression and chemoresistance of ovarian cancer. *Cells*, *9*(5), p.1299.

References:

- Noy, R. and Pollard, J.W., 2014. Tumor-associated macrophages: from mechanisms to therapy. *Immunity*, *41*(1), pp.49-61.
- Nunes, T., Hamdan, D., Leboeuf, C., El Bouchtaoui, M., Gapihan, G., Nguyen, T.T., Meles, S., Angeli, E., Ratajczak, P., Lu, H. and Di Benedetto, M., 2018. Targeting cancer stem cells to overcome chemoresistance. *International journal of molecular sciences*, *19*(12), p.4036.
- Oktem, G., Karabulut, B., Selvi, N., Sezgin, C., Sanli, U.A., Uslu, R., Yurtseven, M.E. and Omay, S.B., 2004. Differential effects of doxorubicin and docetaxel on nitric oxide production and inducible nitric oxide synthase expression in MCF-7 human breast cancer cells. *Oncology Research Featuring Preclinical and Clinical Cancer Therapeutics*, *14*(7-8), pp.381-386.
- Olive, K.P., Tuveson, D.A., Ruhe, Z.C., Yin, B., Willis, N.A., Bronson, R.T., Crowley, D. and Jacks, T., 2004. Mutant p53 gain of function in two mouse models of Li-Fraumeni syndrome. *Cell*, *119*(6), pp.847-860.
- Onder, T.T., Gupta, P.B., Mani, S.A., Yang, J., Lander, E.S. and Weinberg, R.A., 2008. Loss of E-cadherin promotes metastasis via multiple downstream transcriptional pathways. *Cancer research*, *68*(10), pp.3645-3654.
- Onken, M.D., Winkler, A.E., Kanchi, K.L., Chalivendra, V., Law, J.H., Rickert, C.G., Kallogjeri, D., Judd, N.P., Dunn, G.P., Piccirillo, J.F. and Lewis Jr, J.S., 2014. A surprising cross-species conservation in the genomic landscape of mouse and human oral cancer identifies a transcriptional signature predicting metastatic disease. *Clinical Cancer Research*, *20*(11), pp.2873-2884.
- Oren, M. and Rotter, V., 2010. Mutant p53 gain-of-function in cancer. *Cold Spring Harbor perspectives in biology*, *2*(2), p.a001107.

References:

- Ortega, R.A., Barham, W., Sharman, K., Tikhomirov, O., Giorgio, T.D. and Yull, F.E., 2016. Manipulating the NF-κB pathway in macrophages using mannosylated, siRNA-delivering nanoparticles can induce immunostimulatory and tumor cytotoxic functions. *International journal of nanomedicine*, *11*, p.2163.
- Osman, N., Devnarain, N., Omolo, C.A., Fasiku, V., Jaglal, Y. and Govender, T., 2022. Surface modification of nano-drug delivery systems for enhancing antibiotic delivery and activity. *Wiley Interdisciplinary Reviews: Nanomedicine and Nanobiotechnology*, *14*(1), p.e1758.
- Pan, L., Liu, J., He, Q., Wang, L. and Shi, J., 2013. Overcoming multidrug resistance of cancer cells by direct intranuclear drug delivery using TAT-conjugated mesoporous silica nanoparticles. *Biomaterials*, *34*(11), pp.2719-2730.
- Pan, X.Q., Wang, H. and Lee, R.J., 2003. Antitumor activity of folate receptor-targeted liposomal doxorubicin in a KB oral carcinoma murine xenograft model. *Pharmaceutical research*, *20*, pp.417-422.
- Panaro, M.A., Brandonisio, O., Acquafredda, A., Sisto, M. and Mitolo, V., 2003. Evidences for iNOS expression and nitric oxide production in the human macrophages. *Current Drug Targets-Immune, Endocrine & Metabolic Disorders*, *3*(3), pp.210-221.
- Pang, L., Pei, Y., Uzunalli, G., Hyun, H., Lyle, L.T. and Yeo, Y., 2019. Surface modification of polymeric nanoparticles with M2pep peptide for drug delivery to tumor-associated macrophages. *Pharmaceutical research*, *36*, pp.1-12.
- Pelucchi, C., Talamini, R., Negri, E., Levi, F., Conti, E., Franceschi, S. and La Vecchia, C., 2003. Folate intake and risk of oral and pharyngeal cancer. Annals of Oncology, 14(11), pp.1677-1681.

References:

- PeÑarando, J., Aranda, E. and RodrÍguez-Ariza, A., 2019. Immunomodulatory roles of nitric oxide in cancer: Tumor microenvironment says “NO” to antitumor immune response. *Translational Research*, *210*, pp.99-108.
- Pérez-Sayáns, M., Somoza-Martín, J.M., Barros-Angueira, F., Diz, P.G., Rey, J.M.G. and García-García, A., 2010. Multidrug resistance in oral squamous cell carcinoma: the role of vacuolar ATPases. *Cancer Letters*, *295*(2), pp.135-143.
- Perrotta, C., Cervia, D., Di Renzo, I., Moscheni, C., Bassi, M.T., Campana, L., Martelli, C., Catalani, E., Giovarelli, M., Zecchini, S. and Coazzoli, M., 2018. Nitric oxide generated by tumor-associated macrophages is responsible for cancer resistance to cisplatin and correlated with syntaxin 4 and acid sphingomyelinase inhibition. *Frontiers in immunology*, *9*, p.1186.
- Petitprez, F., de Reyniès, A., Keung, E.Z., Chen, T.W.W., Sun, C.M., Calderaro, J., Jeng, Y.M., Hsiao, L.P., Lacroix, L., Bougoüin, A. and Moreira, M., 2020. B cells are associated with survival and immunotherapy response in sarcoma. *Nature*, *577*(7791), pp.556-560.
- Petruzzi, M.N.M.R., Cherubini, K., Salum, F.G. and De Figueiredo, M.A.Z., 2017. Role of tumour-associated macrophages in oral squamous cells carcinoma progression: an update on current knowledge. *Diagnostic pathology*, *12*(1), pp.1-7.
- Pillai, M.R., Chacko, P., Kesari, L.A., Jayaprakash, P.G., Jayaram, H.N. and Antony, A.C., 2003. Expression of folate receptors and heterogeneous nuclear ribonucleoprotein E1 in women with human papillomavirus mediated transformation of cervical tissue to cancer. *Journal of clinical pathology*, *56*(8), pp.569-574.

References:

- Pinto, B., Henriques, A.C., Silva, P.M. and Bousbaa, H., 2020. Three-dimensional spheroids as in vitro preclinical models for cancer research. *Pharmaceutics*, *12*(12), p.1186.
- Pitolli, C., Wang, Y., Mancini, M., Shi, Y., Melino, G. and Amelio, I., 2019. Do mutations turn p53 into an oncogene?. *International journal of molecular sciences*, *20*(24), p.6241.
- Podyacheva, E.Y., Kushnareva, E.A., Karpov, A.A. and Toropova, Y.G., 2021. Analysis of models of doxorubicin-induced cardiomyopathy in rats and mice. A modern view from the perspective of the pathophysiologist and the clinician. *Frontiers in Pharmacology*, *12*, p.670479.
- Pollard, J.W., 2004. Tumour-educated macrophages promote tumour progression and metastasis. Nature Reviews Cancer 4, 71–78.
- Ponte, J.F., Ab, O., Lanieri, L., Lee, J., Coccia, J., Bartle, L.M., Themeles, M., Zhou, Y., Pinkas, J. and Ruiz-Soto, R., 2016. Mirvetuximab soravtansine (IMGN853), a folate receptor alpha–targeting antibody-drug conjugate, potentiates the activity of standard of care therapeutics in ovarian cancer models. *Neoplasia*, *18*(12), pp.775-784.
- Porter, A.G. and Jänicke, R.U., 1999. Emerging roles of caspase-3 in apoptosis. Cell death & differentiation, 6(2), pp.99-104.
- Powan, P., Luanpitpong, S., He, X., Rojanasakul, Y. and Chanvorachote, P., 2017. Detachment-induced E-cadherin expression promotes 3D tumor spheroid formation but inhibits tumor formation and metastasis of lung cancer cells. American Journal of Physiology-Cell Physiology, 313(5), pp.C556-C566.

References:

- Pratt, M.C., White, D., Kushwaha, N., Tibbo, E. and Niu, M.Y., 2007. Cytoplasmic mutant p53 increases Bcl-2 expression in estrogen receptor-positive breast cancer cells. *Apoptosis*, *12*(4), pp.657-669.
- Predina, J.D., Newton, A.D., Xia, L., Corbett, C., Connolly, C., Shin, M., Sulyok, L.F., Litzky, L., Deshpande, C., Nie, S. and Kularatne, S.A., 2018. An open label trial of folate receptor-targeted intraoperative molecular imaging to localize pulmonary squamous cell carcinomas. Oncotarget, 9(17), p.13517.
- Pyonteck, S.M., Akkari, L., Schuhmacher, A.J., Bowman, R.L., Sevenich, L., Quail, D.F., Olson, O.C., Quick, M.L., Huse, J.T., Teijeiro, V. and Setty, M., 2013. CSF-1R inhibition alters macrophage polarization and blocks glioma progression. Nature medicine, 19(10), pp.1264-1272.
- Qian, Y., Qiao, S., Dai, Y., Xu, G., Dai, B., Lu, L., Yu, X., Luo, Q. and Zhang, Z., 2017. Molecular-targeted immunotherapeutic strategy for melanoma via dual-targeting nanoparticles delivering small interfering RNA to tumor-associated macrophages. *ACS nano*, *11*(9), pp.9536-9549.
- Qu, C., Zhang, W., Zheng, G., Zhang, Z., Yin, J. and He, Z., 2014. Metformin reverses multidrug resistance and epithelial–mesenchymal transition (EMT) via activating AMP-activated protein kinase (AMPK) in human breast cancer cells. *Molecular and cellular biochemistry*, *386*, pp.63-71.
- Radha, G. and Raghavan, S.C., 2017. BCL2: A promising cancer therapeutic target. *Biochimica et Biophysica Acta (BBA)-Reviews on Cancer*, *1868*(1), pp.309-314.
- Ramadan, M.A., Shawkey, A.E., Rabeh, M.A. and Abdellatif, A.O., 2019. Expression of P53, BAX, and BCL-2 in human malignant melanoma and squamous cell

References:

carcinoma cells after tea tree oil treatment in vitro. *Cytotechnology*, *71*, pp.461-473.

- Ramadan, S.H., Darwish, Z.E., Elnouaem, M.I., Zeitoun, I.M. and Essawy, M.M., 2020. The role of tumor-associated macrophages in the pathogenesis of oral squamous cell carcinoma correlated with the clinicopathological parameters. *Alexandria Dental Journal*, *45*(3), pp.61-66.
- Ramesh A, Brouillard A, Kumar S, Nandi D, Kulkarni A. Dual inhibition of CSF1R and MAPK pathways using supramolecular nanoparticles enhances macrophage immunotherapy. Biomaterials 2020
- Raniolo, S., Vindigni, G., Ottaviani, A., Unida, V., Iacovelli, F., Manetto, A., Figini, M., Stella, L., Desideri, A. and Biocca, S., 2018. Selective targeting and degradation of doxorubicin-loaded folate-functionalized DNA nanocages. *Nanomedicine: Nanotechnology, Biology and Medicine*, *14*(4), pp.1181-1190.
- Rawat, P.S., Jaiswal, A., Khurana, A., Bhatti, J.S. and Navik, U., 2021. Doxorubicin-induced cardiotoxicity: An update on the molecular mechanism and novel therapeutic strategies for effective management. *Biomedicine & Pharmacotherapy*, *139*, p.111708.
- Retnakumari, A., Setua, S., Menon, D., Ravindran, P., Muhammed, H., Pradeep, T., Nair, S. and Koyakutty, M., 2009. Molecular-receptor-specific, non-toxic, near-infrared-emitting Au cluster-protein nanoconjugates for targeted cancer imaging. Nanotechnology, 21(5), p.055103.
- Rokhlin, O.W., Gudkov, A.V., Kwek, S., Glover, R.A., Gewies, A.S. and Cohen, M.B., 2000. p53 is involved in tumor necrosis factor-α-induced apoptosis in the human prostatic carcinoma cell line LNCaP. *Oncogene*, *19*(15), pp.1959-1968.

References:

- Ross, J.F., Chaudhuri, P.K. and Ratnam, M., 1994. Differential regulation of folate receptor isoforms in normal and malignant tissues in vivo and in established cell lines. Physiologic and clinical implications. *Cancer*, *73*(9), pp.2432-2443.
- Rowley, H., Sherrington, P., Helliwell, T.R., Kinsella, A. and Jones, A.S., 1998. p53 expression and p53 gene mutation in oral cancer and dysplasia. *Otolaryngology--Head and Neck Surgery*, *118*(1), pp.115-123.
- Sabharanjak, S. and Mayor, S., 2004. Folate receptor endocytosis and trafficking. *Advanced drug delivery reviews*, *56*(8), pp.1099-1109.
- Sakai, T., Muramatsu, I., Hayashi, N. and Ishii, Y., 1996. Inhibition of NO synthase induction by an anticancer drug 4'-epi-doxorubicin in rats. *General pharmacology*, *27*(8), pp.1367-1372.
- Sakorafas, G.H. and Safioleas, M., 2009. Breast cancer surgery: an historical narrative. Part I. From prehistoric times to Renaissance. *European journal of cancer care*, *18*(6), pp.530-544.
- Santin, A.D., Hermonat, P.L., Ravaggi, M.C.I., Chiriva-Internat, M., Cannon, M.J., Hiserodt, J.C., Pecorell, S. and Parham, G.P., 1999. Expression of surface antigens during the differentiation of human dendritic cells vs macrophages from blood monocytes in vitro. *Immunobiology*, *200*(2), pp.187-204.
- Satapathy, S.R., Nayak, A., Siddharth, S., Das, S., Nayak, D. and Kundu, C.N., 2018. Metallic gold and bioactive quinacrine hybrid nanoparticles inhibit oral cancer stem cell and angiogenesis by deregulating inflammatory cytokines in p53 dependent manner. *Nanomedicine: Nanotechnology, Biology and Medicine*, *14*(3), pp.883-896.

References:

- Schmitt, M.W., Loeb, L.A. and Salk, J.J., 2016. The influence of subclonal resistance mutations on targeted cancer therapy. Nature reviews Clinical oncology, 13(6), pp.335-347.
- Selvi, B.R., Jagadeesan, D., Suma, B.S., Nagashankar, G., Arif, M., Balasubramanyam, K., Eswaramoorthy, M. and Kundu, T.K., 2008. Intrinsically fluorescent carbon nanospheres as a nuclear targeting vector: delivery of membrane-impermeable molecule to modulate gene expression in vivo. *Nano letters*, *8*(10), pp.3182-3188.
- Shah, J.P. and Gil, Z., 2009. Current concepts in management of oral cancer–surgery. *Oral oncology*, *45*(4-5), pp.394-401.
- Sharma, P., Banerjee, R. and Narayan, K.P., 2016. Mineralocorticoid receptor mediated liposomal delivery system for targeted induction of apoptosis in cancer cells. Biochimica et Biophysica Acta (BBA)-Biomembranes, 1858(2), pp.415-421.
- Sherr, C.J. and McCormick, F., 2002. The RB and p53 pathways in cancer. *Cancer cell*, *2*(2), pp.103-112.
- Shi, Y., Van der Meel, R., Chen, X. and Lammers, T., 2020. The EPR effect and beyond: Strategies to improve tumor targeting and cancer nanomedicine treatment efficacy. *Theranostics*, *10*(17), p.7921.
- Shi, Y., Xie, T., Wang, B., Wang, R., Cai, Y., Yuan, B., Gleber-Netto, F.O., Tian, X., Rodriguez-Rosario, A.E., Osman, A.A. and Wang, J., 2022. Mutant p53 drives an immune cold tumor immune microenvironment in oral squamous cell carcinoma. *Communications Biology*, *5*(1), p.757.
- Shobaki, N., Sato, Y., Suzuki, Y., Okabe, N. and Harashima, H., 2020. Manipulating the function of tumor-associated macrophages by siRNA-loaded lipid nanoparticles for cancer immunotherapy. *Journal of Controlled Release*, *325*, pp.235-248.

References:

- Shrestha, B., Pokhrel, A.R., Darsandhari, S., Parajuli, P., Sohng, J.K. and Pandey, R.P., 2019. Engineering Streptomyces peucetius for doxorubicin and daunorubicin biosynthesis. Pharmaceuticals from Microbes: The Bioengineering Perspective, pp.191-209.
- Silva Servato, J.P., Ueira Vieira, C., de Faria, P.R., Cardoso, S.V. and Loyola, A.M., 2019. The importance of inducible nitric oxide synthase and nitrotyrosine as prognostic markers for oral squamous cell carcinoma. *Journal of Oral Pathology & Medicine*, *48*(10), pp.967-975.
- Singh, R., Letai, A. and Sarosiek, K., 2019. Regulation of apoptosis in health and disease: the balancing act of BCL-2 family proteins. *Nature reviews Molecular cell biology*, *20*(3), pp.175-193.
- Siriwardena, B.S.M.S., Kudo, Y., Ogawa, I., Kitagawa, M., Kitajima, S., Hatano, H., Tilakaratne, W.M., Miyauchi, M. and Takata, T., 2006. Periostin is frequently overexpressed and enhances invasion and angiogenesis in oral cancer. British journal of cancer, 95(10), pp.1396-1403.
- Siu, W.Y., Yam, C.H. and Poon, R.Y., 1999. G1 versus G2 cell cycle arrest after adriamycin-induced damage in mouse Swiss3T3 cells. *FEBS letters*, *461*(3), pp.299-305.
- Song, Y., Tang, C. and Yin, C., 2018. Combination antitumor immunotherapy with VEGF and PIGF siRNA via systemic delivery of multi-functionalized nanoparticles to tumor-associated macrophages and breast cancer cells. *Biomaterials*, *185*, pp.117-132.
- Soussi, T. and Lozano, G., 2005. p53 mutation heterogeneity in cancer. Biochemical and biophysical research communications, 331(3), pp.834-842.

References:

- Sridharan, K., Rathore, B., Yousuf, M., Reddy Rachamalla, H.K., Jinka, S., Jaggarapu, M.M.C.S. and Banerjee, R., 2020. Self-assembling derivative of hydrocortisone as glucocorticoid receptor-targeted nanotherapeutics for synergistic, combination therapy against colorectal tumor. Molecular Pharmaceutics, 18(3), pp.1208-1228.
- Srivastava, S., Gupta, S., Mohammad, S. and Ahmad, I., 2019. Development of α-tocopherol surface-modified targeted delivery of 5-fluorouracil-loaded poly-D, L-lactic-co-glycolic acid nanoparticles against oral squamous cell carcinoma. *Journal of Cancer Research and Therapeutics*, *15*(3), pp.480-490.
- Stasikowska-Kanicka, O., Wągrowska-Danilewicz, M. and Danilewicz, M., 2018. T cells are involved in the induction of macrophage phenotypes in oral leukoplakia and squamous cell carcinoma—a preliminary report. *Journal of Oral Pathology & Medicine*, *47*(2), pp.136-143.
- Stein, Y., Rotter, V. and Aloni-Grinstein, R., 2019. Gain-of-function mutant p53: all the roads lead to tumorigenesis. *International journal of molecular sciences*, *20*(24), p.6197.
- Stornetta, A., Zimmermann, M., Cimino, G.D., Henderson, P.T. and Sturla, S.J., 2017. DNA adducts from anticancer drugs as candidate predictive markers for precision medicine. *Chemical research in toxicology*, *30*(1), pp.388-409.
- Suen, W.L.L. and Chau, Y., 2014. Size-dependent internalisation of folate-decorated nanoparticles via the pathways of clathrin and caveolae-mediated endocytosis in ARPE-19 cells. *Journal of Pharmacy and Pharmacology*, *66*(4), pp.564-573.
- Suh, D.H., Kim, H.S., Kim, B. and Song, Y.S., 2014. Metabolic orchestration between cancer cells and tumor microenvironment as a co-evolutionary source of

References:

chemoresistance in ovarian cancer: a therapeutic implication. *Biochemical pharmacology*, *92*(1), pp.43-54.

- Sun, H., Miao, C., Liu, W., Qiao, X., Yang, W., Li, L. and Li, C., 2018. TGF-β1/TβRII/Smad3 signaling pathway promotes VEGF expression in oral squamous cell carcinoma tumor-associated macrophages. *Biochemical and biophysical research communications*, *497*(2), pp.583-590.
- Sun, J.Y., Shen, J., Thibodeaux, J., Huang, G., Wang, Y., Gao, J., Low, P.S., Dimitrov, D.S. and Sumer, B.D., 2014. In vivo optical imaging of folate receptor-β in head and neck squamous cell carcinoma. *The Laryngoscope*, *124*(8), pp.E312-E319.
- Sun, S.S., Zhou, X., Huang, Y.Y., Kong, L.P., Mei, M., Guo, W.Y., Zhao, M.H., Ren, Y., Shen, Q. and Zhang, L., 2015. Targeting STAT3/miR-21 axis inhibits epithelial-mesenchymal transition via regulating CDK5 in head and neck squamous cell carcinoma. *Molecular cancer*, *14*, pp.1-11.
- Teni, T., Pawar, S., Sanghvi, V. and Saranath, D., 2002. Expression of bcl-2 and bax in chewing tobacco-induced oral cancers and oral lesions from India. *Pathology Oncology Research*, *8*, pp.109-114.
- Tie, Y., Zheng, H., He, Z., Yang, J., Shao, B., Liu, L., Luo, M., Yuan, X., Liu, Y., Zhang, X. and Li, H., 2020. Targeting folate receptor β positive tumor-associated macrophages in lung cancer with a folate-modified liposomal complex. *Signal transduction and targeted therapy*, *5*(1), p.6.
- Tirapu, I., Huarte, E., Guiducci, C., Arina, A., Zaratiegui, M., Murillo, O., Gonzalez, A., Berasain, C., Berraondo, P., Fortes, P. and Prieto, J., 2006. Low surface expression of B7-1 (CD80) is an immunoescape mechanism of colon carcinoma. *Cancer research*, *66*(4), pp.2442-2450.

References:

- Toffoli G, Cernigoi C, Russo A, Gallo A, Bagnoli M, Boiocchi M. 1997. Overexpression of folate binding protein in ovarian cancers. Int J Cancer 74:193±198.
- Toll, A., Masferrer, E., Hernández-Ruiz, M.E., Ferrandiz-Pulido, C., Yébenes, M., Jaka, A., Tuneu, A., Jucglà, A., Gimeno, J., Baró, T. and Casado, B., 2013. Epithelial to mesenchymal transition markers are associated with an increased metastatic risk in primary cutaneous squamous cell carcinomas but are attenuated in lymph node metastases. *Journal of dermatological science*, *72*(2), pp.93-102.
- Topf, M.C., Harshyne, L., Tuluc, M., Mardekian, S., Vimawala, S., Cognetti, D.M., Curry, J.M., Rodeck, U. and Luginbuhl, A., 2019. Loss of CD169+ subcapsular macrophages during metastatic spread of head and neck squamous cell carcinoma. *Otolaryngology–Head and Neck Surgery*, *161*(1), pp.67-73.
- Tsang, W.P., Chau, S.P., Kong, S.K., Fung, K.P. and Kwok, T.T., 2003. Reactive oxygen species mediate doxorubicin induced p53-independent apoptosis. *Life sciences*, *73*(16), pp.2047-2058.
- Tu, B., He, Y., Chen, B., Wang, Y., Gao, Y., Shi, M., Liu, T., Asrorov, A.M. and Huang, Y., 2020. Deformable liposomal codelivery of vorinostat and simvastatin promotes antitumor responses through remodeling tumor microenvironment. Biomaterials Science, 8(24), pp.7166-7176.
- Ughachukwu, P.O. and Unekwe, P.C., 2012. Efflux Pump. Mediated Resistance in Chemotherapy. *Annals of medical and health sciences research*, *2*(2), pp.191-198.
- Ulrich, C.M. and Potter, J.D., 2007. Folate and cancer—timing is everything. Jama, 297(21), pp.2408-2409.
- Van Bambeke, F., Balzi, E. and Tulkens, P.M., 2000. Antibiotic efflux pumps. *Biochemical pharmacology*, *60*(4), pp.457-470.

References:

- Van Dam, G.M., Themelis, G., Crane, L.M., Harlaar, N.J., Pleijhuis, R.G., Kelder, W., Sarantopoulos, A., De Jong, J.S., Arts, H.J., Van Der Zee, A.G. and Bart, J., 2011. Intraoperative tumor-specific fluorescence imaging in ovarian cancer by folate receptor-α targeting: first in-human results. *Nature medicine*, *17*(10), pp.1315-1319.
- Vannini, F., Kashfi, K. and Nath, N., 2015. The dual role of iNOS in cancer. *Redox biology*, *6*, pp.334-343.
- Wan, D.H., Ma, X.Y., Lin, C., Zhu, D.H., Li, X., Zheng, B.Y., Li, J., Ke, M.R. and Huang, J.D., 2020. Noncovalent indocyanine green conjugate of c-phycocyanin: Preparation and tumor-associated macrophages-targeted photothermal therapeutics. *Bioconjugate Chemistry*, *31*(5), pp.1438-1448.
- Wang, D., Xu, X., Zhang, K., Sun, B., Wang, L., Meng, L., Liu, Q., Zheng, C., Yang, B. and Sun, H., 2018. Codelivery of doxorubicin and MDR1-siRNA by mesoporous silica nanoparticles-polymerpolyethylenimine to improve oral squamous carcinoma treatment. *International journal of nanomedicine*, *13*, p.187.
- Wang, F., Wang, Y.C., Dou, S., Xiong, M.H., Sun, T.M. and Wang, J., 2011. Doxorubicin-tethered responsive gold nanoparticles facilitate intracellular drug delivery for overcoming multidrug resistance in cancer cells. *ACS nano*, *5*(5), pp.3679-3692.
- Wang, J., 2017, July. Spatial targeting of tumor-associated macrophage and tumor cells with a designer nanocarrier for cancer chemo-immunotherapy. In *2017 39th Annual International Conference of the IEEE Engineering in Medicine and Biology Society (EMBC)* (pp. 291-291). IEEE.

References:

- Wang, J., Chang, Y., Luo, H., Jiang, W., Xu, L., Chen, T. and Zhu, X., 2020. Designing immunogenic nanotherapeutics for photothermal-triggered immunotherapy involving reprogramming immunosuppression and activating systemic antitumor responses. *Biomaterials*, *255*, p.120153.
- Wang, J., Hu, Y., Escamilla-Rivera, V., Gonzalez, C.L., Tang, L., Wang, B., El-Naggar, A.K., Myers, J.N. and Caulin, C., 2021. Epithelial Mutant p53 Promotes Resistance to Anti-PD-1-Mediated Oral Cancer Immunoprevention in Carcinogen-Induced Mouse Models. *Cancers*, *13*(6), p.1471.
- Wang, J., Wei, Q., Wang, X., Tang, S., Liu, H., Zhang, F., Mohammed, M.K., Huang, J., Guo, D., Lu, M. and Liu, F., 2016. Transition to resistance: an unexpected role of the EMT in cancer chemoresistance. *Genes & diseases*, *3*(1), pp.3-6.
- Wang, J., Xu, Y., Rao, X., Zhang, R., Tang, J., Zhang, D., Jie, X., Zhu, K., Wang, X., Xu, Y. and Zhang, S., 2022. BRD4-IRF1 axis regulates chemoradiotherapy-induced PD-L1 expression and immune evasion in non-small cell lung cancer. *Clinical and Translational Medicine*, *12*(1), p.e718.
- Wang, L.X., Mei, Z.Y., Zhou, J.H., Yao, Y.S., Li, Y.H., Xu, Y.H., Li, J.X., Gao, X.N., Zhou, M.H., Jiang, M.M. and Gao, L., 2013. Low dose decitabine treatment induces CD80 expression in cancer cells and stimulates tumor specific cytotoxic T lymphocyte responses. *PloS one*, *8*(5), p.e62924.
- Wang, T., Zhang, J., Hou, T., Yin, X. and Zhang, N., 2019. Selective targeting of tumor cells and tumor associated macrophages separately by twin-like core–shell nanoparticles for enhanced tumor-localized chemoimmunotherapy. *Nanoscale*, *11*(29), pp.13934-13946.

References:

- Wang, Y., Lin, Y.X., Qiao, S.L., An, H.W., Ma, Y., Qiao, Z.Y., Rajapaksha, R.P.Y.J. and Wang, H., 2017. Polymeric nanoparticles enable reversing macrophage in tumor microenvironment for immunotherapy. *Biomaterials*, *112*(15), p.3e163.
- Wang, Y., Luan, Z., Zhao, C., Bai, C. and Yang, K., 2020. Target delivery selective CSF-1R inhibitor to tumor-associated macrophages via erythrocyte-cancer cell hybrid membrane camouflaged pH-responsive copolymer micelle for cancer immunotherapy. *European Journal of Pharmaceutical Sciences*, *142*, p.105136.
- Wani, N.A., Hamid, A. and Kaur, J., 2008. Folate status in various pathophysiological conditions. IUBMB life, 60(12), pp.834-842.
- Warnakulasuriya, S., 2010. Living with oral cancer: epidemiology with particular reference to prevalence and life-style changes that influence survival. Oral oncology, 46(6), pp.407-410.
- Waters, J.P., Pober, J.S. and Bradley, J.R., 2013. Tumour necrosis factor and cancer. *The Journal of pathology*, *230*(3), pp.241-248.
- Webster, R.M., 2016. Combination therapies in oncology. *Nature reviews. Drug discovery*, *15*(2), p.81.
- Wei, C., Yang, C., Wang, S., Shi, D., Zhang, C., Lin, X. and Xiong, B., 2019. M2 macrophages confer resistance to 5-fluorouracil in colorectal cancer through the activation of CCL22/PI3K/AKT signaling. *OncoTargets and therapy*, *12*, p.3051.
- Wei, C., Yang, C., Wang, S., Shi, D., Zhang, C., Lin, X., Liu, Q., Dou, R. and Xiong, B., 2019. Crosstalk between cancer cells and tumor associated macrophages is required for mesenchymal circulating tumor cell-mediated colorectal cancer metastasis. *Molecular cancer*, *18*(1), pp.1-23.

References:

- Wei, C., Yang, X., Liu, N., Geng, J., Tai, Y., Sun, Z., Mei, G., Zhou, P., Peng, Y., Wang, C. and Zhang, X., 2019. Tumor microenvironment regulation by the endoplasmic reticulum stress transmission mediator Golgi protein 73 in mice. *Hepatology*, *70*(3), pp.851-870.
- Wei, G., Sun, J., Luan, W., Hou, Z., Wang, S., Cui, S., Cheng, M. and Liu, Y., 2019. Natural product albiziabioside A conjugated with pyruvate dehydrogenase kinase inhibitor dichloroacetate to induce apoptosis-ferroptosis-M2-TAMs polarization for combined cancer therapy. *Journal of medicinal chemistry*, *62*(19), pp.8760-8772.
- Wen, Y., Graybill, W.S., Previs, R.A., Hu, W., Ivan, C., Mangala, L.S., Zand, B., Nick, A.M., Jennings, N.B., Dalton, H.J. and Sehgal, V., 2015. Immunotherapy Targeting Folate Receptor Induces Cell Death Associated with Autophagy in Ovarian CancerInhibition of Ovarian Cancer Growth by MORAB-003. *Clinical Cancer Research*, *21*(2), pp.448-459.
- Wilson, T.R., Johnston, P.G. and Longley, D.B., 2009. Anti-apoptotic mechanisms of drug resistance in cancer. *Current cancer drug targets*, *9*(3), pp.307-319.
- Wise-Draper, T.M., Bahig, H., Tonneau, M., Karivedu, V. and Burtness, B., 2022. Current therapy for metastatic head and neck cancer: evidence, opportunities, and challenges. *American Society of Clinical Oncology Educational Book*, *42*, pp.527-540.
- Wu, B., Wu, X., Liu, S., Wang, Z. and Chen, L., 2019. Size-dependent effects of polystyrene microplastics on cytotoxicity and efflux pump inhibition in human Caco-2 cells. *Chemosphere*, *221*, pp.333-341.

References:

- Xu, W., Bae, E.J. and Lee, M.K., 2018. Enhanced anticancer activity and intracellular uptake of paclitaxel-containing solid lipid nanoparticles in multidrug-resistant breast cancer cells. *International journal of nanomedicine*, *13*, p.7549.
- Xue, H.Y., Bendayan, R. and Wong, H.L., 2020. MDR reversal for effective chemotherapy in breast cancer. In Drug Efflux Pumps in Cancer Resistance Pathways: From Molecular Recognition and Characterization to Possible Inhibition Strategies in Chemotherapy (pp. 121-147). Academic Press.
- Yamagata, Y., Tomioka, H., Sakamoto, K., Sato, K., Harada, H., Ikeda, T. and Kayamori, K., 2017. CD163-positive macrophages within the tumor stroma are associated with lymphangiogenesis and lymph node metastasis in oral squamous cell carcinoma. *Journal of Oral and Maxillofacial Surgery*, *75*(10), pp.2144-2153.
- Yamanaka, K., Rocchi, P., Miyake, H., Fazli, L., Vessella, B., Zangemeister-Wittke, U. and Gleave, M.E., 2005. A novel antisense oligonucleotide inhibiting several antiapoptotic Bcl-2 family members induces apoptosis and enhances chemosensitivity in androgen-independent human prostate cancer PC3 cells. *Molecular cancer therapeutics*, *4*(11), pp.1689-1698.
- Yang, J., Ju, Z. and Dong, S., 2017. Cisplatin and paclitaxel co-delivered by folate-decorated lipid carriers for the treatment of head and neck cancer. *Drug delivery*, *24*(1), pp.792-799.
- Yang, L., Song, X., Gong, T., Jiang, K., Hou, Y., Chen, T., Sun, X., Zhang, Z. and Gong, T., 2018. Development a hyaluronic acid ion-pairing liposomal nanoparticle for enhancing anti-glioma efficacy by modulating glioma microenvironment. *Drug Delivery*, *25*(1), pp.388-397.

References:

- Yang, L., Wang, Y., Guo, L., Wang, L., Chen, W. and Shi, B., 2015. The expression and correlation of iNOS and p53 in oral squamous cell carcinoma. *BioMed research international*, *2015*.
- Yang, X., Zhang, C., Li, A., Wang, J. and Cai, X., 2019. Red fluorescent ZnO nanoparticle grafted with polyglycerol and conjugated RGD peptide as drug delivery vehicles for efficient target cancer therapy. *Materials Science and Engineering: C*, *95*, pp.104-113.
- Yang, Y., Yu, Y., Chen, H., Meng, X., Ma, W., Yu, M., Li, Z., Li, C., Liu, H., Zhang, X. and Xiao, H., 2020. Illuminating platinum transportation while maximizing therapeutic efficacy by gold nanoclusters via simultaneous near-infrared-I/II imaging and glutathione scavenging. *ACS nano*, *14*(10), pp.13536-13547.
- Ye, J., Yang, Y., Jin, J., Ji, M., Gao, Y., Feng, Y., Wang, H., Chen, X. and Liu, Y., 2020. Targeted delivery of chlorogenic acid by mannosylated liposomes to effectively promote the polarization of TAMs for the treatment of glioblastoma. *Bioactive Materials*, *5*(3), pp.694-708.
- Yellin, M.J., Sinning, J., Covey, L.R., Sherman, W., Lee, J.J., Glickman-Nir, E., Sippel, K.C., Rogers, J., Cleary, A.M. and Parker, M., 1994. T lymphocyte T cell-B cell-activating molecule/CD40-L molecules induce normal B cells or chronic lymphocytic leukemia B cells to express CD80 (B7/BB-1) and enhance their costimulatory activity. *Journal of immunology (Baltimore, Md.: 1950)*, *153*(2), pp.666-674.
- Yin, X., Han, S., Song, C., Zou, H., Wei, Z., Xu, W., Ran, J., Tang, C., Wang, Y., Cai, Y. and Hu, Q., 2019. Metformin enhances gefitinib efficacy by interfering with interactions between tumor-associated macrophages and head and neck squamous cell carcinoma cells. *Cellular Oncology*, *42*, pp.459-475.

References:

- Yu, Y., Wang, J., Kaul, S.C., Wadhwa, R. and Miyako, E., 2019. Folic acid receptor-mediated targeting enhances the cytotoxicity, efficacy, and selectivity of withania somnifera leaf extract: In vitro and in vivo evidence. *Frontiers in Oncology*, *9*, p.602.
- Yuan, Y.G., Wang, Y.H., Xing, H.H. and Gurunathan, S., 2017. Quercetin-mediated synthesis of graphene oxide–silver nanoparticle nanocomposites: A suitable alternative nanotherapy for neuroblastoma. *International Journal of Nanomedicine*, *12*, p.5819.
- Zhang, F., Wang, H., Wang, X., Jiang, G., Liu, H., Zhang, G., Wang, H., Fang, R., Bu, X., Cai, S. and Du, J., 2016. TGF-β induces M2-like macrophage polarization via SNAIL-mediated suppression of a pro-inflammatory phenotype. *Oncotarget*, *7*(32), p.52294.
- Zhang, J., Yao, H., Song, G., Liao, X., Xian, Y. and Li, W., 2015. Regulation of epithelial-mesenchymal transition by tumor-associated macrophages in cancer. *American journal of translational research*, *7*(10), p.1699.
- Zhang, M., Fang, Z., Cui, M. and Liu, K., 2022. Multifunctional metal complex-based gene delivery for tumour immune checkpoint blockade combination therapy. *Journal of Drug Targeting*, *30*(7), pp.753-766.
- Zhang, X. and Li, B., 2023. Updates of liquid biopsy in oral cancer and multiomics analysis. *Oral Diseases*, *29*(1), pp.51-61.
- Zhang, X., Tian, W., Cai, X., Wang, X., Dang, W., Tang, H., Cao, H., Wang, L. and Chen, T., 2013. Hydrazinocurcumin Encapsuled nanoparticles “re-educate” tumor-associated macrophages and exhibit anti-tumor effects on breast cancer following STAT3 suppression. *PloS one*, *8*(6), p.e65896.

References:

- Zhang, Z., Qiu, C., Li, X., McClements, D.J., Jiao, A., Wang, J. and Jin, Z., 2021. Advances in research on interactions between polyphenols and biology-based nano-delivery systems and their applications in improving the bioavailability of polyphenols. *Trends in Food Science & Technology*, *116*, pp.492-500.
- Zhang, Z., Sun, C., Li, C., Jiao, X., Griffin, B.B., Dongol, S., Wu, H., Zhang, C., Cao, W., Dong, R. and Yang, X., 2020. Upregulated MELK leads to doxorubicin chemoresistance and M2 macrophage polarization via the miR-34a/JAK2/STAT3 pathway in uterine leiomyosarcoma. *Frontiers in oncology*, *10*, p.453.
- Zhao, H., Feng, H., Liu, D., Liu, J., Ji, N., Chen, F., Luo, X., Zhou, Y., Dan, H., Zeng, X. and Li, J., 2015. Self-assembling monomeric nucleoside molecular nanoparticles loaded with 5-FU enhancing therapeutic efficacy against oral cancer. *ACS nano*, *9*(10), pp.9638-9651.
- Zhao, J., Wan, Z., Zhou, C., Yang, Q., Dong, J., Song, X. and Gong, T., 2018. Hyaluronic acid layer-by-layer (LbL) nanoparticles for synergistic chemo-phototherapy. *Pharmaceutical research*, *35*, pp.1-14.
- Zhao, L. and Zhang, B., 2017. Doxorubicin induces cardiotoxicity through upregulation of death receptors mediated apoptosis in cardiomyocytes. *Scientific reports*, *7*(1), p.44735.
- Zhao, X., Qi, X., Lian, W., Tong, X., Wang, H., Su, L., Wei, P., Zhuang, Z., Gong, J. and Bai, L., 2020. Trichomicin suppresses colorectal cancer via comprehensive regulation of IL-6 and TNFα in tumor cells, TAMs, and CAFs. *Frontiers in Pharmacology*, *11*, p.386.

References:

- Zhou, J., Tao, D., Xu, Q., Gao, Z. and Tang, D., 2015. Expression of E-cadherin and vimentin in oral squamous cell carcinoma. *International journal of clinical and experimental pathology*, *8*(3), p.3150.
- Zhou, S., Zhang, T., Peng, B., Luo, X., Liu, X., Hu, L., Liu, Y., Di, D., Song, Y. and Deng, Y., 2017. Targeted delivery of epirubicin to tumor-associated macrophages by sialic acid-cholesterol conjugate modified liposomes with improved antitumor activity. *International journal of pharmaceutics*, *523*(1), pp.203-216.
- Zhou, W., Guo, S., Liu, M., Burow, M.E. and Wang, G., 2019. Targeting CXCL12/CXCR4 axis in tumor immunotherapy. *Current medicinal chemistry*, *26*(17), pp.3026-3041.
- Zhu, Y., Hu, J., Hu, Y. and Liu, W., 2009. Targeting DNA repair pathways: a novel approach to reduce cancer therapeutic resistance. *Cancer treatment reviews*, *35*(7), pp.590-596.
- Zhuo, F., Abourehab, M.A. and Hussain, Z., 2018. Hyaluronic acid decorated tacrolimus-loaded nanoparticles: Efficient approach to maximize dermal targeting and anti-dermatitis efficacy. *Carbohydrate polymers*, *197*, pp.478-489.
- Zou, L., Tao, Y., Payne, G., Do, L., Thomas, T., Rodriguez, J. and Dou, H., 2017. Targeted delivery of nano-PTX to the brain tumor-associated macrophages. *Oncotarget*, *8*(4), p.6564.
- Zwicke, G.L., Ali Mansoori, G. and Jeffery, C.J., 2012. Utilizing the folate receptor for active targeting of cancer nanotherapeutics. *Nano reviews*, *3*(1), p.18496.

Limitations of the research:

Although a variety of receptor-targeted therapeutic approaches have shown promising results in vitro and in pre-clinical models in vivo, several important parameters need to be determined and optimized to ensure successful translation of these technologies to clinical application. Ongoing and future work in the field need to correlate the extent of receptor expression to the amount of ligands needed for effective targeting. It is envisioned that continued research in this area will also enable identification of tumours where receptortargeted approaches can provide additional advantages over non-targeted ones. This information is highly critical, because although several cancers are known to have upregulation of certain receptors, the level of upregulation may or may not be sufficient to warrant additional benefit from active targeting over and above passive accumulation. Furthermore, cancers with high receptor expression are often found to have hypoxic cores that make permeation by delivery systems challenging. Therefore, in such cases even if the particles themselves may have excellent receptor-targeting capability, getting enough particles to penetrate throughout the tumour volume can be a challenge, and this will be a critical component of ongoing and future research.

List of Publications:

Publications related to Thesis

- **Bhattacharya D**, Sakhare K, Dhiman C, Ansari A, Kundu TK, Narayan KP, Banerjee R. Delivery of chemotherapeutic drug targeting folate receptor to oral cancer cells using functionalized carbon nanospheres. Biomedical Materials (Under communication, Manuscript reference: BMM-105376)

- **Elechalawar CK*, Bhattacharya D***, Ahmed MT, Gora H, Sridharan K, Chaturbedy P, Sinha SH, Jaggarapu MM, Narayan KP, Chakravarty S, Eswaramoorthy M. Dual targeting of folate receptor-expressing glioma tumor-associated macrophages and epithelial cells in the brain using a carbon nanosphere–cationic folate nanoconjugate. Nanoscale Advances. 2019;1(9):3555-67.(First author equal contribution)

- **Bhattacharya D**, Sakhare K, Narayan KP, Banerjee R. The prospects of nanotherapeutic approaches for targeting tumor-associated macrophages in oral cancer. Nanomedicine: Nanotechnology, Biology and Medicine. 2021 Jun 1;34:102371.

- Manturthi S, **Bhattacharya D**, Sakhare KR, Narayan KP, Patri SV. Cimetidine-Based Cationic Amphiphiles for In Vitro Gene Delivery Targetable to Colon Cancer. ACS omega. 2022 Aug 25;7(35):31388-402.

- Manturthi S, **Bhattacharya D**, Sakhare KR, Narayan KP, Patri SV. Nicotinic acid-based cationic vectors for efficient gene delivery to glioblastoma cells. New Journal of Chemistry. 2022;46(43):20886-99.

- **Mahadik N*, Bhattacharya D*, Padmanabhan A*, Sakhare K***, Narayan KP, Banerjee R. Targeting steroid hormone receptors for anti-cancer therapy—A review on small molecules and nanotherapeutic approaches. Wiley Interdisciplinary Reviews: Nanomedicine and Nanobiotechnology. 2022 Mar;14(2):e1755.(First author equal contribution)

Publications outside Thesis

- Kumar A, Sakhare K, **Bhattacharya D**, Chattopadhyay R, Parikh P, Narayan KP, Mukherjee A. Communication in non-communicable diseases (NCDs) and role of immunomodulatory nutraceuticals in their management. Frontiers in Nutrition. 2022;9.

List of Conferences:

- Poster presented at 44th All India Cell Biology Conference and International Symposium on Molecular & Cellular Insights of Human Diseases on the topic: ''Folate Receptor targeting Biocompatible nanospheres for augmenting drug uptake in oral squamous cell carcinoma'' organized by Department of Biochemistry,University of Kashmir.

- Poster presented at Virtual 9th Mayo Clinic Symposium on Immuno oncology and Tumor Microenvironment crosstalk 2022 on the topic: '' Folate receptor targeting biocompatible nanospheres for tumor microenvironment manipulation and tumor regression'' organized by School of Continuous Professional development, Mayo clinic, Rochester,USA.

- Poster presented at 45th All India Cell Biology Conference & International Symposium on Biology of Development and Disease on the topic: '' Folate Receptor mediated targeted chemotherapy in a syngeneic mouse model of Oral squamous cell carcinoma'' organized by Department of Zoology,Institute of Science, Banaras Hindu University.

Biography of Dwaipayan Bhattacharya:

Dwaipayan Bhattacharya has done his M.Sc. Biotechnology from Lovely Professional University (LPU), Jalandhar. He then worked as Project Assistant (Level 2) under the supervision of Dr. Sumana Chakravarty on chemical biology and therapy of neurological diseases at CSIR-IICT, Hyderabad from 2013 to 2017. He joined the Ph.D. Program as an Institute Fellow at BITS Pilani, Hyderabad campus in 2018 and has been working as a research scholar on the development and validation of different modes of targeted therapy against oral squamous cell carcinoma from 2018-2023 under the supervision of Prof. Kumar Pranav Narayan. Dwaipayan has attended International and National Conferences and was awarded ICMR-SRF for carrying out his research work in April 2020. He has multiple publications in peer reviewed journals to his credit and wishes to pursue a career in teaching.

Biography of Prof. Kumar Pranav Narayan:

Prof. Kumar Pranav Narayan is working as Professor in the Department of Biological Sciences at BITS Pilani Hyderabad Campus after he joined in June, 2016. Prior to this, he had joined this department in 2008 as Assistant Professor. Prof. Narayan received his Doctoral degree from Jamia Millia Islamia, New Delhi under the joint supervision of Dr. Y. D. Gaur, Division of Microbiology, Indian Agricultural Research Institute, New Delhi and Dr. Arif Ali, Professor, Department of Biosciences, Jamia Millia Islamia, New Delhi. He had been Postdoctoral Senior Research Fellow in the Division of Microbiology, Indian Agricultural Research Institute, New Delhi in the field of molecular biodiversity analysis of cyanobacterial germplasm. He was a Postdoctoral Research Associate in Lipid Science and Technology, Indian Institute of Chemical Technology (IICT), Hyderabad in the field of Gene Therapy for Cancer.

Apart from regularly teaching in programs like M.Sc. Biological Sciences & M. Tech Biotechnology, he works in the areas of cancer therapeutics using targeted drug/gene delivery systems, phyto-compounds for targeted therapeutics, adjuvants for vaccine & immunotherapies and the development of nutraceuticals for cancer patients. Prof. Narayan has also worked in the field of agricultural microbiology on molecular biodiversity of cyanobacteria and bacteriocinogeny for the development of competitive strains of Mesorhizobium ciceri as a potential biofertilizer. Presently, he is using crop residues and waste/weed plants for the development of biopesticides. His research projects are funded by industry, as well as DBT, Govt. of India. He also has internal funding from CHDR-BITS and is shaving active collaborations with reputed organizations like CSIR-IICT(Hyderabad), IIT Hyderabad, NIT Warangal and the Army College of Dental Sciences, Secunderabad.